Electricity market operations under increasing uncertainty

THÈSE N^{O} 7894 (2017)

PRÉSENTÉE LE 25 AOÛT 2017

À LA FACULTÉ DES SCIENCES ET TECHNIQUES DE L'INGÉNIEUR

GROUPE SCI STI RC

PROGRAMME DOCTORAL EN GÉNIE ÉLECTRIQUE

ÉCOLE POLYTECHNIQUE FÉDÉRALE DE LAUSANNE

POUR L'OBTENTION DU GRADE DE DOCTEUR ÈS SCIENCES

PAR

Farzaneh ABBASPOURTORBATI

acceptée sur proposition du jury:

Prof. A. Skrivervik, présidente du jury
Dr S.-R. Cherkaoui, Prof. A. J. Conejo, directeurs de thèse
Prof. A. Bakirtzis, rapporteur
Prof. T. Gomez, rapporteur
Prof. J.-Y. Le boudec, rapporteur

ÉCOLE POLYTECHNIQUE
FÉDÉRALE DE LAUSANNE

Suisse
2017

You are educated when you have the ability to listen to
almost anything without losing your temper or self-confidence.
— Robert Frost

Dedicated to my beloved family.

Abstract

Decision making in electricity markets under uncertainty has worldwide gained attention due to an increasing number of uncertain parameters associated to technology developments and market evolution. Hence, the market operator faces new challenges pertaining to technical and economic aspects of electricity markets. To tackle these challenges, appropriate models are necessary.

This dissertation aims to analyze some of the challenges pertaining to the management in electricity markets under uncertainty and to provide the market operator with the models that enable it to make informed decisions in such uncertain market environments.

In the context above, we categorize market operation problems into the following four groups.

With the aim of obtaining informed day-ahead decisions in the presence of a number of intra-day markets and high renewable production, we propose a multi-stage stochastic clearing model, where the first stage represents the day-ahead market, n stages model n intra-day markets, and a final stage represents real-time operation. The proposed multi-stage clearing model considers not only different realizations of renewable power output, but also how these realizations evolve from day-ahead forecasts into real-time values, and allows flexibility for the contribution of renewable production in both the day-ahead and intra-day markets in form of scheduled productions and their adjustments. This improves the market outcomes and integration of renewable generation.

With the purpose of obtaining marginal prices with cost-recovery features, we develop novel pricing methodologies in the presence of non-convexities and uncertainty in the market. These models minimize the duality gap of a stochastic non-convex clearing model and the dual problem of a relaxed version of this original model subject to primal constraints, dual constraints, cost-recovery constraints, and integrity constraints. The prices obtained deviate in the least possible manner from conventional marginal prices. This implies that a minimum deviation from the optimal value of social welfare is also guaranteed. Moreover, the new prices preserve the short-term economic efficiency and long-term cost recovery properties of

marginal prices, while eliminating a need for uplifts.

We provide insightful analyses on the impact of demand flexibility on the operational and economic aspects of the power system operation. We investigate how market prices are affected by flexible demands and what economic consequences are observed. For this purpose, we consider a system with high renewable production and a number of comparatively expensive fast-ramping units, which are flexible to react to the uncertainty pertaining to renewable power production. We investigate the role of flexible demands from an economic viewpoint, particularly the impact of flexible demands on demand revenues.

Lastly, we develop a risk-neutral two-stage stochastic clearing model and a risk-averse one for reserve markets. We particularly focus on the Swiss reserve market, which consists of a weekly market with a gate closure one week ahead of real-time operation and a daily market with a gate closure two days ahead of real time. The decision-making problem consists of determining which amount of reserves to procure in the weekly market and which one in the daily market. In the proposed two-stage model, the first stage represents the weekly market and the second stage the daily market. The source of uncertainty is the unknown offers in the daily market, which are represented by scenarios. If the system operator aims to minimize the risk pertaining to expensive reserve offers in the daily market, a risk-averse instance of this two-stage clearing model is also proposed.

Key words: Electricity Markets, Multi-Stage Stochastic Programming, Uncertainty Management, Decision Making, Pricing Schemes, Flexible Demands, Reserve Markets, Renewable Production, Intra-Day Markets, Risk, Non-convexity, Uplift, Cost recovery, Value of the Stochastic Solution, Informed Day-ahead Decisions.

Résumé

La prise de décision dans les marchés de l'électricité sujet à l'incertitude attire l'attention à l'échelle mondiale en raison du nombre croissant de paramètres incertains associés aux développements technologiques et à l'évolution du marché. Par conséquent, l'opérateur du marché doit faire face à de nouveaux défis liés aux aspects techniques et économiques des marchés de l'électricité. Pour relever ces défis, des modèles appropriés sont nécessaires.

Cette thèse vise à analyser un certain nombre de défis liés à la gestion des marchés de l'électricité sujet à l'incertitude et à fournir à l'opérateur du marché des modèles permettant de prendre des décisions appropriées dans des environnements de marché aussi incertains. Aussi, dans le contexte ci-dessus, nous classons les problèmes de fonctionnement du marché dans les quatre groupes suivants.

Dans le but d'obtenir des décisions le jour d'avant en présence d'un certain nombre de marchés intra-journaliers et d'une production renouvelable élevée, nous proposons un modèle de marché stochastique à plusieurs étapes, où les étapes représentent respectivement le marché du jour d'avant, N marchés intra journaliers, et un marché en temps réel. Le modèle multi-étapes proposé considère non seulement les différentes réalisations de la production d'énergie renouvelable, mais aussi la façon dont ces réalisations évoluent depuis leur prévision le jour d'avant jusqu'à leur valeur en temps réel. Il permet une flexibilité de la production d'énergie renouvelable dans le marché du jour d'avant et les marchés intra journaliers sous forme de productions programmées et d'ajustement. Cela améliore les résultats du marché ainsi que l'intégration de la production renouvelable.

Dans le but d'obtenir des prix marginaux avec des options de recouvrement des coûts, nous développons un nouveau mécanisme de tarification tenant compte de la présence de non-convexité et d'incertitude dans le modèle de marché. Ce modèle minimise l'écart de dualité entre un modèle de marché stochastique non convexe et sa version duale relaxée tout en tenant compte des contraintes du problème primal, des contraintes duals, des contraintes concernant le recouvrement des coûts et des contraintes sur les variables binaires. Les prix obtenus s'écartent le moins possible des prix marginaux conventionnels. En outre, Ces nouveaux prix préservent l'efficacité économique à court terme et les propriétés de recouvrement des coûts à long terme des prix marginaux tout en éliminant la nécessité des up-lifts.

Ensuite, nous fournissons des analyses approfondies sur l'impact de la flexibilité de la demande sur les aspects opérationnels et économiques de l'exploitation du réseau électrique. Nous étudions comment les prix du marché sont affectés par des demandes flexibles et les conséquences économiques observées. À cet effet, nous considérons un système à forte production renouvelable et un certain nombre d'unités à forte montée en charge et réputées onéreuses. Ces dernières sont considérées suffisamment flexibles pour réagir à l'incertitude relative à la production d'énergie renouvelable. Nous étudions le rôle des demandes flexibles d'un point de vue économique, en particulier l'impact des demandes flexibles sur les revenus de la demande.

Enfin, pour les marchés de réserve, nous développons deux modèles stochastiques à deux étapes respectivement neutre vis-à-vis du risque et robuste face au risque. Nous nous concentrons particulièrement sur le marché de réserve suisse qui comprend un marché hebdomadaire avec clôture une semaine avant l'exploitation en temps réel et un marché quotidien avec clôture deux jours avant le temps réel. Le problème de la prise de décision consiste à déterminer les quantités de réserve à vendre sur le marché hebdomadaire et le marché journalier respectivement. Dans le modèle proposé en deux étapes, la première étape représente le marché hebdomadaire et la deuxième étape représente le marché journalier. La source d'incertitude est liée à l'offre inconnue sur le marché quotidien qui est représentée par des scénarios. Si l'opérateur du système vise à minimiser le risque lié aux prix des offres de réserve sur le marché quotidien, le modèle de marché robuste face au risque est proposée à cet égard.

Mots clefs : Marchés d'électricité, Programmation stochastique à multi-étapes, Gestion de l'incertitude, Prise de décision, Mécanisme de fixation des prix, Demandes flexibles, Marché de réserve, Production renouvelable, Marchés intra journaliers, Risque, Non convexité, Uplift, Recouvrement des coûts, Valeur de la solution stochastique.

Acknowledgements

This thesis summarizes the work done over the course of four years at the Power Systems Group (PWRS) at EPFL. During my PhD, I was also working at the TSO Market Development team at Swissgrid. It has been a wonderful time and unique opportunity for me. I would like to extend my sincere gratitude to everyone I have interacted with, both on a professional and a personal level.

First and foremost, I would like to express my deepest gratitude to my advisors, Dr. Rachid Cherkaoui and Prof. Antonio Conejo, for invaluable help and support. Rachid, thank you for giving me such a wonderful opportunity at EPFL, providing me with flexibility and being patient with me. Thank you for detailed discussions. Antonio, thank you for supporting me with your vast knowledge and patience, and for hosting me at The Ohio State University, which was a turning point in my research. I am grateful to be your 20th graduated PhD student! And also, thank you for writing so many good books! I had been trained by your books years before I had the chance to collaborate with you.

My special thanks go to Dr. Marek Zima, leader of the TSO Market Development team at Swissgrid. Marek, thank you for the courage you gave me to go through this path, and for advising me on my first research work *Combined Auction* when I was just a newbie. The outcome of your idea in this project reported in Chapter 5 of this thesis. Thank you for your support and flexibility over all these years.

Pursuing a PhD at EPFL in Lausanne and a full-time job at Swissgrid in Laufenburg, while living in Zurich was only possible with the flexibility and support that Rachid, Antonio, and Marek provided me. Thank you very much.

I would also like to express my gratitude to the committee members for valuable comments and discussions during and after the PhD exam. Respecting travel distance (!), my sincere thanks goes to Prof. Tomas Gomez. It was a great pleasure to get to know you and to have your opinion on my work. Thank you for insightful comments. I would like to thank the committee member Prof. Anastasios Bakirtzis. It was always a great pleasure for me to have a discussion with you in different conferences. Thank you for constructive comments on my thesis. I would also like to express my gratitude to the committee member Prof. Jean-Yve Le boudec. Thank you for your valuable comments, and careful correction regarding my inaccurate statement on marginal pricing!

It was an incredible luck for me to get to know Prof. Daniel Kuhn. He is a wonderful teacher. I regret that I could not take more courses with him. Should the fundamental knowledge of optimization be a dream, as perhaps the ball in Royal Palace to Cinderella, then I would be confident to nominate Daniel as the fairy Godfather whose magic spell would never wear off! I have learnt a lot from him in convex optimization course.

I would like to express my gratitude to Prof. Göran Andersson, who was also my master thesis advisor, for kindly providing me access to servers in the Power System Laboratory (PSL) at ETH Zurich. This helped me progressing with the work reported in Chapter 3 of this thesis.

I would like to thank Dr. Mokhtar Bozorg and Dr. Mostafa Nick at the Distributed Electrical Systems Laboratory (DESL) at EPFL for their great unconditional help over all these years ranging from administrative issues to detailed technical discussions. I really appreciate your time to listen to my last minute PhD defense rehearsal.

I would like to extend my appreciation to to-be-soon Dr. Stavros Karagiannopoulos and to to-be-soon Prof. Line Roald at the PSL for their computational support and fruitful discussions and collaborations we had in different occasions.

I would like to extend my thanks to my colleagues at Swissgrid and all members of DESL and PWRS for the great time we had together.

Throughout these years, I have been fortunate to work with a number of students. I would like to thank Athanasios Troupakis, Anneta Matenli, Georgios Chatzis, and Haoyuan Qu for their contributions and for choosing to work with me. I would also like to thank my collaborators who co-supervised these projects.

At this point, I would like to thank Dr. Robin Vujanic and to-be-soon Dr. Tobias Sutter for warmly welcoming me in their office over all evenings and weekends at Automatic Control Laboratory (IfA) at ETH Zurich. I am sure that I am a better officemate than Peyman, at least I am more quiet than him!

At a personal level, I want to thank my terrific friends who made my Zurich life memorable, as well as my stays in Boston! Thank you for sharing fun times, brunches, game nights, hikes, but also for standing by me in my difficult moments.

I am greatly indebted to my dear parents, my father, Reza, who taught me being a woman is no excuse for not reaching far, and my mother, Esmat, for encouraging me to explore the world. Thanks to my two wonderful sisters for their unconditional love and empathy. Without them, I would never have been where I am today.

Last, I want to thank my best friend, my discussion partner, and my soulmate, Peyman. When spending all those weekends, evenings, and holidays on my research, you always supported me with compassion and encouragement. Peyman, it has been a long path with many ups and downs. Had I have another chance with you, I would definitely have held your hand more strongly. I can also keep it simple: I love you, too.

Farzaneh Abbaspourtorbati
July 2017
Zurich, Switzerland

Contents

List of Figures

List of Tables

Notations

The notation used in this dissertation is listed below for quick reference; others are defined as required in the text. For the sake of clarity, the symbols used to formulate the proposed models in Chapters 2, 3 and 4 are stated below separately from the symbols used in Chapter 5.

List of Symbols Used in Chapters 2, 3, and 4

Indices, Suberscripts and Sets

t	Index of time periods running from 1 to N_T
n	Index of nodes running from 1 to N_N.
i	Index of generating units running from 1 to N_G.
j	Index of loads running from 1 to N_L.
ω	Index of wind scenarios running from 1 to N_Ω.
q	Index of wind units running from 1 to N_Q.
Λ_n	Set of nodes directly connected to node n.
M_n^{G}	Set of generating units located at node n.
M_n^{L}	Set of loads located at node n.
M_n^{Q}	Set of wind units located at node n.

Constants

α^{WUs_1}	Constant determining the upper limit of wind power output at the day-ahead market.

α^{WDs_1}	Constant determining the lower limit of wind power output at the day-ahead market.
α^{WUs_2}	Constant determining the upper limit of wind power output at the intra-day market.
α^{WDs_2}	Constant determining the lower limit of wind power output at the intra-day market.
$\alpha_{\Delta W}$	Constant determining the upper limit of wind adjustments at the intra-day market.
$\alpha_{\Delta P}$	Constant determining the upper limit of conventional unit adjustments at the intra-day market.
π_{ω}	Probability of wind power scenario ω.
L_{jt}	Power consumption by inflexible demand j in period t [MW].
$P_i^{\max}$	Capacity of unit i [MW].
$P_i^{\min}$	Minimum power output of unit i [MW].
$f_{nr}^{\max}$	Transmission capacity of line (n,r) [MW].
C_i	Variable energy cost of unit i [$/MWh].
K_i^{SU}	Start-up cost of unit i [$].
$R_i^{D,\max}$	Maximum down-reserve that can be provided by unit i [MW].
$R_i^{U,\max}$	Maximum up-reserve that can be provided by unit i [MW].
$R_j^{D,\max}$	Maximum down-reserve that can be provided by flexible demand j [MW].
$R_j^{U,\max}$	Maximum up-reserve that can be provided by flexible demand j [MW].
$D_{jt}^{\min}$	Minimum load required by flexible demand j in period t.
$D_{jt}^{\max}$	Maximum load that can be consumed by flexible demand j in period t.
RU_i	Ramping-up limit of unit i [MW/h].
RD_i	Ramping-down limit of unit i [MW/h].
RU_j	Maximum load pick-up rate of flexible demand j [MW/h].

RD_j Maximum load drop-down rate of flexible demand j [MW/h].

$\overline{D}_{jt}$ Constant load consumed by inflexible demand j in period t [MW].

V_{jt}^{LOL} Value of lost load for load j in period t [$/MWh].

$W_{qt}^{\max}$ Maximum power production of wind unit q in period t [MW].

W_{qt}^{DA} Best forecast of wind power generation for unit q at stage s_1 and period t [MW].

$W_{qt\omega}^{\mathrm{ID}}$ Best forecast of wind power generation for unit q in scenario ω at stage s_2 and period t [MW].

$W_{qt\omega}^{\mathrm{RT}}$ Realization of wind power generation for unit q in scenario ω at stage s_3 and period t [MW].

B_{nr} Susceptance of line (n,r) [per unit].

G Sufficiently large positive constant.

E_j Minimum daily energy consumption by flexible demand j [MWh].

Variables pertaining to Day-ahead Market

C_{it}^{SU} Cost due to the start-up of unit i in period t [$].

P_{it} Power scheduled for unit i in period t at the day-ahead market stage [MW].

D_{jt} Load scheduled for flexible demand j in period t at the day-ahead market stage [MW].

θ_{nt} Angle of node n in period t at the day-ahead market stage [rad].

W_{qt} Power scheduled for wind unit q in period t at the day-ahead market stage [MW].

u_{it} Binary variable that is equal to 1 if unit i is scheduled to be committed in period t.

Variables pertaining to Intra-day Market

$\Delta P_{it\omega}^{\mathrm{U}}$ Upward power adjustment for unit i in scenario ω and period t at the intra-day market [MW].

$\Delta P_{it\omega}^{\mathrm{D}}$ Downward power adjustment for unit i in scenario ω and period t at the intra-day market [MW].

$\Delta W^{\mathrm{U}}_{qt\omega}$ Upward power adjustment for wind unit q in scenario ω and period t at the intra-day market [MW].

$\Delta W^{\mathrm{D}}_{qt\omega}$ Downward power adjustment for wind unit q in scenario ω and period t at the intra-day market [MW].

$\theta^{\mathrm{S}_2}_{nt\omega}$ Angle of node n in scenario ω and period t at the intra-day market [rad].

Variables pertaining to Real-time Operation

$p_{it\omega}$ Actual power output of unit i in period t and scenario ω.

$d_{jt\omega}$ Actual load consumed by flexible demand j in period t and scenario ω.

$r^{\mathrm{U}}_{it\omega}$ Deployed up-reserve by unit i in period t and scenario ω [MW].

$r^{\mathrm{D}}_{it\omega}$ Deployed down-reserve by unit i in period t and scenario ω [MW].

$d^{\mathrm{U}}_{jt\omega}$ Deployed up-reserve by flexible demand j in period t and scenario ω [MW].

$d^{\mathrm{D}}_{jt\omega}$ Deployed down-reserve by flexible demand j in period t and scenario ω [MW].

$\theta_{nt\omega}, \theta^{\mathrm{S}_3}_{nt\omega}$ Angle of node n in period t and scenario ω [rad].

$w^{\mathrm{spill}}_{qt\omega}$ Wind power spillage of unit q in period t and scenario ω [MW].

$L^{\mathrm{shed}}_{jt\omega}$ Involuntarily load shedding of load j in period t and scenario ω [MW].

Acronyms

Con Conventional method without Uplift

U Uplift method

CR Pricing approach with cost recovery at the day-ahead market stage.

AR Pricing approach with average cost recovery.

SR Pricing approach with cost recovery per scenario.

List of Symbols Used in Chapter 5

Indices, Suberscripts and Sets

t Index of time intervals related to the daily reserve market running from 1 to 6.

i	Index of secondary reserve offers running from 1 to N_{SR}.
j	Index of upward tertiary reserve offers running from 1 to N_j.
k	Index of downward tertiary reserve offers running from 1 to N_k.
r	Index of secondary reserve offers belonging to a set of mutually exclusive offers running from 1 to N_r.
m	Index of upward tertiary offers belonging to a set of mutually exclusive offers running from 1 to N_m.
q	Index of downward tertiary offers belonging to a set of mutually exclusive offers running from 1 to N_q.
ω	Index of daily offer scenarios running from 1 to N_{Ω}.

Variables pertaining to Weekly Reserve Market

x^{s}_{ir}	Binary variable that is equal to 1 if secondary reserve offer ir is accepted and 0 if rejected.
x^{up}_{jm}	Binary variable that is equal to 1 if upward tertiary reserve offer jm is accepted and 0 if rejected.
x^{dn}_{kq}	Binary variable that is equal to 1 if downward tertiary reserve offer kq is accepted and 0 if rejected.
$\epsilon^{\mathrm{s+}}$	probability pertaining to the contribution of upward secondary reserves in satisfying the probabilistic criteria.
$\epsilon^{\mathrm{s-}}$	probability pertaining to the contribution of downward secondary reserves in satisfying the probabilistic criteria.
$\epsilon^{\mathrm{o+}}$	probability pertaining to the contribution of upward overall reserves in satisfying the probabilistic criteria.
$\epsilon^{\mathrm{o-}}$	probability pertaining to the contribution of downward overall reserves in satisfying the probabilistic criteria.

Variables pertaining to Daily Reserve Market

$y^{\mathrm{up}}_{t\omega}$	Amount of upward tertiary reserves procured in each four-hour interval t and each scenario ω in the daily market [MW] .

$y^{\mathrm{dn}}_{t\omega}$ Amount of downward tertiary reserves procured in each four-hour interval t and each scenario ω in the daily market [MW].

$\gamma^{\mathrm{up}}_{t\omega}$ Cost of the upward tertiary reserves procured in each four-hour interval t and each scenario ω in the daily market [CHF].

$\gamma^{\mathrm{dn}}_{t\omega}$ Cost of the downward tertiary reserves procured in each four-hour interval t and each scenario ω in the daily market [CHF].

$y^{\mathrm{up}}_{j'm't}$ Binary variable that is equal to 1 if upward tertiary reserve offer $j'm'$ is accepted and 0 if rejected in each four-hour interval t in the daily market.

$y^{\mathrm{dn}}_{k'q't}$ Binary variable that is equal to 1 if downward tertiary reserve offer $k'q'$ is accepted and 0 if rejected in each four-hour interval t in the daily market.

Acronyms

SCR Secondary Reserve.

TR Tertiary Reserve.

1 Introduction

In this dissertation, we analyze some of the challenges pertaining to the management in electricity markets under uncertainty. The objective of this dissertation is to provide the market operator with the models that enable it to make informed decisions in electricity markets where uncertainty matters.

In this chapter, we provide an introduction to the thesis. First, we present an overview of some existing challenges in electricity markets, and how these challenges motivate the problems tackled in this thesis. Next, we provide the descriptions of the corresponding problems, and the approaches used to address them. To contextualized the analysis, a literature review is also carried out. Finally, the objectives and the layout of this dissertation are provided.

1.1 Motivation

Since the liberalization of the electric energy sector in the 90s, electricity markets have been evolving across the world. A key question is whether or not the commitment of a unit is a decision of the owner of that unit or a decision of a central planner, who has detailed information of the system. This has led to two market organizations in practice: self-dispatch markets (i.e., decentralized markets) and central-dispatch markets (i.e., centralized markets). The former is the current practice in many European countries, while the latter is implemented in the US [3, 27, 12, 71].

The self-dispatch market separates energy markets and transmission system operation to a large extent. The unit commitment is left to producers while dispatch decisions are made by the market operator in the day-ahead market [5]. We should note that according to the common practice in Euope, dispatch schedules are decided by Market Operator on portfolio basis and the dispatch of individual units is decided by producers. The production schedules of all units are delivered to the system operator over a specific horizon before real-time operation. The system operator then analyzes the impacts of production schedules on network congestion. In case of congestion, the system operator sends a command of re-dispatching to specific units in order to eliminate congestion. The system balancing is the responsibility of the system operator and it is done by procuring appropriate amounts of reserves in a reserve market (separated from the energy market), and deploying them when appropriate in real-time operation.

In a central-dispatch market, a central operator determines the unit commitment and dispatch schedules of all generating units. These decisions are made considering the technical constraints of the units, offer prices, network constraints, and load over day ahead and real-time horizons. Therefore, the market operator and system operator is the same entity. This gives the possibility of a co-optimization of energy and reserves in the day-ahead market.

Although these market organizations differ in many ways, some of the challenges that they face are similar since these challenges are inherent to the nature of power system.

In electricity markets, obtaining *right* market outcomes necessitates a precise modeling of the power system operation which includes discontinuities (non-convexities) pertaining to the operation of generation units. Thus, the market outcomes (i.e., scheduled power productions and clearing prices) are derived through models with non-convexities. These market-clearing models are formulated as Mixed-Integer Linear Problems (MILP). Obtaining marginal prices (i.e., strict linear clearing prices) directly as dual variables from MILP problems is not possible. In other words, dual variables loose their exact meaning as marginal prices for mixed-integer optimization problems, contrary to linear ones. The lack of marginal prices in terms of strict linear clearing prices in the market may question the market outcomes. That is, clearing prices may not provide dispatch-following incentives to producers, as they may result in inadequate revenues for producers [50]. In other words, some producers may not be able to recover their costs under these prices and they may leave market. This eventually results in market inefficiency.

In short, while from a technical perspective, the use of MILP clearing models might be inevitable, from an economic point of view, these models fail to define clearing marginal prices.

On top of this, the growth of renewable generation adds another layer of complexity to the existing problem: uncertainty. Weather-dependent renewable energy production is uncertain. Therefore, the renewable units cannot be dispatched as conventional units. On the other hand, an efficient use of this energy resource is desired due to its small marginal cost. Therefore, an appropriate clearing model to facilitate the integration of renewable production is required.

From the market operator point of view, the decision making problem is to determine optimal power productions and clearing prices in the presence of non-convexities and uncertainties.

In the context above, the following questions arise:

- How should a clearing model be so that an efficient use of resources is obtained in a market environment under uncertainty?
- How should a pricing scheme be designed to facilitate the operation of the power system in the presence of uncertainty?
- How does uncertainty affect the cost-recovery conditions of producers?
- What is the impact of uncertainty on a pricing scheme with cost-recovery features?

Another facet of managing electricity markets under uncertainty is flexibility. Flexibility is the ability of generating units and demands to be scheduled by the system operator with some degree of freedom. Demand flexibility in form of demand response has gained attention as one of the effective mechanism to facilitate the integration of uncertain renewable production [44]. The operational flexibility of demands and units allows the system operator to adapt them in order to absorb renewable productions to the largest extent, which generally results in reduced cost. Therefore, systems with a high penetration of renewable production generally move toward adopting fast-ramping units and flexible demands. That is, future markets may include comparatively cheap renewable units, comparatively costly fast-ramping units, and flexible demands. In this context, the following questions arise:

- What are the impacts of demand flexibility on the operational and economic dimensions of electricity markets?
- How does demand flexibility facilitate the operation of the power system with uncertain renewable generation?
- Is being flexible advantageous for demands?

The issues thus-far considered are problems faced by an operator in a centrally dispatched market. Next, we turn the view to a self-dispatched market organization, and focus on a uncertainty management problem from the Swiss reserve market. In Switzerland, as in other European countries, the system operator procures the required amount of reserves prior to real-time operation. The reserve market consists of two different market segments with gate closures one week ahead and two days prior to real-time operation (i.e., weekly and daily reserve markets, respectively). Therefore, the decision-making problem of the system operator is to identify which quantity of reserves to purchase in the weekly reserve market and which quantity to procure in the daily reserve market. In this context, the main question is:

- What is an appropriate decision-making model to assist the system operator to procure the *right* quantity of reserve in each reserve market?

This thesis seeks to answer the questions above by providing appropriate models and comprehensive analyses.

1.2 Market Operations

The questions above can be grouped under one umbrella: *market operations under uncertainty*. Market operations include operational aspects involving scheduling problems (i.e., scheduling power productions, scheduling reserves, and scheduling demands) and economic aspects consisting of pricing schemes, producers profits, and consumer payments.

To address the above operation challenges, the problems addressed in this thesis are the following:

- **Multi-Stage Stochastic Market-Clearing Model**

  To obtain efficient market outcomes in the presence of uncertain renewable generation and an increasing number of intra-day markets, we propose a multi-stage clearing model involving the day-ahead market, a number of intra-day markets, and real-time operation. Considering that the two major facets of a market-clearing model are the scheduling problem and the pricing problem, our focus here is the scheduling problem.

- **Pricing Schemes Pertaining to a Stochastic Non-Convex Market-Clearing Model**

  The other facet of a clearing model is the pricing problem. The non-convexities of the stochastic clearing model raise the problem of cost recovery of producers. The uncertainty associated with renewable production adds an additional layer of complexity. We design a pricing model to enforce cost-recovery conditions of producers in a non-convex stochastic market model with imperfect information of renewable production.

- **Economic Impact of Flexible Demands**

  We consider a system with a high penetration of renewable power production and a large-scale flexibility provided by fast-ramping units and flexible demands, as the system in Texas or in Spain. We incorporate demand flexibility in the clearing model, and investigate whether being flexible under marginal pricing is advantageous for demands.

- **Reserve scheduling in the reserve market**

  In the context of a self-dispatch market (with separated energy and reserve markets) in the presence of non-convexity and uncertainty, a system operator may face a decision dilemma for procuring reserves if there exist multiple reserve markets with different gate closures in different points in time. An example of such a market structure is the Swiss reserve market, where the operator may procure reserves in a weekly reserve market and/or a daily one. We propose a two-stage stochastic clearing model appropriately including imperfect market information to identify the best reserve procurement strategy.

1.3 Literature Review

1.3.1 Methodology: Stochastic programming

To address market operation problems under uncertainty, the method used in this thesis is stochastic programming.

Important decisions within an electricity market involve a significant level of uncertainty. To tackle decision-making problems under uncertainty, stochastic programming is an appropriate framework. Stochastic programming models decision-making problems by considering plausible realizations of the uncertain parameters. Therefore, the solution obtained balances all these future realizations.

The major drawback of stochastic programming is the dependency of problem size on the number of scenarios modeling uncertain parameters. On one hand, a high number of scenarios models uncertain parameters in an accurate fashion, but on the other hand, this results in a high number of variables and constraints, which may lead to computational intractability.

The basics and principles of stochastic programming can be found in [4], [17], and [67]. The fundamentals of stochastic programming along with the relevant applications in electricity markets are comprehensively discussed in [14].

When applying a stochastic programming framework to a problem, two relevant questions arises:

1. Why do we use a stochastic approach with high computation efforts instead of a deterministic one, where the uncertain parameters are replaced by their expected values?
2. How much do we gain by improving the scenarios selected to represent the uncertain parameters?

To address the first question, the Value of the Stochastic Solution (VSS) is the relevant metric [4] and [22]. The VSS is the difference between the optimal objective function computed by a stochastic approach and the one computed by a counterpart deterministic one. Therefore, the VSS quantifies the economic advantage of using a stochastic approach over a deterministic one. The Expected Value of Perfect Information (EVPI) is the metric used to answer the second question [4]. The EVPI quantifies how much a decision maker is willing to pay for obtaining perfect information about future, and it is computed as the difference between the optimal value of objective function obtained from a stochastic approach and the optimal objective function of a scenario-dependent instance of the same problem.

A relevant topic within stochastic programming framework is risk. References [37], [57], [60], and [55] provide the risk definition to control the variability associated to uncertain variables in decision-making problems.

Since scenarios are used to represent the uncertain parameters, it is important to consider an adequate number of representative scenarios. In this context, scenario generation techniques ([19], [30], and [42]) and scenario reduction techniques ([20], [25], and [41]) are relevant.

1.3.2 Market Operations: Scheduling of Energy and Reserves

From a market-clearing point of view, it is widely accepted that co-optimizing energy and reserves is the most appropriate scheduling approach. A number of relevant references are provided in the following.

Reference [9] formulates a stochastic security-constrained multi-period electricity clearing problem. Using the same concept, [8] formulates a two-stage stochastic clearing problem, where wind power variability and demand forecast error are the uncertain parameters. Reference [23] applies stochastic programming to an electricity market to schedule energy and reserves, where balance power is considered during primary, secondary and tertiary regulation intervals. Reference [70] proposes a stochastic model to clear the day-ahead market by solving the unit commitment problem as a master problem and wind scenarios as sub-problems. In [40], a stochastic clearing model is proposed to determine the optimal quantity and the costs of spinning and non-spinning reserves in a power system with a high penetration of wind production. Reference [66] considers a system with wind generation and shows the clear advantages of using a stochastic market-clearing model instead of a deterministic one, as the proposed stochastic model results in a less costly and better performing schedules than those of the deterministic model. In [52], a two-stage stochastic unit commitment model is proposed to determine the reserve requirements in a power system with a high penetration of wind power output. This reference suggests a method to generate and to rank scenarios representing wind power output using criteria that capture typical wind behavior. Also, [48] assesses spinning reserve requirements in systems with significant wind power production. Reference [18] proposes a probabilistic method based on empirical load and wind forecast data to quantify reserve requirements in systems with a high wind power production.

All these references mainly focuses on modeling the day-ahead market and real-time operation. However, actual electricity markets have evolved to include intra-day markets [43] and [21]. The structures of intra-day markets differ across the countries. While European intra-day markets relay on continuous trade principles [21], a centralized market-clearing mechanism is in favor of the system operators in the US [26]. Reference [32] highlights the value of intra-day markets in managing wind power uncertainty in competitive electricity markets. This paper, however, does not explicitly model the day-ahead and intra-day market constraints, and therefore, the subsequent prices are missed.

1.3.3 Market Operations: Pricing

It is widely recognized that a non-convex market equilibrium with linear prices [1] may not exist [11]. Many proposed solutions try to *get close* to a convex problem where marginal prices exist.

In the context of *getting close* to a convex problem, [46] proposes to fix the integer decisions at their optimal values obtained from the mixed-integer model, and to derive prices from the resulting continuous problem. An uplift is then paid to each producer incurring losses under these prices. Since uplifts are discriminatory, alternative methods may be desirable. In this context and in a deterministic setting, [59] proposes to obtain prices from a problem whose objective is to minimize the duality gap of the primal problem and dual problem of a relaxed versions of the original primal problem while enforcing primal, dual, integrity and cost recovery constraints. Minimizing the duality gap is a proxy for deviating in the least possible manner from maximum social welfare. An alternative approach is the convex hull pricing techniques that convexify the original market-clearing problem prior to solving it, [24], [68] and [69]. Note that the convex hull approach requires a convexification that is not unique. Thus, the resulting prices depend on the convexification technique selected. The semi-Lagrangean approach has similar issues. Reference [6] presents equilibrium prices composed of an energy price and an uplift charge based on the generation of a condition that supports optimal allocation. Reference [29] proposes a pricing approach based on a minimum uplift payment. Authors in [24] show that the prices proposed in [29] correspond to the optimal Lagrangean multipliers that are also equivalent to the slope of the best convex

[1] Under linear prices, all offers are financially settled at a single price per node (or per market area) and per time period; therefore, no financial losses occur given these linear prices.

dual function of the mixed-integer primal clearing model.

In the context of stochastic market-clearing models, [73] considers a linear model and shows that balancing prices are dual variables of the real-time market model once the wind power uncertainty is actualized, provided that first-stage variables (scheduled quantities) are fixed to their optimal values. This reference also shows that in the presence of uncertainty, cost recovery for producers is not trivial and proposes different settlement schemes based on the expectation of prices. Reference [38] develops a single-period network-constrained linear clearing model focusing on an *energy-only* market[2]. The explicit modeling of the market stages allows to obtain day-ahead and balancing prices. Reference [54] proposes a similar formulation, but allows different offers for energy and reserve deployment. However, this may constitute a gaming incentive for some producers. Both, references [38] and [54], discuss producer cost recovery in expectation.

To the best of our knowledge, no existing reference focuses on the pricing problem in stochastic non-convex electricity markets.

1.3.4 Market Operations: Demand Flexibility

Demand flexibility in form of demand response is recognized to be an effective mechanism for facilitating the integration of renewable production, as well as lowering volatility in market prices, [44] and [62]. Programs promoting demand flexibility in form of demand response are reviewed in [1]. Reference [35] provides an overview of recent regulations, policies, and the status of demand response in Europe.

The contribution of demands in providing flexibility from the system operator point of view is discussed in [33, 39, 75] and [74]. Reference [63] proposes a method for quantifying the effect of demand flexibility on the various categories of market participants.

Since centralized market mechanisms raise communication, computational and privacy issues, [51] proposes an algorithm that combines the optimal solution of centralized coordination problem with decentralized demand participation.

In the context of demand flexibility, dynamic pricing is a relevant topic, where demands are exposed to real-time prices instead of fixed tariffs, and therefore, encouraged to use their flexibility by modifying their consumption patterns [7] and [28]. Reference [28] identifies dynamic pricing as a priority for the implementation of wholesale electricity markets with demand response. However, reference [58] argues that increases in demand response and

[2] In an energy-only market, no unit commitment decisions are made, and thus, the problem is convex.

distributed generation may potentially lead to increased volatility.

Reference [15] proposes an optimization model to adjust the hourly load level of a given consumer in response to hourly electricity prices. Reference [65] proposes a dynamic pricing mechanism that explicitly encourages consumers to shift their peak load, and therefore, this mechanism has the potential to reduce the need for long-term investment in peaking plants.

1.4 Market Operations & Uncertainty Management

In this thesis, market operation problems are segmented into four categories, namely: (i) a multi-stage stochastic clearing model with the aim of obtaining informed day-ahead decisions, (ii) a pricing model addressing cost-recovery conditions of producers in the presence of non-convexities and uncertainty, (iii) insightful analyses on the impact of demand flexibility on the operational and economic aspects of the power system operation, and (iv) a two-stage clearing model for reserve markets in a self-dispatch market organization.

In the rest of this section, we summarize these problems.

- **Multi-stage stochastic clearing model**

  Observing the actual electricity markets, two major factors affect energy trade: a large amount of renewable production and the evolution of markets to include intra-day trading. These factors motivate a revision of the day-ahead clearing approaches.

  We develop a day-ahead clearing model by formulating a multi-stage stochastic programming problem, where the first stage represents the day-ahead market, n additional stages model n intra-day markets, and the last-stage stands for real-time operation. We showcase the performance of the proposed model by applying it to an illustrative example and larger case studies, and benchmark it against the market outcomes obtained from a two-stage stochastic clearing counterpart.

- **Pricing schemes pertaining to a stochastic non-convex market-clearing model**

  Pricing problem is one of the issues inherent to the non-convex nature of the power system. In actual electricity markets, marginal prices are obtained from a linear representative of the actual non-convex clearing model. These marginal prices may only reflect the marginal production cost of energy and not costs pertaining to non-convex decisions such as fixed start-up costs. In such situations, some producers may incur losses and may eventually leave the market. Therefore, the notion of clearing prices with cost-recovery features are considered. In the presence of uncertain renewable production, the definition of cost recovery conditions is not trivial.

We approach this problem by formulating a stochastic non-convex clearing model. Next, we develop a model which guarantees cost-recovery conditions for producers. This model minimizes the duality gap of the stochastic non-convex model and the dual problem of a relaxed version of that model subject to primal constraints, dual constraints, cost-recovery constraints, and integrity constraints. The proposed model is benchmarked against the standard marginal pricing model through a simple example as well as larger case studies.

- **Economic impact of flexible demands**

  This problem focuses on the role of flexible demands in a market with uncertain wind production. While the main stream research enumerates a number of advantages arising from demand flexibility, we take a closer look at the economic impacts of flexible demands: how market prices are affected and what economic consequences are observed.

  We approach the problem by incorporating flexible demands in a stochastic clearing model, where the source of uncertainty is renewable power production. We consider a flexible system with a number of flexible fast-ramping units which are able to react to the uncertainty pertaining to renewable power production. In this market context, we investigate the impact of flexible demands on marginal prices, operation cost, and consumer payment, and compare these outcomes with those pertaining to a case with inflexible demands.

- **Stochastic clearing model for the reserve market**

  In the context of self-dispatch markets with separated energy and reserve market, we present a reserve scheduling problem motivated by the actual reserve market in Switzerland.

  The sequence of the Swiss reserve market includes a weekly market with a gate closure one week ahead of real-time operation and a daily market with a gate closure two-days ahead of real-time operation. The system operator should decide on the amount of reserves to procure in each reserve market.

  We propose a risk-neutral and a risk-averse stochastic clearing model, where the source of uncertainty is the future reserve offers in the daily market. We showcase the clear advantages of the proposed stochastic models as compared to a deterministic model (used in practice) through real cases from the Swiss reserve market.

1.5 Thesis Objectives

In the crossroad of market operations and uncertainty management, this dissertation aims to provide appropriate models to assist the system operator to make informed decisions.

The scope of the thesis is on short-term electricity markets and embraces the daily operation of the power system.

Addressing the market operation problems, previously described, leads to the development of models including a scheduling model and a pricing model, the economic assessment of demand flexibility, and finally, the design and implementation of a reserve-clearing model.

In the following, we elaborate on specific objectives of these models.

1.5.1 Objectives for the Multi-Stage Market-Clearing Model

The specific objectives for the scheduling model are:

- To develop a day-ahead clearing model which considers a number of intra-day markets and uncertain renewable production.
- To formulate the clearing model, described in the previous item, as a multi-stage stochastic programming problem, where the first stage models the day-ahead market, n stages represent n intra-day markets, and a final stage stands for the real-time operation.
- To benchmark the proposed model against a two-stage stochastic model by comparing the market outcomes, the Value of the Stochastic Solution (VSS), and computation time using illustrative examples and larger case studies.

1.5.2 Objectives for the Pricing Scheme Pertaining to a Stochastic Non-Convex Market-Clearing Model

The specific objectives for the pricing model are:

- To develop a pricing scheme for a stochastic non-convex clearing model, where prices shall guarantee cost-recovery conditions for units in the presence of uncertain renewable production.
- To define and formulate cost-recovery conditions of producers in the presence of uncertainty pertaining to renewable production.

- To formulate a novel nonlinear optimization problem which minimizes the gap of the stochastic clearing model and its dual subject to the market and the operation constraints, dual constraints, and cost-recovery constraints.
- To obtain a computationally tractable model of the nonlinear optimization problem, described in the previous item.
- To benchmark the outcomes of the proposed model against the conventional approach using illustrative examples and larger case studies.

1.5.3 Objectives for the Economic Impact of Flexible Demands

The specific objectives related to the impact assessment of flexible demands are:

- To investigate the overall economic impact of large-scale flexible demands, particularly their impact on marginal prices, in a system with flexible units and uncertain renewable production, such as those in Texas and Spain.
- To adapt a two-stage stochastic clearing model to consider demand flexibility.

1.5.4 Objectives for Stochastic Reserve Clearing Model

The specific objectives for the reserve clearing model are:

- To develop a new clearing approach with a focus on the structure of Swiss reserve market.
- To formulate a two-stage stochastic MILP model for clearing the reserve market, described in the previous point, where the first stage represents the weekly reserve market and the second stage stands for the daily reserve market.
- To formulate a risk-averse version of the two-stage model described in the previous item.
- To characterize uncertain offers in the daily market and represent them via scenarios.
- To provide the results using real cases from the Swiss reserve market.

1.6 Thesis Outline

The outline of the thesis is as follows:

Chapter 1 provides an introduction to this dissertation. First, we motivate the problems addressed in this dissertation by reviewing some of the existing challenges in electricity markets. Next, we outline the problems addressed in this thesis. Then, we provide a general overview of the literature relevant to the problems considered in this dissertation. Finally, the approaches and objectives of this thesis are outlined.

Chapter 2 proposes a scheduling model for a system with uncertain power production. If two major facets of a clearing model are considered to be scheduling (technical aspect) and pricing (economic aspect), this chapter focuses on the scheduling problem. The model is formulated as a three-stage stochastic programming problem, where the first stage represents the day-ahead market, the second stage the intra-day market, and the third-stage the real-time operation. We showcase the performance of this model by applying it to an illustrative example and larger case studies, and benchmark it against the market outcomes obtained from a two-stage stochastic market-clearing model.

Chapter 3 proposes pricing methodologies which guarantee cost recovery for units in the presence of non-convexities and uncertainty. Considering two major facets of a clearing model, i.e., scheduling and pricing, this chapter focuses on pricing. The proposed models minimize the duality gap of a stochastic non-convex clearing primal model and the dual problem of a relaxed version of the original primal model subject to primal constraints, dual constraints, cost-recovery constraints, and integrity constraints. The cost-recovery constraints make the proposed problem nonlinear with bi-linear terms. For computational tractability, this problem is linearized and recast as a MILP problem. The proposed models are applied to an illustrative example and larger case studies, and benchmarked against a standard marginal pricing model.

Chapter 4 incorporates flexible demands to a two-stage stochastic market-clearing model, where demand consumption level can be scheduled to some extent by the system operator. The uncertainty related to wind power production is represented via scenarios. We analyze the economic impacts of flexible demands in a system consisting of a generation-mix of comparatively expensive fast-ramping units and comparatively cheap renewable units, which resembles the case of Texas and Spain. The economic assessment of flexible demands include their impacts on operation costs, day-ahead prices, and consequently, consumer payments and producer profits. This assessment is done using a small example and larger case studies.

Chapter 5 develops a two-stage MILP model for the Swiss reserve market. The first stage represents the weekly reserve market, and the second stage the daily reserve market. The first-stage variables denote decisions for the acceptance or rejection of indivisible offers in the weekly reserve market, while the second-stage variables are the quantity of reserves to be procured in the daily market. The decision-making problem is to minimize the expected procurement cost of reserves considering the known offers in the weekly market and the unknown offers in the daily market. We characterize uncertain offers and represent them via scenarios. The results obtained from the implementation of the developed model in the Swiss reserve market are provided. A risk-averse version of the developed model is also formulated and tested.

Chapter 6 provides a summary of the work developed in this thesis accompanied with main conclusions and contributions. Also, some suggestions for future research are listed in this chapter.

Appendix A provides some notions related to a multi-stage stochastic programming.

Appendix B provides the technical characteristics of the IEEE 24-node system used in the case studies of Chapters 2, 3, and 4.

Appendix C provides the mathematical description of minimum up- and down-time constraints pertaining to the operation conditions of generating units.

2 Multi-Stage Stochastic Market-Clearing Model

2.1 Introduction

Since the start of the liberalization in the electricity industry in the 90s, the electricity trade has been subject to short-term transactions in the form of pools dealing with daily operations, and future markets pertaining to mid-term and long-term transactions.

The scope of this chapter is short-term pool-based markets, where electricity is traded in a day-ahead market, in a number of intra-day markets (also known as adjustment markets), as well as in real-time operation.

Traditionally, a pool includes a day-ahead market and a real-time one. In the day-ahead market the on-off status of units and their scheduled production levels are determined considering day-ahead forecasts. In real-time operation, there is a need to compensate mismatches between consumption and production in order to preserve the power balance in the system. For this purpose, reserves are scheduled in the day-ahead market to be eventually deployed in real-time operation. In a system with conventional units, the amount of reserves can be easily determined by considering the factors influencing supply-demand mismatch, such as deviation between the day-ahead load forecast and the actual load, the probability of failure of generating units, etc. From an energy trade perspective, conventional units can be scheduled one day in advance without the need for adjusting their scheduled production levels, and hence, there is usually no need for an extra trading floor between the day-ahead market and the real-time power delivery. Therefore, pools consisting of a day-ahead market and a real-time one fit well a system with conventional units. However, the boom in renewable production challenges this traditional setting.

In the day-ahead market, where scheduling is done, the production ability of renewable units is still uncertain, as renewable power production depends on weather, whose day-ahead forecast still deviates from its actual value. Moving toward real-time operation, a better forecast of weather conditions becomes available that results in a more precise forecast of the renewable power production. Therefore, electricity trades in a horizon between the day-ahead market and real-time operation facilitate the integration of renewable production.

In practice, electricity markets have been evolving to include intra-day trades, where scheduled production levels in the day-ahead market can be adjusted using the best available information related to weather conditions, and thus, renewable production. The intra-day markets facilitate the integration of renewable production as they give renewable units the opportunity of offering closer to power delivery, and thus, with reduced uncertainty [43] and [32].

The structures of intra-day markets differ on both sides of the Atlantic. While European intra-day markets rely on continuous trade principles (i.e., first come, first serve [21]), a centralized market-clearing mechanism is in favor in the US [26]. The gate closure of intra-day markets may vary from several hours to an hour ahead of power delivery. Also, their clearing horizon may include the whole 24 hours or only some hours [45].

While intra-day markets become the norm, actual clearing processes still rely on deterministic models, which are not suitable for systems with a large amount of renewable production. In such systems, a deterministic model generally results in either under-commitment, which is risky, or over-commitment, which is expensive.

As a solution to deal with uncertain renewable production, mainstream research proposes to apply two-stage stochastic programming framework to the traditional market structure, consisting of the day-ahead market and real-time operation. However, consideration of intra-day markets and their mathematical descriptions in clearing models are missing.

Therefore, the evolving market conditions, involving an increasing number of intra-day markets and large amounts of uncertain renewable production, call for a revision in clearing models.

Since our aim is to take informed day-ahead decisions in a trading environment with an increasing number of intra-day markets and a large amount of renewable production, we believe that the transient from a deterministic clearing model to a stochastic one should be a multi-stage clearing model, and not a two-stage one. The corresponding decision-making processes are described in the following.

2.2 Decision-Making Process and Scenario Tree

In a stochastic programming framework, uncertain parameters are represented by a number of scenarios in the form of a scenario tree. A scenario tree schematically describes the decision-making process in term of the sequence of decisions and the order in which uncertainty unfolds. Each stage corresponds to a point in time where a decision has to be made, and it is represented by a node in the scenario tree. The decision points (i.e, stages) are connected through branches, which represent realizations of uncertain parameters. The mathematical description of a multi-stage stochastic programming problem is provided in Appendix A.1.

In an electricity market consisting of a day-ahead market, n number of intra-day markets, and a real-time one, each stage corresponds to a market. That is, the first stage represents the day-ahead market (the decision point for the day-ahead scheduled productions), n stages model n intra-day markets (the decision points for schedule adjustments), and a final stage stands for real-time operation, where uncertain renewable production realizes, and therefore, the balancing actions (i.e., deployed reserves) are taken. The corresponding scenario tree is shown in Fig. 2.1.

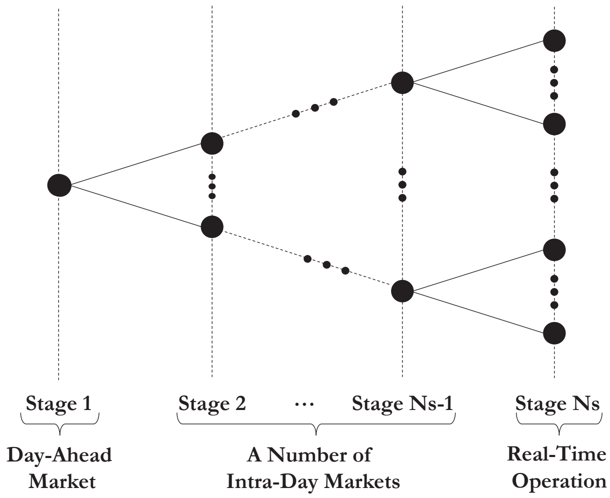

Figure 2.1 – Scenario tree for a multi-stage decision-making process

We consider a market structure including a day-ahead market settling 24 hourly-based schedules with a gate closure in day *d-1*, an intra-day market settling 24 hourly-based adjustments with a gate closure usually several hours ahead of power delivery, and real-time operation. Thus, corresponding to each time period t in day d, there are three points in time when the operator makes a decision: the scheduling decision in the day-ahead market with a gate closure in day *d-1*, the adjustment decision in the intra-day market with a gate closure several hours ahead of power delivery (in day *d-1*), and the deployed reserve decision in real time.

In this context, we propose a three-stage stochastic model, as an instance of a multi-stage stochastic model, to clear the day-ahead market, where uncertainty stems from stochastic renewable generation. The stochastic clearing process includes the first stage representing the day-ahead market, the second stage modeling the intra-day market, and the third stage standing for real-time operation. Therefore, the day-ahead schedules are decided with a detailed prognosis of the future, which includes the intra-day market and real-time operation.

As previously mentioned, a common two-stage model proposed by mainstream research includes the day-ahead market and real-time operation, and does not consider the intra-day market.

The scenario trees corresponding to the three-stage, described above, and its two-stage counterpart are shown in Fig. 2.2.

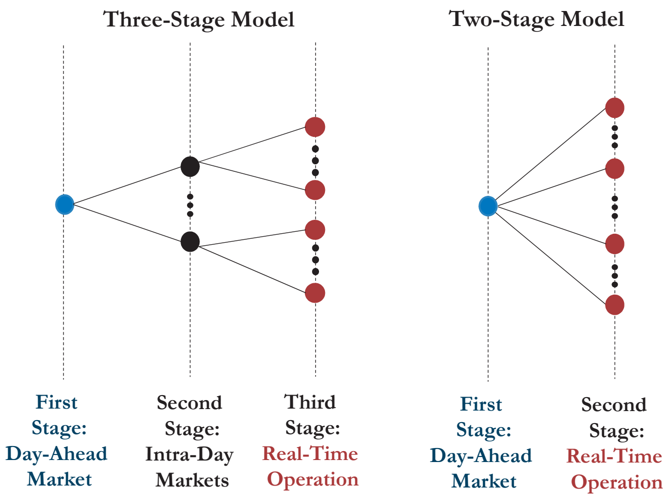

Figure 2.2 – Scenario trees for the three-stage market-clearing model and its two-stage counterpart

Fig. 2.3 depicts an example of a scenario tree corresponding to the three-stage model with two scenarios in the second stage and for each second-stage scenario three scenarios in the third stage. We can see that scenarios ω_1, ω_2, and ω_3 have a common history until the second stage, and thereafter they are represented by different paths. The same observation is valid for scenarios ω_4, ω_5, and ω_6. Therefore, each scenario represents a path from the day-ahead market (the root node) to the real-time operation (the leaf nodes). This is mathematically modeled through *non-anticipativity* constraints, which are mathematically explained in Section 2.4.1.

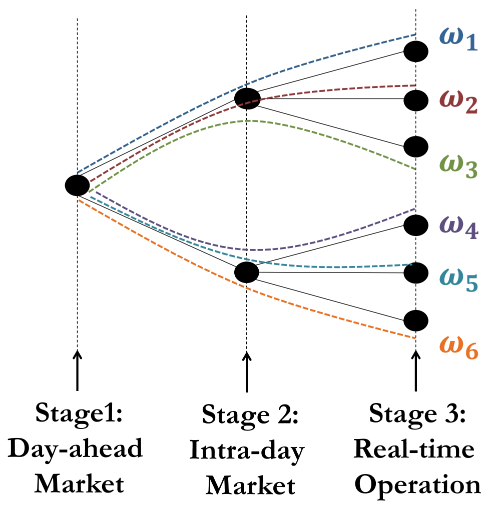

Figure 2.3 – Scenario tree and scenario paths (dashed lines) for a three-stage market-clearing model

2.3 Assumptions

For simplicity and computational tractability, we consider the following assumptions to formulate the three-stage market-clearing model.

- The uncertain renewable resource is wind power generation. The wind generation leads renewable production in term of installed capacity and technological development [31]. Considering other stochastic resources does not change the nature of the model proposed.

- The production of wind units depends on the uncertain wind power output. Wind power production is represented using scenarios. These scenarios are built using historical wind production data as samples without applying any scenario generation/reduction techniques.

- The wind producers are assumed to offer their production at a comparatively small marginal cost.

- A linear representation of the transmission network is considered through a dc load flow model and losses are neglected. The simultaneous consideration of on/off decisions, stochasticity and an ac power flow model leads severally to intractability of the optimization problem.

- We do not consider security criteria, such as n-1, to focus on the treatment of wind uncertainty, and also, to avoid an increase in the size of the model which consequently leads to an increase in computation time.

- All generating units are required to offer energy at marginal cost. This is in line with competitive markets, where market players do not have incentive to offer a price different from their marginal production cost under a marginal pricing scheme. Also, generation cost functions are assumed to be linear for simplicity.
- The costs of the deployed reserves (i.e., balancing energy) is assumed to be equal to the cost of producing energy.
- The stochastic clearing model co-optimizes energy and reserve deployment without explicit reserve offers in the day-ahead market. Units and flexible demands can specify the reserve levels that they are willing to provide, and hence, they are given the opportunity of reserve deployment for a profit.
- Loads are assumed to be inelastic. This assumption is for the sake of simplicity, and can easily be modified by including demands as variables with appropriate utility functions.
- We assume that loads are deterministic. This assumption allows focusing on wind uncertainty. Note that in systems with stochastic wind power production, load variability is generally small in comparison with wind uncertainty.
- Non-convexities considered are solely those due to non-zero minimum power outputs of conventional units and start-up costs. Taking into account other source of non-convexities, such as shut-down costs and minimum up/down time constraints, is straightforward.

2.4 Model Description

In this section, we provide mathematical descriptions of a three-stage clearing model, as well as its two-stage counterpart.

2.4.1 Three-stage Stochastic Clearing Model

The proposed three-stage clearing model seeks to find optimal power production schedules of units, their adjustments, and deployed reserves to minimize the expected cost while satisfying operational constraints.

Decision Variables

The decision variables are categorized into three groups:

- The first-stage decision variables are related to the day-ahead market before the realization of any scenario (actual wind power output). These variables are here-and-now decisions and include:
    - On/off commitment of each unit in each period (u_{it}, binary) and its related cost (C_{it}^{SU}, \$) at the day-ahead market.
    - Scheduled power output (production level) of each conventional unit in each period at the day-ahead market (P_{it}, [MW]).
    - Scheduled power output of each wind unit in each period at the day-ahead market (W_{qt}, [MW]).
    - Angle of each node in each period at the day-ahead market (θ_{nt}, [rad]).
- The second-stage decisions pertain to the intra-day market. They are wait-and-see decisions with respect to the day-ahead market and here-and-now regarding the real-time operation. These decisions are made after the scheduling stage is over and before the realization of any scenario in real-time operation.
    - Upward power adjustment of each conventional unit in each scenario and each period at the intra-day market ($\Delta P_{it\omega}^{\mathrm{U}}$, [MW]).
    - Downward power adjustment of each conventional unit in each scenario and each period at the intra-day market ($\Delta P_{it\omega}^{\mathrm{D}}$, [MW]).
    - Upward power adjustment of each wind unit in each scenario and each period at the intra-day market ($\Delta W_{qt\omega}^{\mathrm{U}}$, [MW]).
    - Downward power adjustment of each wind unit in each scenario and each period at the intra-day market ($\Delta W_{qt\omega}^{\mathrm{D}}$, [MW]).
    - Angle of each node in each scenario and each period at the intra-day market ($\theta_{nt\omega}^{\mathrm{S_2}}$, [rad]).
- The third-stage decision variables are made after the realization of the uncertain wind production in real-time operation. They represent recourse actions compensating for the actual wind power output, and thus, constitute wait-and-see decisions, and are defined for each single scenario considered in the third stage:
    - Deployed up reserve of each conventional unit in each scenario and each period in real-time operation ($r_{it\omega}^{\mathrm{U}}$, [MW]).
    - Deployed down reserve of each conventional unit in each scenario and each period in real-time operation ($r_{it\omega}^{\mathrm{D}}$, [MW]).

- Angle of each node in each scenario and each period in real-time operation ($\theta^{S_3}_{nt\omega}$, [rad]).
- Wind power spillage of each wind unit in each scenario and each period in real-time operation ($w^{\text{spill}}_{qt\omega}$, [MW]).
- Involuntarily load shedding of each load in each scenario and each period in real-time operation ($L^{\text{shed}}_{jt\omega}$, [MW]).

We should note that ω represents a scenario path, as previously described in Section 2.2 and illustrated in Fig. 2.3. Taking the scenario path into account, instead of separately considering second-stage and third-stage scenarios, helps to clarify the mathematical formulation, as the scenarios of the second stage and the scenarios of the third stage do not have to be denoted differently.

Objective Function

The objective function consists of three terms pertaining to the cost in the day-ahead market, the expected cost in the intra-day market, and the expected balancing cost in real-time operation:

- The day-ahead cost includes the start-up cost and production costs of conventional units, as well as the production cost of wind units over all periods of the market horizon:

$$\sum_{t=1}^{N_T}\Big[\sum_{i=1}^{N_G}[C^{\text{SU}}_{it}+C_iP_{it}]+\sum_{q=1}^{N_Q}C_qW_{qt}\Big] \tag{2.1}$$

- The expected intra-day cost results from the adjustments of day-ahead scheduled productions of conventional units as well as wind units in the intra-day market. Since schedule adjustments depend on the wind power output represented by scenarios, the intra-day cost depends on scenarios:

$$\sum_{t=1}^{N_T}\sum_{\omega=1}^{N_\Omega}\pi_\omega\Big[\sum_{i=1}^{N_G}C_i(\Delta P^{\text{U}}_{it\omega}-\Delta P^{\text{D}}_{it\omega})+\sum_{q=1}^{N_Q}C_q(\Delta W^{\text{U}}_{qt\omega}-\Delta W^{\text{D}}_{qt\omega})\Big] \tag{2.2}$$

- The expected balancing cost results from the deployed reserves (first term in equation (2.3)), actual wind power output and its spillage (second term in equation (2.3)), and involuntary load shedding (third term in equation (2.3)) in real-time operation. The expected balancing cost also depends on scenarios representing wind power output, as the third-stage decisions compensate for the realization of the wind power production:

$$\sum_{t=1}^{N_T}\sum_{\omega=1}^{N_\Omega}\pi_\omega\big[\sum_{i=1}^{N_G}C_i(r^{\mathrm{U}}_{it\omega}-r^{\mathrm{D}}_{it\omega})+\sum_{q=1}^{N_Q}C_q(W^{\mathrm{RT}}_{qt\omega}-W_q-\Delta W^{\mathrm{U}}_{qt\omega}+\Delta W^{\mathrm{D}}_{qt\omega}-w^{\mathrm{spill}}_{qt\omega})$$
$$+\sum_{j=1}^{N_L}V^{\mathrm{LOL}}_{jt}L^{\mathrm{shed}}_{jt\omega}\big] \tag{2.3}$$

The summation of these cost components results in the total cost. The objective of the three-stage clearing model is to minimize this cost, as expressed by (2.4).

$$\underset{\Xi_{3s}}{\text{Minimize}}$$
$$\sum_{t=1}^{N_T}\left[\sum_{i=1}^{N_G}C^{\mathrm{SU}}_{it}+\sum_{\omega=1}^{N_\Omega}\pi_\omega\Big[\sum_{i=1}^{N_G}C_i(P_{it}+\Delta P^{\mathrm{U}}_{it\omega}-\Delta P^{\mathrm{D}}_{it\omega}+r^{\mathrm{U}}_{it\omega}-r^{\mathrm{D}}_{it\omega})+\sum_{q=1}^{N_Q}C_q(W^{\mathrm{RT}}_{qt\omega}-w^{\mathrm{spill}}_{qt\omega})\right.$$
$$\left.+\sum_{j=1}^{N_L}V^{\mathrm{LOL}}_{jt}L^{\mathrm{shed}}_{jt\omega}\Big]\right] \tag{2.4}$$

The minimization is over the set of variables $\Xi_{3s}=\{C^{\mathrm{SU}}_{it},u_{it},P_{it},\forall i,\forall t;W_{qt},\forall q,\forall t;\theta_{nt},\forall n,\forall t;$ $\Delta P^{\mathrm{U}}_{it\omega},\Delta P^{\mathrm{D}}_{it\omega},\forall i,\forall t,\forall\omega;\Delta W^{\mathrm{U}}_{qt\omega},\Delta W^{\mathrm{D}}_{qt\omega},\forall q,\forall t,\forall\omega;r^{\mathrm{U}}_{it\omega},r^{\mathrm{D}}_{it\omega},\forall i,\forall t,\forall\omega;w^{\mathrm{spill}}_{qt\omega},\forall q,\forall t,\forall\omega;\theta^{s_2}_{nt\omega},$ $\theta^{s_3}_{nt\omega},\forall n,\forall t,\forall\omega;L^{\mathrm{shed}}_{jt\omega},\forall j,\forall t,\forall\omega\}$, as described in Section 2.4.1.

We note here that reserve offer prices are not considered in the objective function. We allow units to indicate their reserve levels (MW) that they are willing to provide, thus give them the opportunity of reserve deployment for a profit.

Constraints

There are four categories of constraints: the constraints pertaining to the day-ahead market, those accounting for the intra-day market, the constraints representing the real-time operation, and finally, the non-anticipativity constraints implying that decisions must be equal if the realizations of stochastic parameter are equal.

First-Stage Constraints (Day-ahead Market):

Any market seeks to balance supply and demand. In power systems with a large amount of stochastic wind generation, a share of the energy supply is uncertain at the scheduling stage occurring in the day-ahead market. This implies that the day-ahead scheduled productions (first-stage decisions) shall account for the impact of uncertain wind power production. Therefore, units shall be scheduled such that the power system is able to absorb actual wind power output at minimum cost.

We represent the contribution of wind unit q in the power balance equation at the day-ahead market through variable W_{qt}, and formulate the power balance equation for each node n and period t as follows:

$$\sum_{i\in M_n^{\mathrm{G}}} P_{it} + \sum_{q\in M_n^{\mathrm{Q}}} W_{qt} - \sum_{j\in M_n^{\mathrm{L}}} L_{jt} - \sum_{r\in\Lambda_n} B_{nr}(\theta_{nt}-\theta_{rt}) = 0, \quad \forall n, \forall t \tag{2.5}$$

The term $\sum_{r\in\Lambda_n} B_{nr}(\theta_{nt}-\theta_{rt})$ represents the power flows (dc model) between node n and the nodes connected to it, denoted by $r\in\Lambda_n$, at period t.

The production level of conventional units is limited by their minimum and maximum power output:

$$u_{it}P_i^{\min} \le P_{it} \le u_{it}P_i^{\max}, \quad \forall i, \forall t \tag{2.6}$$

The wind production is also bounded within a range. We consider coefficients α^{WDs_1} and α^{WUs_1} to specify the limits of wind production with respect to its best available day-ahead forecast W_{qt}^{DA}:

$$\alpha^{\mathrm{WDs}_1} W_{qt}^{\mathrm{DA}} \le W_{qt} \le \alpha^{\mathrm{WUs}_1} W_{qt}^{\mathrm{DA}}, \quad \forall q, \forall t \tag{2.7}$$

In the objective function (2.4), the start-up cost of conventional units C_{it}^{SU} is one of the cost terms in the day-ahead market. This cost results from a change in the status of a conventional unit and is modeled using the commitment variable u_{it} and the start-up cost K_i^{SU} as follows:

$$K_i^{\mathrm{SU}}(u_{it}-u_{i,t-1}) \le C_{it}^{\mathrm{SU}}, \quad \forall i, \forall t \tag{2.8}$$

$$C_{it}^{\mathrm{SU}} \ge 0, \quad \forall i, \forall t \tag{2.9}$$

$$u_{it} \in \{0,1\}, \quad \forall i, \forall t \tag{2.10}$$

Equations (2.8) and (2.9) enforce that variable C_{it}^{SU} equals either zero or the start-up cost K_i^{SU}.

Other technical constraints that must be considered at the day-ahead market are the ramp limits of generators. In a multi-period model, the scheduled production of a unit over the periods shall respect its minimum and maximum ramping limits, denoted by RD_i and RU_i respectively:

$$RD_i \le P_{it} - P_{i,t-1} \le RU_i, \quad \forall i, \forall t \tag{2.11}$$

Finally, the slack bus is considered to be node 1:

$$\theta_{1t} = 0, \quad \forall t \tag{2.12}$$

Second-Stage Constraints (Intra-day Market):

The second-stage constraints include the constraints modeling the intra-day market and involve variables pertaining to adjustments of day-ahead scheduled productions of units (i.e., conventional units as well as wind units).

The intra-day market allows upward or downward power adjustments in order to adopt to the best available forecast of wind power output $W^{\mathrm{ID}}_{qt\omega}$ in each scenario. Therefore, the second-stage constraints are defined for each scenario.

Given the best available forecast of wind power output $W^{\mathrm{ID}}_{qt\omega}$ and the wind scheduled production W_{qt} decided at the day-ahead market, a set of adjustment decisions (i.e., $\Delta P^{\mathrm{U}}_{it\omega}$, $\Delta P^{\mathrm{D}}_{it\omega}, \forall i, \forall t, \forall \omega$; $\Delta W^{\mathrm{U}}_{qt\omega}$, $\Delta W^{\mathrm{D}}_{qt\omega}, \forall q, \forall t, \forall \omega$) are made to compensate for wind changes of $W^{\mathrm{ID}}_{qt\omega} - W_{qt}$. The adjustment decisions shall respect the power balance in the system:

$$\begin{aligned}
&\sum_{i \in M^{\mathrm{G}}_n} \Delta P^{\mathrm{U}}_{it\omega} - \Delta P^{\mathrm{D}}_{it\omega} + \sum_{q \in M^{\mathrm{Q}}_n} W^{\mathrm{ID}}_{qt\omega} - W_{qt} - \Delta W^{\mathrm{U}}_{qt\omega} + \Delta W^{\mathrm{D}}_{qt\omega} \\
&- \sum_{r \in \Lambda_n} B_{nr}(\theta^{\mathrm{s}_2}_{nt\omega} - \theta^{\mathrm{s}_2}_{rt\omega} - \theta_{nt} + \theta_{rt}) = 0, \quad \forall n, \forall \omega, \forall t
\end{aligned} \tag{2.13}$$

We enforce that the day-ahead scheduled productions and their power adjustments satisfy generation capacity limits through equation (2.14). Also, we consider that power adjustments are limited to $\alpha_{\Delta P}$% of the maximum power output, as enforced by equations (2.15) and (2.16). A zero value of $\alpha_{\Delta P}$ means that there is no power adjustment possible in the intra-day market, and a value of 1 (or 100%) extends the power adjustments to full generation capacity, $P^{\max}_i$:

$$u_i P^{\min}_i \le P_{it} + \Delta P^{\mathrm{U}}_{it\omega} - \Delta P^{\mathrm{D}}_{it\omega} \le u_{it} P^{\max}_i, \quad \forall i, \forall \omega, \forall t \tag{2.14}$$

$$0 \le \Delta P^{\mathrm{U}}_{it\omega} \le \alpha_{\Delta P} P^{\max}_i, \quad \forall i, \forall \omega, \forall t \tag{2.15}$$

$$0 \le \Delta P^{\mathrm{D}}_{it\omega} \le \alpha_{\Delta P} P^{\max}_i, \quad \forall i, \forall \omega, \forall t \tag{2.16}$$

Constraint (2.17) enforces that the wind scheduled production adapted by their corresponding power adjustments stay within a range specified by a percentage of $W^{\mathrm{ID}}_{qt\omega}$. This range is not necessarily symmetric; hence, constants α^{WDs_2} and α^{WUs_2} are considered differently from each other in equation (2.17):

$$\alpha^{\mathrm{WDs_2}} W^{\mathrm{ID}}_{qt\omega} \le W_{qt} + \Delta W^{\mathrm{U}}_{qt\omega} - \Delta W^{\mathrm{D}}_{qt\omega} \le \alpha^{\mathrm{WUs_2}} W^{\mathrm{ID}}_{qt\omega}, \quad \forall q, \forall \omega, \forall t \tag{2.17}$$

For individual up and down power adjustments of each wind unit, we assume a limit prescribed by $\alpha_{\Delta W}$ % of installed capacity, as in (2.18) and (2.19). A zero value of $\alpha_{\Delta W}$ means that no power adjustments are possible for wind units in the intra-day market, and a value of 100% allows power adjustments to full installed capacity, $W^{\max}_q$:

$$0 \le \Delta W^{\mathrm{U}}_{qt\omega} \le \alpha_{\Delta W} W^{\max}_q, \quad \forall q, \forall \omega, \forall t \tag{2.18}$$

$$0 \le \Delta W^{\mathrm{D}}_{qt\omega} \le \alpha_{\Delta W} W^{\max}_q, \quad \forall q, \forall \omega, \forall t \tag{2.19}$$

The power scheduled for each unit modified by its adjustments shall respect the ramping limits:

$$RD_i \le \left(P_{it} + \Delta P^{\mathrm{U}}_{it\omega} - \Delta P^{\mathrm{D}}_{it\omega}\right) - \left(P_{i,t-1} + \Delta P^{\mathrm{U}}_{i,t-1,\omega} - \Delta P^{\mathrm{D}}_{i,t-1,\omega}\right) \le RU_i, \quad \forall i, \forall \omega, \forall t \tag{2.20}$$

Finally, the slack variable in node 1 is enforced by equation (2.21):

$$\theta^{\mathrm{s_2}}_{1t\omega} = 0 : \sigma_{1t\omega}, \quad \forall \omega, \forall t \tag{2.21}$$

Third-Stage Constraints (Real-Time Operation):

The third-stage constraints pertain to the actual power system operation in real time and involve the third-stage decisions made to balance the actual wind power output in real-time operation, which is modeled through scenarios. Hence, these constraints and decisions are defined per scenario.

Once the wind power output realizes in real-time operation, preserving the energy balance in the system necessitates to deploy upward or/and downward reserves, to spill wind power, and as a last measure, to eventually shed the load. The power balance in real-time operation is modeled through equation (2.22), where upward reserve deployment $r^{\mathrm{U}}_{it\omega}$, downward reserve deployment $r^{\mathrm{D}}_{it\omega}$, and wind spillage $w^{\mathrm{spill}}_{qt\omega}$ compensate for the actual wind power output $W^{\mathrm{RT}}_{qt\omega}$ considering the wind power scheduled in the day-ahead market, W_{qt}, and its adjustments in the intra-day stage, $\Delta W^{\mathrm{U}}_{qt\omega}$ and $\Delta W^{\mathrm{D}}_{qt\omega}$. Load shedding $L^{\mathrm{shed}}_{jt\omega}$ is the last resort to preserve the power balance in the system:

$$\sum_{q\in M_n^{\mathrm{Q}}} (W_{qt\omega}^{\mathrm{RT}} - W_{qt} - \Delta W_{qt\omega}^{\mathrm{U}} + \Delta W_{qt\omega}^{\mathrm{D}} - w_{qt\omega}^{\mathrm{spill}}) + \sum_{i\in M_n^{\mathrm{G}}} (r_{it\omega}^{\mathrm{U}} - r_{it\omega}^{\mathrm{D}})$$
$$- \sum_{r\in\Lambda_n} B_{nr}(\theta_{nt\omega}^{s_3} - \theta_{rt\omega}^{s_3} - \theta_{nt\omega}^{s_2} + \theta_{rt\omega}^{s_2}) + \sum_{j\in M_n^{\mathrm{L}}} L_{jt\omega}^{\mathrm{shed}} = 0, \quad \forall n, \forall\omega, \forall t \tag{2.22}$$

The term $B_{nr}(\theta_{nt\omega}^{s_3} - \theta_{rt\omega}^{s_3} - \theta_{nt\omega}^{s_2} + \theta_{rt\omega}^{s_2})$ models the power flow (dc approximation) through the line connecting nodes n and r per scenario ω. In each scenario, the power flow must be within thermal limits of each line. This is modeled through equation (2.23):

$$- f_{nr}^{\max} \le B_{nr}(\theta_{nt\omega}^{s_3} - \theta_{rt\omega}^{s_3}) \le f_{nr}^{\max}, \quad \forall n, \forall r \in \Lambda_n, \forall\omega, \forall t \tag{2.23}$$

Note that enforcing line limit constraints is not generally required in the day-ahead and intra-day markets. However, in real-time operation actual power flows must remain within the line limits in any realization of the wind power outputs.

Node 1 is set to be the reference node:

$$\theta_{1t\omega}^{s_3} = 0, \quad \forall\omega, \forall t \tag{2.24}$$

The final power output of each unit involves its scheduled production level at the day-ahead market, its power adjustment in the intra-day market, and eventually, its reserve deployment in real-time operation for each scenario. This power output is denoted by $P_{it} + \Delta P_{it\omega}^{\mathrm{U}} - \Delta P_{it\omega}^{\mathrm{D}} + r_{it\omega}^{\mathrm{U}} - r_{it\omega}^{\mathrm{D}}$ and needs to be within the generation capacity limits:

$$u_{it} P_i^{\min} \le P_{it} + \Delta P_{it\omega}^{\mathrm{U}} - \Delta P_{it\omega}^{\mathrm{D}} + r_{it\omega}^{\mathrm{U}} - r_{it\omega}^{\mathrm{D}} \le u_{it} P_i^{\max}, \quad \forall i, \forall\omega, \forall t \tag{2.25}$$

Additionally, equation (2.26) enforces that the final power output of each unit meets its ramping constraints:

$$RD_i \le \left(P_{it} + \Delta P_{it\omega}^{\mathrm{U}} - \Delta P_{it\omega}^{\mathrm{D}} + r_{it\omega}^{\mathrm{U}} - r_{it\omega}^{\mathrm{D}}\right)$$
$$- \left(P_{i,t-1} + \Delta P_{i,t-1,\omega}^{\mathrm{U}} - \Delta P_{i,t-1,\omega}^{\mathrm{D}} + r_{i,t-1,\omega}^{\mathrm{U}} - r_{i,t-1,\omega}^{\mathrm{D}}\right) \le RU_i, \quad \forall i, \forall\omega, \forall t \tag{2.26}$$

Finally, we describe the limits of the third-stage decision variables in the following.

The up/down deployed reserves of each unit are limited between zero and the corresponding up/down reserve offers:

$$0 \le r^{\mathrm{U}}_{it\omega} \le R^{\mathrm{U,max}}_{i}, \forall i, \forall \omega, \forall t \tag{2.27}$$
$$0 \le r^{\mathrm{D}}_{it\omega} \le R^{\mathrm{D,max}}_{i}, \forall i, \forall \omega, \forall t \tag{2.28}$$

Involuntary load shedding $L^{\mathrm{shed}}_{jt\omega}$ vary between zero and the actual load L_{jt}:

$$0 \le L^{\mathrm{shed}}_{jt\omega} \le L_{jt}, \quad \forall j, \forall \omega, \forall t \tag{2.29}$$

Additionally, wind power spillage is below the actual wind power output:

$$0 \le w^{\mathrm{spill}}_{qt\omega} \le W^{\mathrm{RT}}_{qt\omega}, \quad \forall q, \forall \omega, \forall t \tag{2.30}$$

Non-Anticipativity Constraints:

The fourth group of constraints is the non-anticipativity of decisions, which implies that if the realizations of stochastic wind power output are identical up to stage s, the value of decisions shall be then identical up to stage s. In other words, if scenarios ω and $\hat{\omega}$, which represent two realizations of wind power output, are equal, the decisions depending on these scenarios must be also equal.

The non-anticipativity of the intra-day decisions is mathematically expressed as:

$$\begin{aligned}
&\Delta P^{\mathrm{U}}_{it\omega} = \Delta P^{\mathrm{U}}_{it\hat{\omega}}, \Delta P^{\mathrm{D}}_{it\omega} = \Delta P^{\mathrm{D}}_{it\hat{\omega}}, \quad \forall i, \forall \omega, \hat{\omega} | \omega = \hat{\omega}, \forall t \\
&\Delta W^{\mathrm{U}}_{qt\omega} = \Delta W^{\mathrm{U}}_{qt\hat{\omega}}, \Delta W^{\mathrm{D}}_{q\omega} = \Delta W^{\mathrm{D}}_{q\hat{\omega}}, \quad \forall q, \forall \omega, \hat{\omega} | \omega = \hat{\omega}, \forall t \\
&\theta^{s_2}_{nt\omega} = \theta^{s_2}_{nt\hat{\omega}}, \quad \forall n, \forall \omega, \hat{\omega} | \omega = \hat{\omega}, \forall t
\end{aligned} \tag{2.31}$$

An example of the non-anticipativity of the decisions at the second stage is described in Fig 2.3. The corresponding mathematical statements are as follow. The non-anticipativity of the intra-day decisions let $\theta^{s_2}_{n\omega_1} = \theta^{s_2}_{n\omega_2} = \theta^{s_2}_{n\omega_3}$ and $\theta^{s_2}_{n\omega_4} = \theta^{s_2}_{n\omega_5} = \theta^{s_2}_{n\omega_6}$, $\Delta P^{\mathrm{U}}_{i\omega_1} = \Delta P^{\mathrm{U}}_{i\omega_2} = \Delta P^{\mathrm{U}}_{i\omega_3}$ and $\Delta P^{\mathrm{U}}_{i\omega_4} = \Delta P^{\mathrm{U}}_{i\omega_5} = \Delta P^{\mathrm{U}}_{i\omega_6}$, $\Delta W^{\mathrm{U}}_{q\omega_1} = \Delta W^{\mathrm{U}}_{q\omega_2} = \Delta W^{\mathrm{U}}_{q\omega_3}$ and $\Delta W^{\mathrm{U}}_{q\omega_4} = \Delta W^{\mathrm{U}}_{q\omega_5} = \Delta W^{\mathrm{U}}_{q\omega_6}$, and similar equalities for downward schedule adjustments.

Complete Formulation

The complete formulation of the proposed three-stage clearing model is as follows:

$$\underset{\Xi_{3s}}{\text{Minimize}}$$
$$\sum_{t=1}^{N_T}\Bigg[\sum_{i=1}^{N_G} C_{it}^{\text{SU}} + \sum_{\omega=1}^{N_\Omega} \pi_\omega \Big[\sum_{i=1}^{N_G} C_i(P_{it} + \Delta P_{it\omega}^{\text{U}} - \Delta P_{it\omega}^{\text{D}} + r_{it\omega}^{\text{U}} - r_{it\omega}^{\text{D}})$$
$$+ \sum_{q=1}^{N_Q} C_q(W_{qt\omega}^{\text{RT}} - w_{qt\omega}^{\text{spill}}) + \sum_{j=1}^{N_L} V_{jt}^{\text{LOL}} L_{jt\omega}^{\text{shed}}\Big]\Bigg] \tag{2.32a}$$

subject to

First-stage constraints:

$$\sum_{i\in M_n^{\text{G}}} P_{it} + \sum_{q\in M_n^{\text{Q}}} W_{qt} - \sum_{j\in M_n^{\text{L}}} L_{jt} - \sum_{r\in\Lambda_n} B_{nr}(\theta_{nt} - \theta_{rt}) = 0, \forall n, \forall t \tag{2.32b}$$

$$u_{it} P_i^{\min} \le P_{it} \le u_{it} P_i^{\max}, \forall i, \forall t \tag{2.32c}$$

$$\alpha^{\text{WDs}_1} W_{qt}^{\text{DA}} \le W_{qt} \le \alpha^{\text{WUs}_1} W_{qt}^{\text{DA}}, \forall q, \forall t \tag{2.32d}$$

$$K_i^{\text{SU}}(u_{it} - u_{i,t-1}) \le C_{it}^{\text{SU}}, \forall i, \forall t \tag{2.32e}$$

$$u_{it} \in \{0,1\}, \forall i, \forall t \tag{2.32f}$$

$$RD_i \le P_{it} - P_{i,t-1} \le RU_i, \forall i, \forall t \tag{2.32g}$$

$$\theta_{1t} = 0, \forall t \tag{2.32h}$$

Second-stage constraints:

$$\sum_{i\in M_n^{\text{G}}} \Delta P_{it\omega}^{\text{U}} - \Delta P_{it\omega}^{\text{D}} + \sum_{q\in M_n^{\text{Q}}} W_{qt\omega}^{\text{ID}} - W_{qt} - \Delta W_{qt\omega}^{\text{U}} + \Delta W_{qt\omega}^{\text{D}}$$
$$- \sum_{r\in\Lambda_n} B_{nr}(\theta_{nt\omega}^{\text{s}_2} - \theta_{rt\omega}^{\text{s}_2} - \theta_{nt} + \theta_{rt}) = 0, \forall n, \forall \omega, \forall t \tag{2.32i}$$

$$u_i P_i^{\min} \le P_{it} + \Delta P_{it\omega}^{\text{U}} - \Delta P_{it\omega}^{\text{D}} \le u_{it} P_i^{\max}, \forall i, \forall \omega, \forall t \tag{2.32j}$$

$$\alpha^{\text{WDs}_2} W_{qt\omega}^{\text{ID}} \le W_{qt} + \Delta W_{qt\omega}^{\text{U}} - \Delta W_{qt\omega}^{\text{D}} \le \alpha^{\text{WUs}_2} W_{qt\omega}^{\text{ID}}, \forall q, \forall \omega, \forall t \tag{2.32k}$$

$$\Delta P_{it\omega}^{\text{U}} \le \alpha_{\Delta P} P_i^{\max}; \Delta P_{it\omega}^{\text{D}} \le \alpha_{\Delta P} P_i^{\max}, \forall i, \forall \omega, \forall t \tag{2.32l}$$

$$\Delta W_{qt\omega}^{\text{U}} \le \alpha_{\Delta W} W_q^{\max}; \Delta W_{qt\omega}^{\text{D}} \le \alpha_{\Delta W} W_q^{\max}, \forall q, \forall \omega, \forall t \tag{2.32m}$$

$$RD_i \le (P_{it} + \Delta P_{it\omega}^{\text{U}} - \Delta P_{it\omega}^{\text{D}}) - (P_{i,t-1} + \Delta P_{i,t-1,\omega}^{\text{U}} - \Delta P_{i,t-1,\omega}^{\text{D}}) \le RU_i, \forall i, \forall \omega, \forall t \tag{2.32n}$$

$$\theta_{1t\omega}^{\text{s}_2} = 0 : \sigma_{1t\omega}, \forall \omega, \forall t \tag{2.32o}$$

Third-stage constraints:

$$\sum_{q\in M_n^{\text{Q}}} (W_{qt\omega}^{\text{RT}} - W_{qt} - \Delta W_{qt\omega}^{\text{U}} + \Delta W_{qt\omega}^{\text{D}} - w_{qt\omega}^{\text{spill}}) + \sum_{i\in M_n^{\text{G}}} (r_{it\omega}^{\text{U}} - r_{it\omega}^{\text{D}})$$
$$- \sum_{r\in\Lambda_n} B_{nr}(\theta_{nt\omega}^{\text{s}_3} - \theta_{rt\omega}^{\text{s}_3} - \theta_{nt\omega}^{\text{s}_2} + \theta_{rt\omega}^{\text{s}_2}) + \sum_{j\in M_n^{\text{L}}} L_{jt\omega}^{\text{shed}} = 0, \forall n, \forall \omega, \forall t \tag{2.32p}$$

$$u_{it}P_i^{\min} \leq P_{it} + \Delta P_{it\omega}^{\mathrm{U}} - \Delta P_{it\omega}^{\mathrm{D}} + r_{it\omega}^{\mathrm{U}} - r_{it\omega}^{\mathrm{D}} \leq u_{it}P_i^{\max}, \forall i, \forall \omega, \forall t \tag{2.32q}$$

$$r_{it\omega}^{\mathrm{U}} \leq R_i^{\mathrm{U,max}}, \forall i, \forall \omega, \forall t \tag{2.32r}$$

$$r_{it\omega}^{\mathrm{D}} \leq R_i^{\mathrm{D,max}}, \forall i, \forall \omega, \forall t \tag{2.32s}$$

$$L_{jt\omega}^{\mathrm{shed}} \leq L_{jt}, \forall j, \forall \omega, \forall t \tag{2.32t}$$

$$w_{qt\omega}^{\mathrm{spill}} \leq W_{qt\omega}^{\mathrm{RT}}, \forall q, \forall \omega, \forall t \tag{2.32u}$$

$$-f_{nr}^{\max} \leq B_{nr}(\theta_{nt\omega}^{s_3} - \theta_{rt\omega}^{s_3}) \leq f_{nr}^{\max}, \forall n, \forall r \in \Lambda_n, \forall \omega, \forall t \tag{2.32v}$$

$$\begin{aligned} RD_i \leq & \left(P_{it} + \Delta P_{it\omega}^{\mathrm{U}} - \Delta P_{it\omega}^{\mathrm{D}} + r_{it\omega}^{\mathrm{U}} - r_{it\omega}^{\mathrm{D}}\right) \\ & - \left(P_{i,t-1} + \Delta P_{i,t-1,\omega}^{\mathrm{U}} - \Delta P_{i,t-1,\omega}^{\mathrm{D}} + r_{i,t-1,\omega}^{\mathrm{U}} - r_{i,t-1,\omega}^{\mathrm{D}}\right) \leq RU_i, \forall i, \forall \omega, \forall t \end{aligned} \tag{2.32w}$$

$$\theta_{1t\omega}^{s_3} = 0, \forall \omega, \forall t \tag{2.32x}$$

Non-anticipativity constraints:

$$\begin{aligned} & \Delta P_{it\omega}^{\mathrm{U}} = \Delta P_{it\hat{\omega}}^{\mathrm{U}}, \Delta P_{it\omega}^{\mathrm{D}} = \Delta P_{it\hat{\omega}}^{\mathrm{D}}, \forall i, \forall \omega, \hat{\omega} | \omega = \hat{\omega}, \forall t \\ & \Delta W_{qt\omega}^{\mathrm{U}} = \Delta W_{qt\hat{\omega}}^{\mathrm{U}}, \Delta W_{q\omega}^{\mathrm{D}} = \Delta W_{q\hat{\omega}}^{\mathrm{D}}, \forall q, \forall \omega, \hat{\omega} | \omega = \hat{\omega}, \forall t \\ & \theta_{nt\omega}^{s_2} = \theta_{nt\hat{\omega}}^{s_2}, \forall n, \forall \omega, \hat{\omega} | \omega = \hat{\omega}, \forall t \end{aligned} \tag{2.32y}$$

Variable declarations:

$$\begin{aligned} & 0 \leq P_{it}, C_{it}^{\mathrm{SU}}, \forall i, \forall t \\ & 0 \leq W_{qt}, \forall q, \forall t \\ & 0 \leq \Delta P_{it\omega}^{\mathrm{U}}, \Delta P_{it\omega}^{\mathrm{D}}, r_{it\omega}^{\mathrm{U}}, r_{it\omega}^{\mathrm{D}}, \forall i, \forall \omega, \forall t \\ & 0 \leq \Delta W_{qt\omega}^{\mathrm{U}}, \Delta W_{qt\omega}^{\mathrm{D}}, w_{qt\omega}^{\mathrm{spill}}, \forall q, \forall \omega, \forall t \\ & 0 \leq L_{jt\omega}^{\mathrm{shed}}, \forall j, \forall \omega, \forall t \end{aligned} \tag{2.32z}$$

The problem (2.32) minimizes the expected operation cost (2.32a) considering day-ahead market constraints (2.32b)-(2.32h), intra-day market constraints (2.32i)-(2.32o), real-time operation constraints (2.32p)-(2.32x), non-anticipativity constraints (2.32y), and constraints (2.32z) expressing variable declarations.

Problem (2.32) models the realizations of wind power output through a finite number of scenario paths ω. A scenario path establishes how the wind power output evolves from its day-ahead forecast, W_{qt}^{DA}, and the intra-day forecast, $W_{qt\omega}^{\mathrm{ID}}$, to its realization denoted by $W_{qt\omega}^{\mathrm{RT}}$.

We should note that through the power balance equations (2.32b), (2.32i), and (2.32p), the production limit constraints (2.32j), (2.32k), and (2.32q), and the ramping limit equations (2.32n) and (2.32w), the day-ahead decisions are coupled to the intra-day decisions, and the intra-day decisions are linked to the operation decisions made in real time. These constraints are called *linking constraints* or *coupling constraints* in stochastic programming framework, as they couple the first-stage, second-stage, and third-stage decisions.

2.4.2 Two-stage Stochastic Clearing Model

A common two-stage model involves the day-ahead market and real-time operation without the intra-day market. Thus, the three-stage model (2.32) can be easily recast as a two-stage one by eliminating all variables and constraints pertaining to the intra-day market. The decision-making problem is, thus, to take day-ahead decisions taking into account uncertain wind power output in real-time operation. That is, the day-ahead decisions and constraints remain the same as those of the three-stage model. To avoid repeating the detailed description of the market, but to mathematically clarify the two-stage model, we briefly describe variables, objective function, and constraints of the two-stage model in the sequel.

Variables

We categorize the decisions into two groups: decisions pertaining to the day-ahead market, and decisions related to real-time operation.

- The first-stage variables pertain to the day-ahead market, similar to those in the three-stage model. They are decided before any realization of wind power output, and hence, these variables are here-and-now decisions and include:
  - On/off commitment of each unit in each period (u_{it}, binary) and its related cost (C_{it}^{SU}, \$).
  - Scheduled power output (production level) for each conventional unit at the day-ahead market in period t (P_{it}, [MW]).
  - Scheduled power output for each wind unit at the day-ahead market in each period (W_{qt}, [MW]).
  - Angle of each node at the day-ahead market in each period (θ_{nt}, [rad]).
- The second-stage variables pertain to the realization of wind power production in real-time operation. These decisions compensate for actual wind power output, and thus, defined for each single scenario. The operation decisions are wait-and-see decisions and involve:
  - Deployed up reserve by each conventional unit in each scenario and each period in real-time operation ($r_{it\omega}^{\mathrm{U}}$, [MW]).
  - Deployed down reserve by each conventional unit in each scenario and each period in real-time operation ($r_{it\omega}^{\mathrm{D}}$, [MW]).

– Angle of each node in each scenario and each period in real-time operation ($\theta_{nt\omega}$, [rad]).
– Wind power spillage of each wind unit in each scenario and each period in real-time operation ($w^{\text{spill}}_{qt\omega}$, [MW]).
– Involuntarily load shedding of each load in each scenario and each period in real-time operation ($L^{\text{shed}}_{jt\omega}$, [MW]).

We should note here that in the three-stage model, variables of two stages (i.e., second and third stages) are defined per scenario. Thus, superscripts s_2 and s_3 are used for the clarity of formulation. In the two-stage model, there is only one stage whose variables are defined per scenario, and thus, we do use any extra superscript.

Objective Function

The objective function consists of two components representing the cost in the day-ahead market, which is the same as the day-ahead cost in the three-stage model expressed in (2.1), and the expected balancing cost pertaining to real-time operation stated in (2.33).

$$\sum_{t=1}^{N_T}\sum_{\omega=1}^{N_\Omega}\pi_\omega\Big(\sum_{i=1}^{N_G}C_i(r^{\text{U}}_{it\omega}-r^{\text{D}}_{it\omega})+\sum_{q=1}^{N_Q}C_q(W^{\text{RT}}_{qt\omega}-W_q-w^{\text{spill}}_{qt\omega})+\sum_{j=1}^{N_L}V^{\text{LOL}}_{jt}L^{\text{shed}}_{jt\omega}\Big) \tag{2.33}$$

Thus, the objective function of the two-stage clearing model is:

$$\sum_{t=1}^{N_T}\left[\sum_{i=1}^{N_G}C^{\text{SU}}_{it}+\sum_{\omega=1}^{N_\Omega}\pi_\omega\Big[\sum_{i=1}^{N_G}C_i(P_{it}+r^{\text{U}}_{it\omega}-r^{\text{D}}_{it\omega})+\sum_{q=1}^{N_Q}C_q(W^{\text{RT}}_{qt\omega}-w^{\text{spill}}_{qt\omega})+\sum_{j=1}^{N_L}V^{\text{LOL}}_{jt}L^{\text{shed}}_{jt\omega}\Big]\right] \tag{2.34}$$

The minimization is over the set of variables $\Xi=\{C^{\text{SU}}_{it},u_{it},P_{it},\forall i,\forall t;W_{qt},\forall q,\forall t;\theta_{nt},\forall n,\forall t;r^{\text{U}}_{it\omega}, r^{\text{D}}_{it\omega},\forall i,\forall t,\forall\omega;w^{\text{spill}}_{qt\omega},\forall q,\forall t,\forall\omega;\theta_{nt\omega},\forall n,\forall t,\forall\omega;L^{\text{shed}}_{jt\omega}\forall j,\forall t,\forall\omega\}$, as described in Section 2.4.2.

Constraints

First-Stage Constraints (Day-ahead Market Constraints):

The first-stage constraints of the two-stage model remain the same as those representing the day-ahead market in the three-stage model. Detailed descriptions of these constraints are provided by equations (2.5)-(2.12).

Second-Stage Constraints (Real-Time Operation Constraints):

The second-stage constraints pertain to real-time operation, where uncertain wind power output is modeled through scenarios, and hence, the corresponding constraints are defined per scenario.

After the actual wind power output is realized in real time, the system energy balance must be preserved. This is done through second-stage decisions involving upward reserve deployment $r^{\mathrm{U}}_{it\omega}$, downward reserve deployment $r^{\mathrm{D}}_{it\omega}$, wind spillage $w^{\mathrm{spill}}_{qt\omega}$, and as the last resort, load shedding $L^{\mathrm{shed}}_{jt\omega}$. Constraint (2.35) enforces the power balance in each node, each scenario and each time period:

$$\sum_{i\in M_n^{\mathrm{G}}}(r^{\mathrm{U}}_{it\omega}-r^{\mathrm{D}}_{it\omega})+\sum_{q\in M_n^{\mathrm{Q}}}(W^{\mathrm{RT}}_{qt\omega}-W_{qt}-w^{\mathrm{spill}}_{qt\omega})+\sum_{r\in\Lambda_n}B_{nr}(\theta_{nt}-\theta_{nt\omega}-\theta_{rt}+\theta_{rt\omega})$$
$$+\sum_{j\in M_n^{\mathrm{L}}}L^{\mathrm{shed}}_{jt\omega}=0,\forall n,\forall t,\forall\omega \tag{2.35}$$

Equation (2.36) enforces the power flow to be within the thermal limits of lines:

$$-f^{\max}_{nr}\le B_{nr}(\theta_{nt\omega}-\theta_{rt\omega})\le f^{\max}_{nr},\forall n,\forall r\in\Lambda_n,\forall t,\forall\omega \tag{2.36}$$

The final power output of each unit $P_{it}+r^{\mathrm{U}}_{it\omega}-r^{\mathrm{D}}_{it\omega}$ is enforced to be within the generation capacity limits:

$$u_{it}P^{\min}_i\le P_{it}+r^{\mathrm{U}}_{it\omega}-r^{\mathrm{D}}_{it\omega}\le u_{it}P^{\max}_i,\forall i,\forall t,\forall\omega \tag{2.37}$$

Additionally, the final power output of each unit is enforced to meet its ramping limits:

$$RD_i\le\left(P_{it}+r^{\mathrm{U}}_{it\omega}-r^{\mathrm{D}}_{it\omega}\right)-\left(P_{i,t-1}-r^{\mathrm{U}}_{i,t-1,\omega}+r^{\mathrm{D}}_{i,t-1,\omega}\right)\le RU_i,\forall i,\forall t,\forall\omega \tag{2.38}$$

The up/down deployed reserves are limited between zero and the corresponding up/down reserve offers:

$$0\le r^{\mathrm{U}}_{it\omega}\le R^{\mathrm{U,max}}_{it},\forall i,\forall t,\forall\omega \tag{2.39}$$
$$0\le r^{\mathrm{D}}_{it\omega}\le R^{\mathrm{D,max}}_{it},\forall i,\forall t,\forall\omega \tag{2.40}$$

The load can be shed within zero and the actual load L_{jt}:

$$0\le L^{\mathrm{shed}}_{jt\omega}\le L_{jt},\forall j,\forall t,\forall\omega \tag{2.41}$$

Additionally, the wind power output can be spilled within zero and its actual value:

$$0 \leq w_{qt\omega}^{\text{spill}} \leq W_{qt\omega}^{\text{RT}}, \forall q, \forall t, \forall \omega \tag{2.42}$$

Finally, node 1 is set to be the reference node:

$$\theta_{1t\omega} = 0, \forall t, \forall \omega \tag{2.43}$$

Complete Formulation of Two-Stage Model

The complete formulation of the two-stage clearing model is as follows:

$$\underset{\Xi}{\text{Minimize}}$$

$$\sum_{t=1}^{N_T} \left[\sum_{i=1}^{N_G} C_{it}^{\text{SU}} + \sum_{\omega=1}^{N_\Omega} \pi_\omega \left[\sum_{i=1}^{N_G} C_i(P_{it} + r_{it\omega}^{\text{U}} - r_{it\omega}^{\text{D}}) + \sum_{q=1}^{N_Q} C_q(W_{qt\omega}^{\text{RT}} - w_{qt\omega}^{\text{spill}}) + \sum_{j=1}^{N_L} V_{jt}^{\text{LOL}} L_{jt\omega}^{\text{shed}} \right] \right] \tag{2.44a}$$

subject to

First-stage constraints:

$$\sum_{i \in M_n^{\text{G}}} P_{it} + \sum_{q \in M_n^{\text{Q}}} W_{qt} - \sum_{j \in M_n^{\text{L}}} L_{jt} - \sum_{r \in \Lambda_n} B_{nr}(\theta_{nt} - \theta_{rt}) = 0, \forall n, \forall t \tag{2.44b}$$

$$u_{it} P_i^{\min} \leq P_{it} \leq u_{it} P_i^{\max}, \forall i, \forall t \tag{2.44c}$$

$$\alpha^{\text{WDs}_1} W_{qt}^{\text{DA}} \leq W_{qt} \leq \alpha^{\text{WUs}_1} W_{qt}^{\text{DA}}, \forall q, \forall t \tag{2.44d}$$

$$K_i^{\text{SU}}(u_{it} - u_{i,t-1}) \leq C_{it}^{\text{SU}}, \forall i, \forall t \tag{2.44e}$$

$$u_{it} \in \{0, 1\}, \forall i, \forall t \tag{2.44f}$$

$$RD_i \leq P_{it} - P_{i,t-1} \leq RU_i, \forall i, \forall t \tag{2.44g}$$

$$\theta_{1t} = 0, \forall t \tag{2.44h}$$

Second-stage constraints:

$$\sum_{q \in M_n^{\text{Q}}} (W_{qt\omega}^{\text{RT}} - W_{qt} - w_{qt\omega}^{\text{spill}}) + \sum_{i \in M_n^{\text{G}}} (r_{it\omega}^{\text{U}} - r_{it\omega}^{\text{D}}) - \sum_{r \in \Lambda_n} B_{nr}(\theta_{nt\omega} - \theta_{rt\omega} - \theta_{nt} + \theta_{rt})$$
$$+ \sum_{j \in M_n^{\text{L}}} L_{jt\omega}^{\text{shed}} = 0, \forall n, \forall \omega, \forall t \tag{2.44i}$$

$$u_{it} P_i^{\min} \leq P_{it} + r_{it\omega}^{\text{U}} - r_{it\omega}^{\text{D}} \leq u_{it} P_i^{\max}, \forall i, \forall \omega, \forall t \tag{2.44j}$$

$$r_{it\omega}^{\text{U}} \leq R_i^{\text{U,max}}, \forall i, \forall \omega, \forall t \tag{2.44k}$$

$$r_{it\omega}^{\text{D}} \leq R_i^{\text{D,max}}, \forall i, \forall \omega, \forall t \tag{2.44l}$$

$$L_{jt\omega}^{\text{shed}} \leq L_{jt}, \forall j, \forall \omega, \forall t \tag{2.44m}$$

$$w_{qt\omega}^{\text{spill}} \leq W_{qt\omega}^{\text{RT}}, \forall q, \forall \omega, \forall t \tag{2.44n}$$

$$-f_{nr}^{\max} \leq B_{nr}(\theta_{nt\omega} - \theta_{rt\omega}) \leq f_{nr}^{\max}, \forall n, \forall r \in \Lambda_n, \forall \omega, \forall t \tag{2.44o}$$

$$RD_i \leq \left(P_{it} + r_{it\omega}^{\text{U}} - r_{it\omega}^{\text{D}}\right) - \left(P_{i,t-1} + r_{i,t-1,\omega}^{\text{U}} - r_{i,t-1,\omega}^{\text{D}}\right) \leq RU_i, \forall i, \forall \omega, \forall t \tag{2.44p}$$

$$\theta_{1t\omega} = 0, \forall \omega, \forall t \tag{2.44q}$$

Variable declarations:

$$\begin{aligned}
&0 \leq P_{it}, C_{it}^{\text{SU}}, \forall i, \forall t \\
&0 \leq W_{qt}, \forall q, \forall t \\
&0 \leq r_{it\omega}^{\text{U}}, r_{it\omega}^{\text{D}}, \forall i, \forall \omega, \forall t \\
&0 \leq w_{qt\omega}^{\text{spill}}, \forall q, \forall \omega, \forall t \\
&0 \leq L_{jt\omega}^{\text{shed}}, \forall j, \forall \omega, \forall t
\end{aligned} \tag{2.44r}$$

The problem (2.44) minimizes the expected operation cost (2.44a) subject to day-ahead constraints (2.44b)-(2.44h), real-time operation constraints (2.44i)-(2.44q), and constraints (2.44r) expressing variable declarations. The linking constraints coupling the first-stage and second-stage variables are the power balance equation (2.44i), generation capacity constraint (2.44j), and generation ramping constraint (2.44p) in real-time operation.

2.4.3 Metrics for Performance Evaluation

Using a stochastic model requires complexity and high computational burden, as compared with using a deterministic model, where the random parameters are replaced by their deterministic average values. To justify the use of a stochastic model over a deterministic one, the notion of *Value of the Stochastic Solution* (VSS) is relevant [22].

Computing the VSS for a two-stage stochastic model is straightforward: first, the uncertain parameters are replaced by their mean value, and a deterministic problem without recourse is solved. We call this problem MV model (standing for Mean-Value) and the corresponding solution to first-stage variables x^{MV}. Next, the first-stage variables in the stochastic problem are fixed at x^{MV}, and the resulting problem is solved for the set of scenarios. The optimal value of the objective function of this problem (z^D) minus the optimal value of the objective function of the stochastic problem (z^*) results in the VSS:

$$\text{VSS} = \text{z}^{\text{D}} - \text{z}^{*} \tag{2.45}$$

The VSS can be also expressed as a percentage of the optimal value of the stochastic problem:

$$\mathrm{VSS} = \frac{z^D - z^*}{z^*} \tag{2.46}$$

A small VSS means that the deterministic MV model is a good approximation of the stochastic one. In other words, the uncertain parameters can be approximated by their expected value and the resulting deterministic problem can be then solved instead of a stochastic problem.

In a multi-stage problem, there is not a unique VSS as variables can be fixed to the solution of the MV model in different stages. In a multi-stage problem with s_N stages, the VSS_{s_n} is defined for stage s_n as follows. The decisions of stages s_1 to s_{n-1} are fixed at the solution of the MV model corresponding to stages s_1 to s_{n-1}. The resulting problem is solved for each scenario and the expected optimal value of objective function is computed over the set of scenarios. In other words, the optimal solution of this problem is obtained using the MV solution up to stage s_{n-1}. Denoting it by z^{D,s_n}, the VSS_{s_n} is:

$$\mathrm{VSS}_{s_n} = z^{D,s_n} - z^*, \quad \forall n > 1 \tag{2.47}$$

and as a percentage of the optimal value of stochastic problem:

$$\mathrm{VSS}_{s_n\%} = \frac{z^{D,s_n} - z^*}{z^*}, \quad \forall n > 1 \tag{2.48}$$

The mathematical details of computing the VSS for a multi-stage stochastic problem is provided in Appendix A.2.

Since our focus is to obtain the day-ahead informed decisions, the VSS_{s_2} is used. Note that the optimal solution z^{D,s_2} is obtained by fixing the day-ahead variables at the corresponding MV solution. This makes this VSS calculation consistent for three-stage and two-stage models.

2.4.4 Economic Aspect: Pricing Scheme, Cost-Recovery Conditions & Notion of Uplift

Below, we describe the pricing approach used in this chapter.

Marginal (clearing) prices are obtained from the dual problem of the market-clearing model if it is convex. The marginal prices are the dual variables of the power balance equations as they represent the sensitivity of objective function (i.e., expected cost) to the right hand side of the power balance equation (i.e., load). However, market model (2.32) is a MILP problem. Clearing prices cannot be obtained from a MILP problem as its dual problem cannot mathematically defined.

As a solution, [46] proposes to fix the integer variable at their optimal values obtained from the MILP model, and to derive prices from the dual problem of the resulting continuous problem. However, obtaining prices from a relaxed continuous version of the original mixed-integer clearing problem may yield situations where some producers cannot recover their costs, and consequently, they may leave the market. The reason is that such pricing approaches do not fully reflect costs pertaining to integer decisions, such as the start-up cost of a unit. To avoid this, a side-payment called uplift is paid to each unit incurring losses under these prices. Note that the uplift makes the losses of these units zero without extra profit.

Given the power outputs and prices from the three-stage model, the day-ahead profit and the expected profit are formulated by equations (2.49) and (2.50), respectively, for individual unit i located in node n.

$$\text{Profit}_i^{\text{DA}} = \sum_t \Big[P_{it}(\lambda_{nt} - C_i) - C_{it}^{\text{SU}} \Big], \quad \forall i \tag{2.49}$$

where λ_{nt} is the day-ahead marginal price at node n and time t. Since unit i is located at node n, λ_{nt} is the price that this unit receives for its power output P_{it}.

$$\begin{aligned} \text{Profit}_i^{\text{exp}} = \sum_t \Big[& P_{it}(\lambda_{nt} - C_i) - C_{it}^{\text{SU}} \\ & + \sum_\omega \pi_\omega \big[(\Delta P_{it\omega}^{\text{U}} - \Delta P_{it\omega}^{\text{D}})(\lambda_{nt\omega}^{\text{s}_2}/\pi_\omega - C_i) + (r_{it\omega}^{\text{U}} - r_{it\omega}^{\text{D}})(\lambda_{nt\omega}^{\text{s}_3}/\pi_\omega - C_i) \big] \Big], \quad \forall i \end{aligned} \tag{2.50}$$

where $\lambda_{nt\omega}^{\text{s}_2}$ and $\lambda_{nt\omega}^{\text{s}_3}$ are, respectively, probability-affected intra-day prices and probability-affected balancing prices at node n, scenario ω and time t. Note that the expected intra-day cost (2.2) and the expected operation cost (2.3) have the probability term π_ω, and hence, the corresponding prices are probability-affected. To have them in the same order of magnitude of the day-ahead prices, we consider the probability-removed intra-day prices $\frac{\lambda_{nt\omega}^{\text{s2}}}{\pi_\omega}$ and probability-removed balancing prices $\frac{\lambda_{nt\omega}^{\text{s3}}}{\pi_\omega}$.

Note that $\lambda_{nt\omega}^{\text{s}_2}$ and $\lambda_{nt\omega}^{\text{s}_3}$ are not actual intra-day and balancing prices. Rather, they can be translated as forecast prices given wind power scenarios. If any wind power scenario considered will realized in real-time operation, these forecast prices will be correspondingly actualized.

We should note that the uplift is calculated based on day-ahead losses and formulated as:

$$\text{Uplift}_i = \max\{0, \sum_t (P_{it}(C_i - \lambda_{nt}) + C_{it}^{\text{SU}})\}, \quad \forall i \tag{2.51}$$

A detailed description of the issues related to the pricing scheme for a MILP problem is provided in Chapter 3, where pricing schemes are considered.

2.5 Illustrative Example

To illustrate the advantages of the clearing model (2.32), we apply it to a small example, and provide the corresponding market outcomes in this section.

2.5.1 Data

The example considered is based on a three-node system, as depicted in Fig. 2.4. The planning horizon spans two time periods.

The system includes three conventional units and one wind unit. The data of the conventional units are provided in Table 2.1. The maximum reserves $R_i^{\mathrm{U,max}}$ and $R_i^{\mathrm{D,max}}$ are assumed to be equal to $P_i^{\max}$ for all units. These units can be therefore scheduled for both energy and reserve.

The load L_3, located at node 3, is 230 MW and 320 MW at periods t_1 and t_2, respectively. A value of lost load equal to $2000/MWh is considered in real-time operation.

Table 2.1 – Data of generating units.

Unit	K_i^{SU} ($)	C_i ($/MWh)	$P_i^{\max}$ (MW)	$P_i^{\min}$ (MW)	$R_i^{\mathrm{U,max}}$ (MW)	$R_i^{\mathrm{D,max}}$ (MW)
U_1	10.01	3.03	102.00	10.00	102.00	102.00
U_2	10.20	4.01	101.00	10.00	101.00	101.00
U_3	50.06	5.09	100.00	10.00	100.00	100.00

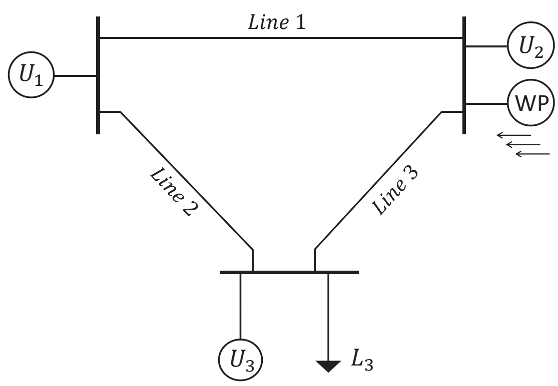

Figure 2.4 – Test system

The wind unit is located at node 2. A small production cost of $0.3/MWh is assumed for this unit. We consider two scenarios, *high* and *low*, to characterize wind production in the intra-day market, and for each second-stage scenario, three scenarios, namely, *high*, *medium* and *low*, are considered in real-time operation. There are in total six scenarios at each time period, as presented in Table 2.2. Also, we assume that these are equi-probable scenarios. The other assumption is that at the day-ahead market, the wind power output can be scheduled within ±20% of its best available forecast W_{qt}^{DA}, which are 58 MW and 87 MW at periods t_1 and t_2, respectively ($\alpha^{\mathrm{WUs}_1} = 1.2$, $\alpha^{\mathrm{WDs}_1} = 0.8$). On the other hand, the intra-day up and down adjustments of power schedules of conventional units and wind production are assumed to be limited to 25% of the maximum power outputs and wind installed capacity, respectively ($\alpha_{\Delta P} = \alpha_{\Delta W} = 25\%$).

Table 2.2 – Wind scenarios [MW] over time periods t_1 and t_2

	period t_1		period t_2	
scenario	ID stage	RT stage	ID stage	RT stage
ω_1 :(High, High)	60	91	89	99
ω_2 :(High, Medium)	60	71	89	85
ω_3 :(High, Low)	60	49	89	21
ω_4 :(Low, High)	35	67	46	91
ω_5 :(Low, Medium)	35	37	46	48
ω_6 :(Low, Low)	35	9	46	11

Finally, line reactances and capacities are all equal to 0.13 p.u. and 500 MW, respectively. A line capacity of 500 MW is high enough to avoid congestion in any of the scenarios considered. Thus, prices do not change across nodes.

2.5.2 Outcomes of the Three-Stage Model

Figs. 2.5 and 2.6 show the scheduled quantities, the adjustments, and the deployed reserves for periods t_1 and t_2, respectively, at the day-ahead market, intra-day market, and real-time operation.

To get insight into the decision-making process, we focus on period t_1 and scenario ω_1, where the realization of wind power output is 91 MW. The wind unit is scheduled to produce 53 MW in the day-ahead market considering that the wind power output may increase to 60 MW, for which a downward wind schedule adjustment of 5 MW is decided by the three-stage model. As a consequent, the day-ahead scheduled power output of the wind unit is adjusted to produce 48 MW in the intra-day market. The difference of 12 MW between a wind power output of 60 MW and a wind scheduled production of 48 MW is compensated by adjusting unit U_2 in the downward direction. After the realization of 91 MW of wind power output in real-time

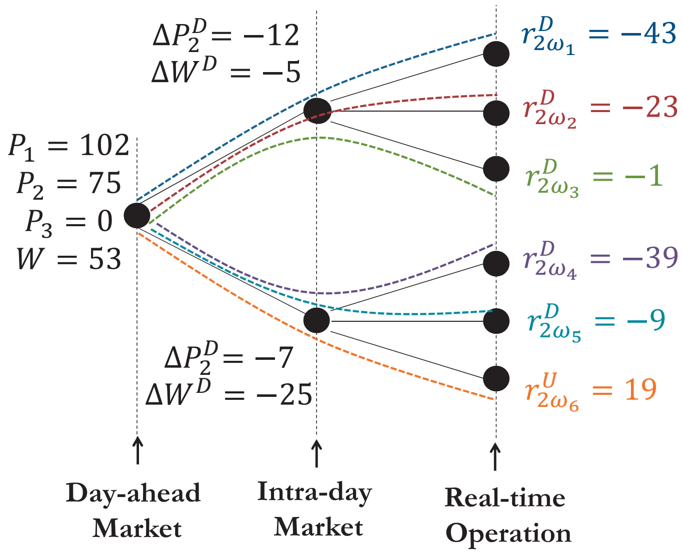

Figure 2.5 – Scheduled power productions, power adjustments, and deployed reserves in period t_1

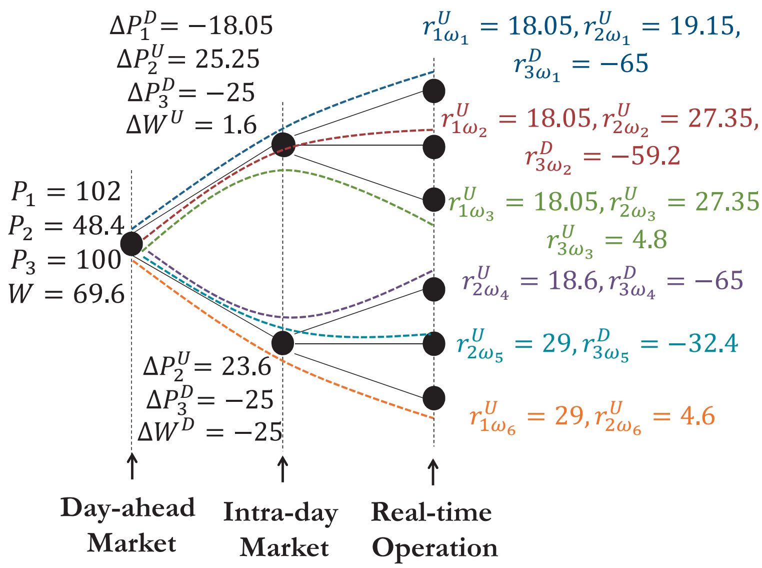

Figure 2.6 – Scheduled power productions, power adjustments, and deployed reserves in period t_2

operation, reserves must be deployed downward for an amount of 43 MW (91 MW - 48 MW) in order to accommodate the total 91 MW of wind power output in the system without spillage and load shedding. This is done by decreasing the production level of unit $U2$ by 43 MW.

The other extreme point regarding wind power output occurs in scenario ω_6, where the realization of wind power production is 9 MW. The day-ahead power scheduled for the wind unit is 53 MW, which is reduced to 28 MW in the intra-day market if the wind power forecast of 35 MW occurs. In real-time operation, if the wind power output realizes to be 9 MW, there is a supply deficit of 19 MW (9 MW - 28 MW), which is compensated by an upward reserve deployment by unit U_2.

The total expected cost is \$1515.1.

Table 2.3 provides the day-ahead, intra-day, and balancing prices, denoted by λ_{nt}, $\lambda^{S_2}_{nt\omega}$, and $\lambda^{S_3}_{nt\omega}$, respectively. The day-ahead prices in period t_2 are higher than those in period t_1 resulting from a higher load in period t_2. This trend is also observed in the intra-day market, as well as in real-time operation, except for period t_2 and scenario *high*, where balancing price $\lambda^{S_3}_{t_2\omega_1}$ is \$4.01/MWh. The reason is that the marginal unit from which clearing prices are driven is unit U_2 in this scenario; however, the marginal unit is unit U_3 in scenarios *medium* and *low*.

Table 2.3 – Day-ahead, intra-day, and balancing clearing prices [\$/MWh]

		$\lambda^{S_2}_{n\omega}/\pi_\omega$		$\lambda^{S_3}_{n\omega}/\pi_\omega$		
	λ_n	High	Low	High	Medium	Low
period t_1	4.01	4.01	4.01	4.01	4.01	4.01
period t_2	4.73	4.73	4.73	4.01	5.09	5.09

Given these scheduled power outputs and prices, Table 2.4 provides the day-ahead profit, stated in (2.49), and the expected profit, expressed in (2.50).

Focusing on the day-ahead market and unit U_3, this unit earns $4.73 \times 100 = \$473$, while its total start-up and production cost is $5.09 \times 100 + 50.06 = \$559.06$. Therefore, unit U_3 incurs a loss of \$86.06 at the day-ahead market. At the intra-day stage, the profit of unit U_3 increases by $(4.73 - 5.09) \times (-25) = \$9$ if either scenarios *high* or *low* realizes. In real-time operation, the profit of unit U_3 increases only under scenarios ω_1 and ω_4. However, none of these increases in profit can cover the loss of \$86.06 at day-ahead market. Therefore, unit U_3 suffers a loss on average as well as under any scenario.

To avoid this loss, an uplift of \$86.06 is paid by the load to unit U_3. As previously mentioned, an uplift is a side-payment paid only to those units incurring losses at the day-ahead market with the purpose of making the losses of these units zero.

Without uplift, the payment of load L_3 at the day-ahead market is $4.01 \times 230 = \$922.3$ and $4.73 \times 320 = \$1513.6$ at periods t_1 and t_2, respectively. The total payment over the two periods (\$2435.9) is equal to the summation of total day-ahead profit of all units (\$706.9) and the

Table 2.4 – Day-ahead and Expected profits [$]

	unit U_1	unit U_2	unit U_3	wind	Total
DA profit	263.40	24.60	-86.06	504.90	706.90
Total expected profit	263.40	62.50	-53.70	397.50	669.70

day-ahead cost ($1729). Considering the uplift of $86.06, L_3 finally pays $2521.96. Table 2.5 provides these outcomes in details.

Table 2.5 – Consumer payment with and without uplift [$]

Day-ahead cost	Day-ahead profit	Uplift	Cons. pay. with uplift	Cons. pay. without uplift
1729.00	706.90	86.06	2521.96	2435.9

2.5.3 Performance of the Three-Stage Model vs. the Two-Stage One

In this section, we provide a comparison between the outcomes of the three-stage model (2.32) and those from the two-stage model (2.44).

The scenarios representing real-time operation for the two-stage model are the same as those modeling real-time operation of the three-stage model (RT stage in Table 2.2).

The production schedules for the two-stage model are shown in Figs. 2.7 and 2.8 for periods t_1 and t_2, respectively.

We first elaborate on the day-ahead scheduled power outputs obtained from the two-stage model, and compare them to those obtained from the three-stage model, previously shown in Figs. 2.5 and 2.6.

The wind unit is scheduled to produce 46.4 MW in period t_1 which turns out to be 91 MW in scenario ω_1. Therefore, the system requires a total reserve deployments of 44.6 MW in the downward direction. We recall that the day-ahead power scheduled for the wind unit is 53 MW from the three-stage model which can be adjusted to be 48 MW in intra-day market. This eventually results in a smaller amount of deployed reserves as compared to that from the two-stage one (43 MW vs. 44.6 MW in scenario ω_1). In period t_2, the two-stage model allocates a production of 104.4 MW to the wind unit, which is higher than the day-ahead power scheduled for the wind unit by the three-stage model (69.9 MW). Consequently, a higher amount of reserves is deployed using the two-stage model, as compared to the amount of deployed reserves using the three-stage one.

Table 2.6 provides the day-ahead and balancing prices obtained from the two-stage model. The day-ahead prices at period t_2 obtained from the two-stage model are higher than those of the three-stage model. Depending on scenarios, the balancing prices of the two-stage model are equal to or higher than those obtained from the three-stage model. This is the result of the reduced wind scenario information in the two-stage model.

Table 2.6 – Clearing prices obtained from two-stage model [$/MWh]

	λ_n	$\lambda_{n\omega_1}$	$\lambda_{n\omega_2}$	$\lambda_{n\omega_3}$	$\lambda_{n\omega_4}$	$\lambda_{n\omega_5}$	$\lambda_{n\omega_6}$
period t_1	4.01	4.01	4.01	4.01	4.01	4.01	4.01
period t_2	5.09	5.09	5.09	5.09	5.09	5.09	5.09

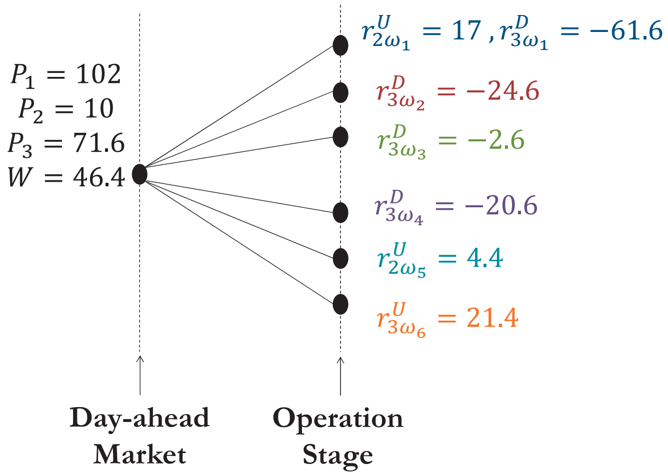

Figure 2.7 – Scheduled productions and deployed reserves result from two-stage model in period t_1.

The day-ahead cost expressed in equation (2.1), the expected intra-day cost stated in equation (2.2), and the expected balancing cost formulated in equation (2.3) are provided in Table 2.7 for both models. The three-stage model results in a higher day-ahead cost than that of the two-stage model, but a lower balancing cost, which finally results in a lower total expected cost. The main reason to have a lower day-ahead cost in the two-stage model is scheduled wind power. The total wind power scheduled is 150.8 MW over the two periods in the two-stage model, which is higher than 122.6 MW scheduled wind production in the three-stage model. This, however, results in a higher amount of deployed reserves. That is why the balancing cost is higher in the two-stage model than that of the three-stage model.

Table 2.8 provides the profit of the units (conventional units and wind unit) at each stage and in total for both models without uplifts. The total expected profit of producers is lower in the three-stage model than that in the two-stage model. This observation does not reverse

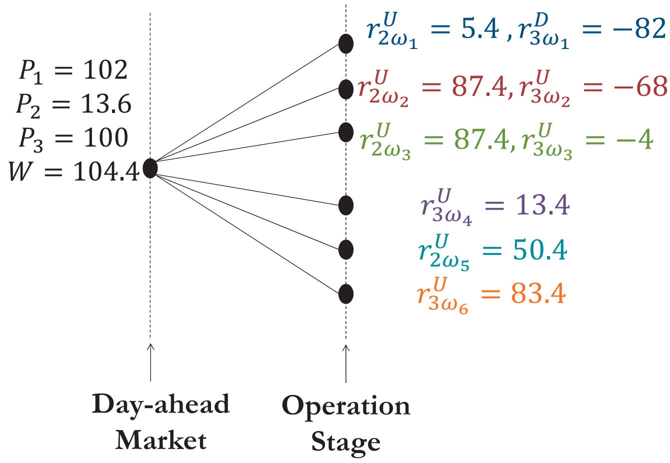

Figure 2.8 – Scheduled productions and deployed reserves result from two-stage model in period t_2.

Table 2.7 – costs [$]; three-stage model vs. two-stage model

	Three-stage model	Two-stage model
Day-ahead market	1729.00	1540.80
Intra-day market	-102.80	–
Real-time Operation	-111.10	162.70
Total expected cost	1515.10	1703.50

after adding the uplift, that is $60.86 for the two-stage model and $80.06 for the three-stage model. Note that the unit profits in real-time operation are zero under the two-stage model; the reason is that unit U_2 and unit U_3 are deployed under balancing prices equal to their marginal costs.

Table 2.8 – Producers profit[$]; three-stage model vs. two-stage model and no uplift

Three-stage model	unit U_1	unit U_2	unit U_3	wind	all units
Day-ahead	263.40	24.60	-86.00	504.90	706.90
Intra-day	-15.30	17.60	9.00	-107.50	-96.20
Real-time operation	15.30	20.30	23.40	0.00	59.00
Total exp. profit	263.40	62.50	-53.70	397.50	**669.70**
Two-stage model	unit U_1	unit U_2	unit U_3	wind	all units
Day-ahead	300.07	98.88	-60.86	672.20	1010.30
Real-time operation	0.00	0.00	0.00	0.00	0.00
Total exp. profit	300.07	98.88	-60.86	672.20	**1010.30**

The consumer payment is the summation of day-ahead cost and day-ahead profit. Given the day-ahead costs and day-ahead unit profits, the consumer payment without uplift is \$2551.1 for the two-stage model and \$2435.9 for the three-stage model. That is, the consumer payment from the two-stage model is higher than that from the three-stage model. Uplift does not change this result, as it increases the consumer payment to \$2611.9 (\$2551.1+ uplift of \$60.86) and \$2521.9 (\$2435.9+ uplift of \$80.06) for the two-stage model and the three stage model, respectively.

2.6 Case Studies

We first present the outcomes of a base case study involving a single load profile. Next, in order to gain insight on the performance of the three-stage model, we consider different bounds for the system constraints using the same load profile and explore how these bounds influence the results. Finally, different load profiles and different bounds are considered.

These case studies aim to appraise the performance of three-stage model by comparing its outcomes to those from a two-stage model.

2.6.1 Data

We use a 24-node system based on the single-area IEEE Reliability Test System (RTS).

To facilitate the analysis of the results, we have modified some of the original characteristics of this test system. We consider that the system has 34 lines, 9 conventional generating units, and 1 wind power unit. The data of conventional generating units are provided in Table 2.9. We assume that hydro units 2, 4, and 8 (i.e., U_{50}) offer its energy production at zero price.

Table 2.10 provides the total demand over the 24 periods, while the demand locations and the corresponding shares are provided in Table 2.11.

Table 2.9 – Characteristics of the Generating Units

Type	U_{90}	U_{50}	U_{155}	U_{76}	U_{197}	U_{400}
Unit i	1	2,4,8	3,6	5	7	9
Node	2	7,15,22	10,18	16	21	23
$P_i^{\max}$ (MW)	90.00	50.00	155.00	76.00	197.00	400.00
$P_i^{\min}$ (MW)	25.00	15.00	55.00	15.20	69.00	100.00
k_i^{SU} (\$)	300.00	100.00	320.00	400.00	300.00	1000.00
C_i (\$/MW)	19.67	0.00	10.68	11.89	11.09	5.53

The wind power unit is located at node 7. We assume that the wind unit has an installed

Table 2.10 – Total demand in [MW] from period t_1 to period t_{24}

period	t_1	t_2	t_3	t_4	t_5	t_6	t_7	t_8
demand	828.10	831.00	842.00	923.00	943.00	1103.60	1185.30	1139.00
period	t_9	t_{10}	t_{11}	t_{12}	t_{13}	t_{14}	t_{15}	t_{16}
demand	1137.50	1121.00	1123.00	1099.00	1088.00	1100.00	1103.00	1119.00
period	t_{17}	t_{18}	t_{19}	t_{20}	t_{21}	t_{22}	t_{23}	t_{24}
demand	1125.00	1143.00	1115.00	1109.00	1101.20	1080.10	1037.00	800.00

Table 2.11 – Demand location and share

demand	L_1	L_2	L_3	L_4	L_5	L_6	L_7	L_8	
location	1	2	3	4	5	6	7	8	
share [%]	21.5	16.4	11.7	3.5	5.1	4.8	4.3	4.8	
demand	L_9	L_{10}	L_{11}	L_{12}	L_{13}	L_{14}	L_{15}	L_{16}	L_{17}
location	9	10	13	14	15	16	18	19	20
share [%]	4.1	2	2.4	2.8	2.5	2.6	4.3	3.4	3.8

capacity is 600 MW. To generate wind power scenarios, we use wind speed historical data from Austin, Texas, which are available in the System Advisor Model (SAM) [2]. To obtain hourly wind power scenarios for 24 time periods, we apply the power curve of a 2-MW Vestas V80/2000 wind turbine with a hub height of 80 m. The power curve of this turbine model can be found in [16].

We should note that we built up the scenarios employing historical data without applying scenario generation/reduction techniques.

2.6.2 Scenarios

The following process is used for scenario generation. We generate N_{Ω_1} scenarios prior to the day-ahead gate closure, using all the historical data available up to this time. Each scenario involves 24 values for the output of the wind power unit pertaining to the 24 time periods of day d. Then, conditioned to the actual values of each scenario during the hours between the day-ahead gate closure and the intra-day gate closure, we generate N_{Ω_2} new scenarios for each one of the original N_{Ω_1} scenarios, resulting in a total number of N_Ω scenarios, where $N_\Omega = N_{\Omega_1} \times N_{\Omega_2}$. The decision-making tree is shown in Figure 2.9. For the case study, we consider 10 scenarios at the intra-day market, and corresponding to each second-stage scenario 15 scenarios in real-time operation; therefore, there are in total 150 equi-probable scenarios at each time period for the three-stage model. The corresponding two-stage model is assumed

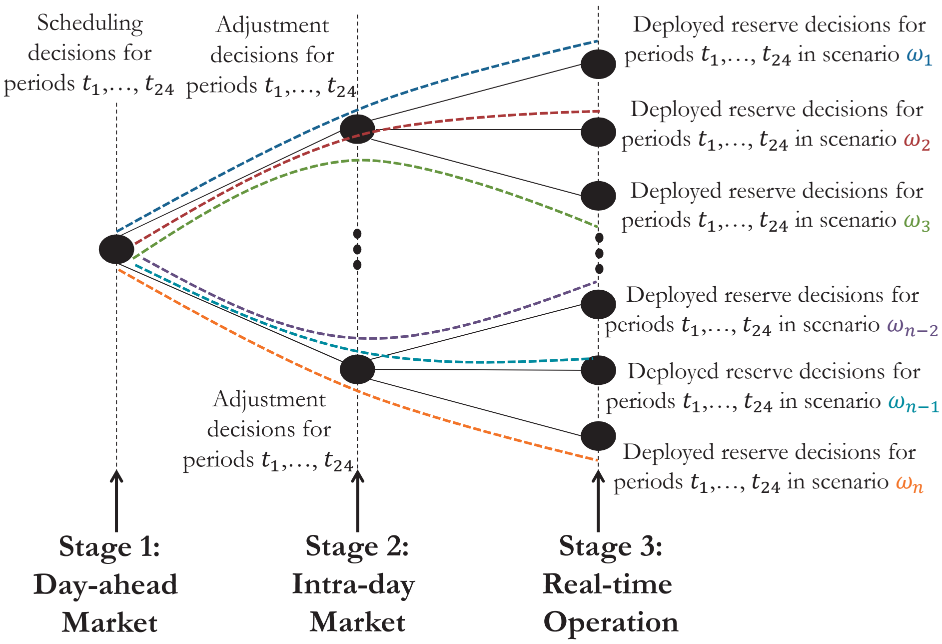

Figure 2.9 – Scenario tree for the three stages of day-ahead market, intra-day market, and real-time operation. Each scenario involves 24 values for the wind power output of wind unit.

to have the same 150 equi-probable scenarios in real-time operation.

2.6.3 Base Case

The base case maintains the assumptions used in the example in Section 2.5, namely $\alpha^{\mathrm{WUs}_1} = \alpha^{\mathrm{WUs}_2} = 1.2$, $\alpha^{\mathrm{WDs}_1} = \alpha^{\mathrm{WDs}_2} = .8$, $\alpha_{\Delta W} = 0.25\%$, $\alpha_{\Delta P} = 0.25\%$, and the limit of reserve capacity is equal to the production capacity of each conventional unit.

Table 2.12 provides details regarding day-ahead profit, expected profit, day-ahead cost, expected cost, and consumer payment resulting from both models.

Under both models, U_{90} and U_{76} incur losses at the day-ahead market, but only U_{90} has a negative expected profit. The total day-ahead producer profit is higher in the three-stage model than in the two-stage model, whereas the total expected profit from the three-stage model is lower than that of the two-stage model. The main reason is that scheduled power of the wind unit has a higher value in the three-stage model than in the two-stage one (1471.3 MW vs 1265.5 MW) that translates to a high profit (as its cost is small). This is the result of

Table 2.12 – Base Case

	3-stage Model		2-stage Model	
Unit i	DA Profit ($)	Exp. Profit ($)	DA Profit ($)	Exp. Profit ($)
1	-8489.42	-4581.29	-10998.97	-3696.75
2	13471.36	13818.44	4575.19	14043.00
3	2175.66	3174.24	3622.79	3896.70
4	13042.15	13400.31	6332.85	14043.00
5	-612.19	282.04	-34.44	136.41
6	2109.44	3269.33	3664.89	3896.70
7	2064.74	2173.20	3435.12	3540.08
8	12954.63	13531.14	4142.90	14043.00
9	42299.73	51345.17	55651.98	59056.00
Wind	16627.21	21358.15	11626.71	11626.71
Total	95643.31	117770.74	82019.03	120584.85
	DA Cost ($)	Exp. Cost ($)	DA Cost ($)	Exp. Cost ($)
	192507.85	174401.51	217498.08	190554.00
	Cons. pay. ($)	Uplift ($)	Cons. pay. ($)	Uplift ($)
	288151.16	9101.61	299517.11	11033.41

information asymmetry on wind production. Also, the day-ahead losses of units U_{90} and U_{76} are higher under the two-stage model that make the total day-ahead profit smaller than that of the three-stage model.

The three-stage model also results in lower day-ahead cost, expected cost, and consumer payment than those from the two-stage model. The savings in expected cost and consumer payment obtained in the three-stage model as a percentage of the corresponding values in the two-stage model are 8.48% and 3.79%, respectively.

For the purpose of comparing day-ahead prices, Fig. 2.10 shows the day-ahead prices obtained from the three-stage and two-stage models. At period t_7 (morning peak), the two-stage model results in a higher price than that of the three-stage model. Also, at period t_{24} (when the lowest load occurs) the price from the three-stage model is considerably lower than that of the two-stage model.

Despite the higher prices obtained from the two-stage model over several periods, an uplift of \$11,033.41 is still required, and this uplift is higher than the uplift of the three-stage model (\$9101.00). As mentioned above, units U_{90} and U_{76} incur losses in the day-ahead market under both models, and thus, they are paid an uplift. Unit U_{90} is paid an uplift of \$8489.42 under the three-stage model, and \$10998.97 under the two-stage model, while Unit U_{76} receives an uplift of \$612.19 under the three-stage model, and \$34.44 under the two-stage model.

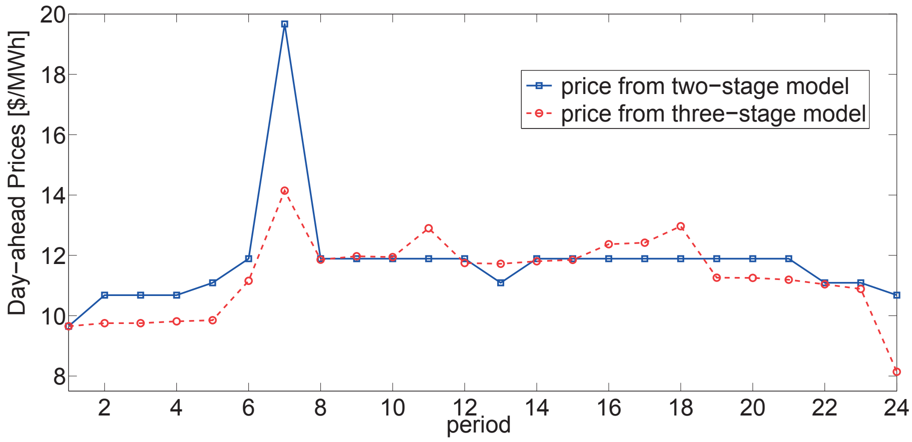

Figure 2.10 – Day-ahead clearing prices from the three-stage model and the two-stage model over all periods.

2.6.4 Analyses of Flexibility of Units for Reserve Provision and Different Adjustment Bounds

The objective of this section is to gain insight on the performance of the three-stage model. For this purpose, we investigate the impact of the availability of reserves and of diverse limits on the intra-day power adjustments considering the following cases:

- Case 1 (not limited):
  - All conventional units provide reserves: $R_i^{\mathrm{U,max}} = R_i^{\mathrm{D,max}} = P_i^{\max}, \forall i$.
  - Wind production at the day-ahead market is limited by the wind installed capacity. That is, the limit of the wind unit is $0 \le W_{qt} \le W_q^{\max}$ in the day-ahead market (constraint (2.7)). Also, for consistency, $0 \le W_{qt} + \Delta W_{qt\omega}^{\mathrm{U}} - \Delta W_{qt\omega}^{\mathrm{D}} \le W_q^{\max}$ (constraint (2.17)).
  - The up/down wind adjustments are limited by the wind installed capacity at the intra-day market. That is, $\Delta W_{qt\omega}^{\mathrm{U}} \le W_q^{\max}$ and $\Delta W_{qt\omega}^{\mathrm{D}} \le W_q^{\max}$ (i.e., $\alpha_{\Delta W} = 1$ in constraint (2.18)).
  - Up/down adjustments of conventional units are up to their maximum power output. That is, $\alpha_{\Delta P} = 1$ in constraint (2.15), and thus, $\Delta P_{it\omega}^{\mathrm{U}} \le P_i^{\max}$ and $\Delta P_{it\omega}^{\mathrm{D}} \le P_i^{\max}$.
- Case 2 (partly limited):

Table 2.13 – Savings in the expected cost and consumer payment for the different cases

	Saving in expected cost (%)	Saving in consumer payment (%)
Case 1	81.54	63.91
Case 2	8.48	3.79
Case 3	8.19	5.61

- All conventional units provide reserves: $R_i^{\mathrm{U,max}} = R_i^{\mathrm{D,max}} = P_i^{\max}, \forall i$.
- Wind production at the day-ahead market is limited at ±20% of the best available wind production forecast. That is, $\alpha^{\mathrm{WDs}_1} = 0.8$ and $\alpha^{\mathrm{WUs}_1} = 1.2$, and thus, $0.8W_{qt}^{\mathrm{DA}} \leq W_{qt} \leq 1.2W_{qt}^{\mathrm{DA}}$ (constraint (2.7)).
- The up/down power adjustments of units at the intra-day stage are limited by 25% of installed capacity. That is, $\alpha_{\Delta P} = \alpha_{\Delta W} = 0.25$, and thus, $\Delta P_{it\omega}^{\mathrm{U}} \leq 0.25P_i^{\max}$ and $\Delta P_{it\omega}^{\mathrm{D}} \leq 0.25P_i^{\max}$, and $\Delta W_{qt\omega}^{\mathrm{U}} \leq 0.25W_q^{\max}$ and $\Delta W_{qt\omega}^{\mathrm{D}} \leq 0.25W_q^{\max}$.

- Case 3 (highly limited):
  - Nuclear and hydro units (U_{400} and U_{50}) do not provide reserves.
  - Wind production at the day-ahead market is limited at ±20% of the best available wind production forecast. That is, $\alpha^{\mathrm{WDs}_1} = 0.8$ and $\alpha^{\mathrm{WUs}_1} = 1.2$, and thus, $0.8W_{qt}^{\mathrm{DA}} \leq W_{qt} \leq 1.2W_{qt}^{\mathrm{DA}}$ (constraint (2.7)).
  - The up/down power adjustments of units at the intra-day stage are limited by 25% of installed capacity. That is, $\alpha_{\Delta P} = \alpha_{\Delta W} = 0.25$, and thus, $\Delta P_{it\omega}^{\mathrm{U}} \leq 0.25P_i^{\max}$ and $\Delta P_{it\omega}^{\mathrm{D}} \leq 0.25P_i^{\max}$, and $\Delta W_{qt\omega}^{\mathrm{U}} \leq 0.25W_q^{\max}$ and $\Delta W_{qt\omega}^{\mathrm{D}} \leq 0.25W_q^{\max}$.

Fig. 2.11 shows that the total expected profit, the expected cost, and the consumer payment obtained from the two-stage model are higher than those of the three-stage model. The savings in expected cost and consumer payment obtained in the three-stage model as a percentage of the corresponding values in the two-stage model are provided in Table 2.13. The difference between these outcomes is larger for case 1 (less restricted), and smaller for the more restricted cases 2 and 3. Therefore, irrespective of the limits imposed on reserves and intra-day unit adjustments, we conclude that the three-stage model has a better performance from the consumer point of view.

The uplift, however, follows a different trend (bottom plot in Fig. 2.11). The three-stage model results in a larger uplift for case 1, while a smaller uplift for case 2 and case 3 than those of the two-stage model. The uplift from the two-stage model is similar in all cases; however the uplift from the three-stage model decreases along with the increase in the restrictions. Note that the uplift amount is small and does not reverse the fact that the consumer payment obtained from the three-stage model is smaller. Understanding this is easy by observing the day-ahead prices in Fig. 2.12. The prices from the three-stage model are lower in case 1 than those in cases 2 and 3. This results in smaller uplifts in cases 2 and 3. Also, these prices are of the same order of magnitude as the day-ahead prices from the two-stage model, and hence, the consumer payments are of the same order of magnitude in case 2 and case 3. In addition, the day-ahead prices from the three-stage model and those from the two-stage model get closer to each other as cases become increasingly restricted.

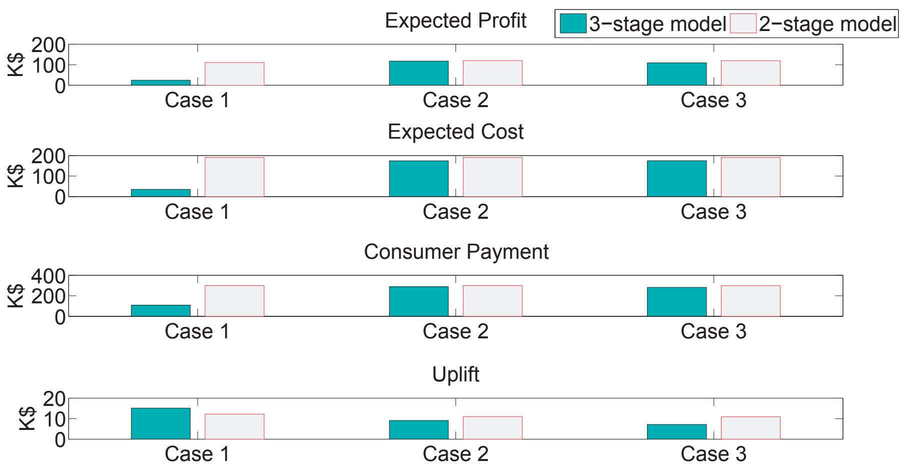

Figure 2.11 – Expected profit, expected cost, consumer payment, and uplift for different cases.

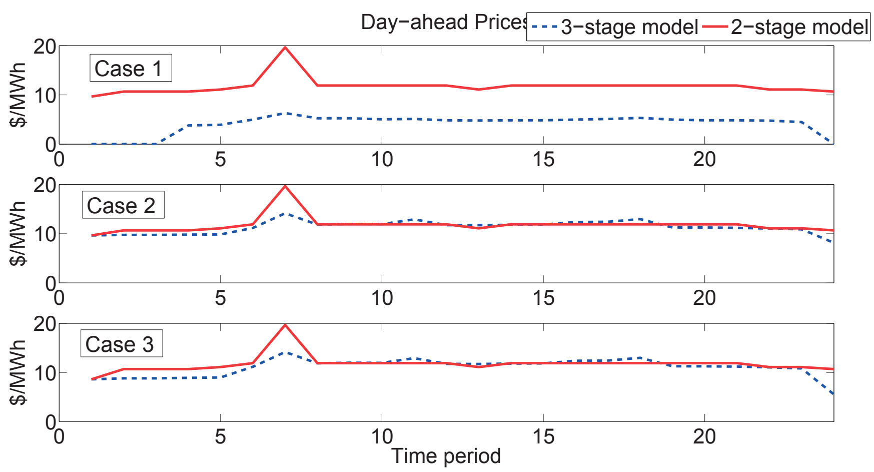

Figure 2.12 – Day-ahead clearing prices for different cases

We also simulate these models on different load profiles (shown in Fig. 2.13) and observe similar outcomes.

Fig. 2.14 shows that a higher expected cost is obtained by using the two-stage model than that of the three-stage model irrespective of the limiting bounds for five different load profiles and the different cases. Note that the large difference between expected costs of the three stage model and the two stage model for case 1 is due to the wide (and rather unrealistic) bounds assumed for the intra-day power adjustments of the wind unit as well as conventional units. The expected costs of the three-stage model get closer to those from the two-stage model when bounds become tighter, as in case 2 and case 3.

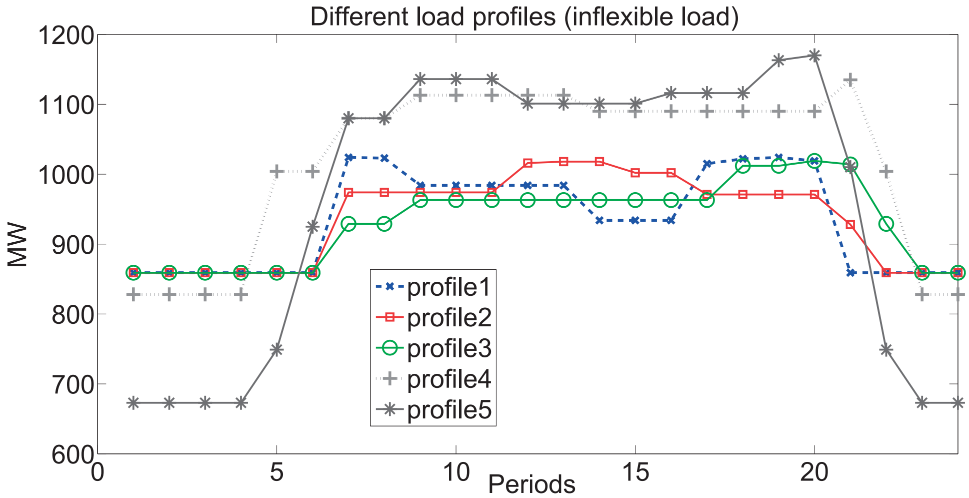

Figure 2.13 – Different load profiles

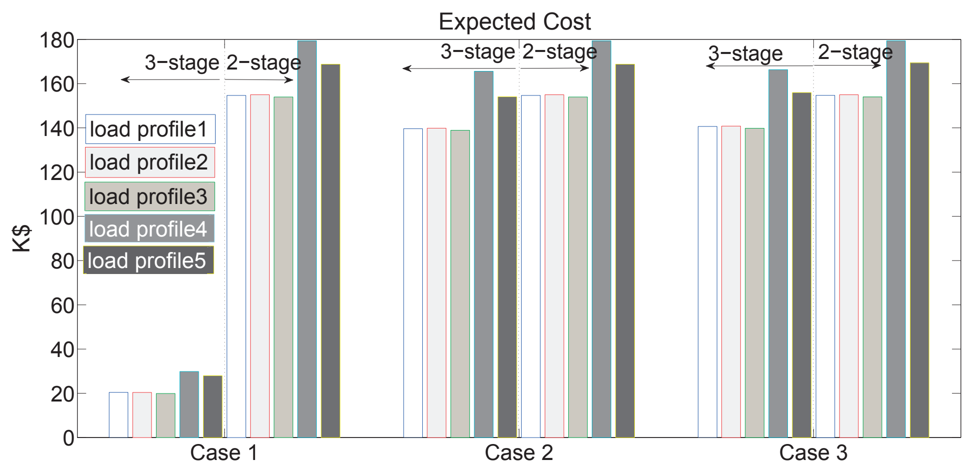

Figure 2.14 – Expected costs for different load profiles and different limited cases

Table 2.14 provides the savings in expected cost and consumer payment obtained in the three-stage model as a percentage of the corresponding values in the second-stage model. The savings in case 1 are large due to the wide bounds assumed for the intra-day power adjustments of the wind unit as well as the conventional units.

Table 2.14 – Savings in expected cost and consumer payment for the different load profiles [%]

	Savings in Exp. Cost			Savings in Consumer Pay.		
Load profile	case 1	case 2	case 3	case 1	case 2	case 3
1	86.80	9.72	9.07	75.78	6.29	11.85
2	86.85	9.75	9.16	74.60	6.34	11.94
3	87.07	9.79	9.20	73.75	6.71	12.63
4	83.36	7.66	7.28	66.22	3.18	5.42
5	83.42	8.71	7.93	67.44	7.57	8.75

In addition to the expected value, another metric to evaluate the performance of stochastic optimization problems is the standard deviation. It is desirable to have a cost with both small expected value and small variance, since this means that the operation cost is expected to be small with a low probability of obtaining a cost very different from the expected cost.

The standard deviations for the different load profiles considered and the different cases analyzed are provided in Table 2.15.

The standard deviations of both models are of the same order of magnitude for case 1 (all load profiles). For case 2, the standard deviations from the two-stage model are smaller than those from the three-stage model. This observation is, however, reversed for case 3. Therefore, a general conclusion regarding the standard deviation of cost from these instances cannot be obtained. In other words, none of these models guarantee a smaller variability of cost as compared to the other one. That is, the three-stage model improves the cost in term of expectation, but the variability of the cost around the expected value is similar to that of the two-stage model.

Table 2.15 – Standard deviations from the three-stage model and the two-stage model for the different load profiles [$]

	Case 1		Case 2		Case 3	
Load profile	3-stage model	2-stage model	3-stage model	2-stage model	3-stage model	2-stage model
1	1.10×10^4	3.61×10^4	3.08×10^4	7.45×10^3	7.58×10^3	1.32×10^4
2	1.05×10^4	3.53×10^4	3.04×10^4	6.71×10^3	9.20×10^3	1.18×10^4
3	9.30×10^3	4.33×10^4	2.95×10^4	7.84×10^3	6.28×10^3	1.21×10^4
4	1.09×10^4	4.52×10^4	3.57×10^4	6.76×10^3	1.02×10^4	1.34×10^4
5	1.19×10^4	4.04×10^4	3.28×10^4	1.44×10^4	7.34×10^3	8.74×10^3

Finally, the VSS calculated for the three-stage model is compared with that of the two-stage model. The results are provided in Table 2.16.

The three-stage model has a better performance than the two-stage model (i.e, higher VSS) for all case studies except for those pertaining to load profile 4. In this case, the use of the optimal first-stage solution of the deterministic model without recourse, denoted by x^{MV} in Section 2.4.3, causes load-shedding in real-time operation, where the wind power output is realized under the two-stage model. This results in a high cost, and consequently, a large difference between the optimal value of the two-stage model and that of the deterministic model.

Table 2.16 – The VSS [%]

	Three-stage model			Two-stage model		
Load profile	case 1	case 2	case 3	case 1	case 2	case 3
1	4.94	0.32	0.31	0.01	0.01	0.01
2	4.96	0.12	0.11	0.01	0.01	0.01
3	5.06	0.23	0.22	0.01	0.01	0.01
4	3.79	1.31	1.30	6.19	6.19	6.19
5	3.71	0.22	0.22	1.41	1.41	1.41

2.6.5 Computation Time

In this section, we elaborate on the computational aspect of the proposed model by considering different number of scenarios and different number of units.

For the simulations, we use CPLEX 12.5.0 under MATLAB on a computer with two Intel(R) Core(TM) processors clocking at 2.7 GHz and 8 GB of RAM. The sizes of the proposed models in terms of numbers of variables and constraints, and computation time for the base case are provided in Table 2.17.

Table 2.17 – Dimension of the three-stage and two-stage models (base case)

	3-stage Model	2-stage Model
No. of binary variables	216	216
No. of continuous variables	375432	217232
No. of total variables	375648	217248
No. of constraints	786744	409320
Computation time (s)	123	48

We should note that the computation times reported are an indication of the tractability of a three-stage model, and that using industry-grade computers and parallelization should allow achieving the required solution times.

First, we fix the number of scenarios to 15 in the third stage and consider different numbers of scenarios in the second stage. The corresponding computation time and the expected cost are provided in Table 2.18.

The computation time increases with the problem size. However, it remains within an acceptable range (e.g., less than 8 minute for a problem size larger than 0.7 million variables and 1.5 million constraints). The increases in the total number of scenarios (from 150 to 225 and from 150 to 300) result in the same expected cost, which is slightly higher than the expected cost obtained in the case with 150 scenarios. In other words, the sensitivity of the expected cost decreases as the number of second-stage scenarios increases.

Table 2.18 – Computation time for different number of scenarios in the second stage (10 units, 24 buses, 15 scenarios in the third stage)

No. of scenarios in the second stage	10	15	20
No. of scenarios in the third stage	15	15	15
Total No. of scenarios	150	225	300
Total No. of constraints	786,744	1,179,264	1,571,784
Total No. of decision variables	375,648	562,848	750,048
Expected cost ($)	1.74×10^5	1.77×10^5	1.77×10^5
Computation time (s)	123	235	445

Table 2.19 provides the computation time for different number of the scenarios in the third stage if the number of the second-stage scenarios is fixed to 10. The computation time does not change significantly from 150 scenarios to 250 scenarios, while it increases to 491 s if considering 350 scenarios, for which the size of the problem is significantly larger (i.e., 0.9 million variables and 1.8 million constraints). The increases in the total number of scenarios (from 150 to 250 and from 150 to 350) result in the same expected cost, which is slightly higher than the expected cost obtained in the case with 150 scenarios. In other words, the sensitivity of the expected cost decreases as the number of third-stage scenarios increases.

Given Tables 2.19 and 2.18, we infer that the sensitivity of the expected cost decreases as the total number of scenarios increases.

In short, an increase in the number of scenarios involves a better uncertainty description, and hence, a possible change in expected cost. However, this is valid up to a certain number of scenarios (in the case study, 225). Once this number of scenarios is reached, the uncertainty description is accurate enough and the expected cost remains unaltered. If this number of

Table 2.19 – Computation time for different number of scenarios in the third stage (10 units, 24 buses, 10 scenarios in the second stage)

No. of scenarios in the second stage	10	10	10
No. of scenarios in the third stage	15	25	35
Total No. of scenarios	150	250	350
Total No. of constraints	786,744	1,317,144	1,847,544
Total No. of decision variables	375,648	562,848	750,048
Expected cost ($)	1.74×10^5	1.77×10^5	1.77×10^5
Computation time (s)	123	147	491

scenarios is increased, the expected cost remains the same, whereas the computation time increases.

Table 2.20 – Computation time for the different number of generators (24 buses, 150 scenarios)

No. of units	10	15	20
No. of binary variables	216	336	456
Total No. of decision variables	375,648	448,008	520,368
Total No. of constraints	786,744	964,944	1,143,144
Expected cost ($)	1.74×10^5	1.75×10^5	1.75×10^5
Computation time (s)	123	182	590

Finally, Table 2.20 provides computation times for different number of units if 150 scenarios are considered. With the increase in the number of units, the size of the problem and the number of binary commitment variables increase, and hence, the computation time increases as well.

2.6.6 Case Study Conclusion

We present a three-stage stochastic model to clear the day-ahead market, which explicitly represents an intra-day market and real-time operation. We then compare the outcomes of this model with results from a two-stage model, which includes a prognosis solely of real-time operation.

The simulation outcomes show that the proposed three-stage model has a better performance than the two-stage one as a result of more informed decisions at the day-ahead market. That is, the three-stage model results in lower day-ahead cost, expected cost, total expected profit, and consumer payment than those from the two-stage model.

Additionally, the day-ahead peak prices obtained from the three-stage model are lower than those from a two-stage model. This results from the use of information about evolving wind power forecast across market stages in the three-stage model, and therefore, more efficient "positioning" of the units in term of day-ahead power production schedules, as well as intra-day power adjustments and deployed reserves.

The VSS also confirms that the use of three-stage model is beneficial to a system with a large amount of uncertain wind production over a two-stage one.

Regarding computation time, our analyses show that although the computation time increases with the problem size, it remains still within an acceptable range. The sensitivity of the expected cost decreases as the number of the scenarios increases. An increase in the number of scenarios involves a better uncertainty description (and consequently a possible change in the expected cost), but up to a certain number of scenarios. Once this number is reached, the uncertainty description cannot improve additionally and the expected cost remains the same, whereas the computation time increases. The computation times reported are an indication of the tractability of a three-stage model. Using industry-grade computers and parallelization techniques should help achieving the required solution times.

The remarks above are concluded by applying the three-stage model to different load profiles, and by considering different limits on adjustment bounds and flexibility of units to provide reserves. Our simulation results indicate that the outcomes from the three-stage model and the two-stage one get closer as restrictions get tighter. The small bounds are translated into less energy trading in the intra-day market, and hence, the results of the three-stage model get closer to those from two-stage one.

These outcomes suggest that replacing a deterministic model with a three-stage model, not a two-stage one, has clear advantages. In other words, if the industry decides to move toward using a a stochastic clearing algorithm (and if it has sufficient computational resources to do so), such a clearing algorithm should be a three-stage one, not a two-stage one.

2.7 Summary and Conclusion of the Chapter

The evolving market conditions, including an increasing number of intra-day markets (from the energy trading point of view) and the growth of renewable generation (from the technology point of view), call for a revise in market-clearing models.

With the aim of obtaining better informed day-ahead decisions, we propose a multi-stage stochastic clearing model. In other words, we argue that if the use of a stochastic clearing model is adopted in systems with a large amount of renewable production, it should be a multi-stage stochastic model, and not a two-stage one.

In a multi-stage clearing model, not only different realizations of renewable power output are considered, but also how these realizations evolve from day-ahead forecasts into real-time values are taken into account. A multi-stage model allocates flexibility for the contribution of renewable production in both the day-ahead and intra-day markets in form of scheduled productions and their adjustments. In other words, the information on how uncertain renewable production develops across the market floors, as well as, allowing flexibility for the contribution of renewable generation in both the day-ahead and intra-day markets improve the market outcomes and integration of renewable generation.

3 Pricing Schemes Pertaining to A Stochastic Non-Convex Market-Clearing Model

3.1 Introduction

When it comes to electricity markets, an accurate modeling of the underlying physics of power systems is important to obtain *right* market outcomes. Market outcomes include scheduled power productions that must respect the non-continuous operating nature (non-convexities) of power system elements, in particular generating units.

To precisely model non-convexities pertaining to the technical characteristics and operation conditions of power system elements, integer variables are the key. For instance, to model physical conditions of generating units such as the start-up and shut-down sequences, binary variables are used. Therefore, the corresponding clearing problem is formulated as a Mixed-Integer Linear Programming problem (MILP). Although the MILP problem allows to obtain production schedules consistent with the operation conditions of the power system, it results in a number of challenges pertinent to economic aspects of the market.

To trade the electric energy, marginal prices are recognized to provide the *right* market signals in competitive markets, as they are appropriate prices to achieve short-term economic efficiency and long-term cost recovery [53]. Among other relevant properties of marginal prices, reaching market equilibrium is a distinguished feature. In an equilibrium, market prices are such that all participants are better off to follow market outcomes. That is, no agent incurs losses under these prices and no agent earns a higher profit by deviating from the schedule assigned. This implies that market players have no incentive to submit inaccurate information. In other words, marginal pricing promotes *truth-telling* in the market [61]. Marginal prices can be obtained as dual variables of power balance equations for convex market-clearing problems. This connection is, however, missing in MILP problems due to the inherent non-convex structure, which often leads to a non-zero duality gap between the primal and dual counterparts.

In the presence of non-convexities, different pricing approaches are proposed to tackle this problem in practice. As a solution, [46] proposes to fix the integer decisions at their optimal values obtained from sloving the MILP model, and to derive prices from the dual problem of the resulting continuous primal problem. The clearing prices obtained from this approach are the closest valid prices that can be defined for the corresponding non-convex clearing problem. This approach seems to be satisfactory in practice, as PJM follows a similar implementation [46] . However, obtaining prices from the dual problem of a relaxed continuous version of the original MILP clearing problem may yield situations where some producers cannot recover their costs. The reason is that such pricing approaches do not fully reflect costs pertaining to discrete decisions, such as the start-up cost of a unit. In other words, the prices obtained do not encompass cost-recovery of discontinuous costs. Such marginal prices may lead to situations where financial losses occur to an extent that the corresponding producers may leave the market. This may eventually lead to a financial loss of welfare and market inefficiency.

To mitigate this problem, a common practice is to compensate each producer incurring losses through a side-payment called uplift. A simple example is as follows. Suppose that a thermal unit is scheduled to generate a certain power under a marginal price which is equal to its marginal production cost. Therefore, the unit cannot recover its start-up cost. This fixed cost is, thus, compensated using an uplift, which is paid by all demands to this thermal unit. In such a situation, the owner of the unit may try to suggest a higher start-up cost than its real one to earn more money by being paid a higher uplift than the actual cost.

This example shows that uplift is not economically a neat concept. Uplifts do not promote truth-telling in the market, rather they encourage strategic pay-as-bid behavior. The uplifts are discriminatory, and their implementation requires a detailed regulation. Hence, alternative pricing methods in non-convex electricity markets are of interest of the electricity market community.

Thus far, we have described the existing pricing issue in deterministic markets. As presented in the previous chapter, a high penetration of renewable generation calls for the use of stochastic market-clearing models, where the system power balance results in a significant connection between power production schedules in the day-ahead market, power adjustments in intra-day markets, and deployed reserves in real-time operation. These connections in the quantities of different market stages result in links between the prices obtained from the corresponding market stages. Therefore, moving toward the use of stochastic market-clearing models increases the degree of complexity of the pricing problem.

In short, in a system with a large amount of renewable generation, day-ahead prices are effected by non-convexities due to operational conditions, as well as by uncertainty associated with renewable generation. In this context, we strive to derive a new pricing scheme with the aim of obtaining a set of uniform day-ahead prices with cost-recovery properties at the crossroads of stochasticity and non-convexity.

3.2 A New Pricing Mechanism with Cost Recovery

We, first, elaborate on the desired properties that a pricing scheme is expected to meet.

Our focus is to obtain a set of day-ahead prices in a market environment with stochastic renewable generation. A desired property of these prices is to reflect the uncertainty associated to renewable generation. Therefore, these prices must be obtained from a model which appropriately considers stochastic renewable generation. Referring to Chapter 2, to optimally integrate renewable generation, the power production outputs of conventional units (e.g., thermal and hydro units) are scheduled in the day-ahead market considering all possible realizations of renewable generation at real-time operation. Therefore, the day-ahead scheduled productions are affected by stochastic generation, and the day-ahead prices as well. In other words, uncertain renewable generation transfers its impact on day-ahead prices through day-ahead scheduled productions. Furthermore, realizations of renewable production require reserve deployments in real-time operation, and consequently, result in balancing prices which are linked to the day-ahead prices. That is, uncertain renewable generation has additionally an impact on day-ahead prices through balancing prices.

Therefore, explicitly modeling the sequence of decision-making process is important. This entails the day-ahead market, a number of intra-day markets, and real-time operation, and implies the use of a multi-stage stochastic clearing model, similar to the one proposed in Chapter 2.

The marginal prices obtained using the conventional pricing approach do not embody cost-recovery features. This motivates a new pricing mechanism, where day-ahead prices guarantee cost-recovery conditions to producers. The cost-recovery conditions need to be defined in the presence of high renewable production, and then, considered as market constraints in a clearing model. Such a clearing model results in marginal prices with cost-recovery features that eliminate a need for uplifts.

We should note here that two types of uplift are identified by economists: *make-whole payments* and *lost opportunity profits*.

Make-whole payments ensure that each unit can recover its incurred cost by producing the energy at the level assigned to it in the market. This type of uplift does, therefore, focus on the production cost of the unit (marginal production cost and fixed cost). On the other hand, the uplift related to lost opportunity profits ensures that each online unit receives its maximum possible profit under the existing market prices. Some units may be willing to produce more under the final prices, but fulfilling such a wish may not be possible as it may cause that the market would not be in equilibrium. A solution to encourage units to still follow the assigned productions is to pay them their lost opportunity profits through a side-payment.

Our focus is to remove the need for uplift in term of make-whole payments. Therefore, the final day-ahead prices provided by the methodology proposed may cause some units to experience lost opportunity profits. That is, considering the final prices some units are willing to produce more, but this is not possible for the market to be in equilibrium. Uplifts (of reduced magnitude) can be used to remedy this side effect and to cover the lost opportunity revenue. These uplifts are then socialized among consumers. For the sake of simplicity, we do not consider the lost opportunity profits.

Finally, the new day-ahead prices obtained shall deviate in the least possible manner from conventional marginal prices. This implies that social welfare deviates the least from its maximum value.

Regarding the desired properties above and inspired by the approach in [59], we provide a pricing scheme for a non-convex stochastic clearing model such that the producers do not incur losses.

The proposed approach is as follows:

1. We formulate a stochastic market-clearing model with binary unit-commitment variables, which results in a MILP problem.
2. The binary variables are relaxed to be continuous to obtain a relaxed linear primal problem.
3. The dual of the relaxed linear primal problem is then obtained.
4. Next, we formulate a primal-dual minimization problem whose objective function is the duality gap and that is subject to primal and dual constraints. Since the integrity constraints of the primal problem are also included, the primal-dual problem is a MILP. The quantities and prices are output of this model. It is important to note that minimizing the duality gap is tantamount of getting as close as possible to maximum welfare, but ensuring cost recovery.

5. To guarantee cost recovery for producers, we incorporate cost-recovery equations as extra constraints in the primal-dual problem.

In the presence of stochasticity, the definition of cost-recovery conditions for producers is not unique. In this sense, three views can be expressed:

1. Cost-recovery conditions in the day-ahead market: To satisfy cost-recovery conditions in the day-ahead market, the day-ahead prices must ensure that the day-ahead profit of each unit is not negative. That is, the day-ahead revenues minus the day-ahead costs (including marginal production costs and fixed costs) must be either zero or a positive value.
2. Cost-recovery conditions in expectation: In the same vein, cost-recovery conditions in expectation are imposed. That is, average cost recovery of each unit over all realizations of stochastic generation is guaranteed, i.e., the expected revenue minus the expected cost of each unit is required to be non-negative.
3. Cost-recovery conditions per scenario: The most conservative interpretation of cost-recovery conditions indicates that for each individual realization of stochastic generation the per scenario profit of each unit is required to be non-negative.

3.3 Assumptions

We consider the following assumptions to formulate the proposed pricing optimization model. Many of these assumptions are similar to those stated in Section 2.3.

- The uncertain renewable resource is wind power generation. Wind generation leads renewable production in term of installed capacity and technological development [31]. Considering other stochastic resources does not change the nature of the model proposed.
- The production of wind units depends on the uncertain wind power realization. Wind power production is represented using scenarios. These scenarios are built using historical wind production data as samples without applying any scenario generation and scenario reduction techniques.
- The wind producers are assumed to offer their production at zero cost. This is in line with the actual market practice of wind production in some countries, where as much wind generation as possible shall be absorbed.

- We assume that loads are deterministic. This assumption allows focusing on wind uncertainty. Note that in systems with imperfect wind power production, load variability is generally small in comparison with wind uncertainty.

- Loads are assumed to be inelastic. This assumption can easily be removed from the model without modeling or computational complications.

- Generation cost functions are assumed to be linear for simplicity. However, note that quadratic cost functions can be accurately approximated using piecewise linear functions. Also, all generating units are required to offer their energy at marginal costs.

- The costs of the deployed reserves is assumed to be equal to the cost of producing energy. Other criteria about the cost of the deployed reserves could be straightforwardly considered in the proposed formulation.

- The stochastic clearing model co-optimizes energy and reserve deployment without explicit reserve offers in the day-ahead market. Units and flexible demands can specify the reserve levels that they are willing to provide, and hence, we given them the opportunity of reserve deployment for a profit.

- A linear representation of the transmission network is considered through a dc load flow model where losses are neglected.

- We do not consider security criteria, such as n-1, to focus on the analyses of wind uncertainty, and also, to avoid an increase in the size of the model which consequently leads to an increase in computation time.

- The non-convexities considered are solely those due to non-zero minimum power outputs of conventional units, start-up costs, and binary unit-commitment variables. Taking into account other source of non-convexities, such as shut-down costs and minimum up/down time constraints, is straightforward.

These assumptions are made for convenience, simplicity, and the sake of computational tractability.

3.4 Decision-Making Process

The decision-making process is based on the multi-stage stochastic clearing model described in Section 2.2. To reduce complexity but still satisfying the need for a stochastic clearing model in the presence of uncertainty, we consider the two-stage model (2.44) in this chapter. Note that the principles of the proposed pricing approach are fully applicable to any multi-stage stochastic clearing model, and the use of two-stage model is for the sack of simplicity.

The decision-making sequence involves day-ahead market and real-time operation. The day-ahead outcomes, including scheduled power outputs and prices, are here-and-now decisions as they are made before uncertain parameters are realized, while in real time deployed reserves (balancing actions) and balancing prices represent wait-and-see decisions which are recourse actions taken after uncertainty realizes.

3.5 Model Description

In this section, we provide the mathematical description of the proposed pricing scheme. For this purpose, we first present the primal two-stage clearing model in Section 3.5.1. Next, We formulate the corresponding dual problem in Section 3.5.2, and the corresponding primal-dual problem in Section 3.5.3. Section 3.5.4 provides mathematical descriptions of cost-recovery conditions for units. Next, the linearization of cost-recovery conditions is presented in Section 3.5.5. Finally, we provide the complete linear mixed-integer model in Section 3.5.6.

3.5.1 Primal Problem: Two-Stage Clearing Model

The first step of the proposed pricing approach is to formulate a two-stage clearing model. We take the two-stage model (2.44) and skip to elaborate on the details as this model is described in details in Section 2.4. We just slightly modify the two-stage model (2.44) according to the simplifying assumptions indicated in Section 3.3. These modifications are related to wind production as follow.

The wind producers are assumed to offer their production at zero cost. That is, C_q is zero in the cost function (2.34). Therefore, the objective function includes the following two components:

- The day-ahead cost involving the start-up costs and production costs of conventional units over all periods of the market horizon:

$$\sum_{t=1}^{N_T} \sum_{i=1}^{N_G} (C_{it}^{\mathrm{SU}} + C_i P_{it}) \tag{3.1}$$

- The expected balancing cost involving the cost of deployed reserves and involuntary load shedding:

$$\sum_{\omega=1}^{N_\Omega} \pi_\omega \Big[\sum_{t=1}^{N_T} \big(\sum_{i=1}^{N_G} C_i (r_{it\omega}^{\mathrm{U}} - r_{it\omega}^{\mathrm{D}}) + \sum_{j=1}^{N_L} V_{jt}^{\mathrm{LOL}} L_{jt\omega}^{\mathrm{shed}} \big) \Big] \tag{3.2}$$

Additionally, we assume that wind power output can be scheduled within a range of zero and the installed capacity in the day-ahead market. Therefore, constraint (2.7) changes to:

$$0 \le W_{qt} \le W_q^{\max} \tag{3.3}$$

The formulation of the two-stage MILP clearing model is provided in the following. We should note that the corresponding dual variables are listed in front of the constraints that are used when formulating the dual problem.

$$\underset{\Xi_p}{\text{Minimize}}$$

$$\sum_{t=1}^{N_T} \sum_{i=1}^{N_G} C_{it}^{\mathrm{SU}} + \sum_{\omega=1}^{N_\Omega} \pi_\omega \Big[\sum_{t=1}^{N_T} \big(\sum_{i=1}^{N_G} C_i (P_{it} + r_{it\omega}^{\mathrm{U}} - r_{it\omega}^{\mathrm{D}}) + \sum_{j=1}^{N_L} V_{jt}^{\mathrm{LOL}} L_{jt\omega}^{\mathrm{shed}} \big) \Big] \tag{3.4a}$$

subject to

Day-ahead constraints:

$$\sum_{i \in M_n^{\mathrm{G}}} P_{it} + \sum_{q \in M_n^{\mathrm{Q}}} W_{qt} - \sum_{j \in M_n^{\mathrm{L}}} L_{jt} - \sum_{r \in \Lambda_n} B_{nr}(\theta_{nt} - \theta_{rt}) = 0 : (\lambda_{nt}), \forall n, \forall t \tag{3.4b}$$

$$-f_{nr}^{\max} \le B_{nr}(\theta_{nt} - \theta_{rt}) \le f_{nr}^{\max} : (\epsilon_{nrt}^{-\max}, \epsilon_{nrt}^{\max}), \forall n, \forall r \in \Lambda_n, \forall t \tag{3.4c}$$

$$u_{it} P_i^{\min} \le P_{it} \le u_{it} P_i^{\max} : (\phi_{it}^{\min}, \phi_{it}^{\max}), \forall i, \forall t \tag{3.4d}$$

$$W_{qt} \le W_q^{\max} : (\rho_{qt}^{\mathrm{W}}), \forall q, \forall t \tag{3.4e}$$

$$K_i^{\mathrm{SU}}(u_{it} - u_{i,t-1}) \le C_{it}^{\mathrm{SU}} : (\beta_{it}), \forall i, \forall t \tag{3.4f}$$

$$RD_i \le P_{it} - P_{i,t-1} \le RU_i : (\psi_{it}^{\min}, \psi_{it}^{\max}), \forall i, \forall t \tag{3.4g}$$

$$\theta_{1t} = 0 : (\sigma_{1t}), \forall t \tag{3.4h}$$

$$u_{it} \in \{0, 1\}, \forall i, \forall t \tag{3.4i}$$

Real-time operation constraints:

$$\sum_{i \in M_n^{\mathrm{G}}} (r_{it\omega}^{\mathrm{U}} - r_{it\omega}^{\mathrm{D}}) + \sum_{q \in M_n^{\mathrm{Q}}} (W_{qt\omega}^{\mathrm{RT}} - W_{qt} - w_{qt\omega}^{\mathrm{spill}})$$

$$+ \sum_{r \in \Lambda_n} B_{nr}(\theta_{nt} - \theta_{nt\omega} - \theta_{rt} + \theta_{rt\omega}) + \sum_{j \in M_n^{\mathrm{L}}} L_{jt\omega}^{\mathrm{shed}} = 0 : (\lambda_{nt\omega}), \forall n, \forall t, \forall \omega \tag{3.4j}$$

$$-f_{nr}^{\max} \le B_{nr}(\theta_{nt\omega} - \theta_{rt\omega}) \le f_{nr}^{\max} : (\epsilon_{nr\omega t}^{-\max}, \epsilon_{nr\omega t}^{\max}), \forall n, \forall r \in \Lambda_n, \forall t, \forall \omega \tag{3.4k}$$

$$P_{it} + r_{it\omega}^{\mathrm{U}} - r_{it\omega}^{\mathrm{D}} \le u_{it} P_i^{\max} : (\phi_{it\omega}^{\max}), \forall i, \forall t, \forall \omega \tag{3.4l}$$

$$-P_{it} - r^{\mathrm{U}}_{it\omega} + r^{\mathrm{D}}_{it\omega} \le -u_{it}P^{\min}_{i} : (\phi^{\min}_{it\omega}), \forall i, \forall t, \forall \omega \tag{3.4m}$$

$$RD_i \le \left(P_{it} + r^{\mathrm{U}}_{it\omega} - r^{\mathrm{D}}_{it\omega}\right) - \left(P_{i,t-1} + r^{\mathrm{U}}_{i,t-1,\omega} - r^{\mathrm{D}}_{i,t-1,\omega}\right) \le RU_i :$$
$$(\psi^{\min}_{it\omega}, \psi^{\max}_{it\omega}), \forall i, \forall t, \forall \omega \tag{3.4n}$$

$$r^{\mathrm{U}}_{it\omega} \le R^{\mathrm{U,max}}_{it} : (\alpha^{\mathrm{U}}_{it\omega}), \forall i, \forall t, \forall \omega \tag{3.4o}$$

$$r^{\mathrm{D}}_{it\omega} \le R^{\mathrm{D,max}}_{it} : (\alpha^{\mathrm{D}}_{it\omega}), \forall i, \forall t, \forall \omega \tag{3.4p}$$

$$L^{\mathrm{shed}}_{jt\omega} \le L_{jt} : (\mu_{jt\omega}), \forall j, \forall t, \forall \omega \tag{3.4q}$$

$$w^{\mathrm{spill}}_{qt\omega} \le W^{\mathrm{RT}}_{qt\omega} : (\gamma_{qt\omega}), \forall q, \forall t, \forall \omega \tag{3.4r}$$

$$\theta_{1t\omega} = 0 : (\sigma_{1t\omega}), \forall t, \forall \omega \tag{3.4s}$$

Variable declarations:

$$0 \le P_{it}, C^{\mathrm{SU}}_{it}, \forall i, \forall t$$
$$0 \le W_{qt}, \forall q, \forall t$$
$$0 \le r^{\mathrm{U}}_{it\omega}, r^{\mathrm{D}}_{it\omega}, \forall i, \forall t, \forall \omega$$
$$0 \le w^{\mathrm{spill}}_{qt\omega}, \forall q, \forall t, \forall \omega$$
$$0 \le L^{\mathrm{shed}}_{jt\omega}, \forall j, \forall t, \forall \omega \tag{3.4t}$$

The problem (3.4) minimizes the expected operation cost (3.4a) considering day-ahead scheduling constraints (3.4b)-(3.4i), real-time operation constraints (3.4j)-(3.4s), and variable declarations (3.4t). The minimization is over the set of primal variables $\Xi_p = \{C^{\mathrm{SU}}_{it}, u_{it}, P_{it}, \forall i, \forall t; W_{qt}, \forall q, \forall t; \theta_{nt}, \forall n, \forall t; r^{\mathrm{U}}_{it\omega}, r^{\mathrm{D}}_{it\omega}, \forall i, \forall t, \forall \omega; w^{\mathrm{spill}}_{qt\omega}, \forall q, \forall t, \forall \omega; \theta_{nt\omega}, \forall n, \forall t, \forall \omega; L^{\mathrm{shed}}_{jt\omega}, \forall j, \forall t, \forall \omega;\}$, as described in Chapter 2.

3.5.2 Dual Problem of Two-stage Clearing Model

The second step of the proposed approach is to obtain a dual formulation of the primal clearing model (3.4). For this purpose, the integrity constraint (3.4i) in problem (3.4) is relaxed to be:

$$0 \le u_{it} \le 1, \forall i, \forall t : (\upsilon^{\min}_{it}, \upsilon^{\max}_{it}) \tag{3.5}$$

where $\upsilon^{\min}_{it}$ and $\upsilon^{\max}_{it}$ are the corresponding dual variables.

This relaxed problem is a simple linear program whose dual problem is straightforward to be obtained.

As a reminder, the dual problem of the LP problem in general from (3.6) is formulated in (3.7)

[36].

$$\underset{\mathrm{x}\geq 0}{\text{Minimize}} \quad c^{\mathrm{T}}\mathrm{x} \tag{3.6a}$$

subject to:

$$A\mathrm{x} \geq \mathrm{b}, \quad (\mu) \tag{3.6b}$$

$$C\mathrm{x} = \mathrm{d}, \quad (\lambda) \tag{3.6c}$$

where $\mathrm{x} \in \mathbb{R}^n$, $c \in \mathbb{R}^n$, $A \in \mathbb{R}^{m\times n}$, $\mathrm{b} \in \mathbb{R}^{\mathrm{m}}$, $C \in \mathbb{R}^{q\times n}$, and $\mathrm{d} \in \mathbb{R}^{\mathrm{q}}$.

$$\underset{\mu\geq 0,\lambda}{\text{Maximize}} \quad b^{\mathrm{T}}\mu + d^{\mathrm{T}}\lambda \tag{3.7a}$$

$$\text{subject to:} \quad A^{\mathrm{T}}\mu + C^{\mathrm{T}}\lambda \leq c \tag{3.7b}$$

where $\mu \in \mathbb{R}^m$ and $\lambda \in \mathbb{R}^q$.

In the same vein, the dual formulation of relaxed primal problem (3.4) is:

$$\begin{aligned}
&\underset{\Xi_d}{\text{Maximize}}\\
&\sum_t \Big[-\sum_{n,j\in M_n^{\mathrm{L}}} \lambda_{nt} L_{jt} - \sum_{n,r\in\Lambda_n} (f_{nr}^{\max}\epsilon_{nrt}^{\max} - f_{nr}^{\max}\epsilon_{nrt}^{-\max}) + \sum_i (-\upsilon_{it}^{\max} - \psi_{it}^{\max} RU_i + \psi_{it}^{\min} RD_i)\\
&+ \sum_\omega \Big(-\sum_q \gamma_{qt\omega} W_{qt\omega}^{\mathrm{RT}} - \sum_j \mu_{jt\omega} L_{jt} - \sum_i \psi_{it\omega}^{\max} RU_i + \sum_i \psi_{it\omega}^{\min} RD_i\\
&- \sum_i \alpha_{it\omega}^{\mathrm{U}} R_{it}^{\mathrm{U,max}} - \sum_i \alpha_{it\omega}^{\mathrm{D}} R_{it}^{\mathrm{D,max}} - \sum_{n,r\in\Lambda_n} (f_{nr}^{\max}\epsilon_{nrt\omega}^{\max} - f_{nr}^{\max}\epsilon_{nrt\omega}^{-\max})\Big)\Big]
\end{aligned} \tag{3.8a}$$

subject to

$$C_i + \lambda_{nt} + \rho_{it} + \psi_{it}^{\max} + \psi_{it}^{\min} + \psi_{it\omega}^{\max} - \psi_{it\omega}^{\min} + \phi_{it\omega}^{\max} - \phi_{it\omega}^{\min} \geq 0, \forall i \in M_n^{\mathrm{G}}, \forall n, \forall \omega, \forall t \tag{3.8b}$$

$$\lambda_{nt} + \lambda_{nt\omega} + \rho_{qt}^{\mathrm{W}} \geq 0, \forall q \in M_n^{\mathrm{L}}, \forall n, \forall \omega, \forall t \tag{3.8c}$$

$$1 - \beta_{it} \geq 0, \forall i, \forall t \tag{3.8d}$$

$$\pi_\omega C_i + \lambda_{nt\omega} + \psi_{it\omega}^{\max} - \psi_{it\omega}^{\min} + \alpha_{it\omega}^{\mathrm{U}} + \phi_{it\omega}^{\max} - \phi_{it\omega}^{\min} \geq 0, \forall i \in M_n^{\mathrm{G}}, \forall n, \forall \omega, \forall t \tag{3.8e}$$

$$-\pi_\omega C_i - \lambda_{nt\omega} - \psi_{it\omega}^{\max} + \psi_{it\omega}^{\min} - \alpha_{it\omega}^{\mathrm{D}} - \phi_{it\omega}^{\max} + \phi_{it\omega}^{\min} \geq 0, \forall i \in M_n^{\mathrm{G}}, \forall n, \forall \omega, \forall t \tag{3.8f}$$

$$\sigma_{1t_{|n=1}} + \sum_{r\in\Lambda_n} B_{nr}(\epsilon_{nrt}^{\max} - \epsilon_{nrt}^{-\max}) - \sum_{r\in\Lambda_n} B_{nr}\Big(\lambda_{nt} - \lambda_{rt} + \lambda_{nt\omega} - \lambda_{rt\omega}\Big) = 0, \forall n, \forall \omega, \forall t \tag{3.8g}$$

$$\sigma_{1t\omega_{|n=1}} + \sum_{r\in\Lambda_n} B_{nr}(\epsilon_{nrt}^{\max} - \epsilon_{nrt}^{-\max}) + \sum_{r\in\Lambda_n} B_{nr}(\lambda_{nt\omega} - \lambda_{rt\omega}) = 0, \forall n, \forall \omega, \forall t \tag{3.8h}$$

$$\beta_{it}K_i^{\mathrm{SU}} - \phi_{it}^{\max}P_i^{\max} + \phi_{it}^{\min}P_i^{\min} - \phi_{it\omega}^{\max}P_i^{\max} + \phi_{it\omega}^{\min}P_i^{\min} + \upsilon_{it}^{\max} \geq 0, \forall i, \forall \omega, \forall t \quad (3.8i)$$

$$\pi_\omega V_{jt}^{\mathrm{LOL}} + \lambda_{nt\omega} + \mu_{jt\omega} \geq 0, \forall j \in M_n^{\mathrm{L}}, \forall n, \forall \omega, \forall t \quad (3.8j)$$

$$\lambda_{nt\omega} + \gamma_{qt\omega} \geq 0, \forall q \in M_n^{\mathrm{Q}}, \forall \omega, \forall t \quad (3.8k)$$

$$\epsilon_{nrt}^{\max}, \epsilon_{nrt}^{-\max} \geq 0, \forall n, \forall r \in \Lambda_n, \forall t \quad (3.8l)$$

$$\epsilon_{nrt\omega}^{\max}, \epsilon_{nrt\omega}^{-\max} \geq 0, \forall n, \forall r \in \Lambda_n, \forall \omega, \forall t \quad (3.8m)$$

$$\upsilon_{it}^{\max}, \beta_{it}, \phi_{it}^{\max}, \phi_{it}^{\min}, \psi_{it}^{\max}, \psi_{it}^{\min} \geq 0, \forall i, \forall t \quad (3.8n)$$

$$\rho_{qt}^{\mathrm{W}} \geq 0, \forall q, \forall t \quad (3.8o)$$

$$\phi_{it\omega}^{\max}, \phi_{it\omega}^{\min}, \psi_{it\omega}^{\max}, \psi_{it\omega}^{\min}, \alpha_{it\omega}^{\mathrm{U}}, \alpha_{it\omega}^{\mathrm{D}} \geq 0, \forall i, \forall \omega, \forall t \quad (3.8p)$$

$$\mu_{jt\omega} \geq 0, \forall j, \forall \omega, \forall t, \quad \gamma_{qt\omega} \geq 0, \forall q, \forall \omega, \forall t \quad (3.8q)$$

where $\Xi_d = \{\lambda_{nt}, \forall n, \forall t; \lambda_{nt\omega}, \forall n, \forall t, \forall \omega; \epsilon_{nrt}^{\max}, \epsilon_{nrt}^{-\max}, \forall n, \forall r \in \Lambda_n, \forall t; \epsilon_{nrt\omega}^{\max}, \epsilon_{nrt\omega}^{-\max}, \forall n, \forall r \in \Lambda_n, \forall t, \forall \omega; \phi_{it}^{\max}, \phi_{it}^{\min}, \upsilon_{it}^{\max}, \beta_{it}, \psi_{it}^{\max}, \psi_{it}^{\min}, \forall i, \forall t; \rho_{qt}^{\mathrm{W}}, \forall q, \forall t; \phi_{it\omega}^{\max}, \phi_{it\omega}^{\min}, \psi_{it\omega}^{\max}, \psi_{it\omega}^{\min}, \alpha_{it\omega}^{\mathrm{U}}, \alpha_{it\omega}^{\mathrm{D}}, \forall i, \forall t, \forall \omega; \mu_{jt\omega}, \forall j, \forall t, \forall \omega; \gamma_{qt\omega} \forall q, \forall t, \forall \omega\}$ are the variables of the dual problem.

Among them and of utmost importance are λ_{nt} and $\frac{\lambda_{nt\omega}}{\pi_\omega}$ which are the day-ahead prices and probability-removed balancing prices, respectively.

3.5.3 Primal-Dual Problem

The next step is to formulate the primal-dual form of problem (3.4). The advantage of the primal-dual problem is to allow simultaneously controlling primal variables, i.e., quantities, and dual variables, i.e., prices.

To obtain the primal-dual formulation, we proceed as follows. We first provide the primal-dual formulation in general form using the LP problem (3.6) and its dual problem (3.7). We next apply this mathematical framework to the problem (3.4) and its dual problem (3.8).

Since primal problem (3.6) is convex, its Karush-Kuhn-Tucker (KKT) optimality conditions are necessary and sufficient, and can be formulated as [36]:

Complementarity of primal problem (3.6):

$$A\mathrm{x} \geq \mathrm{b} \quad (3.9a)$$

$$C\mathrm{x} = \mathrm{d} \quad (3.9b)$$

$$\mu^{\mathrm{T}}(A\mathrm{x} - \mathrm{b}) = 0 \quad (3.9c)$$

$$\lambda^{\mathrm{T}}(C\mathrm{x} - \mathrm{d}) = 0 \quad (3.9d)$$

$$\mu \geq 0 \quad (3.9e)$$

Complementarity of dual problem (3.7):

$$A^{\mathrm{T}}\mu + C^{\mathrm{T}}\lambda \leq c \tag{3.9f}$$

$$\mathrm{x}^{\mathrm{T}}(\mathrm{c} - \mathrm{A}^{\mathrm{T}}\mu - \mathrm{C}^{\mathrm{T}}\lambda) = 0 \tag{3.9g}$$

$$\mathrm{x} \geq 0 \tag{3.9h}$$

Primal-dual formulation is [59]:

$$\underset{\mathrm{x},\mu,\lambda}{\text{Minimize}} \quad c^{\mathrm{T}}\mathrm{x} - \mathrm{b}^{\mathrm{T}}\mu - \mathrm{d}^{\mathrm{T}}\lambda \tag{3.10a}$$

subject to

$$A\mathrm{x} \geq \mathrm{b} \tag{3.10b}$$

$$C\mathrm{x} = \mathrm{d} \tag{3.10c}$$

$$A^{\mathrm{T}}\mu + C^{\mathrm{T}}\lambda \leq c \tag{3.10d}$$

$$\mathrm{x} \geq 0, \quad \mu \geq 0 \tag{3.10e}$$

The objective function in problem (3.10) is the duality gap, $c^{\mathrm{T}}\mathrm{x} - \mathrm{b}^{\mathrm{T}}\mu - \mathrm{d}^{\mathrm{T}}\lambda$. Problem (3.10) minimizes this gap subject to primal constraints (3.10b) and (3.10c), the dual constraint (3.10d), and the variable declaration (3.10e). If the optimal value of the objective function (3.10a) is zero (i.e., the duality gap is therefore zero), strong duality hold. That is, the primal problem and dual problem have the same optimal value of objective function, and problems (3.9) and (3.10) are, thus, equivalent.

The advantage of problem (3.10) is to provide the possibility of including additional constraints at the cost of deviating from a zero duality gap. Therefore, the cost recovery conditions of producers can be added to the primal-dual form of the problem as extra constraints. Before elaborating on it, we provide the primal-dual formulation of the two-stage clearing problem:

$$\begin{aligned}
&\underset{\Xi_p,\Xi_d}{\text{Minimize}} \\
&\sum_{t=1}^{N_T}\sum_{i=1}^{N_G} C_{it}^{\mathrm{SU}} + \sum_{\omega=1}^{N_\Omega}\pi_\omega\Big[\sum_{t=1}^{N_T}\big(\sum_{i=1}^{N_G} C_i(P_{it} + r_{it\omega}^{\mathrm{U}} - r_{it\omega}^{\mathrm{D}}) + \sum_{j=1}^{N_L} V_{jt}^{\mathrm{LOL}} L_{jt\omega}^{\mathrm{shed}}\big)\Big] \\
&-\sum_t\Big[-\sum_{n,j\in M_n^{\mathrm{L}}}\lambda_{nt}L_{jt} - \sum_{n,r\in\Lambda_n}(f_{nr}^{\max}\epsilon_{nrt}^{\max} - f_{nr}^{\max}\epsilon_{nrt}^{-\max}) - \sum_i \upsilon_{it}^{\max} \\
&-\sum_i \psi_{it}^{\max} RU_i + \sum_i \psi_{it}^{\min} RD_i + \sum_\omega\Big(-\sum_q \gamma_{qt\omega} W_{qt\omega}^{\mathrm{RT}} - \sum_j \mu_{jt\omega} L_{jt} \\
&-\sum_i \psi_{it\omega}^{\max} RU_i + \sum_i \psi_{it\omega}^{\min} RD_i - \sum_i \alpha_{it\omega}^{\mathrm{U}} R_{it}^{\mathrm{U,max}} - \sum_i \alpha_{it\omega}^{\mathrm{D}} R_{it}^{\mathrm{D,max}} \\
&-\sum_{n,r\in\Lambda_n}(f_{nr}^{\max}\epsilon_{nr\omega t}^{\max} - f_{nr}^{\max}\epsilon_{nr\omega t}^{-\max})\Big)\Big]
\end{aligned} \tag{3.11a}$$

subject to

Primal constraints:

$$\sum_{i\in M_n^{\mathrm{G}}} P_{it} + \sum_{q\in M_n^{\mathrm{Q}}} W_{qt} - \sum_{j\in M_n^{\mathrm{L}}} L_{jt} - \sum_{r\in\Lambda_n} B_{nr}(\theta_{nt}-\theta_{rt}) = 0, \forall n, \forall t \tag{3.11b}$$

$$-f_{nr}^{\max} \le B_{nr}(\theta_{nt}-\theta_{rt}) \le f_{nr}^{\max}, \forall n, \forall r\in\Lambda_n, \forall t \tag{3.11c}$$

$$u_{it}P_i^{\min} \le P_{it} \le u_{it}P_i^{\max}, \forall i, \forall t \tag{3.11d}$$

$$W_{qt} \le W_q^{\max}, \forall q, \forall t \tag{3.11e}$$

$$K_i^{\mathrm{SU}}(u_{it}-u_{i,t-1}) \le C_{it}^{\mathrm{SU}}, \forall i, \forall t \tag{3.11f}$$

$$RD_i \le P_{it} - P_{i,t-1} \le RU_i, \forall i, \forall t \tag{3.11g}$$

$$\theta_{1t} = 0, \forall t \tag{3.11h}$$

$$u_{it} \in \{0,1\}, \forall i, \forall t \tag{3.11i}$$

$$\sum_{i\in M_n^{\mathrm{G}}} (r_{it\omega}^{\mathrm{U}} - r_{it\omega}^{\mathrm{D}}) + \sum_{q\in M_n^{\mathrm{Q}}} (W_{qt\omega}^{\mathrm{RT}} - W_{qt} - w_{qt\omega}^{\mathrm{spill}}) + \sum_{r\in\Lambda_n} B_{nr}(\theta_{nt} - \theta_{nt\omega}$$
$$-\theta_{rt} + \theta_{rt\omega}) + \sum_{j\in M_n^{\mathrm{L}}} L_{jt\omega}^{\mathrm{shed}} = 0, \forall n, \forall t, \forall\omega \tag{3.11j}$$

$$-f_{nr}^{\max} \le B_{nr}(\theta_{nt\omega}-\theta_{rt\omega}) \le f_{nr}^{\max}, \forall n, \forall r\in\Lambda_n, \forall t, \forall\omega \tag{3.11k}$$

$$P_{it} + r_{it\omega}^{\mathrm{U}} - r_{it\omega}^{\mathrm{D}} \le u_{it}P_i^{\max}, \forall i, \forall t, \forall\omega \tag{3.11l}$$

$$-P_{it} - r_{it\omega}^{\mathrm{U}} + r_{it\omega}^{\mathrm{D}} \le -u_{it}P_i^{\min}, \forall i, \forall t, \forall\omega \tag{3.11m}$$

$$RD_i \le \left(P_{it} + r_{it\omega}^{\mathrm{U}} - r_{it\omega}^{\mathrm{D}}\right) - \left(P_{i,t-1} + r_{i,t-1,\omega}^{\mathrm{U}} - r_{i,t-1,\omega}^{\mathrm{D}}\right) \le RU_i, \forall i, \forall t, \forall\omega \tag{3.11n}$$

$$r_{it\omega}^{\mathrm{U}} \le R_{it}^{\mathrm{U,max}}, \forall i, \forall t, \forall\omega \tag{3.11o}$$

$$r_{it\omega}^{\mathrm{D}} \le R_{it}^{\mathrm{D,max}}, \forall i, \forall t, \forall\omega \tag{3.11p}$$

$$L_{jt\omega}^{\mathrm{shed}} \le L_{jt}, \forall j, \forall t, \forall\omega \tag{3.11q}$$

$$w_{qt\omega}^{\mathrm{spill}} \le W_{qt\omega}^{\mathrm{RT}}, \forall q, \forall t, \forall\omega \tag{3.11r}$$

$$\theta_{1t\omega} = 0, \forall t, \forall\omega \tag{3.11s}$$

$$0 \le P_{it}, C_{it}^{\mathrm{SU}}, \forall i, \forall t$$
$$0 \le W_{qt}, \forall q, \forall t$$
$$0 \le r_{it\omega}^{\mathrm{U}}, r_{it\omega}^{\mathrm{D}}, \forall i, \forall t, \forall\omega$$
$$0 \le w_{qt\omega}^{\mathrm{spill}}, \forall q, \forall t, \forall\omega$$
$$0 \le L_{jt\omega}^{\mathrm{shed}}, \forall j, \forall t, \forall\omega \tag{3.11t}$$

Dual constraints:

$$C_i + \lambda_{nt} + \rho_{it} + \psi_{it}^{\max} + \psi_{it}^{\min} + \psi_{it\omega}^{\max} - \psi_{it\omega}^{\min}$$
$$+\phi_{it\omega}^{\max} - \phi_{it\omega}^{\min} \ge 0, \forall i\in M_n^{\mathrm{G}}, \forall n, \forall\omega, \forall t \tag{3.11u}$$

$$\lambda_{nt} + \lambda_{nt\omega} + \rho^{\mathrm{W}}_{qt} \geq 0, \forall q \in M^{\mathrm{L}}_{n}, \forall n, \forall \omega, \forall t \tag{3.11v}$$

$$1 - \beta_{it} \geq 0, \forall i, \forall t \tag{3.11w}$$

$$\begin{aligned}&\pi_{\omega} C_i + \lambda_{nt\omega} + \psi^{\max}_{it\omega} - \psi^{\min}_{it\omega} + \alpha^{\mathrm{U}}_{it\omega}\\&+ \phi^{\max}_{it\omega} - \phi^{\min}_{it\omega} \geq 0, \forall i \in M^{\mathrm{G}}_{n}, \forall n, \forall \omega, \forall t\end{aligned} \tag{3.11x}$$

$$\begin{aligned}&- \pi_{\omega} C_i - \lambda_{nt\omega} - \psi^{\max}_{it\omega} + \psi^{\min}_{it\omega} - \alpha^{\mathrm{D}}_{it\omega}\\&- \phi^{\max}_{it\omega} + \phi^{\min}_{it\omega} \geq 0, \forall i \in M^{\mathrm{G}}_{n}, \forall n, \forall \omega, \forall t\end{aligned} \tag{3.11y}$$

$$\begin{aligned}&\sigma_{1t_{|n=1}} + \sum_{r \in \Lambda_n} B_{nr} (\epsilon^{\max}_{nrt} - \epsilon^{-\max}_{nrt})\\&- \sum_{r \in \Lambda_n} B_{nr} \Big(\lambda_{nt} - \lambda_{rt} + \lambda_{nt\omega} - \lambda_{rt\omega} \Big) = 0, \forall n, \forall \omega, \forall t\end{aligned} \tag{3.11z}$$

$$\begin{aligned}&\sigma_{1t\omega_{|n=1}} + \sum_{r \in \Lambda_n} B_{nr} (\epsilon^{\max}_{nrt} - \epsilon^{-\max}_{nrt})\\&+ \sum_{r \in \Lambda_n} B_{nr} (\lambda_{nt\omega} - \lambda_{rt\omega}) = 0, \forall n, \forall \omega, \forall t\end{aligned} \tag{3.11aa}$$

$$\begin{aligned}&\beta_{it} K^{\mathrm{SU}}_{i} - \phi^{\max}_{it} P^{\max}_{i} + \phi^{\min}_{it} P^{\min}_{i}\\&- \phi^{\max}_{it\omega} P^{\max}_{i} + \phi^{\min}_{it\omega} P^{\min}_{i} + \upsilon^{\max}_{it} \geq 0, \forall i, \forall \omega, \forall t\end{aligned} \tag{3.11ab}$$

$$\pi_{\omega} V^{\mathrm{LOL}}_{jt} + \lambda_{nt\omega} + \mu_{jt\omega} \geq 0, \forall j \in M^{\mathrm{L}}_{n}, \forall n, \forall \omega, \forall t \tag{3.11ac}$$

$$\lambda_{nt\omega} + \gamma_{qt\omega} \geq 0, \forall q \in M^{\mathrm{Q}}_{n}, \forall \omega, \forall t \tag{3.11ad}$$

$$\epsilon^{\max}_{nrt}, \epsilon^{-\max}_{nrt} \geq 0, \forall n, \forall r \in \Lambda_n, \forall t \tag{3.11ae}$$

$$\epsilon^{\max}_{nr\omega t}, \epsilon^{-\max}_{nr\omega t} \geq 0, \forall n, \forall r \in \Lambda_n, \forall \omega, \forall t \tag{3.11af}$$

$$\upsilon^{\max}_{it}, \beta_{it}, \phi^{\max}_{it}, \phi^{\min}_{it}, \psi^{\max}_{it}, \psi^{\min}_{it} \geq 0, \forall i, \forall t \tag{3.11ag}$$

$$\rho^{\mathrm{W}}_{qt} \geq 0, \forall q, \forall t \tag{3.11ah}$$

$$\phi^{\max}_{it\omega}, \phi^{\min}_{it\omega}, \psi^{\max}_{it\omega}, \psi^{\min}_{it\omega}, \alpha^{\mathrm{U}}_{it\omega}, \alpha^{\mathrm{D}}_{it\omega} \geq 0, \forall i, \forall \omega, \forall t \tag{3.11ai}$$

$$\mu_{jt\omega} \geq 0, \forall j, \forall \omega, \forall t, \quad \gamma_{qt\omega} \geq 0, \forall q, \forall \omega, \forall t. \tag{3.11aj}$$

Problem (3.11) minimizes a social welfare gap since the objective function (3.11a) is the difference of the primal objective function, which is the expected social welfare, and the dual objective function, which is the expected social welfare as well. In other words, the gap in equation (3.11a) is zero if no integrality or other constraints are imposed. Note that problem (3.11) with relaxed integrality constraints (equation (3.11i)) is fully equivalent to either the primal problem (3.4) with relaxed integrality constraints or the dual problem (3.8), but embodies both primal and dual variables.

As stated above, the advantage of problem (3.11) is to allow controlling simultaneously quantities and prices and to provide the possibility of introducing additional constraints to the problem.

Additionally, it should be noted that minimizing the duality gap is a proxy for deviating the least from maximum social welfare.

The remaining steps of the proposed pricing model are to formulate cost-recovery conditions of producers and to incorporate them in problem (3.11).

3.5.4 Cost Recovery Conditions

To incorporate cost-recovery conditions in problem (3.11), we consider the following three variants:

- **Cost-recovery at the day-ahead market (CR case):**

  Day-ahead cost-recovery conditions guarantee that no producer incurs losses following day-ahead scheduled productions P_{it} under day-ahead prices λ_{nt}. That is, under day-ahead prices λ_{nt}, unit i, located at node n, has a revenue of $\sum_t \lambda_{nt} P_{it}$ and a cost of $\sum_t C_i P_{it} + C^{\text{SU}}_{it}$. Through the cost-recovery constraints at the day-ahead market, the day-ahead profit of each producer is enforced to be non-negative:

$$\sum_t \big((\lambda_{nt} - C_i)P_{it} - C^{\text{SU}}_{it}\big) \geq 0 \quad \forall i \in M^{\text{G}}_n \quad . \tag{3.12}$$

- **Cost-recovery in expectation (AR case):**

  Cost-recovery conditions in expectation (or average cost-recovery conditions) guarantee a non-negative expected profit for producers. The expected profit of unit i, located at node n, includes the day-ahead profit $\sum_t \big((\lambda_{nt} - C_i)P_{it}\big) - C^{\text{SU}}_{it}\big)$ and the average profit $\sum_t \sum_\omega \pi_\omega (\lambda_{nt\omega}/\pi_\omega - C_i)(r^{\text{U}}_{it\omega} - r^{\text{D}}_{it\omega})$ pertaining to real-time operation:

$$\sum_t \big[(\lambda_{nt} - C_i)P_{it} - C^{\text{SU}}_{it} + \sum_\omega \pi_\omega (\lambda_{nt\omega}/\pi_\omega - C_i)(r^{\text{U}}_{it\omega} - r^{\text{D}}_{it\omega})\big] \geq 0, \forall i \in M^{\text{G}}_n \quad . \tag{3.13}$$

  As previously mentioned, $\lambda_{nt\omega}$ are the probability-affected balancing prices (linked to the term $\pi_\omega C_i$ in the objective function) that need to be divided by π_ω to make the balancing prices comparable with the day-ahead prices. It is important to note that if no integrality or cost-recovery constraint is imposed, then $\lambda_{nt} = \sum_\omega \pi_\omega (\lambda_{nt\omega}/\pi_\omega)$.

- **Cost-recovery per scenario (SR case):**

  Although the expected profit of each producer is guaranteed to be non-negative under cost-recovery conditions in expectation, it can still happen that a unit incurs losses in one of the scenarios [38]. Cost-recovery conditions per scenario ensure the actual cost recovery if that scenario is a good approximation of real-time operation. The cost recovery condition of unit i enforced in each scenario is:

$$\sum_t \left[(\lambda_{nt} - C_i)P_{it} - C^{\mathrm{SU}}_{it} + (\lambda_{nt\omega}/\pi_\omega - C_i)(r^{\mathrm{U}}_{it\omega} - r^{\mathrm{D}}_{it\omega})\right] \geq 0, \forall \omega, \forall i \in M^{\mathrm{G}}_n \quad . \tag{3.14}$$

3.5.5 Linearization of Cost-Recovery Conditions

The cost-recovery constraints, formulated in equations (3.12)-(3.14), contain products of quantities (primal variables) and prices (dual variables). That is, the producer revenues from the day-ahead market are calculated using the product of day-ahead quantities and day-ahead prices ($\lambda_{nt}P_{it}$), and their revenues from real-time operation are obtained by the product of the deployed quantities and the probability-removed balancing prices ($\frac{\lambda_{nt\omega}}{\pi_\omega}(r^{\mathrm{U}}_{it\omega} - r^{\mathrm{D}}_{it\omega})$). In short, the cost-recovery constraints contain bi-linear terms.

Optimization problems with bi-linear terms in their constraints are categorized into non-linear optimization problems that are in general hard to solve and no state-of-the-art solver is available to guarantee the convergence or optimality of these problems. Hence, for computational tractability, bi-linear terms are usually linearized. To linearize bi-linear equations (3.12)-(3.14), a binary expansion is used as follows [59].

- **Linearization of cost-recovery constraints at the day-ahead market**:

  The day-ahead cost-recovery constraints include the bi-linear term $P_{it}\lambda_{nt}$. To linearize this term, equations (3.15) are used:

$$P_{it} = \sum_k y_{itk}\hat{p}_{itk}, \quad \sum_k y_{itk} = 1, \quad \forall i, \forall t \tag{3.15a}$$

$$0 \leq \lambda_{nt} - z_{itk} \leq G(1 - y_{itk}), \quad \forall k, \forall i \in M^{\mathrm{G}}_n, \forall t \tag{3.15b}$$

$$0 \leq z_{itk} \leq G y_{itk}, \quad \forall k, \forall i, \forall t \tag{3.15c}$$

$$0 \leq \sum_t \sum_k (z_{itk}\hat{p}_{itk}) - C_i P_{it} - C^{\mathrm{SU}}_{it}, \quad \forall i \tag{3.15d}$$

$$y_{itk} \in \{0,1\}, \quad \forall k, \forall i, \forall t \quad . \tag{3.15e}$$

  In equation (3.15a), the continuous production P_{it} is replaced by $\sum_k y_{itk}\hat{p}_{itk}$, which discretely approximates P_{it}. Index k denotes discretization index running from 1 to K and $\hat{p}_{itk}$ denotes the discretization step. Since the variables y_{itk} are binary, as stated in equation (3.15e), $\sum_{k=1}^{K} y_{itk} = 1$ ensures that P_{it} is approximated by only one discrete value. Replacing $\lambda_{nt}P_{it}$ by $\lambda_{nt}\sum_k y_{itk}\hat{p}_{itk}$ needs a further linearization step. For this purpose, equations (3.15b) and (3.15c) are included, where z_{itk} denotes a continuous variable representing day-ahead price and G denotes a sufficiently large positive constant. The value of G must be chosen such that equations (3.15b) and (3.15c) are not binding at the solution, for example, the value of G can be ten times the value of the maximum price offer. Finally, the day-ahead cost-recovery constraint (3.12) is approximated by equation (3.15d).

As an example, if at $k=k'$, $y_{itk'}=1$ (i.e., $y_{it1}=y_{it2}=\cdots=y_{itk'-1}=0, y_{itk'}=1, y_{itk'+1}=\cdots=y_{itK}=0$), then $P_{it}=\hat{p}_{itk'}$ (obtained from equation (3.15a)) and $0\le\lambda_{nt}-z_{itk'}\le G(1-1)$ (obtained from equation (3.15b)) that results in $\lambda_{nt}=z_{itk'}$. Then, $0\le\sum_t z_{itk'}\hat{p}_{itk'}-C_iP_{it}-C^{\mathrm{SU}}_{it}$ that is equal to equation (3.12) if $\lambda_{nt}P_{it}$ is replaced by $z_{itk'}\hat{p}_{itk'}$.

- **Linearization of cost-recovery constraints in expectation**:

  In the same vein, we linearize the product of deployed reserves and balancing prices. Therefore, the expected cost-recovery constraint (3.13) is recast as:

$$P_{it}=\sum_k y_{itk}\hat{p}_{itk},\quad \sum_k y_{itk}=1,\quad \forall i,\forall t \tag{3.16a}$$

$$0\le\lambda_{nt}-z_{itk}\le G(1-y_{itk}),\quad \forall k,\forall i\in M^{\mathrm{G}}_n,\forall t \tag{3.16b}$$

$$0\le z_{itk}\le G y_{itk},\quad \forall k,\forall i,\forall t \tag{3.16c}$$

$$y_{itk}\in\{0,1\},\quad \forall k,\forall i,\forall t \tag{3.16d}$$

$$r^{\mathrm{U}}_{it\omega}=\sum_m y^{\mathrm{U}}_{it\omega m}\hat{r}^{\mathrm{U}}_{it\omega m},\quad \forall i,\forall\omega,\forall t \tag{3.16e}$$

$$r^{\mathrm{D}}_{it\omega}=\sum_m y^{\mathrm{D}}_{it\omega m}\hat{r}^{\mathrm{D}}_{it\omega m},\quad \forall i,\forall\omega,\forall t \tag{3.16f}$$

$$\sum_m y^{\mathrm{U}}_{it\omega m}=1,\quad \forall i,\forall\omega,\forall t \tag{3.16g}$$

$$\sum_m y^{\mathrm{D}}_{it\omega m}=1,\quad \forall i,\forall\omega,\forall t \tag{3.16h}$$

$$0\le\lambda_{n\omega t}-z^{\mathrm{U}}_{it\omega m}\le G(1-y^{\mathrm{U}}_{it\omega m}),\quad \forall m,\forall i\in M^{\mathrm{G}}_n,\forall\omega,\forall t \tag{3.16i}$$

$$0\le\lambda_{n\omega t}-z^{\mathrm{D}}_{it\omega m}\le G(1-y^{\mathrm{D}}_{it\omega m}),\quad \forall m,\forall i\in M^{\mathrm{G}}_n,\forall\omega,\forall t \tag{3.16j}$$

$$0\le z^{\mathrm{U}}_{it\omega m}\le G y^{\mathrm{U}}_{it\omega m},\quad \forall m,\forall i,\forall t,\forall\omega \tag{3.16k}$$

$$0\le z^{\mathrm{D}}_{it\omega m}\le G y^{\mathrm{D}}_{it\omega m},\quad \forall m,\forall i,\forall t,\forall\omega \tag{3.16l}$$

$$0\le\sum_t\Bigg(-C_iP_{it}-C^{\mathrm{SU}}_{it}+\sum_k z_{itk}\hat{p}_{itk}+ \tag{3.16m}$$

$$\sum_\omega\pi_\omega\Big[\sum_m\big(z^{\mathrm{U}}_{it\omega m}\hat{r}^{\mathrm{U}}_{it\omega m}-z^{\mathrm{D}}_{it\omega m}\hat{r}^{\mathrm{D}}_{it\omega m}\big)/\pi_\omega-C_i(r^{\mathrm{U}}_{it\omega}-r^{\mathrm{D}}_{it\omega})\Big]\Bigg),\quad \forall i$$

$$y^{\mathrm{U}}_{it\omega m},y^{\mathrm{D}}_{it\omega m}\in\{0,1\},\quad \forall m,\forall i,\forall\omega,\forall t\quad . \tag{3.16n}$$

In equations (3.16a), (3.16e), and (3.16f), the scheduled production P_{it}, upward deployed reserve $r^{\mathrm{U}}_{it\omega}$, and downward deployed reserve $r^{\mathrm{D}}_{it\omega}$ are replaced by the discrete approximations of $\sum_k y_{itk}\hat{p}_{itk}$, $\sum_m y^{\mathrm{U}}_{it\omega m}\hat{r}^{\mathrm{U}}_{it\omega m}$ and $\sum_m y^{\mathrm{D}}_{it\omega m}\hat{r}^{\mathrm{U}}_{it\omega m}$, respectively. As stated above, index k denotes discretization index running from 1 to K and $\hat{p}_{itk}$ denotes the discretization step pertaining to scheduled production P_{it}. In the same vein, index m denotes discretization index pertaining to deployed reserves that runs from 1 to M, and $\hat{r}^{\mathrm{U}}_{it\omega m}$ and $\hat{r}^{\mathrm{D}}_{it\omega m}$ denote the discretization steps related to upward and downward deployed reserves, $r^{\mathrm{U}}_{it\omega}$ and $r^{\mathrm{D}}_{it\omega}$.

The variables y_{itk}, $y^{\mathrm{U}}_{it\omega m}$, and $y^{\mathrm{D}}_{it\omega m}$ are binary as stated in equations (3.16a) and (3.16n), respectively. Therefore, $\sum_{k=1}^{K} y_{itk} = 1$ ensures that P_{it} is approximated by only one discrete value, $\sum_m y^{\mathrm{U}}_{it\omega m} = 1$ guarantees that one discrete value ($\hat{r}^{\mathrm{U}}_{it\omega m}$) approximates $r^{\mathrm{U}}_{it\omega}$, and finally, $\sum_m y^{\mathrm{D}}_{it\omega m} = 1$ imposes that $r^{\mathrm{U}}_{it\omega}$ is approximated by only one discrete value ($\hat{r}^{\mathrm{D}}_{it\omega m}$).

To replace $\lambda_{nt}P_{it}$ by $\lambda_{nt}\sum_k y_{itk}\hat{p}_{itk}$, $\lambda_{nt\omega}r^{\mathrm{U}}_{it\omega}$ by $\lambda_{nt\omega}\sum_m y^{\mathrm{U}}_{it\omega m}\hat{r}^{\mathrm{U}}_{it\omega m}$, and $\lambda_{nt\omega}r^{\mathrm{D}}_{it\omega}$ by $\lambda_{nt\omega}\sum_m y^{\mathrm{D}}_{it\omega m}\hat{r}^{\mathrm{D}}_{it\omega m}$, equations (3.16b), (3.16c), (3.16i)-(3.16l) are included. In these equations, z_{itk}, $z^{\mathrm{U}}_{it\omega m}$, and $z^{\mathrm{D}}_{it\omega m}$ denote continuous variables representing day-ahead price, probability-affected balancing price associated to upward deployed reserves, and probability-affected balancing price associated to downward deployed reserves. As stated above, G denotes a sufficiently large positive constant. Finally, the expected cost-recovery constraint (3.13) is approximated by equation (3.16m).

- **Linearization of cost-recovery constraints per scenario**:

  Cost-recovery constraint per scenario (3.14) is linearized by (3.17).

  The description of the variables and constraints needed for approximating and linearizing are similar to those related to equations (3.16a)-(3.16n), described above, but the expected cost recovery equation (3.16m) is replaced by equation (3.17m) expressing cost recovery per scenario:

$$P_{it} = \sum_k y_{itk}\hat{p}_{itk}, \quad \sum_k y_{itk} = 1, \quad \forall i, \forall t \tag{3.17a}$$

$$0 \le \lambda_{nt} - z_{itk} \le G(1 - y_{itk}), \quad \forall k, \forall i \in M^{\mathrm{G}}_n, \forall t \tag{3.17b}$$

$$0 \le z_{itk} \le G y_{itk}, \quad \forall k, \forall i, \forall t \tag{3.17c}$$

$$y_{itk} \in \{0,1\}, \quad \forall k, \forall i, \forall t \tag{3.17d}$$

$$r^{\mathrm{U}}_{it\omega} = \sum_m y^{\mathrm{U}}_{it\omega m}\hat{r}^{\mathrm{U}}_{it\omega m}, \quad \forall i, \forall \omega, \forall t \tag{3.17e}$$

$$r^{\mathrm{D}}_{it\omega} = \sum_m y^{\mathrm{D}}_{it\omega m}\hat{r}^{\mathrm{D}}_{it\omega m}, \quad \forall i, \forall \omega, \forall t \tag{3.17f}$$

$$\sum_m y^{\mathrm{U}}_{it\omega m} = 1, \quad \forall i, \forall \omega, \forall t \tag{3.17g}$$

$$\sum_m y^{\mathrm{D}}_{it\omega m} = 1, \quad \forall i, \forall \omega, \forall t \tag{3.17h}$$

$$0 \leq \lambda_{n\omega t} - z^{\mathrm{U}}_{it\omega m} \leq G(1 - y^{\mathrm{U}}_{it\omega m}), \quad \forall m, \forall i \in M^{\mathrm{G}}_n, \forall \omega, \forall t \tag{3.17i}$$

$$0 \leq \lambda_{n\omega t} - z^{\mathrm{D}}_{it\omega m} \leq G(1 - y^{\mathrm{D}}_{it\omega m}), \quad \forall m, \forall i \in M^{\mathrm{G}}_n, \forall \omega, \forall t \tag{3.17j}$$

$$0 \leq z^{\mathrm{U}}_{it\omega m} \leq G y^{\mathrm{U}}_{it\omega m}, \quad \forall m, \forall i, \forall t, \forall \omega \tag{3.17k}$$

$$0 \leq z^{\mathrm{D}}_{it\omega m} \leq G y^{\mathrm{D}}_{it\omega m}, \quad \forall m, \forall i, \forall t, \forall \omega \tag{3.17l}$$

$$0 \leq \sum_t \Bigg(- C_i P_{it} - C^{\mathrm{SU}}_{it} + \sum_k z_{itk} \hat{p}_{itk} + \tag{3.17m}$$

$$\sum_m (z^{\mathrm{U}}_{it\omega m} \hat{r}^{\mathrm{U}}_{it\omega m} - z^{\mathrm{D}}_{it\omega m} \hat{r}^{\mathrm{D}}_{it\omega m}) / \pi_\omega - C_{it}(r^{\mathrm{U}}_{it\omega} - r^{\mathrm{D}}_{it\omega}) \Bigg), \quad \forall i, \forall \omega$$

$$y^{\mathrm{U}}_{it\omega m}, y^{\mathrm{D}}_{it\omega m} \in \{0, 1\}, \quad \forall m, \forall i, \forall \omega, \forall t \quad . \tag{3.17n}$$

3.5.6 Complete Model

To summarize, primal-dual problem (3.11) with equations (3.15a)-(3.15e) results in prices guaranteeing cost-recovery conditions at the day-ahead market, problem (3.11) with constraints (3.16a)-(3.16n) materializes prices ensuring cost-recovery conditions in expectation, and finally this model with equations (3.17a)-(3.17n) achieves prices with the feature of cost-recovery conditions per scenario.

We should note that the primal-dual problem (3.11) with cost-recovery constraints optimizes over the primal variables (in set Ξ_p) and the dual variables (in set Ξ_d), as well as additional variables introduced in this section for linearization, i.e., $\Xi_l = \{z_{itk}, y_{itk}, \forall i, \forall t, \forall k; z^{\mathrm{U}}_{it\omega m}, y^{\mathrm{U}}_{it\omega m}, z^{\mathrm{D}}_{it\omega m}, y^{\mathrm{D}}_{it\omega m}, \forall i, \forall t, \forall \omega, \forall m\}$.

3.6 Illustrative Example

For the sake of illustration, in this section, we apply the proposed pricing approaches to a simple system, and compare the market outcomes obtained from these approaches to those from the conventional pricing method with uplift.

We reiterate that the prices from the conventional method are obtained by freezing binary variables at their optimal value, which result from solving the primal problem (3.4), and computing prices as dual variables of the corresponding LP problem [46].

3.6.1 Data

We consider a three-node system over a two-period time horizon. The system is shown in Fig. 3.1.

The system includes three conventional units and a wind power unit. The data of generating units are provided in Table 3.1. The maximum reserves $R_i^{\text{U,max}}$ and $R_i^{\text{D,max}}$ are assumed to be equal to $P_i^{\max}$. Therefore, all units are flexible and can be dispatched for both energy and reserve purposes. The start-up costs and marginal production costs of the units are chosen with the purpose of highlighting unit U_3 as expensive.

The load is considered to be 110 MW and 280 MW in periods t_1 and t_2, respectively. The load is chosen so that expensive unit U_3 must be dispatched in period t_2. This allows analyzing the cost recovery for unit U_3 under the different approaches. A value of lost load equal to $2000/MWh is considered in real-time operation.

The wind unit is located at node 2 and has an installed capacity of 120 MW. The uncertain power output of this wind unit is modeled using two scenarios, *high* (with a probability of 0.6) and *low* (with a probability of 0.4), for each time period as presented in Table 3.2.

Table 3.1 – Data of generating units.

Unit	K_i^{SU} [$]	C_i [$/MWh]	$P_i^{\max}$ [MW]	$P_i^{\min}$ [MW]	$R_i^{\text{U,min}}$ [MW]	$R_i^{\text{D,max}}$ [MW]
U_1	101.1	20.03	95	10	95	95
U_2	103.2	50.06	100	10	100	100
U_3	2001.06	100.01	105	10	105	105

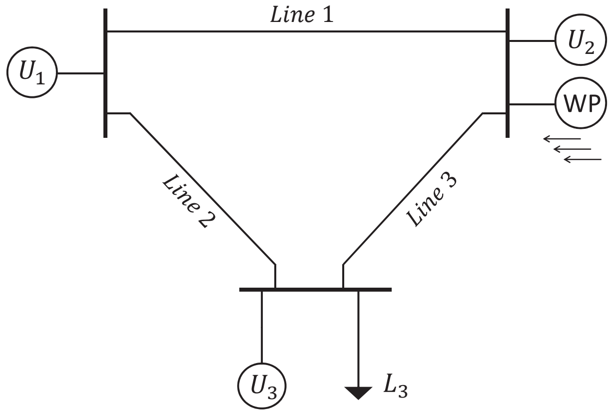

Figure 3.1 – Test system

Table 3.2 – Wind scenarios [MW]

Period	High	Low
t_1	59	13
t_2	111	17

Finally, line reactances and capacities are all equal to 0.13 p.u. and 500 MW, respectively. This line capacity is sufficiently high to avoid congestion in any of the scenarios considered in order to analyze solely the impact of uncertain wind production in this example.

3.6.2 Market Outcomes

We start discussing the results by providing quantities including the day-ahead scheduled productions and the deployed reserves in real-time operation, as shown in Fig. 3.2.

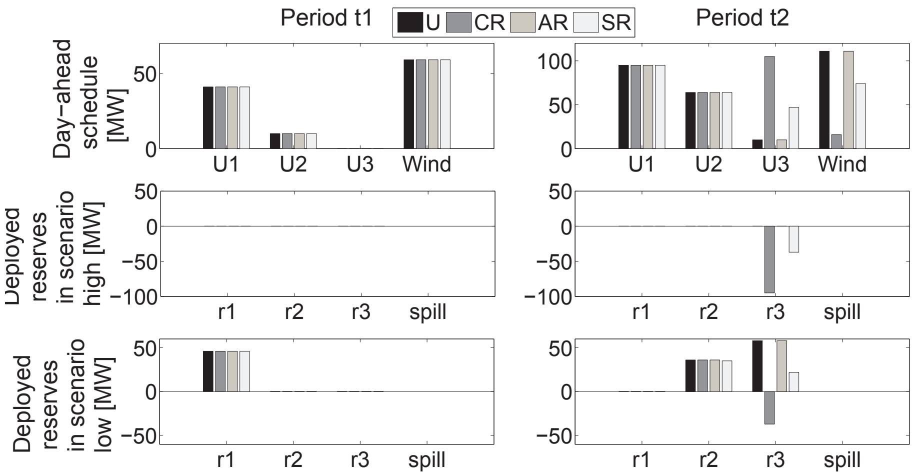

Figure 3.2 – Scheduled productions and deployed reserves obtained from the conventional method and the proposed pricing approaches.

Focusing on period t_1, the different approaches result in similar day-ahead scheduled productions for all units. That is, all approaches allocate 41 MW to unit U_1, 10 MW to unit U_2 and 59 MW to wind unit, which is the wind power output in scenario *High*. If scenario *High* occurs in real-time operation, there is no need to deploy reserves, and if scenario *Low* occurs, where the wind power output is 13 MW, unit U_1 is deployed 46 MW.

In period t_2, the scheduled productions of unit U_3 (the expensive unit) and wind unit differ under the different approaches. The approach with day-ahead cost-recovery conditions schedules unit U_3 to produce up to its capacity generation, i.e., 105 MW, while allocating 16 MW to wind unit. In other words, this approach allocates the highest production to unit U_3 and the lowest to wind unit comparing to the corresponding production levels from the other approaches. To assess these differences, we look at their impacts on the prices obtained from the different approaches.

Table 3.3 provides the day-ahead prices from the proposed approaches and from the conventional approach. Since there is no congestion in any of the two scenarios considered, prices do not change across nodes.

The day-ahead prices are higher in period t_2 than in period t_1 due to a higher load in this period (110 MW and 280 MW, respectively).

The approach with the day-ahead cost-recovery constraints results in the highest day-ahead price, which is \$119.06/MWh in period t_2.

In the following, we elaborate on the impact of these prices on the unit profits.

Table 3.3 – Day-ahead prices [\$/MWh]

method	λ_{t_1}	λ_{t_2}
U	20.03	70.04
CR	33.84	119.06
AR	33.84	103.87
SR	33.84	103.47

Fig. 3.3 depicts the producer profits at the day-ahead market, $\sum_t \left[P_{it}(\lambda_{nt} - C_i) - C^{\text{SU}}_{it}\right], \forall i$, and in expectation, $\sum_t \left[P_{it}(\lambda_{nt} - C_i) - C^{\text{SU}}_{it} + \sum_\omega \pi_\omega\big((r^{\text{U}}_{it\omega} - r^{\text{D}}_{it\omega})(\lambda_{nt\omega}/\pi_\omega - C_i)\big)\right], \forall i$, under the different pricing approaches considered.

We should note that the profits obtained from the conventional method with uplift (black bars) and without uplift (white bars) differ only for units incurring losses in the day-ahead market, as uplift is paid only to these units.

Focusing on the performance of the conventional method in the day-ahead market and unit U_3, this unit earns $10 \times 70.04 = \$700.4$ (\$70.04/MWh is the marginal price at period t_2) while its total cost, including production and start-up costs, is $10 \times 100.01 + 2001.06 = \$3001.16$. Therefore, the profit of unit U_3 resulting from the day-ahead market is \$-2300.7. To prevent unit U_3 from incurring losses, the conventional method proposes to pay an uplift. We reiterate that uplifts are paid only to those units incurring losses as a side-payment with the purpose of reducing these losses to zero, and not to provide an extra profit. Since uplift takes actual losses into account, it is computed based on the day-ahead scheduled productions and prices as follows: $|\max\{0, \sum_t (c_i - \lambda_{nt})P_{it} + C^{\text{SU}}_{it}\}| = |\max\{0, (100.01 - 70.04)10 + 2001.06\}| = 2300.7$. As depicted at the top plot in Fig. 3.3, the day-ahead profit of unit U_3 is zero under the method with uplift (denoted by U) and negative under the method without uplift (denoted by Con). The profits from the method with uplift (black bars) and without uplift (white bars) are the same for units U_1 and U_2 as they do not incur losses, and therefore, do not receive uplifts.

This figure also shows that units U_1 and U_2 earn a higher day-ahead profit under the approaches with cost-recovery constraints than that under the method with uplift.

Focusing on unit U_3, the approach with day-ahead cost-recovery constraints results in a zero day-ahead profit. This is a better outcome in comparison to the negative day-ahead profits resulting from the expected cost-recovery and per-scenario cost-recovery approaches. However, the day-ahead cost-recovery approach does not prevent a negative profit in real-time operation, as depicted at the bottom plot in Fig. 3.3.

Considering the expected profit (bottom plot in Fig. 3.3), the proposed approaches result in higher expected profits for units U_1 and U_2 than those from the conventional method. We reiterate that uplift is zero for these units, and hence, their expected profits are not affected by uplifts, i.e., the white bars and black bars are the same for units U_1 and U_2. This observation does not hold for unit U_3. The approaches with average cost-recovery and per-scenario cost-recovery constraints as well as the method with uplift result in a zero expected profit.

The total day-ahead profits (i.e., summation of the day-ahead profits of all units) obtained from the approaches CR, AR, SR, as well as the method with uplift are \$14,023.87, \$9646.88, \$9707.19, and \$5525.07, respectively. These outcomes are in line with the day-ahead prices presented above: the day-ahead prices resulting from the approach with day-ahead cost recovery are the highest, whereas those from the conventional method are the lowest.

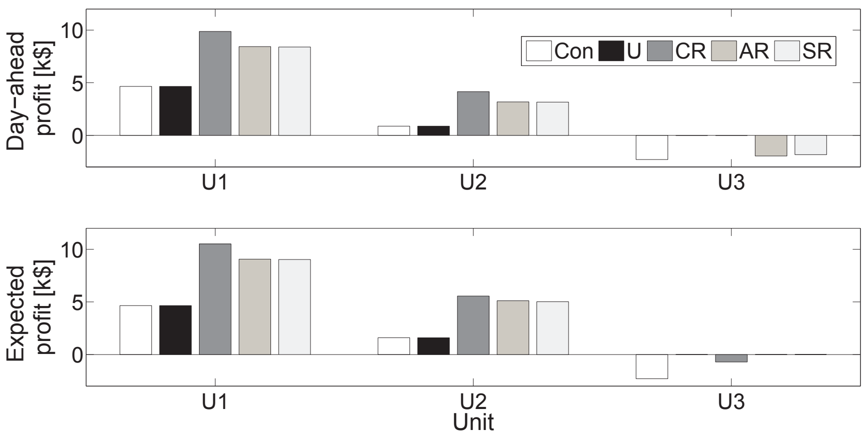

Figure 3.3 – Day-ahead profit and expected profit

Table 3.4 provides the expected costs and the consumer payments, as well as the duality gaps under the different pricing schemes. The methods with cost-recovery constraints in expectation results in the same optimal expected cost as the primal clearing problem (i.e., the optimal expected cost of the conventional method). The approaches with day-ahead cost-recovery constraints and with cost-recovery constraints per scenario increase the expected cost by about 0.04% and 0.16%, respectively.

Under the approaches with cost-recovery conditions, the consumer payments are higher than those from the method with uplift. The increases in consumer payments obtained from the proposed approaches as a percentage of the consumer payment from the method with uplift are also listed in this table. We should note that these large (unrealistic) differences are due to the fact that this example does not represent a realistic case-study. Using a realistic case-study, these differences get smaller.

Consumer payment consists of the day-ahead cost and the day-ahead profit. Noting comparatively small differences in the costs from the different approaches, the higher consumer payments from the proposed approaches result from higher day-ahead profits caused by higher day-ahead prices obtained from the proposed approaches.

The last row of Table 3.4 provides the social welfare gaps of the proposed pricing schemes. Also, these gaps are listed as a percentage of the optimal expected cost of $13049.23. Although it may seem that these gaps are not small enough in comparison with the optimal expected cost obtained from the primal problem (3.4) (i.e., $13,044.5 in this example), one should notice that the illustrative example presented does not represent a realistic case-study. It is provided for the sake of clarity. Social welfare gaps obtained from applying the proposed pricing scheme to realistic cases are provided in Section 3.7.5.

Table 3.4 – Expected cost, consumer payment, and duality gap in [$]

	CR	AR	SR	U
Expected cost	13054.09	13049.23	13069.95	13049.23
Consumer payment	33158.80	19280.86	23041.54	15159.05
	(118.7%)	(27.2%)	(51.2%)	–
Gap	2061.06 (15.8%)	1524.56 (11.7%)	1530.08 (11.7%)	–

3.7 Case Studies

The case studies provided in this section aim to appraise the performance of the proposed pricing schemes in a larger power system. To this aim, the outcomes of the proposed approaches are benchmarked against the outputs of the conventional method with uplift.

3.7.1 Data

We apply the proposed approaches to a 24-node system based on the single-area IEEE Reliability Test System (RTS) [72]. To facilitate the analysis of the results, some of the original characteristics of this test system are modified.

We consider the system to have 34 lines, 8 conventional generating units, 1 wind power unit, and 5 loads.

The data of conventional generating units are provided in Table 3.5. We assume that hydro unit U_{50} offers its energy at zero cost. The amount of reserve capacity that each generating unit is willing to provide, either downward or upward, is assumed to be equal its production capacity except from nuclear unit U_{400} that does not provide reserve.

The wind power unit, located at node 7, has an installed capacity of 600 MW. To generate wind power scenarios, we use wind speed historical data from Austin, Texas, which are available in the System Advisor Model (SAM) [2]. To obtain hourly wind power scenarios for 24 time periods, we apply the power curve of a 2-MW Vestas V80/2000 wind turbine with a hub height of 80 m. The power curve of this turbine model can be found in [16].

We should note that we built up the scenarios employing historical data without applying scenario reduction techniques.

We consider 25 equi-probable scenarios for the wind power output in real-time operation.

Table 3.5 – Characteristics of the Generating Units

	U_{76}	U_{50}	U_{155}	U_{50}	U_{197}	U_{50}	U_{400}
Node	2	7	15, 18	15	21	22	23
$P_i^{\max}$ [MW]	76	50	155	50	197	50	400
$P_i^{\min}$ [MW]	15	15	55	15	69	15	100
$R_i^{\mathrm{U,max}}$ [MW]	76	50	155	50	197	50	0
$R_i^{\mathrm{D,max}}$ [MW]	76	50	155	50	197	50	0
C_i^{SU} [\$]	400	100	320	100	300	100	1000
C_i [\$/MWh]	13.89	0	10.68	0	11.09	0	5.53

Table 3.6 provides the total demand over the 24 periods, while the demand locations and the corresponding shares are provided in Table 3.7.

Table 3.6 – Total demand in [MW]

t_1	t_2	t_3	t_4	t_5	t_6	t_7	t_8	t_9	t_{10}	t_{11}	t_{12}
441.1	481	482	483	490	1021.6	1132	1097	960.5	910.2	910	941.2
t_{13}	t_{14}	t_{15}	t_{16}	t_{17}	t_{18}	t_{19}	t_{20}	t_{21}	t_{22}	t_{23}	t_{24}
943	960	970	1031	1123	1130	1112	1101	998	930.1	780	440

Table 3.7 – Demand location

Demand	D_1	D_2	D_3	D_4	D_5
Node	1	4	13	14	20
Share %	33.5	18.9	14.9	16.2	16.5

3.7.2 Case I: No Network Congestion

In this case, the thermal limits of lines are considered to be high so that no congestion appears. Therefore, the prices do not change across nodes

Since the driving factor of this chapter is the cost-recovery conditions of producers, we present the market outcomes starting with producer profits.

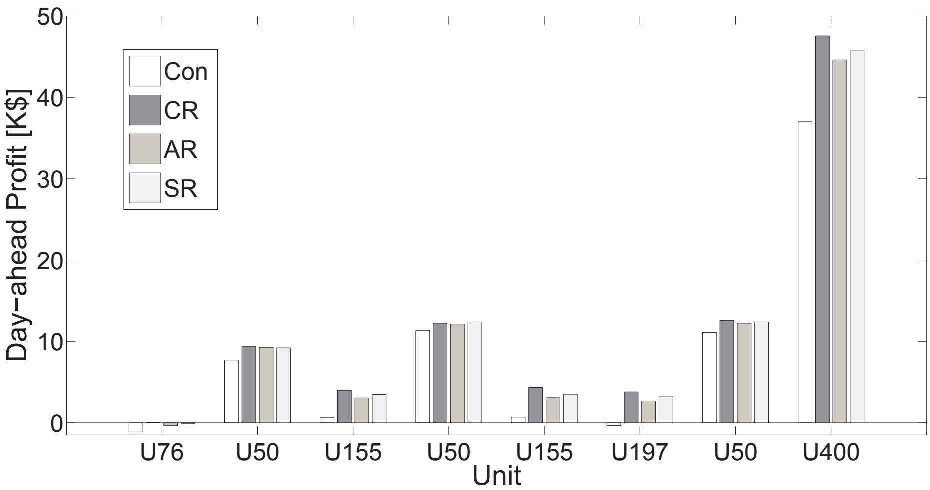

Figure 3.4 – Day-ahead Profit (RTS no congestion case).

Fig. 3.4 shows the day-ahead profit obtained from the different approaches. Under the conventional approach without uplift (white bars), units U_{76} and U_{197} incur losses (negative day-ahead profits), and therefore, two uplifts totaling $1465 are required.

Using the proposed approaches, unit U_{197} has a positive day-ahead profit, and thus, does not need uplift. However, unit U_{76} still incurs losses under the approaches with cost-recovery constraints in expectation and per scenario, as these approaches do not enforce cost-recovery conditions at the day-ahead market. The day-ahead profit of other units increases using the proposed approaches. Among them, the day-ahead cost-recovery approach results in the largest day-ahead profits. This is caused by the day-ahead prices, as described in the following.

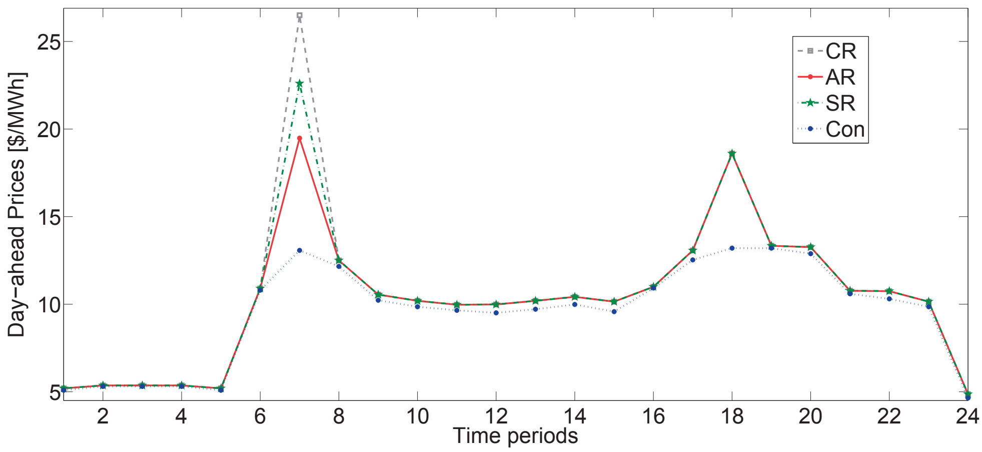

Figure 3.5 – Day-ahead prices at node 2 under different approaches (RTS no congestion case).

Fig. 3.5 depicts the day-ahead prices at node 2, where unit U_{76} is located, over the 24-hour horizon. Since there is no congestion, the prices are the same at all nodes. Apart from period t_7 (morning peak) and period t_{18} (evening peak), the prices obtained from the approaches with cost-recovery constraints are either equal or slightly higher than the prices obtained by the conventional method. In period t_{18}, the day-ahead prices obtained from the approaches with cost-recovery constraints are the same and higher than the conventional marginal price. However, a different behavior is observed in period t_7. The approach with day-ahead cost-recovery constraints results in a higher day-ahead price than those from the other approaches. This consequently leads to a higher day-ahead profit from this approach, as observed in Fig. 3.4.

Fig. 3.6 shows the expected profit of the producers. In this figure, we distinguish the producer profits with and without uplift by U and Con, respectively. One can observe that unit U_{76} cannot recover its expected cost under the prices obtained from the conventional method without uplift (white bars). However, it attains a non-negative expected profit from the approaches with cost-recovery constraints. Other units achieve higher profits under the pricing approaches proposed than under the conventional method with uplift.

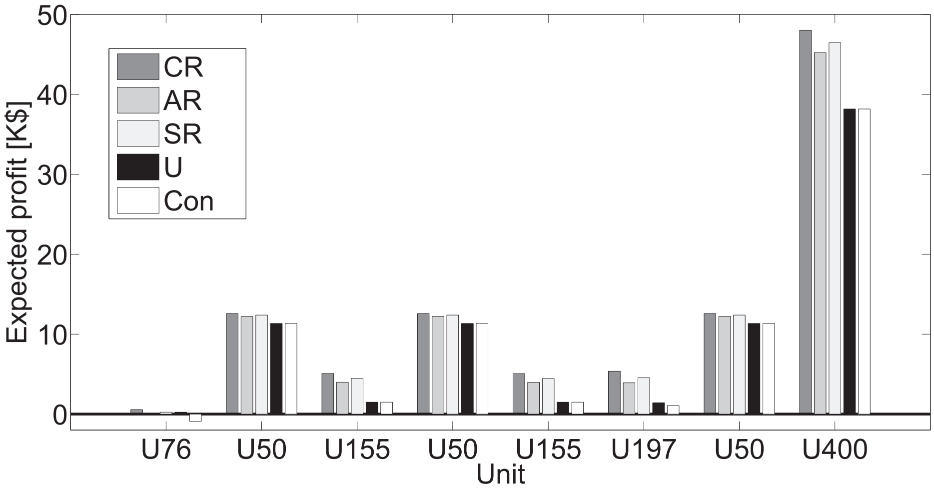

Figure 3.6 – Expected Profit (RTS no congestion case).

Therefore, the proposed pricing approaches demonstrate the performance desired: the approach with day-ahead cost-recovery constraints guarantees non-negative day-ahead profit, and the approaches with cost-recovery constraints in expectation and per scenario result in non-negative expected profits. However, it is important to assess at what expenses these outcomes are obtained. For this purpose, we provide the expected cost, consumer payment as well as the duality gap in Table 3.8. The pricing methodologies with cost-recovery constraints result in slightly higher expected cost than the one from the conventional method.

The approaches with cost-recovery conditions result in higher consumer payments than the method with uplift. The increase in the consumer payments obtained from the proposed approaches as a percentage of the consumer payment from the method with uplift is also listed in Table 3.8. Note that consumer payment comprises day-ahead costs and day-ahead profits. Higher day-ahead profits from the proposed approaches, described above, derive higher consumer payments in these approaches as compared to those from the method with uplift.

Finally, one can observe that the social welfare gaps in the last row are small in comparison with the expected optimal social welfare from primal problem (3.4); they are of order of 0.3% of the optimal expected cost of $127,066.

We should note that these differences are small, but also, they get smaller using a realistic power system, as in a power system with a high penetration of renewable energy, gas units are dominated technology among the conventional units due to their fast-ramping ability. Gas units have small start-up costs and minimum production limits as compared to coal units.

Table 3.8 – Expected cost, consumer payment and duality gap for the RTS system [$] (RTS no congestion case)

	CR	AR	SR	U
Expected cost	127,066	127,169	127,153	127,066
Consumers payment	2.42×10^5	2.34×10^5	2.38×10^5	2.17×10^5
	(11.5%)	(7.8%)	(9.7%)	–
Gap	288.24 (0.2%)	384.80 (0.3%)	371.10 (0.3%)	–

Therefore, we obtain a set of uniform prices under which cost-recovery conditions of producers are guaranteed without a need of uplift at the expense of deviating about 0.3% from the optimal social welfare.

For these simulation, we use CPLEX 12.1 under MATLAB on a computer Intel(R) Xeon(R) with two processors clocking at 2.2 GHz and 512 GB of RAM. The sizes of the proposed models in terms of number of variables and constraints as well as the computation time are provided in Table 3.9. We elaborate on computation time in section 3.7.5.

Table 3.9 – Size of the proposed models

	CR	AR	SR	U
No. of continuous variables	93368	96968	96968	27600
No. of integer variables	1560	5160	5160	1176
No. of total variables	94928	102128	102128	28776
No. of constraints	95361	108561	108585	65384
Computation time (s)	22705	14231	1624	57

3.7.3 Impact of Minimum Up/Down Time Constraints

We have assumed start-up costs and minimum generation capacity as the only non-convexities involved. However, other sources of non-convexity can be included without modeling difficulty, but different computational efforts. In this context, we investigate the impact of minimum up/down time constraints in this section. We should note that these constraints mostly pertain to old coal units and not to modern gas units. In a system with a large-scale renewable penetration, it is expected that flexible gas units have a higher share of supply than coal units. Therefore, the clearing model without these constraints represents a common future power system, where a generation mix consists of renewable units and flexible units.

The mathematical formulation of these constraints are provided in Appendix C.

We consider the minimum up time to be equal to the minimum down time for each conventional unit, as provided in Table 3.10. A minimum up time of 3 hours is considered for unit U_{76} in order to ensure that its respective minimum up time constraint is binding, and therefore, the commitment of this unit is different from the commitment without considering that constraint.

Table 3.11 provides the expected costs, the consumer payments, and the gaps obtained from the different cost-recovery approaches under minimum up/down time constraints. The increases in the consumer payments as a percentage of the consumer payment obtained from the method with uplift are provided in Table 3.11. The gaps as a percentage of the optimal expected cost of primal problem ($127,112) are also listed in this table.

Comparing these results to the outcomes from the formulation without minimum time constraints (Table 3.8), we conclude that the expected costs, the consumer payments, and the gaps are similar. That is, the performance of the proposed approaches are not affected by minimum up/down time constraints.

From the computational point of view, the approaches with day-ahead cost-recovery constraints and average cost-recovery constraints take the same computational efforts as the simulations without minimum up/down time constraints. The computation time for the approach with cost-recovery conditions per scenario, however, increases from 1624 s (for the model without minimum up/down time constraints) to 4479 s (for the model with these constraints).

Table 3.10 – Minimum Up/Down Time of Units

	U_{76}	U_{50}	U_{155}	U_{50}	U_{197}	U_{50}	U_{400}
T_{min}[h]	3	3	5	3	8	3	10

Table 3.11 – Expected cost, consumer payment and duality gap for the RTS system: No congestion case incorporating minimum Up/Down Time Constraints [$].

	CR	AR	SR	U
Expected cost	127,112	127,218	127,252	127,112
Consumers payment	2.37×10^5 (9.2%)	2.34×10^5 (7.8%)	2.39×10^5 (10 %)	2.17×10^5 –
Gap	275.5 (0.2%)	433.5 (0.3%)	471.3 (0.4%)	–

3.7.4 Case II: Network Congestion

The purpose of this case is to explore the impact of congestion on day-ahead prices, and consequently, on consumer payments.

To create network congestion, transmission limits of lines between node 2 and node 4, node 2 and node 6, node 3 and node 9, and node 6 to node 10 are set to be comparatively small (i.e., 60 MW). As examples, the day-ahead prices at periods t_{18} and t_{21} are chosen for illustration and depicted in Fig. 3.7. The prices from other periods also show the same behavior.

In period t_{18}, the day-ahead prices obtained from the conventional method and the approaches with cost-recovery conditions are the same over all nodes apart from node 6, where the average cost-recovery method results in a lower price. In period t_{21}, the prices from the conventional method and the cost-recovery approaches are almost equal over all nodes; there are small price differences only at nodes 2, 4 and 6.

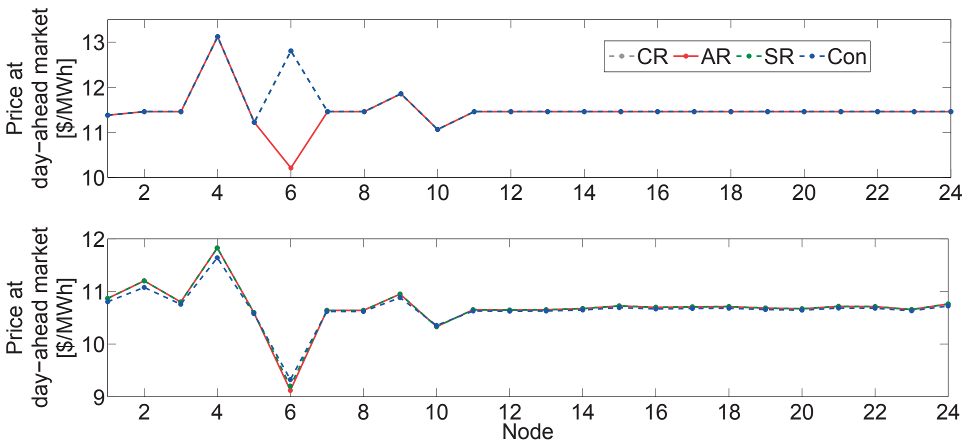

Figure 3.7 – LMPs at t_{18} (up) and t_{21} (down) obtained by the different approaches.

Table 3.12 provides the expected costs, the consumer payments, and the duality gaps obtained from the different approaches. The expected costs obtained from different approaches are of the same order of magnitude. The consumer payments from the approaches with cost-recovery constraints are of the same order of magnitude, and generally, about 3% higher than that from the method with uplift. Similar to the non-congested case, the social welfare gaps are small; these gaps are of order of 0.13% of the optimal expected cost ($170257).

Table 3.12 – Expected cost, consumer payment and duality gap for the RTS system with congestion [$].

	CR	AR	SR	U
Expected cost	170,257	170,271	170,273	170,257
Consumers payment	2.87×10^5	2.85×10^5	2.86×10^5	2.77×10^5
	(3.6%)	(2.9%)	(3.2%)	–
Gap	211.58 (0.1%)	174.27 (0.1%)	230.91 (0.1%)	–

3.7.5 Discussion on Social Welfare Gap and Computation Time

In this section, we elaborate on the computational aspects of the proposed models and the relevance of the deviation from the expected optimal social welfare, i.e., the social welfare gap. For this purpose, we simulate the proposed approaches using a number of different load profiles for both no-congestion and congestion cases.

Outcomes show the same trend as those reported in Sections 3.7.2 and 3.7.4. That is, the day-ahead prices obtained from the proposed approaches guarantee cost-recovery conditions at the expense of an increase in the expected cost. The relevant metrics providing this information are the expected cost and consumer payment, as described in the following.

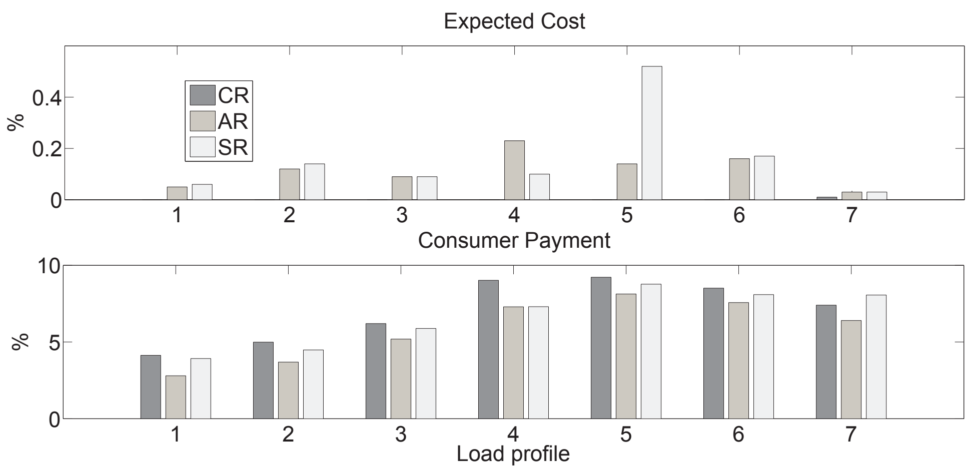

Figure 3.8 – Cost increase in percent, and consumer payment increase in percent for different load profiles (RTS no congested case)

Fig. 3.8 shows the increase in the expected cost using the cost-recovery approaches as a percentage of the optimal expected cost of primal problem (3.4), and the increase in consumer payment obtained from the cost-recovery approaches as a percentage of the payment resulting from the method with uplift. A similar trend is observed in case of congestion, as depicted in

Fig. 3.9. The increases in the expected cost are of order of less than 0.5%, and the increases in the consumer payments are of order of less than 9%.

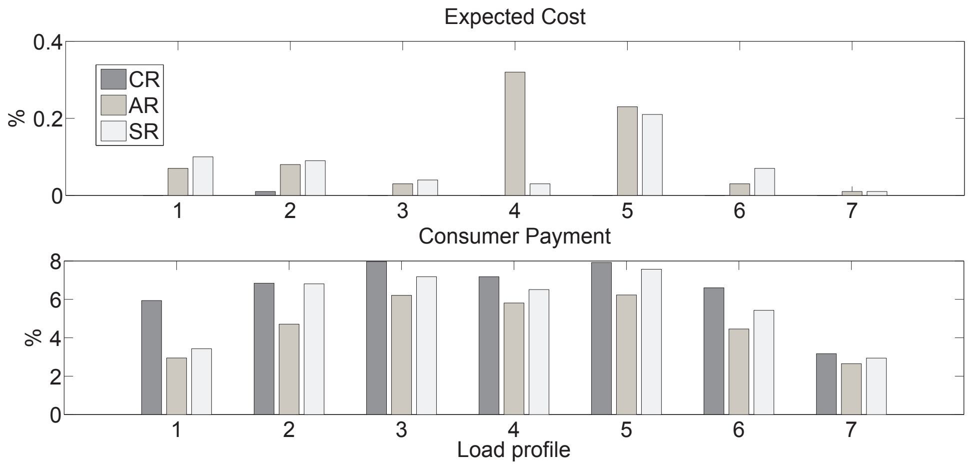

Figure 3.9 – Cost increase in percent, and consumer payment increase in percent for different load profiles (RTS congestion case)

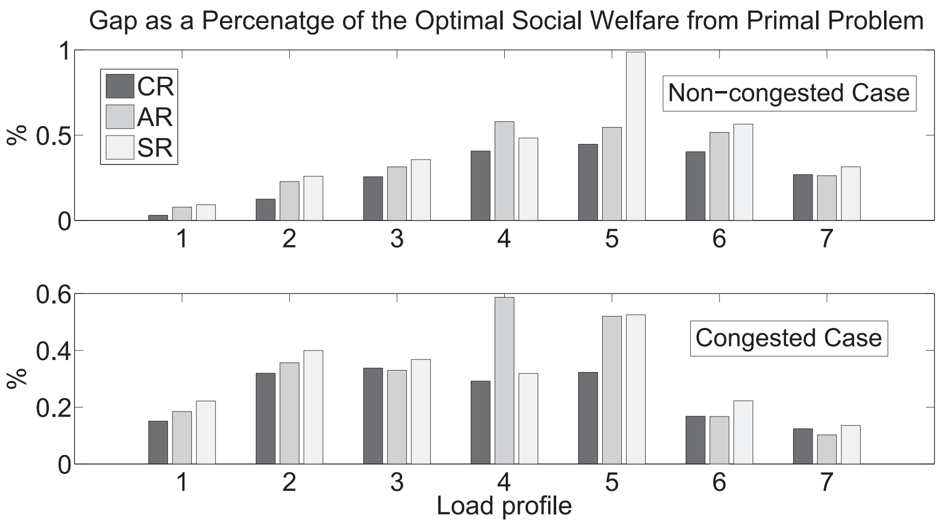

Figure 3.10 – Social welfare gaps as a percentage of the optimal expected cost obtained from primal problem 3.4 for different load profiles

The social welfare gaps as a percentage of the optimal expected cost obtained from primal problem (3.4) for different load profiles are shown in Fig. 3.10. The gaps obtained from the different proposed approaches are of the same order of magnitude, and small in comparison with the optimal expected cost.

Referring to Table 3.9, the approach with day-ahead cost-recovery constraints requires a high computation time. This can be partly explained by the small gap obtained from this approach for all load profiles in the non-congested case and for most of the profiles in the congested case (see Fig. 3.10). Note, however, that for MILP models, there is no linear relationship between the size of the problem and the required computation time. In other words, a smaller problem (with smaller number of variables and constraints) may take longer to solve than a larger problem.

The average computation time considering different load profiles for models CR, AR, and SR are, respectively, 5473 s, 4964 s, and 4479 s, which are not significantly different. Note that the computation burden may be considerably reduced by carefully adjusting the linearization of the cost-recovery conditions. By doing this, computation requirements are expected to be not much higher than those of a standard stochastic clearing model. We elaborate on the impact of linearization steps on computation time in the next section.

3.7.6 Impact of Linearization Step

The impact of linearization steps on the problem outcomes is elaborated in this section.

On one hand, a smaller linearization step approximates more precisely the problem, but on the other hand, significantly increases the dimension of the problem and its computational burden.

Computational burden particularly matters when considering small linearization steps for the deployed reserves in the approach with cost-recovery constraints in expectation and the approach with cost-recovery constraints per scenario. The reason is that the number of required decision variables ($y^{\mathrm{U}}_{it\omega m}$, $y^{\mathrm{D}}_{it\omega m}$, $z^{\mathrm{U}}_{it\omega m}$, and $z^{\mathrm{D}}_{it\omega m}$, $\forall i, \forall t, \forall \omega, \forall m$), and constraints, (constraints (3.16i)-(3.16l) for the approach with average cost-recovery conditions, and constraints (3.17i)-(3.17l) for the approach with per-scenario cost-recovery conditions) significantly increase.

In the simulations, thus far presented, linearization steps of 5 MW and 19 MW have been considered, respectively, for the day-ahead scheduled productions and the deployed reserves. We next consider a linearization step of 2 MW for both the day-ahead productions and deployed reserves (a drastic reduction) and provide the outcomes in Table 3.13. Comparing these outcomes with those provided in Table 3.8 (with linearization steps of 5 MW and 19 MW), we conclude that this smaller linearization step results in very similar expected costs (less than 0.03% differences), but smaller gaps for all proposed approaches. It also results in smaller consumer payments for the approach with day-ahead cost-recovery constraints (2.5% reduction) and the approach with average cost-recovery constraints (0.4% reduction), and the same consumer payment for the approach with cost-recovery constraints per scenario.

From a computational point of view, the smaller linearization steps of 2 MW increase the computation time from 14321 s to 19581 s for the approach with cost-recovery constraints in expectation, and from 1624 s to 10983 s for the approach with cost-recovery constraints per scenario. The computation time for the approach with day-ahead cost-recovery constraints remains the same as the one for the linearization steps of 5 MW and 19 MW.

To summarize, a smaller linearization step leads to slightly more precise results at the expense of higher computation time, while still the same conclusions are derived.

Table 3.13 – Expected cost, consumer payment and duality gap for the RTS system: no congestion case and linearization steps of 2MW for both schedules and deployed reserves.

	CR	AR	SR
Expected cost	127055	127122	127131
Consumers payment	2.36×10^5	2.33×10^5	2.38×10^5
Gap	282.8	347.6	359.9

3.7.7 Case Study Conclusion

We propose pricing approaches with cost-recovery conditions at the day-ahead, in expectation, and per scenario for a stochastic non-convex clearing model.

Day-ahead prices obtained from the proposed approaches are higher than conventional marginal prices in some periods. This, consequently, causes higher producer profits, and therefore, higher consumer payments. However, the new prices eliminate the need of uplifts and allow the market to fully rely on these new marginal prices. These conclusions are not affected by network congestion, as well as by considering other sources of non-convexity such as minimum up/down time constraints of units.

The increase in consumer payment varies from 3% to 9% of a payment derived from the method with uplift considering different load profiles and network congestion.

From a social welfare point of view, the proposed approaches with cost-recovery features imply deviating the least possible amount from the optimal value of the expected cost. The approach with day-ahead cost-recovery constraints results in the same expected cost as the original primal two-stage problem for the different load profiles considered. The other proposed approaches also attain optimal expected costs close to the one of the primal problem. The increases in expected costs are of order of 0.5% of the optimal expected cost. In the same vein, the duality gaps are also small. Considering different load profiles, the duality gaps are of order of 0.5% of the optimal social welfare.

From the computational point of view, the models proposed have bi-linear terms, which need to be linearized using integer variables. In this process, a smaller linearization step leads to slightly more precise results at the expense of higher computation burden, but still the same conclusions are derived. Generally, the models proposed are tractable and solvable in a reasonable time using a MILP state-of-the-art solver.

3.8 Summary and Conclusion of the Chapter

Pricing schemes in non-convex electricity markets constitute an active area of research. Recently, the growth of renewable generation and the possibility of using of stochastic clearing models have added a new dimension to the traditional pricing problem: uncertainty.

This chapter proposes pricing methodologies in the presence of non-convexity and stochasticity in electricity markets. The proposed approaches result in locational marginal prices which guarantee cost-recovery conditions for producers, and therefore, eliminate a need for uplifts. The prices obtained deviate in the least possible manner from conventional marginal prices. This implies that a minimum deviation from the optimal value of social welfare is also guaranteed. Moreover, the new prices preserve the short-term economic efficiency and long-term cost recovery properties of marginal prices.

The proposed pricing methods may be of interest for regulators to replace the existing pricing methods that require uplifts.

4 Economic Impact of Flexible Demands

4.1 Introduction

In the previous chapters, we have focused on market-clearing models as tools facilitating a large-scale integration of renewable generation. In this chapter, we change the view from the role of tools to the role of market players, particularly demands.

A high penetration of renewable generation requires a system with sufficient flexibility. Flexibility is the operational ability of a generating unit or a demand to be scheduled by the system operator with some degree of freedom. The operational flexibility of demands and units allows the system operator to adjust them in order to absorb renewable production to the largest extent at a minimum cost. While flexibility of a generating unit is reflected in its ramping capability, demand flexibility includes the ability to move consumption across periods, and to change the consumption level per period. Hence, a system with a large amount of renewable generation needs to promote demand flexibility and building fast-ramping units. This implies that a common future power generation mix may consist of comparatively cheap renewable units and comparatively expensive fast-ramping units.

Given that the driving factors behind marginal prices are the production costs of units, a swing between high marginal prices (due to high production costs of fast-ramping units) and low marginal prices (due to small production costs of renewable units) seems likely. But also, high demand flexibility may alter energy prices such that what is known nowadays as peak and off-peak prices may fade by demand flexibility, as it basically shifts energy consumption from peak periods to off-peak periods.

The interaction between energy prices and flexible demands is complex. On one hand, demand flexibility is recognized to be beneficial to the system as a whole since such flexibility facilitates the integration of renewable generation with a reduced operation cost, but on the other hand, shifting demands from peak periods to off-peak periods may influence prices to an extent that affects the willingness of demands to be flexible.

Therefore, in a power system with a high penetration of cheap renewable production and expensive fast-ramping units, a legitimate question is whether being flexible is advantageous for demands.

To address this question, this chapter analyzes the operational and economic impacts of demand flexibility, particularly demand revenues.

Note that the contribution of demands in providing flexibility to assist the integration of renewable generation ([44] and [1]) from the system point of view is discussed in [39], [75], and [74]. However, analyses focusing on the economic impacts of demand flexibility are not common in the literature, particularly the impact of different degrees of demand flexibility on day-ahead prices.

4.2 Approach

We investigate the economic consequences resulting from flexible demand actions in a market involving a significant amount of cheap renewable power production and expensive fast-ramping units. To this aim, we use a two-stage stochastic clearing model, similar to the model introduced in Chapter 2. However, this model is carefully adapted to consider demand flexibility.

We should note that the use of a two-stage model is solely for the sake of convenience. A multi-stage model comprising a number of intra-day markets in addition to the day-ahead market and real-time one can be considered without difficulties. Note that this does not change the outcome of the analyses in this chapter.

An actual system exhibiting the properties described above is the one in mainland Spain, a system mostly based on gas and wind units. The energy prices may swing between high prices driven by comparatively expensive gas units and low prices driven by comparatively cheap wind units. Inspired by this system, we consider a power system with a generation mix of wind and gas units for our analyses and investigate the impact of demand flexibility in such a system by following the steps below:

- We consider flexible demands with a certain minimum daily energy consumption, and the ability to move their consumptions across time periods.
- We use a two-stage model to obtain the day-ahead market outcomes including sched-

uled power production of units, scheduled power consumptions of demands, and day-ahead prices.

- The prices are obtained using the prevalent price scheme in industry [46] that is described as the conventional pricing approach in Chapter 3. We should note that if pricing schemes other than the one adopted [46] are used, e.g., a convex-hull pricing [24], the problem of concern remains the same, and therefore, the choice of pricing scheme is not particularly relevant.
- Next, we consider demands to be inflexible with the same daily energy consumptions as those considered for flexible demands, and we obtain the day-ahead market outcomes.
- Finally, the results of the case with flexible demands are compared to the outcomes obtained from inflexible demands.

4.3 Assumptions

Before elaborating on the mathematical formulation of the clearing model with flexible demands, we list below the assumptions considered for the sake of simplicity and convenience.

- A generation mix of wind units and gas units are considered for our analyses. Wind power output is considered to be the only source of uncertainty.
- Wind power output is represented by a number of scenarios. These scenarios are built using historical wind production data as samples without applying any scenario generation/reduction techniques.
- The wind producers are assumed to offer their production at a comparatively small cost.
- For simplicity, the cost functions of generating units and utility functions of flexible demands are assumed to be linear.
- The cost of deploying reserve is the cost of energy production if the source for reserve deployment is a unit, and if the source is a flexible demand, the utility of demand is the cost of deploying reserve.

  the utility of a flexible demand if the source is a demand.
- The stochastic clearing model co-optimizes energy and reserve deployment without explicit reserve offers in the day-ahead market. Units and flexible demands can specify the reserve limits (MW) that they are willing to provide, and hence, we give them the opportunity of reserve deployment for a profit.

- A linear representation of the transmission network is considered through a dc load flow model where losses are neglected.

- We do not consider security criteria, such as n-1, to focus on the analyses of wind uncertainty.

- The non-convexities considered are solely those due to non-zero minimum power outputs of conventional units, start-up costs, and binary unit-commitment variables. Taking into account other source of non-convexities, such as shut-down costs and minimum up/down time constraints, is straightforward.

4.4 Model Description: Two-Stage Stochastic Clearing with Flexible Demands

The decision-making sequence of the two-stage model is described in Chapter 2. Hence, we do not repeat the description of variables and constraints. However, the two-stage model still needs to be adapted to consider flexible demands.

In the following, we first list variables and constraints pertaining to demand flexibility, and next, we provide the mathematical description of the two-stage model with flexible demands followed by a brief description of the constraints.

4.4.1 Flexible Demands as Decision Variables

Similar to generating units, flexible demands are scheduled in the day-ahead market before wind power output is realized. These flexible demands can also react to actual wind power output in real-time operation by deploying reserves.

Therefore, the day-ahead demand schedules are first-stage variables, while flexible demands in term of providing reserve deployments are second-stage variables. We define actual loads as second-stage variables that result from the day-ahead demand schedules and real-time deployments, i.e., $d_{jt\omega} = D_{jt} + d^{\mathrm{D}}_{jt\omega} - d^{\mathrm{U}}_{jt\omega}$.

Therefore, the following variables are considered in addition to the set of variables described in Section 2.4.2, i.e., $\Xi = \{C^{\mathrm{SU}}_{it}, u_{it}, P_{it}, \forall i, \forall t; W_{qt}, \forall q, \forall t; \theta_{nt}, \forall n, \forall t; r^{\mathrm{U}}_{it\omega}, r^{\mathrm{D}}_{it\omega}, \forall i, \forall t, \forall \omega; w^{\mathrm{spill}}_{qt\omega}, \forall q, \forall t, \forall \omega; \theta_{nt\omega}, \forall n, \forall t, \forall \omega; L^{\mathrm{shed}}_{jt\omega} \forall j, \forall t, \forall \omega\}$:

- Load scheduled for each flexible demand in each period at the day-ahead market (D_{jt}, [MW]).

- Deployed up-reserve by each flexible demand in each period and each scenario in real-time operation ($d^{\mathrm{U}}_{jt\omega}$, [MW]).
- Deployed down-reserve by each flexible demand in each period and each scenario in real-time operation ($d^{\mathrm{D}}_{jt\omega}$, [MW]).
- Actual load consumed by each flexible demand in each period and each scenario in real-time operation ($d_{jt\omega}$, [MW]).
- Final power output of each generating unit in each period and each scenario in real-time operation ($p_{jt\omega}$, [MW]).

Objective Function

In the presence of flexible demands, the objective function to be maximize is the expected social welfare, and it includes the following terms:

- The day-ahead cost that includes the start-up cost and production costs of conventional units, the production cost of wind units, and the utility of flexible demands over all periods of the market horizon:

$$\sum_{t=1}^{N_T}\Big(\sum_{i=1}^{N_G}(C^{\mathrm{SU}}_{it}+C_iP_{it})+\sum_{q=1}^{N_Q}C_qW_{qt}-\sum_{j=1}^{N_L}U_{jt}D_{jt}\Big) \tag{4.1}$$

- The expected balancing cost that results from the deployed reserves by conventional units and flexible demands, and involuntary load shedding in real-time operation:

$$\begin{aligned}&\sum_{t=1}^{N_T}\sum_{\omega=1}^{N_\Omega}\pi_\omega\Big[\sum_{i=1}^{N_G}C_i(r^{\mathrm{U}}_{it\omega}-r^{\mathrm{D}}_{it\omega})+\sum_{q=1}^{N_Q}C_q(W^{\mathrm{RT}}_{qt\omega}-W_q-w^{\mathrm{spill}}_{qt\omega})\\&+\sum_{j=1}^{N_L}V^{\mathrm{LOL}}_{jt}L^{\mathrm{shed}}_{jt\omega}-U_{jt}(d^{\mathrm{D}}_{jt\omega}-d^{\mathrm{U}}_{jt\omega})\Big]\end{aligned} \tag{4.2}$$

Thus, the expected social welfare is:

$$\sum_{t=1}^{N_T}\sum_{i=1}^{N_G}-C^{\mathrm{SU}}_{it}-\sum_{\omega=1}^{N_\Omega}\pi_\omega\Big[\sum_{t=1}^{N_T}\Big(\sum_{i=1}^{N_G}C_ip_{it\omega}+\sum_{q=1}^{N_Q}C_q(W^{\mathrm{RT}}_{qt\omega}-w^{\mathrm{spill}}_{qt\omega})+\sum_{j=1}^{N_L}(V^{\mathrm{LOL}}_{jt}L^{\mathrm{shed}}_{jt\omega}-U_{jt}d_{jt\omega})\Big)\Big] \tag{4.3}$$

where $p_{it\omega}=P_{it}+r^{\mathrm{U}}_{it\omega}-r^{\mathrm{D}}_{it\omega}$ and $d_{jt\omega}=D_{jt}+d^{\mathrm{D}}_{jt\omega}-d^{\mathrm{U}}_{jt\omega}$.

We should note that demand utilities are equivalent to bid prices, submitted by demands to the market, and thus, the model proposed incorporates demand bids in form of $U_{jt}d_{jt\omega}$, i.e., $U_{jt}(D_{jt}+d^{\mathrm{D}}_{jt\omega}-d^{\mathrm{U}}_{jt\omega})$.

4.4.2 Constraints pertinent to Demand Flexibility

We define demand flexibility to be the ability of demands to move their consumption across periods, and to change their consumption level per period. That is, demands provide a consumption range to the system operator within which they can vary according to the preference of the operator (to benefit the system), but they have a certain energy consumption that must be respected by the system operator.

In this context, we introduce the following new constraints pertaining to flexible demands in the day-ahead market as well as in real-time operation:

Day-ahead Market Constraints

Considering the power balance equation in the day-ahead market expressed in (2.5), the inflexible demand L_{jt} changes to flexible demand D_{jt} of which schedule is determined in the market:

$$\sum_{i\in M_n^{\mathrm{G}}} P_{it} + \sum_{q\in M_n^{\mathrm{Q}}} W_{qt} - \sum_{j\in M_n^{\mathrm{L}}} D_{jt} - \sum_{r\in\Lambda_n} B_{nr}(\theta_{nt}-\theta_{rt}) = 0, \forall n, \forall t \tag{4.4}$$

The day-ahead demand schedules are enforced to be within the minimum and maximum limits in each period:

$$D_{jt}^{\min} \le D_{jt} \le D_{jt}^{\max}, \forall j, \forall t \tag{4.5}$$

Similar to the ramping limits of units, demands have pick-up and drop-down rate limits. The pick-up/drop-down rates represent how a flexible load can increase or decrease its consumption. The day-ahead demand schedules are enforced to respect these limits in each period:

$$RD_j \le D_{jt} - D_{j,t-1} \le RU_j, \forall j, \forall t \tag{4.6}$$

Real-time Operation Constraints

Considering the power balance equation in real-time operation expressed in (2.35), apart from units, flexible demands also provide deployed reserves:

$$\sum_{i\in M_n^{\mathrm{G}}}(r^{\mathrm{U}}_{it\omega}-r^{\mathrm{D}}_{it\omega})+\sum_{q\in M_n^{\mathrm{Q}}}(W^{\mathrm{RT}}_{qt\omega}-W_{qt}-w^{\mathrm{spill}}_{qt\omega})-\sum_{j\in M_n^{\mathrm{L}}}(d^{\mathrm{D}}_{jt\omega}-d^{\mathrm{U}}_{jt\omega}+L^{\mathrm{shed}}_{jt\omega})$$
$$+\sum_{r\in\Lambda_n}B_{nr}(\theta_{nt}-\theta_{nt\omega}-\theta_{rt}+\theta_{rt\omega})=0,\forall n,\forall t,\forall\omega \tag{4.7}$$

The actual load, resulting from the reserve deployment provided by the flexible demands, is enforced to be within the demand limits in real-time operation for each scenario and each time period:

$$D^{\min}_{jt}\le d_{jt\omega}\le D^{\max}_{jt},\forall j,\forall t,\forall\omega \tag{4.8}$$

The pick-up/drop-down rate limits of flexible demand j shall be respected in real-time operation for each scenario and each time period:

$$RD_j\le d_{jt\omega}-d_{j,t-1,\omega}\le RU_j,\forall j,\forall t,\forall\omega \tag{4.9}$$

The total consumption of actual demand $d_{jt\omega}$ over all periods shall respect the minimum daily energy consumption of flexible demand j, denoted by E_j. This is enforced by constraint (4.10):

$$E_j\le\sum_{t=1}^{N_T}d_{jt\omega},\forall j,\forall\omega \tag{4.10}$$

The deployed reserves are limited between zero and the available amount of reserves offered by flexible demands:

$$0\le d^{\mathrm{D}}_{jt\omega}\le R^{\mathrm{D,max}}_{jt},\forall j,\forall t,\forall\omega \tag{4.11}$$
$$0\le d^{\mathrm{U}}_{jt\omega}\le R^{\mathrm{U,max}}_{jt},\forall j,\forall t,\forall\omega \tag{4.12}$$

4.4.3 Mathematical Model

The MILP market-clearing model including flexible demands is as follows:

$$\underset{\Xi_D}{\text{Maximize}}$$

$$\sum_{t=1}^{N_T}\sum_{i=1}^{N_G} -C_{it}^{\mathrm{SU}} - \sum_{\omega=1}^{N_\Omega}\pi_\omega\Big[\sum_{t=1}^{N_T}\Big(\sum_{i=1}^{N_G} C_i p_{it\omega} + \sum_{q=1}^{N_Q} C_q(W_{qt\omega}^{\mathrm{RT}} - w_{qt\omega}^{\mathrm{spill}}) + \sum_{j=1}^{N_L}(V_{jt}^{\mathrm{LOL}} L_{jt\omega}^{\mathrm{shed}} - U_{jt} d_{jt\omega})\Big)\Big] \tag{4.13a}$$

subject to

First-stage constraints:

$$\sum_{i\in M_n^{\mathrm{G}}} P_{it} + \sum_{q\in M_n^{\mathrm{Q}}} W_{qt} - \sum_{j\in M_n^{\mathrm{L}}} D_{jt} - \sum_{r\in\Lambda_n} B_{nr}(\theta_{nt}-\theta_{rt}) = 0, \forall n, \forall t \tag{4.13b}$$

$$K_i^{\mathrm{SU}}(u_{it} - u_{i,t-1}) \le C_{it}^{\mathrm{SU}}, \forall i, \forall t \tag{4.13c}$$

$$u_{it} \in \{0,1\}, \forall i, \forall t \tag{4.13d}$$

$$u_{it} P_i^{\min} \le P_{it} \le u_{it} P_i^{\max}, \forall i, \forall t \tag{4.13e}$$

$$D_{jt}^{\min} \le D_{jt} \le D_{jt}^{\max}, \forall j, \forall t \tag{4.13f}$$

$$W_{qt} \le W_q^{\max}, \forall q, \forall t \tag{4.13g}$$

$$RD_i \le P_{it} - P_{i,t-1} \le RU_i, \forall i, \forall t \tag{4.13h}$$

$$RD_j \le D_{jt} - D_{j,t-1} \le RU_j, \forall j, \forall t \tag{4.13i}$$

$$\theta_{1t} = 0, \forall t \tag{4.13j}$$

Second-stage constraints:

$$\sum_{i\in M_n^{\mathrm{G}}}(r_{it\omega}^{\mathrm{U}} - r_{it\omega}^{\mathrm{D}}) + \sum_{q\in M_n^{\mathrm{Q}}}(W_{qt\omega}^{\mathrm{RT}} - W_{qt} - w_{qt\omega}^{\mathrm{spill}}) - \sum_{j\in M_n^{\mathrm{L}}}(d_{jt\omega}^{\mathrm{D}} - d_{jt\omega}^{\mathrm{U}} + L_{jt\omega}^{\mathrm{shed}})$$
$$+ \sum_{r\in\Lambda_n} B_{nr}(\theta_{nt} - \theta_{nt\omega} - \theta_{rt} + \theta_{rt\omega}) = 0, \forall n, \forall t, \forall\omega \tag{4.13k}$$

$$p_{it\omega} = P_{it} + r_{it\omega}^{\mathrm{U}} - r_{it\omega}^{\mathrm{D}} \tag{4.13l}$$

$$d_{jt\omega} = D_{jt} + d_{jt\omega}^{\mathrm{D}} - d_{jt\omega}^{\mathrm{U}} \tag{4.13m}$$

$$u_{it} P_i^{\min} \le p_{it\omega} \le u_{it} P_i^{\max}, \forall i, \forall t, \forall\omega \tag{4.13n}$$

$$D_{jt}^{\min} \le d_{jt\omega} \le D_{jt}^{\max}, \forall j, \forall t, \forall\omega \tag{4.13o}$$

$$RD_i \le p_{it\omega} - p_{i,t-1,\omega} \le RU_i, \forall i, \forall t, \forall\omega \tag{4.13p}$$

$$RD_j \le d_{jt\omega} - d_{j,t-1,\omega} \le RU_j, \forall j, \forall t, \forall\omega \tag{4.13q}$$

$$-f_{nr}^{\max} \le B_{nr}(\theta_{nt\omega} - \theta_{rt\omega}) \le f_{nr}^{\max}, \forall n, \forall r \in \Lambda_n, \forall t, \forall\omega \tag{4.13r}$$

$$E_j \le \sum_{t=1}^{N_T} d_{jt\omega}, \forall j, \forall\omega \tag{4.13s}$$

$$r_{it\omega}^{\mathrm{U}} \le R_{it}^{\mathrm{U,max}}, \forall i, \forall t, \forall\omega \tag{4.13t}$$

$$r_{it\omega}^{\mathrm{D}} \le R_{it}^{\mathrm{D,max}}, \forall i, \forall t, \forall\omega \tag{4.13u}$$

$$d_{jt\omega}^{\mathrm{D}} \le R_{jt}^{\mathrm{D,max}}, \forall j, \forall t, \forall\omega \tag{4.13v}$$

$$d_{jt\omega}^{\mathrm{U}} \le R_{jt}^{\mathrm{U,max}}, \forall j, \forall t, \forall\omega \tag{4.13w}$$

$$L^{\text{shed}}_{jt\omega} \leq d_{jt\omega}, \forall j, \forall t, \forall \omega \tag{4.13x}$$

$$w^{\text{spill}}_{qt\omega} \leq W^{\text{RT}}_{qt\omega}, \forall q, \forall t, \forall \omega \tag{4.13y}$$

$$\theta_{1t\omega} = 0, \forall t, \forall \omega \tag{4.13z}$$

$$0 \leq P_{it}, C^{\text{SU}}_{it}, \forall i, \forall t, \quad 0 \leq W_{qt}, \forall q, \forall t$$

$$0 \leq r^{\text{U}}_{it\omega}, r^{\text{D}}_{it\omega}, \forall i, \forall t, \forall \omega, \quad 0 \leq w^{\text{spill}}_{qt\omega}, \forall q, \forall t, \forall \omega$$

$$0 \leq L^{\text{shed}}_{jt\omega}, d^{\text{U}}_{jt\omega}, d^{\text{D}}_{jt\omega}, \forall j, \forall t, \forall \omega \tag{4.13aa}$$

where $\Xi_D = \{C^{\text{SU}}_{it}, P_{it}, \forall i, \forall t; W_{qt}, \forall q, \forall t; D_{jt}, \forall j, \forall t; \theta_{nt}, \forall n, \forall t; p_{it\omega}, r^{\text{U}}_{it\omega}, r^{\text{D}}_{it\omega}, \forall i, \forall t, \forall \omega; d_{jt\omega}, d^{\text{U}}_{jt\omega}, d^{\text{D}}_{jt\omega}, L^{\text{shed}}_{jt\omega}, \forall j, \forall t, \forall \omega; w^{\text{spill}}_{qt\omega}, \forall q, \forall t, \forall \omega; \theta_{nt\omega}, \forall n, \forall t, \forall \omega\}$ is the set of optimization variables.

The problem (4.13) maximizes the expected social welfare (4.13a) considering the day-ahead constraints (4.13b)-(4.13j), the real-time operation constraints (4.13k)-(4.13z), and variable declarations expressed in (4.13aa).

A brief description of the constraints is as follows. Constraint (4.13b) represents the power balance in the day-ahead market, where scheduled power production of units and scheduled loads of flexible demands are determined. The start-up costs are modeled by equation (4.13c), which depend on the on/off status of each generating unit via binary variable u_{it} in constraint (4.13d). The limits of production of conventional units, flexible demands, and wind production in the day-ahead market are represented by constraints (4.13e), (4.13f) and (4.13g), respectively. Constraint (4.13h) enforces the ramping limits of generating units. Similarly, constraint (4.13i) enforces the pick-up/drop-down rate limits of flexible demands in the day-ahead market. Constraint (4.13j) establishes that node 1 is the reference node in the day-ahead market.

Constraint (4.13k) stands for power balance in real-time operation, where actual wind power output is compensated by deploying reserves provided by conventional units and flexible demands, as well as (in rare cases) load shedding. The power output of unit i during period t and scenario ω is described by equation (4.13l), and the actual load for flexible demand j in period t and scenario ω by equation (4.13m). The reserve deployment provided by the conventional units shall respect the generation limits, and the reserve deployment provided by the flexible demands must be within the demand limits in real-time operation. These limits are considered in constraints (4.13n) and (4.13o), respectively. Constraint (4.13p) represents the ramping limits of generating units, and constraint (4.13q) represents the pick-up/drop-down rate limits of flexible demands in real-time operation. Constraint (4.13r) enforces that the line flows stay within the transmission capacity limits at real-time operation. Note that enforcing this constraint is not generally required in the day-ahead market. The day-ahead schedules can violate these limits as long as actual power flows are still within the transmission limits in any realization of the wind scenario in real-time operation. A minimum daily energy consumption of flexible demand j is enforced by (4.13s). Constraints (4.13t) and (4.13u), (4.13v) and (4.13w) stand for maximum up and down reserve limits provided by conventional units and flexible demands, respectively. The limits of load shedding and wind spillage are provided in constraints (4.13x) and (4.13y), respectively. Constraint (4.13z) establishes node 1 as the reference node in real-time operation.

Non-negativity of scheduled productions and consumptions, start-up costs, wind productions, deployed reserves, wind spillage, and load shedding are enforced by constraints (4.13aa).

We should note that in the case of inflexible demands, variables $d^{\mathrm{U}}_{jt\omega}$ and $d^{\mathrm{D}}_{jt\omega}$ are set to zero, and consequently, constraint (4.13m) change to $d_{jt\omega} = D_{jt}$, where D_{jt} is equal to the constant L_{jt}, representing an inflexible load pattern. Note also that, contrary to flexible demands, inflexible demands cannot vary within a range.

4.5 Illustrative Example

For illustration purposes, we apply the clearing problem (4.13) to a simple system to show how consumption levels are allocated differently in a flexible demand case and in an inflexible demand case, and how this different allocation affects prices, and consequently, producer profits and consumer payments.

4.5.1 Data

The test system is depicted in Fig. 4.1. We consider a scheduling horizon of two periods for this analysis. The system includes three conventional units, three demands and a wind unit, as described in the following.

The data of the conventional units are provided in Table 4.1. The maximum reserves $R_i^{\mathrm{U,max}}$ and $R_i^{\mathrm{D,max}}$ provided by these units are assumed to be equal to P_i^{max}. Hence, all units can be dispatched for both energy and reserve. Also, no limitations are assumed for the ramping rates of the conventional units.

We consider demand utilities to be zero. The prices are therefore driven solely by the production costs of the units. We also assume that demands do not provide reserve and that flexibility for demands is the ability of shifting load across time periods. We consider a minimum energy consumption (E_j) of 180 MWh, 111 MWh, and 209 MWh for demands D_1, D_2, and D_3, respectively. A value of lost load equal to \$2000/MWh is considered in real-time operation.

The wind power plant, at node 2, has an installed capacity of 300 MW. A small production cost of \$0.3/MWh is assumed for this unit. Two equi-probable scenarios are used to model the wind power output uncertainty for each time period, as provided in Table 4.2. We should note that period t_1 represents a period with a high wind power production while at period t_2 the wind power output significantly decreases.

All line reactances are equal to 0.13 p.u. and all line capacities are set to be high enough to avoid congestion.

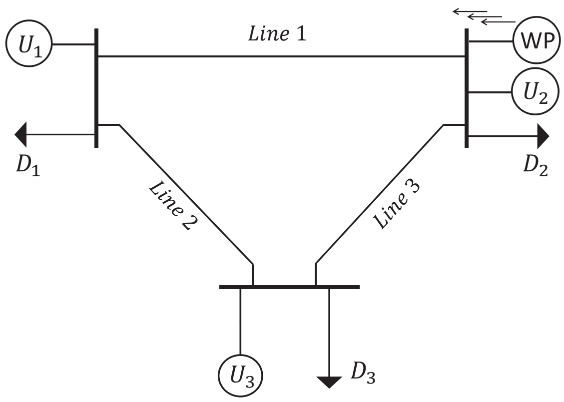

Figure 4.1 – Test system

Table 4.1 – Data of generating units.

Unit	K_i^{SU} [\$]	C_i [\$/MWh]	$P_i^{\max}$[MW]	$P_i^{\min}$ [MW]	$R_i^{\mathrm{U,max}}$ [MW]	$R_i^{\mathrm{D,max}}$ [MW]
U_1	300.01	10.03	95	15	95	95
U_2	102.2	30.02	100	10	100	100
U_3	101.2	31.01	105	5	105	105

Table 4.2 – Wind scenarios ($W_{qt\omega}^{\mathrm{RT}}$) [MW]

Period	scenario ω_1	scenario ω_2
t_1	283	299
t_2	10	13

4.5.2 Market Outcomes

Below, we present the results, including day-ahead schedules and day-ahead prices, for two cases, one with flexible demands and other with inflexible demands.

Fig. 4.2 shows the day-ahead scheduled production (upper plots) and scheduled demands (bottom plots) for the cases described.

In the case with inflexible demands, the consumption is assumed to be fixed to 283 MW in period t_1 and to 217 MW in period t_2 (total 500 MW).

In this allocation, none of the conventional units is scheduled in period t_1 (the load is covered solely by the wind unit), whereas all of them are scheduled in period t_2. On the other hand, in the case with flexibility, demand is moved from period t_2 to period t_1 so that a larger load share (378 MW from 500 MW) is allocated to period t_1 and a smaller one (122 MW from 500 MW) to period t_2. Note that this is the outcome that we aim to obtain in order to be able to explore the impact of flexible demands on marginal prices.

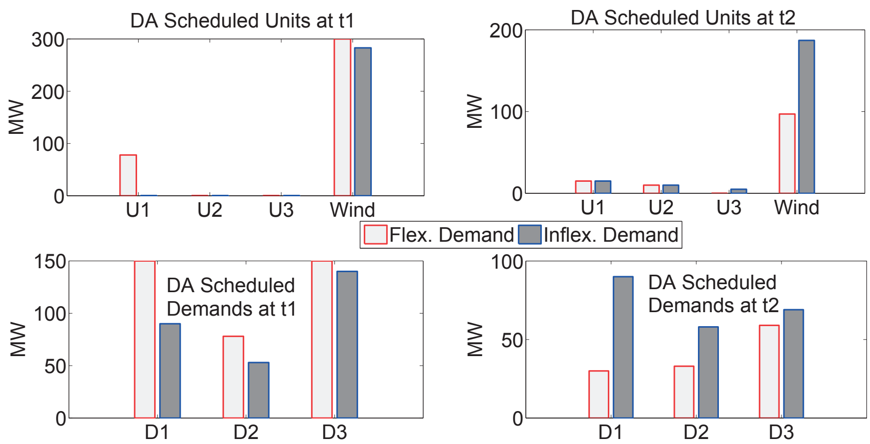

Figure 4.2 – Day-ahead scheduled units and demands - illustrative example

Table 4.3 provides the day-ahead prices λ_t and the probability-removed balancing prices $\lambda_{t\omega}/\pi_\omega$ per scenario. Since there is no congestion in any of the scenarios considered, electricity prices do not change across nodes.

As mentioned in the previous chapters, these prices are obtained as dual variables of power balance equations after setting the binary unit-commitment variables to their optimal values [46].

In period t_1, the price from the inelastic demand case is the lowest, whereas it is the highest in period t_2. This is due to the commitment decisions: since none of the conventional units is committed in period t_1, the corresponding prices obtained are solely driven by the small cost of the wind unit. However, in period t_2 all conventional units are online and the corresponding prices are driven by the marginal production cost of unit U_3. Under flexible demands, the shift of demands from period t_2 to period t_1 turns unit U_1 on in period t_1, which results in a higher price (\$10.03/MWh) than that of the inflexible demand case (\$0.3/MWh).

Table 4.3 – Day-ahead and probability-removed balancing prices (\$/MWh)

	Flexible demand		Inflexible demand	
	t_1	t_2	t_1	t_2
λ	10.03	30.02	0.3	31.01
$\lambda_{\omega_1}/\pi_{\omega_1}$	10.03	30.02	0.3	31.01
$\lambda_{\omega_2}/\pi_{\omega_2}$	10.03	30.02	0.3	31.01

Therefore, demand flexibility results in higher prices in valley and slightly lower prices in peak.

Given these schedules and prices, Table 4.4 provides the day-ahead profit, expected profit, day-ahead cost, expected cost, consumer payment, and uplift for the different cases.

Table 4.4 – Market outcomes of three-node system

	Flexible demand		Inflexible demand	
Unit	DA Profit (\$)	Exp. Profit (\$)	DA Profit (\$)	Exp. Profit (\$)
U_1	-0.16	1599.04	14.69	1693.09
U_2	-102.20	-102.20	-92.30	-3.20
U_3	0.00	0.00	-101.20	-101.20
Wind	5801.84	5801.84	5742.77	5742.77
Total	5699.48	7298.68	5563.96	7331.46
	DA	Exp.	DA	Exp.
Cost (\$)	1754.30	2783.70	1250.10	4872.20
	Consumer Payment (\$)		Consumer Payment (\$)	
	7453.80		6814.10	
	Uplift (\$)		Uplift (\$)	
	102.36		193.50	

The inflexible demand case results in a higher expected cost and a lower day-ahead cost than those from the case with flexibility. The comparatively lower day-ahead cost of the inflexible demand case is due to a higher amount of wind power scheduled in the day-ahead market. However, this requires a high expected balancing cost of deployed reserves, and eventually, leads to a higher total expected cost than that of the case with flexibility.

This observation confirms that demand flexibility is beneficial to the system, as it decreases the operation cost.

Focusing on unit profits, the inflexible demand case results in a smaller total day-ahead profit (i.e., \$5563.96 vs \$5699.48), but a larger total expected profit than those from the flexible demand case. The smaller total day-ahead profit is due to the low prices (i.e., \$0.3/MWh) that are driven by the off status of the conventional units in period t_1, and a larger total expected profit results from high prices (i.e., \$31/MWh) obtained in period t_2.

Note that under the day-ahead prices obtained, units U_1 and U_2 cannot recover their production costs in the flexible demand case, as well as units U_2 and U_3 in the inflexible demand case. These losses disappear or decrease, if the respective units are deployed at the operation stage, such as unit U_1 in the flexible demand case and unit U_2 in the inflexible demand case. Adopting the common practice of uplifts, these side-payments are provided for both cases.

Finally, the consumer payment, which is the summation of the day-ahead cost and total day-ahead profit, is smaller under the inflexible demands than that under flexible demands. Note that the flexible demand case results in a smaller day-ahead cost, but a higher total day-ahead profit. The latter causes a higher consumer payment under this case than that of the inflexible demand case. In other words, demand flexibility results in prices that increase unit profits, and consequently, the demand payments.

Therefore, although demand flexibility is beneficial to the system as a whole, it may result in prices not beneficial for the flexible demands.

4.6 Case Studies

In this section, we present two case studies: one without network congestion and without ramping limits of units, and another with both network congestion and ramping limits of units.

Similar to the illustrative example and for simplicity, the utility of demands is considered to be zero. Therefore, the marginal prices are linked to the production costs of units.

In other words, we explore a situation where demands support the system operator with a full scale flexibility free of charge, and compare the operational and economic outcomes to the case with inflexible demands.

4.6.1 Data

The test system is a modified version of the 24-node system based on the single-area IEEE RTS [72] including a generation mix of expensive fast-ramping units and one wind unit to facilitate the analyses of the results.

The system considered has 34 lines, 8 conventional units, and 1 wind power unit. The data of conventional units are provided in Table 4.5. Note that apart from hydro units U_{50}, the rest of the units have relatively high production costs as compared to the cheap wind unit. As previously mentioned, such a generation mix is motivated by the case of mainland Spain, whose generation mix is dominated by gas and wind units. Considering this generation mix, we note that gas units (CCGTs) are generally not subject to minimum up/down time constraints. Therefore, these constraints are not considered. We assume that the limit of reserve capacity is equal to the capacity of each conventional unit.

Table 4.5 – Characteristics of the Generating Units

	U_{90}	U_{50}	U_{155}	U_{76}	U_{197}
Node	2	7,15	10,18	16	21,22
$P_i^{\max}$ [MW]	90	50	20	76	197
$P_i^{\min}$ [MW]	25	15	12	15.2	69
K_i^{SU} [$]	400	100	400	400	300
C_i [$/MWh]	19.67	0.2	10.68	11.89	18.09
$R_i^{\mathrm{U,max}}$[MW]	90	50	20	76	197
$R_i^{\mathrm{D,max}}$[MW]	90	50	20	76	197

Table 4.6 provides demand data including their location and minimum energy consumption E_j.

The wind power unit, located at node 7, has an installed capacity of 1000 MW. To generate wind power scenarios, we use wind speed historical data from Austin, Texas, which are available in the System Advisor Model (SAM) [2]. To obtain hourly wind power scenarios for 24 time periods, we apply the power curve of a 2-MW Vestas V80/2000 wind turbine with a hub height of 80 m. The power curve of this turbine model can be found in [16].

We should note that we built up the scenarios employing historical data without applying scenario reduction techniques.

We consider 30 equi-probable scenarios for the wind power output in real-time operation.

Table 4.6 – RTS case: Demand Information

Demand	D1	D2	D3	D4	D5	D6	D7	D8
Node	1	2	3	4	5	6	7	8
Minimum Energy (MWh)	775	1415	2675	1005	896	1165	1065	1505
Demand	D9	D10	D11	D12	D13	D14	D15	D16
Node	9	10	13	14	15	16	18	19
Minimum Energy (MWh)	1287	1129	988	1021	1275	955	1085	1430

4.6.2 Base Case: No Congestion

For first case, we consider high enough transmission capacity so that no congestion occurs. Therefore, prices are the same across nodes. Also, the ramping limits of units are assumed to be equal to their capacities.

For the case with inflexible demands, demands D_{jt} are fixed to given load value L_{jt}, i.e., $D_{jt} = L_{jt}$, with off-peak values during the early morning and the late evening, and peak values over day hours.

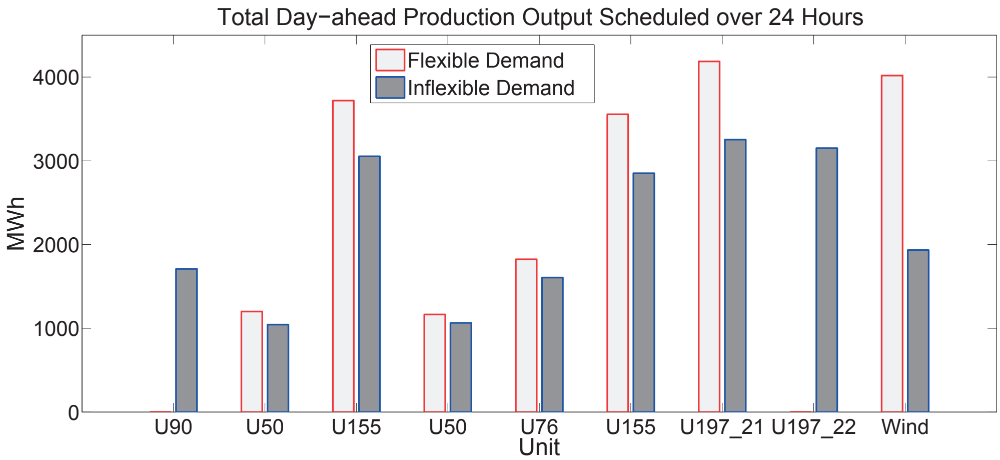

Figure 4.3 – Day-ahead production scheduled over 24 periods (RTS system)

Fig. 4.3 shows the day-ahead energy production of all units scheduled over all periods. In the flexible demand case, the wind power output scheduled is almost twice than that in the inflexible demand case. This observation confirms the impact of demand flexibility in integrating wind production. Also, units U_{90} and U_{197} (the one located at node 22) stay offline in the flexible demand case, while all conventional units, including expensive unit U_{90}, are scheduled in the inflexible demand case. The impact of unit U_{90} on the day-ahead prices is elaborated below.

Figs. 4.4 and 4.5 show the total scheduled demand and the day-ahead prices, respectively.

In the case with inflexible demands (blue and squares), during periods $t_1 - t_4$ demands are relatively small and can be supplied solely by wind generation. In the mid-day hours, demand grows while wind generation decreases. Therefore, to cover the demands, other units are required. Focusing on the outcome from flexible demands (red and circles), demands are shifted to periods $t_1 - t_5$ and periods $t_{20} - t_{24}$ which are periods with cheap wind generation.

Correspondingly, the day-ahead prices have a different pattern for these cases: in the case with inflexible demands, in periods $t_1 - t_3$ and $t_{22} - t_{24}$ the day-ahead prices are derived from the small production cost of wind unit, and therefore, are very low. With the load increase starting at period t_4, the prices increase until period t_{20}, when the load decreases. In the flexible demand case, the day-ahead prices are relatively high for all periods, however, still smaller than the peak price of the inflexible demand case. They are overall high since demands are shifted to low-demand periods (night hours). Increasing the demands in these periods that now require both wind and conventional units (except from expensive unit U_{90}) results in overall high prices. Due to the off status of unit U_{90}, the peak price of the case with flexible demands is smaller than that of the inflexible demand case.

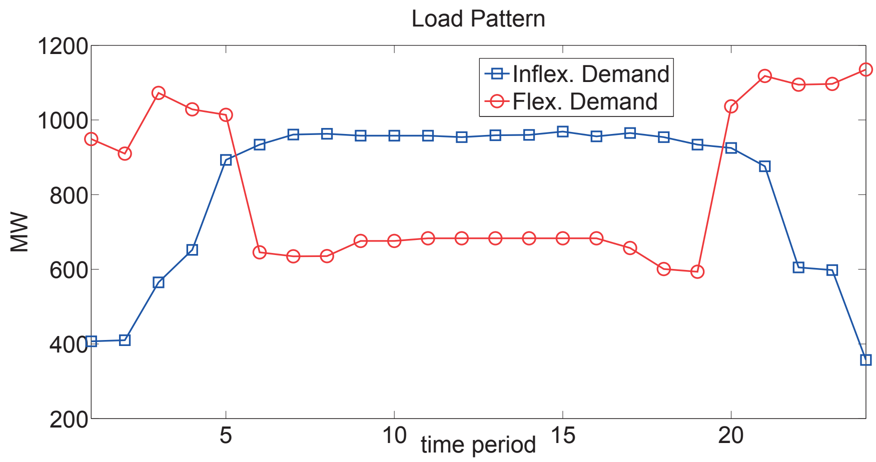

Figure 4.4 – Demand pattern obtained from the flexible and inflexible demand cases (RTS system)

Table 4.7 provides details regarding day-ahead profits, expected profits, day-ahead costs, expected costs (i.e., the total of day-ahead cost and balancing cost[1]), consumer payments, uplifts, and total day-ahead scheduled demand resulting from the two case: flexible and inflexible demands.

For the same amount of scheduled demand (i.e., 19,671 MWh), moving from the case with inflexible demands to the case with flexibility, a cost saving of 24% is obtained in the day-ahead

[1]The day-ahead cost, the expected balancing cost, and the total expected cost are formulated in (4.1), (4.2), (4.3), respecively.

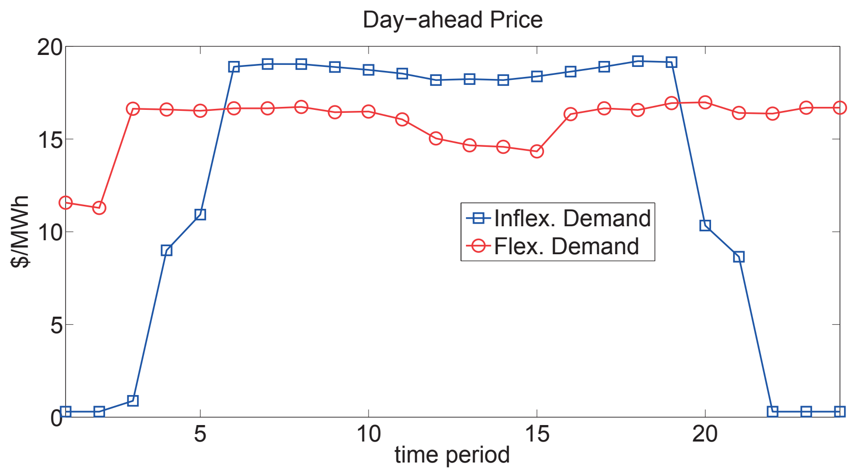

Figure 4.5 – Day-ahead prices obtained from the flexible and inflexible demand cases (RTS system)

market, and a reduction of 23% is achieved in the total expected cost.

The smaller day-ahead cost results from a higher day-ahead wind production in the case with flexibility (see Fig. 4.3), as compared to the counterpart values in the case with inflexible demands. This is possible due to the flexible demands which are able to be shifted to periods, where the wind blows.

It is of interest to note that in both cases, the day-ahead costs are higher than the total expected cost, implying that the clearing model allocates a high share of supply to wind unit in the day-ahead market, and deploy reserves in the downward direction to follow the actual wind power output. The expected balancing cost in the case with flexibility is \$34,820, which is 24% of total expected cost in this case, while the expected balancing cost of the case with inflexible demands is \$47,820 which owns a share of 25% of total expected cost.

Focusing on unit profits, only unit U_{197}, located in node 21, cannot recover its production cost in the case of flexibility, while both units U_{197} (located at nodes 21 and 22) and unit U_{90} incur losses under the inflexible demand case. This consequently leads to a higher uplift for the case with inflexible demands than that of the case with demand flexibility. In the case with flexibility, other units have higher profits, among which the profit of wind unit is the highest, as compared to those in the case with inflexible demands. Higher day-ahead profit of units in the flexible demand case results from overall higher day-ahead prices in this case, as shown in Fig. 4.5. The high profit of the wind unit is a result of high day-ahead prices and its day-ahead production schedule of about 4 GWh (see Fig. 4.3). Consequently, higher day-ahead and expected profits result from the flexible demand case than from the case with inflexible demands.

Table 4.7 – Economic Outcomes (base case - RTS system)

Unit	Flexible demand DA Profit ($)	Flexible demand Exp. Profit ($)	Inflexible demand DA Profit ($)	Inflexible demand Exp. Profit ($)
U_{90}	0.00	0.00	-8672.29	-2697.86
U_{50}	17691.48	17698.02	13310.71	14015.00
U_{155}	18744.00	19343.47	13672.96	15189.82
U_{50}	17146.79	17698.02	13955.38	14015.00
U_{76}	6779.69	7406.56	3388.50	6055.38
U_{155}	17740.75	19343.46	13358.34	15282.41
$U_{197_{n21}}$	-8163.73	-2309.13	-4619.08	-1555.64
$U_{197_{n22}}$	0.00	0.00	-4179.50	-1555.64
Wind	60924.56	60924.56	7341.70	7341.70
Total	130863.54	140104.95	47556.73	66090.18
	DA	Exp.	DA	Exp.
Cost ($)	180420.00	145600.00	236780.00	188960.00
	Consumer Payment ($)		Consumer Payment ($)	
	311280.00		284340.00	
	Uplift ($)		Uplift ($)	
	8163.70		17471.00	
	Total DA Demand (MWh)		Total DA Demand (MWh)	
	19671.00		19671.00	

Therefore, the case with flexibility results in a smaller day-ahead cost and a smaller uplift, but a higher total day-ahead profit which leads to 9.5% increase in consumer payment, as compared to those from the case with inflexible demands.

This observation shows an inherent conflict in incorporating demand flexibility into an electricity market: on one hand, the system benefits from the reduced operation cost caused by demand flexibility, but on the other hand, the resulting prices increases the demand expenses. Thus, demands might be better off being inflexible.

4.6.3 Impact of Ramping Limits and Congestion

In this section, we consider that the ramping capability of each unit is half of its capacity. That is, reduced flexibility is provided by the conventional units to the system as compared to the base case, i.e., the previous case. Also, in order to create congestion, we consider reduced transmission capacity for the lines connecting node 2 to 1, to 4, and to 6, node 4 to 9, node 5 to

10 (i.e., line limits of 50 MW), and node 17 to 18, and to 22 (i.e., line limits of 137MW and 179 MW, respectively). With this consideration, congestion appears mainly in peak periods.

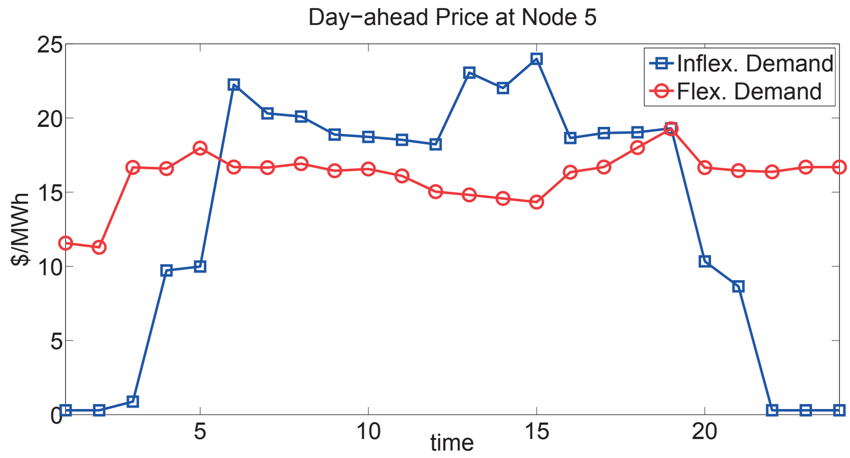

Figure 4.6 – The day-ahead prices at node 5 over different periods (ramping limits and congestion case)

As an example of the day-ahead prices obtained, Fig. 4.6 shows the prices at node 5 over the 24-hour study horizon. Similar to the trend observed in the case without congestion, the prices from the flexible demand case are higher over the off-peak periods and lower over the peak-periods with respect to the prices from the case with inflexible demands.

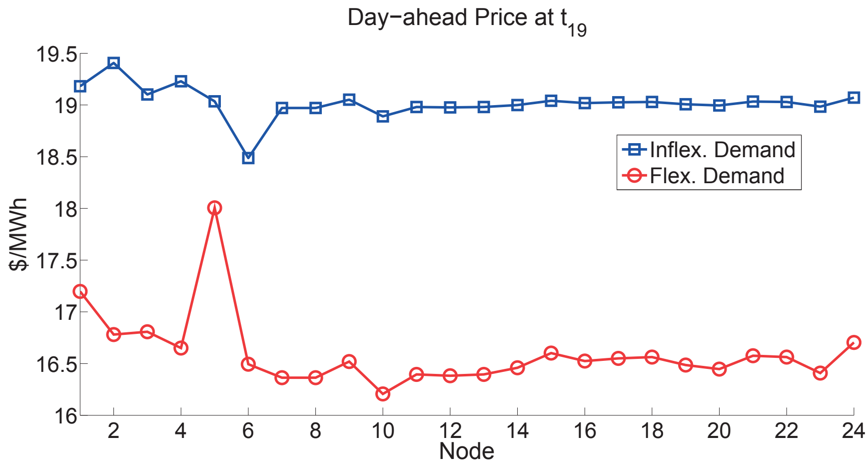

Figure 4.7 – RTS case study with congestion: nodal day-ahead prices in period t_{19}

As an example of the nodal prices (i.e., prices across the nodes), the day-ahead prices in period t_{19} are shown in Fig. 4.7. The nodal prices from the inflexible case are higher than those from the flexible demand case in this period. This observation is also valid for the other peak periods, when price differentiation across nodes appears. Note that congestion does not occur over the off-peak periods. In other words, the case with inflexible demand results in higher prices over the peak periods, and congestion does not generally change this trend.

Similar to the base case, economic metrics involving producer profits and operation costs, as well as consumer payments and uplifts are provided in Table 4.8. The total consumption remains the same at 19,671 MWh.

Table 4.8 – Economic Outcomes; RTS system including ramping limits and congestion

	Flexible demand no reserves		Inflexible demand	
Unit	DA Profit ($)	Exp. Profit ($)	DA Profit ($)	Exp. Profit ($)
U_{90}	0.00	0.00	-7361.58	-2328.60
U_{50}	17654.27	17660.88	13949.36	14051.56
U_{155}	18537.21	19298.32	12533.66	15202.75
U_{50}	17700.20	17705.86	14127.06	14202.31
U_{76}	6359.70	7419.09	3802.66	6277.80
U_{155}	18419.18	19377.62	14644.06	15710.47
$U_{197_{n21}}$	-8004.79	-2305.46	-5179.46	-1301.82
$U_{197_{n22}}$	0.00	0.00	-4831.20	-1311.11
Wind	61744.36	61744.36	5424.60	5424.60
Total	132410.14	140900.68	47109.16	65927.95
	DA	Exp.	DA	Exp.
Cost ($)	178494.71	145601.59	239971.32	190137.53
	Consumer Payment ($)		Consumer Payment ($)	
	311789.61		289790.00	
	Uplift ($)		Uplift ($)	
	8004.79		17372.00	

The case with flexible demands results in a reduction of about 26% in the day-ahead cost and 23% in the total expected cost, as compared to those from the case with inflexible demands. This is similar to the observation in the base case. In principle, demand flexibility allows consumption shift from peak periods to off-peak periods, when cheap wind production is available, irrespective of network congestion and unit (ramping) flexibility.

The case with inflexible demands results in a lower day-head producer profit, and a lower expected total producer profit, and a higher uplift than those from the flexible demand case.

Finally, the comparatively high day-ahead profit from the case with flexibility (about $130,000) leads to an increase of 7.5% in the consumer payment.

Therefore, congestion and ramping limits of the conventional units do not change the conclusions from the previous case, of which the most important one is that demands incur higher expenses under the flexible demand case.

4.6.4 Case Study Conclusions

To get insights about the impact of demand flexibility, we compare two cases: one with highly flexible demands in term of their ability to shift consumption across periods in the day-ahead market without considering the demand ability of reserve provision for real-time deployment; and the case with inflexible demands including inelastic demands following a traditional consumption pattern with peak consumption in day hours and off-peak consumption in night hours. The common feature of the two cases is that demands have the same total energy consumption over the entire clearing horizon. Therefore, we are able to explore producers and consumers expenses for the same amount of energy consumption. Based on the observations in these case studies, we conclude the followings:

1. Demand flexibility is beneficial to the system, as it shifts consumption from day hours to night hours, when cheap wind production is available. In other words, demand flexibility adapts its consumption pattern to the production pattern of the wind unit. Specifically, the scheduled production of the wind unit (i.e., the contribution of wind production in energy supply) is almost twice in the case with flexibility. This leads to a cost reduction of about 25%, as compared to the cost obtained from the case with inflexible demands.

2. Due to the notable shift in consumption in the case with demand flexibility, a price shift occurs: the prices from the flexible demand case are comparatively higher over the off-peak periods and comparatively lower over the peak-periods with respect to the prices from the case with inflexible demands. Network congestion and ramping limits of the conventional units do not change these conclusions.

3. Higher off-peak prices result in a higher consumer payment in the flexible demand case than that of the case with inflexible demands. The increase in consumer payment is 9% in the base case and 7.5% in the case with congestion and limited ramping capability.

4. The observations from the case studies show an inherent conflict in incorporating demand flexibility to an electricity market: on one hand, the system benefits from the reduced operation cost caused by demand flexibility, but on the other hand, the resulting prices increases the demand expenses. Thus, demands might be better off being inflexible.

4.7 Summary and Conclusion of the Chapter

This chapter is devoted to analyze the economic consequences resulting from the actions of flexible demands in a common future market consisting of a significant amount of renewable power production with comparatively low marginal cost and fast-ramping units with comparatively high marginal cost, such as combined-cycle gas turbines.

On one hand, demand flexibility (the ability of some demands to move load from peak periods to off-peak periods) is beneficial for the system as a whole since it decreases the expected operation cost, but on the other hand, demand flexibility can result in price increases that in turn increase demand expenses. Therefore, demands might be better off being inflexible in systems with a generation mix dominated by comparatively cheap renewable units and comparatively expensive fast-ramping units.

We should note that if pricing schemes other than the one adopted [46] are used, e.g., a convex-hull pricing [24], the conclusions derived in our study are likely to remain valid provided that the final prices do not deviate significantly from marginal prices.

We should also note that the use of a stochastic clearing model is for the purpose of obtaining optimal outcomes in a market with a high penetration of renewable generation, and the choice of clearing model, i.e., a deterministic or a stochastic one, does not change the conclusion above.

The observations in this chapter call for new settlement approaches seeking to encourage demand flexibility.

5 Two-Stage Stochastic Clearing Model for the Reserve Market

5.1 Introduction

The system operator is responsible to ensure system security in power systems. A mechanism to do so is reserve; in real-time operation, there is a need to compensate mismatches between supply and demand in order to preserve the power balance in the system. For this purpose, reserves are scheduled in *a market* prior to real time to be eventually deployed in real-time operation. The structure of this market (e.g., gate closure, type of offers, etc.) depends on the market organization, i.e., a centralized market organization and a decentralized one.

In a centralized market organization, such as electricity markets in the US, reserves are scheduled in the day-ahead market co-optimizing energy and reserves (this is similar to the clearing models in Chapter 2), whereas in a decentralized market organization, such as electricity markets in Europe, reserves are procured in reserve markets separately from energy markets. In a centralized market, the system operator and market operator are generally the same entity. However, a decentralized market separates energy transactions and system operations to a large extent; the former is done by the market operator, whereas the latter is the responsibility of the Transmission System Operator (TSO) [3].

The common practice in many European countries, as examples of the decentralized market organization, is first to determine fixed amounts of reserves (of different types) using technical (security) criteria, and then, to procure them in reserve markets. We challenge this practice as it decouples technical criteria from market aspects, which may result in economic inefficiencies.

The particular focus of this chapter is the reserve market in Switzerland, as an example of a decentralized market organization. We use two-stage stochastic clearing models to show the advantages of our proposed model with respect to deterministic one, not only through simulated case studies, but also through the outcomes of the actual implementation of the proposed two-stage clearing model.

The lay-out of this chapter is as follows. We first describe the Swiss reserve market in Section 5.2. Next, the decision-making process and scenarios are described in Sections 5.3 and 5.4, respectively. Section 5.5 provides the assumptions that we use to model the reserve market. Section 5.6 provides the mathematical descriptions of the proposed risk-neutral two-stage stochastic model (in Section 5.6.1), of the proposed risk-averse counterpart (in Section 5.6.2), and of a common deterministic model (in Section 5.6.3). Also, we formulate how to obtain a perfect information solution as well as the actual cost of the two-stage model in Section 5.6.4. The proposed models are showcased through real cases from the Swiss reserve market in Section 5.7. Finally, relevant remarks are concluded in Section 5.8.

5.2 The Swiss Reserve Market

In this section, we briefly describe the Swiss reserve market that is similar to those of other countries in continental Europe.

5.2.1 Technical Description of Reserves in Europe

According to European Network of Transmission System Operators for Electricity (ENTSO-E) definition, reserves are categorized as primary, secondary, and tertiary [47]. [1]

Primary reserves react to frequency deviations in the interconnected Continental Europe irrespective of the location of the contingencies. The corresponding amount is determined by ENTSO-E and shared among all involved countries on an annual basis. Secondary reserves automatically react to power imbalances within a time varying from a few seconds to several minutes (e.g., load fluctuations). Finally, tertiary reserves are manually deployed to replace secondary reserves [56, 34] if any power mismatch with a time duration more than several minutes occurs (e.g., a constant (load) forecast error lasting more than 15 minute or an outage of a power plant). In other words, secondary reserves compensate for spontaneous power imbalances lasting a few to several seconds, while along with secondary reserves, tertiary reserves are deployed to cover overall power mismatches lasting more than several minutes. Therefore, secondary reserves are continuously in use, and hence, tertiary reserves cannot be deployed without already-deployed secondary reserves. Fig. 5.1 illustrates the reaction

[1] In Guideline Electricity Balancing, reserves are called frequency containment reserves (FCR), frequency restoration reserves (FRR) and replacement reserves (RR) [13]. Also, frequency restoration reserves are categorized into automatic frequency restoration reserves (aFRR) and manual frequency restoration reserves (mFRR). The FCR and aFRR stand for primary and secondary reserves, respectively, while the mFRR is interpreted to be fast tertiary reserves and the RR is considered as slow tertiary reserves.

time of reserves after an outage of a power plant in France. Immediately after the outage, the frequency in the interconnected transmission system of continental Europe drops from nominal value of 50 Hz to 49.935 Hz. Primary reserves over Europe, colored map in light pink, immediately react to bring the frequency back to an acceptable value. However, a frequency error still remains since primary reserves are purely proportional. This frequency error is regulated to zero by secondary reserves in the area where the outage occurs. In this example, the map of France is in dark pink as secondary reserves in this country react to the power plant outage. Secondary reserves automatically react to the frequency drop a few seconds after the outage. Finally, tertiary reserves are manually deployed to relieve secondary reserves several minutes after the outage. Tertiary reserves are not necessarily from the location of disturbance; in this example, two units in France and one unit in Spain (in red) are deployed.

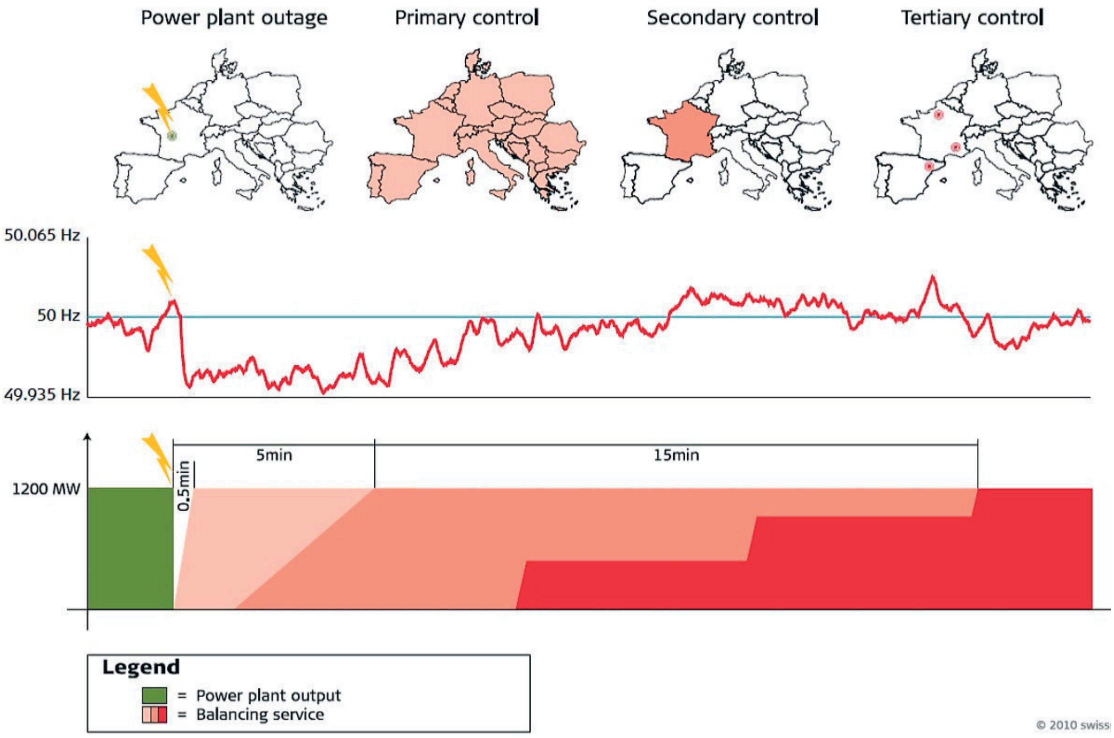

Figure 5.1 – Reaction time of primary, secondary, and tertiary reserves to a power plant outage in France [64]

As opposed to primary reserves, which are centrally decided by ENTSO-E, amounts of secondary and tertiary reserves are the responsibility of each system operator. The process of determining the required amounts of reserves is called *dimensioning reserves* by ENTSO-E.

As previously mentioned, secondary reserves are continuously in use, and therefore, tertiary reserves cannot be deployed without considering already-deployed secondary reserves. Therefore, two types of reserves are categorized for the reserve dimensioning process: secondary and overall reserves. Overall reserves represent the total of secondary and tertiary reserves. The system operator first determines the necessary amounts of secondary reserves and overall reserves. The required amount of tertiary reserves is then obtained by subtracting the amount of secondary reserves from the amount of overall reserves.

We should note that since determining the amount of primary reserves is the responsibility of ENTSO-E, and not the TSOs, it is not consider in this chapter.

5.2.2 Reserve Dimensioning Criteria

In Switzerland, the dimensioning criteria that determine the required amount of reserves include a probabilistic criterion and a deterministic one, as described in the following.

Probability Criterion:

The probability criterion states that the amount of reserves must be determined such that power mismatches are regulated to zero with a probability of 99.8%. This implies that the power balance in the system cannot be violated more than 0.2% of all hours over a year. Therefore, the reserve amount R is determined by the 99.8% quantile of the power imbalance distribution as expressed in inequality (5.1):

$$\mathbb{P}(\Delta p \leq R) \geq 99.8\% \tag{5.1}$$

which is equivalent to:

$$\mathbb{P}(\Delta p > R) \leq 0.2\% \tag{5.2}$$

Inequality (5.2) describes the probability that a certain power deviation (Δp) exceeds a certain quantity (R). This is translated to the probability that a certain amount of reserves (R) cannot cover a certain power deviation. In other words, inequality (5.2) enforces that the probability of the deficit of reserve (i.e., *reserve deficit probability*) must be equal to or smaller than 0.2%.

Given that there are two types of reserves (i.e., secondary and tertiary reserves), the probability criterion is translated into the following. The portion of time over a year that secondary reserves are not sufficient to cover spontaneous power mismatches and that the total of secondary and tertiary reserves are not enough to cover power mismatches cannot exceed

0.2%. Therefore, inequality (5.2) is recast to:

$$\mathbb{P}(\Delta p^{\mathrm{s},+} > R^{\mathrm{s,up}}) + \mathbb{P}(\Delta p^{\mathrm{s},-} > R^{\mathrm{s,dn}}) + \mathbb{P}(\Delta p^{\mathrm{o},+} > R^{o,\mathrm{up}}) + \mathbb{P}(\Delta p^{\mathrm{o},-} > R^{o,\mathrm{dn}}) \leq 0.2\% \quad (5.3)$$

where $\Delta p^{\mathrm{s},+}$, $\Delta p^{\mathrm{s},-}$, $\Delta p^{\mathrm{o},+}$, $\Delta p^{\mathrm{o},-}$ denote positive spontaneous power imbalance, negative spontaneous power imbalance, positive overall power imbalance, and negative overall power imbalance, respectively. Positive spontaneous power imbalances denote power mismatches resulting from situations where consumption exceeds generation within durations of order of seconds. Therefore, upward secondary reserves $R^{\mathrm{s,up}}$ are deployed to keep the system power balance. Negative spontaneous power imbalances represent power mismatches resulting from situations where generation exceeds consumption within durations of order of seconds. Thus, downward secondary reserves $R^{\mathrm{s,dn}}$ are deployed to keep the system power balance. Positive overall power imbalances represent power mismatches resulting from situations where consumption exceeds generation within durations of order of minutes. Therefore, upward overall reserves $R^{\mathrm{o,up}}$ are deployed to keep the system power balance. Negative overall power imbalances denote power mismatches resulting from situations where generation exceeds consumption within durations of order of minutes. Thus, downward overall reserves $R^{\mathrm{o,dn}}$ are deployed to keep the system power balance.

To evaluate the deficit probability, the system operator identifies the factors driving power imbalances and their corresponding probability functions. These factors include load oscillations, load forecast errors, forecast errors of renewable generation, outages of power plants, etc. We should note that some of these factors drive spontaneous power imbalances such as load oscillations, while some others have a more permanent impact, such as outages of power plants.

The Swiss TSO, Swissgrid, does not have a database with detailed information on the individual factors deriving power imbalances. The available data only involves measurements of Area Control Error (ACE) [34] [2] and deployed secondary and tertiary reserves. Therefore, spontaneous power imbalances are calculated by adding the deployed secondary reserves to the ACE measurements, and the overall power imbalances are computed by adding the deployed secondary and tertiary reserves to the measurements of the ACE using the historical data over a year.

Next, these datasets are used to statistically derive the corresponding cumulative distribution functions. The advantage of using cumulative distribution functions is that these functions easily describe the relationship between the deficit probability and the reserves.

[2] ACE is defined as the difference between scheduled power production and actual power within a control area on the power grid, taking frequency bias into account

Fig. 5.2 shows the cumulative distribution functions of power imbalances in the Swiss power system in 2013. The larger the imbalance is, the smaller its probability is. Spontaneous power imbalances (in blue) determine the amount of secondary reserves while overall imbalances (in red) determine the amount of overall reserves.

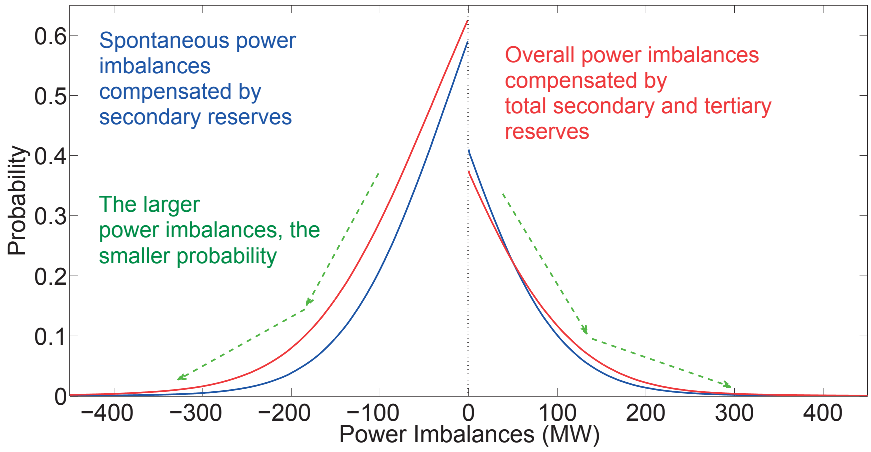

Figure 5.2 – Cumulative distribution functions of spontaneous power imbalances and overall power imbalance using data of the Swiss power system over 2013.

We should note that probability criterion does not specify how the 99.8% quantile of the power imbalance distribution should be allocated to positive and negative imbalances, as well as to spontaneous imbalances and overall imbalances. Therefore, any amounts of secondary and tertiary reserves in any upward and/or downward directions that satisfy a deficit probability of 0.2% are the appropriate amounts. In other words, there is a set of solutions representing the amounts of reserves, and not only fixed single amounts of secondary and tertiary reserves.

However, for clarity and simplicity, the TSOs prefer to have a fixed amount of each upward/-downward secondary and tertiary reserves to be able to buy this amount in the corresponding reserve market. For this purpose, a common practice is to equally allocate the deficit probability to positive and negative imbalances, as well as spontaneous imbalances and overall imbalances. Therefore, instead of considering the 99.8% quantile of power imbalance distribution, the common practice takes into account the 99.9% quantile of spontaneous power imbalance distribution to determine secondary reserves and the 99.9% quantile of overall power imbalance distribution to determine overall reserves:

$$\mathbb{P}(\Delta p^{\mathrm{s},+} > R^{\mathrm{s,up}}) + \mathbb{P}(\Delta p^{\mathrm{s},-} > R^{\mathrm{s,dn}}) \leq 0.1\% \tag{5.4}$$

$$\mathbb{P}(\Delta p^{\mathrm{o},+} > R^{o,\mathrm{up}}) + \mathbb{P}(\Delta p^{\mathrm{o},-} > R^{o,\mathrm{dn}}) \leq 0.1\% \tag{5.5}$$

This is shown in Fig. 5.3, where the amounts of reserves are as follow: upward secondary reserve is 355 MW, downward secondary reserve is 415 MW, upward tertiary reserve is 65 MW (i.e., 420MW-355 MW), and downward tertiary reserve is 120 MW (i.e., 535MW-415 MW).

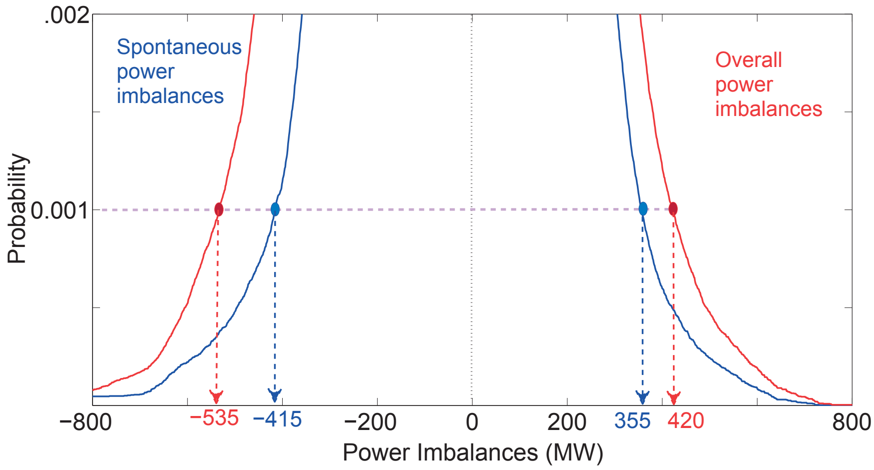

Figure 5.3 – Amounts of reserves obtained from equally allocating the probability criterion to power imbalances (data of 2013).

This approach ignores other possible solutions obtained from allocating differently the deficit probability without considering their costs, which is in contradiction to the TSO obligation to procure reserves at minimum cost. Fig. 5.4 illustrates two examples of allocating differently the deficit probability.

In Fig. 5.4(a), the amounts of secondary reserves can be determined by the 99.85% quantile of spontaneous power imbalance distribution, while the amounts of overall reserves are determined by the 99.95% quantile of overall power imbalance distribution:

$$\mathbb{P}(\Delta p^{\mathrm{s},+} > R^{\mathrm{s,up}}) + \mathbb{P}(\Delta p^{\mathrm{s},-} > R^{\mathrm{s,dn}}) \leq 0.15\% \tag{5.6}$$

$$\mathbb{P}(\Delta p^{\mathrm{o},+} > R^{o,\mathrm{up}}) + \mathbb{P}(\Delta p^{\mathrm{o},-} > R^{o,\mathrm{dn}}) \leq 0.05\% \tag{5.7}$$

The amounts of reserves are $R^{\mathrm{s,up}}$ =325 MW, $R^{\mathrm{s,dn}} = -380$ MW, $R^{\mathrm{o,up}}$ =490 MW, and $R^{\mathrm{o,dn}} = -605$ MW.

Other alternative is to asymmetrically allocate the 99.8% quantile to positive and negative power imbalances. An example is depicted in Fig. 5.4(b), where the deficit criterion is met by:

$$\mathbb{P}(\Delta p^{\mathrm{s},+} > R^{\mathrm{s,up}}) + \mathbb{P}(\Delta p^{\mathrm{o},+} > R^{\mathrm{o,up}}) \leq 0.15\% \tag{5.8}$$

$$\mathbb{P}(\Delta p^{\mathrm{s},-} > R^{s,\mathrm{dn}}) + \mathbb{P}(\Delta p^{\mathrm{o},-} > R^{o,\mathrm{dn}}) \leq 0.05\% \tag{5.9}$$

Therefore, the amounts of reserves are $R^{\mathrm{s,up}}$ =325 MW, $R^{\mathrm{s,dn}} = -495$ MW, $R^{\mathrm{o,up}}$ =380 MW, and $R^{\mathrm{o,dn}} = -605$ MW.

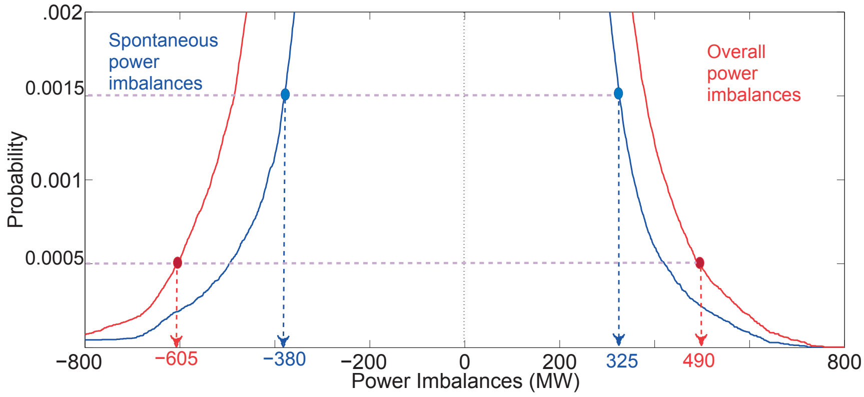

(a) Reserve amounts are determined by $\mathbb{P}(\Delta p^{\mathrm{s},+} > R^{\mathrm{s,up}}) + \mathbb{P}(\Delta p^{\mathrm{s},-} > R^{\mathrm{s,dn}}) \leq 0.15$ and $\mathbb{P}(\Delta p^{\mathrm{o},+} > R^{o,\mathrm{up}}) + \mathbb{P}(\Delta p^{\mathrm{o},-} > R^{o,\mathrm{dn}}) \leq 0.05$

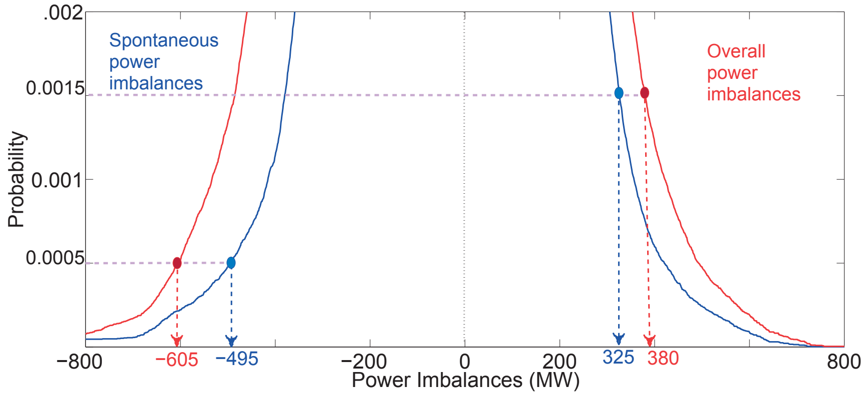

(b) Reserve amounts are determined by $\mathbb{P}(\Delta p^{\mathrm{s},+} > R^{\mathrm{s,up}}) + \mathbb{P}(\Delta p^{\mathrm{o},+} > R^{\mathrm{o,up}}) \leq 0.15\%$ and $\mathbb{P}(\Delta p^{\mathrm{s},-} > R^{s,\mathrm{dn}}) + \mathbb{P}(\Delta p^{\mathrm{o},-} > R^{o,\mathrm{dn}}) \leq 0.05\%$

Figure 5.4 – The amounts of reserves can be determined by any allocation of the deficit probability.

Without considering reserve procurement costs, the TSOs consider the quantities of reserves resulting from inequalities (5.4) and (5.5), and nor those obtained from inequalities (5.8) and (5.9), neither inequalities (5.6) and (5.7).

Deterministic Criterion:

A common approach based on the n-1 security criterion indicates that the total amount of reserves must be able to cover the largest possible incident in the power system regardless of its (low) probability. In Switzerland, the largest possible incidence is the outage of a power plant with a generation capacity of 1.2 GW (nuclear unit Leibstadt).

Additionally, there are contractual agreements between Switzerland and its neighboring countries called Mutual Emergency Ancillary Services (MEAS). According to the MEAS contracts, the countries involved have an exchange of a certain amount of reserves in emergency situations. The MEAS contracts imply that the system operator does not have to procure reserves to fully cover the largest possible incidence. Given a low probability of such an incidence, the system operator can rely on the MEAS amount from the countries involved.

Currently, the most binding MEAS contract of Swissgrid is an agreement with the French TSO, RTE, indicating the availability of 400 MW upward reserves. Therefore, the deterministic criterion is interpreted to ensure 400 MW of upward tertiary reserves:

$$400 \leq R^{\mathrm{T,up}} \tag{5.10}$$

5.2.3 Structure of the Swiss Reserve Market

The Swiss reserve market consists of a weekly market and a daily market. Secondary reserves are procured in the weekly market, while tertiary reserves can be procured in both weekly and daily markets.

The weekly market has a delivery period of a week with a gate closure a week ahead of the delivery period. That is, considering week *w*, the gate closure of the weekly market is at *w-1* and the reserve offers accepted in this market must be available to the system operator for the entire week *w*.

The daily market considered for day *d* has a gate closure at *d-2*. Reserve offers accepted in the daily auction have a delivery period of four hours. That is, the daily market is composed of six auctions, each standing for a four-hour interval. These auctions include the following hours 00:00-04:00, 04:00-08:00, 08:00-12:00, 12:00-16:00, 16:00-20:00, 20:00-24:00 per day. A market agent can choose to offer reserves in a subset of these auctions (e.g., submitting offers only in the time interval of 04:00-08:00) or all of them. Therefore, the daily market is of interest for small market players who cannot guarantee the delivery period of one whole week (e.g., small power units and demand side management).

The scheme of the Swiss reserve market, described above, is illustrated in Fig 5.5, where the reserves for the entire week *w* are procured partly in the weekly market with a delivery period of a week (in red) and partly in the daily market with a delivery period of four hours (in green).

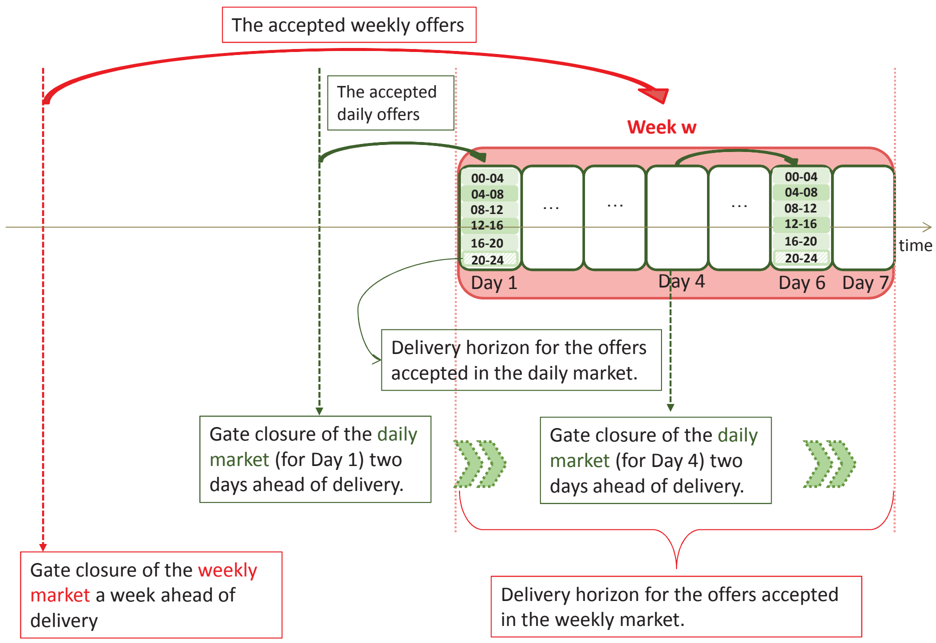

Figure 5.5 – Scheme of the weekly and daily reserve markets in Switzerland.

Offer Structure

Market participants submit their offers consisting of a quantity in MW and a price in CHF[3]/MW without any information about the locations of the generating units, as the reserve market is cleared without network constraints [4].

The offers are indivisible. That is, an offer cannot be partly accepted; it is either completely accepted or rejected. Offers can be mutually exclusive. Such offers are a set of offers that a market participant submits in the reserve market, while only one of them can be accepted by the system operator. [5]

Offers of secondary reserves need to be symmetric. That is, an offer of x MW represents the ability of its unit to provide x MW of secondary reserve in the upward direction and x MW in the downward direction. However, offers of tertiary reserves can be asymmetric; that is, a

[3]CHF denotes Swiss Francs

[4]The Swiss transmission system is a highly meshed network with a few congested operating conditions per year. Since the system is not sensitive to the location of reserves, the reserve market is cleared without locational information.

[5]As an example, if market player A submits 100 MW, 120 MW and 150 MW as mutually exclusive offers, the TSO can accept only one of them.

producer can offer x MW in the upward direction and y MW in the downward direction.

Remuneration

The remuneration of reserves follows the pay-as-bid scheme (not a marginal pricing scheme). That is, the market participant whose offer is accepted is paid its price offer submitted irrespective of the deployment in real-time operation [6].

We should note that the focus of this chapter is on the reserve market, and not reserve deployment. Thus, topics pertaining to the reserve deployment are out of our scope.

5.2.4 Drawbacks of the Common Practice

The main drawback of the common practice is that it disregards a set of possible solutions of reserve amounts without considering their costs. However, secondary reserves should generally replace tertiary reserves as far as this substitution does not yield a higher reserve cost. In other words, market aspects (economic objectives) and technical (dimensioning) criteria are inefficiently separated in the common practice. As an example, symmetric offers of secondary reserves imply that upward and downward secondary reserves must be represented by one single amount. Considering the example of Fig. 5.3, where the corresponding secondary amounts are 355 MW and −415 MW, the question is what amount the TSO should procure in the reserve market. The current practice does not provide an optimal answer to this.

Another issue that the common practice does not optimally address is related to the allocation of tertiary reserves in the weekly and daily markets. If the amounts of upward and downward tertiary reserves are determined to be $\hat{R}^{\mathrm{T,up}}$ and $\hat{R}^{\mathrm{T,dn}}$, respectively, the question is how the system operator should allocate these amounts to the weekly and daily markets.

The common practice fixes the reserve amounts in the weekly and daily markets to predefined values based on judgment and experience. These markets are cleared independently from each other without considering that offers may be cheaper in one of these market than in the other.

To summarize, the common practice of the Swiss reserve market suffers from the following drawbacks:

- The market aspects and the technical dimensioning criteria are decoupled.
- The potential substitution of secondary and tertiary reserves are not reflected.

[6] The choice of renumeration scheme is a regulatory decision out of the scope of this thesis.

- A link between the weekly and daily markets is missing.

These drawbacks call for an update of the clearing approach in the Swiss reserve market.

In this context, we propose a new clearing approach based on stochastic programming with the purpose of actual implementation in the Swiss reserve market. This implies that major changes in the structure and properties of the existing Swiss reserve market must be avoided. Therefore, the new approach preserves the IT infrastructures, the structure of offers, and the gate closure sequences of the weekly and daily markets. Additionally, a reasonable computation time is desired.

5.3 Decision-Making Process

The TSO decides on the amounts of secondary reserves, upward and downward tertiary reserves in the weekly market as well as in the daily market at minimum cost. There are two points in time when the TSO makes decisions: at the gate closure of the weekly market, and at the gate closure of the daily market. The beginning of the decision-making horizon is at the gate closure of the weekly market, where offers of the daily market are still not available. Unknown daily offers are translated to uncertainty, and therefore, the problem above is a decision-making problem under uncertainty. To tackle this decision-making problem, we use a stochastic programming model.

Therefore, we define a stage corresponding to each decision point in time. The first stage represents the weekly market and the second stage models the daily market. The uncertain daily offers are modeled through scenarios. Fig. 5.6 shows the scenario tree of this two-stage clearing model for the reserve market. A two-stage stochastic optimization model clears the weekly market with the objective of minimizing expected reserve cost subject to dimensioning criteria and market properties (e.g., mutually exclusive and indivisible offers). In the first-stage weekly market, the decision is on the optimal level of reserves by accepting/rejecting available weekly offers while considering scenarios representing uncertain offers of the daily market. In the second-stage daily market, when offers are realized, the TSO determines the amount of tertiary reserves by accepting/rejecting available daily offers while taking into account the outcomes of the weekly market.

5.4 Scenarios Modeling Reserve Offers in Daily Market

As previously mentioned, the source of uncertainty in this reserve clearing problem is the unknown daily offers. The question is how to select scenarios representing daily offers.

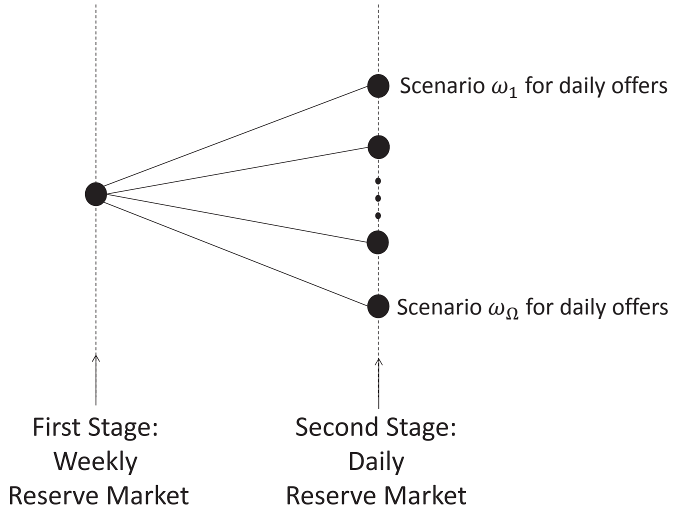

Figure 5.6 – Scenario tree of the two-stage Swiss reserve market

In a stochastic programming framework, scenarios are either historical samples or samples generated by a distribution which is constructed based on the historical data. In both cases, sufficient data is necessary.

We should note that we cannot assume a true-cost bidding behavior, as the market follows a pay-as-bid scheme, which does not promote truth-telling. We should also note that Swissgrid does not know true costs of generation units to estimate reserve offers. Therefore, historical data of offers in the daily market need to be used.

The Swiss daily market was launched in February 2010, and we have data available up to 2012. At the first glance, it seems that there is sufficient data (data over two yeas). However, a careful look indicates otherwise. The Swiss power system is a hydro-based system where hydrological conditions play an important role in the reserve market. That is, electricity generation is high in late spring and summer, and low in winter time and the beginning of spring. Correspondingly, the reserve offers follow a hydrological trend. Therefore, the daily offers in week w can be related to the previous weeks in the same month, or/and the same week in the previous years (e.g., the offers in the daily market at week w-2 and the same year, at week w in the previous year), and not to other weeks over that year. This implies that to model daily offers, there are only few historical samples (and not the data of two years) available, which are not sufficient to build-up a model.

Due to the limited data available, we invoke the experience and judgment of the operators to select representative scenarios.

Considering the daily market in week w, the most recently-submitted offers are those of week *w-2* (and not week *w-1*). The reason is as follows. The scenarios must be ready at the gate closure of the weekly market which is at week *w-1*. At this time, not all daily markets in week *w-1* are closed. Therefore, considering day *d1* to day *d7* in week *w*, the best available data is the daily offers of day *d1* to day *d7* in week *w-2*.

5.5 Practical Aspects

The proposed clearing approach is intended for an actual implementation, and hence, from a practical point of view, drastic changes in the structure of the existing Swiss reserve market shall be avoided in order to facilitate the acceptance of the new clearing model among market players. Hence, the following points should be noted:

- The co-optimization of energy and reserves is not applicable to the Swiss electricity market. As previously mentioned, the Swiss electricity market follows the principles of a decentralized market, where energy and reserve markets are separately cleared by the market operators and the TSO, respectively.

- A nodal market clearing model is not applicable to the Swiss reserve market, as offers do not include locational information.

- The new approach does not alter the settlement scheme. That is, the pay-as-bid rule remains as the settlement scheme.

- The new approach preserves the current practice of uncoupling reserve acquisition and reserve deployment.

Therefore, we focus on an optimization model with minimum changes in communication and rules from the viewpoint of market participants.

5.6 Model Description

In this section, we provide the mathematical descriptions of the proposed models, including a risk-neutral two-stage model and a risk-averse one, as well as the reference model (common practice). Next, we describe the notion of perfect information model and how to obtain the actual cost.

5.6.1 Risk-Neutral Model

In the following, we first describe the optimization variables, the objective function, and the constraints. Next, we provide the mathematical description of the risk-neutral two-stage model.

Decision Variables

We categorize the decisions into to groups:

- The first-stage variables are related to the weekly market that clears before the realization of any scenario of daily offers. These variables are here-and-now decisions and include:
  - Binary variables representing the acceptance or the rejection of each secondary reserve offer with a quantity of p^{s}_{ir} in MW and an offered price of c^{s}_{ir} in CHF/MW in the weekly market [$x^{\mathrm{s}}_{ir} \in \{0,1\}$]. Each secondary offer can belong to a set of mutually exclusive N_r offers.
  - Binary variables representing the acceptance or the rejection of each upward tertiary reserve offer with a quantity of p^{up}_{jm} in MW and an offered price of c^{up}_{jm} in CHF/MW in the weekly market [$x^{\mathrm{up}}_{jm} \in \{0,1\}$]. Each upward tertiary offer can belong to a set of mutually exclusive N_m offers.
  - Binary variables representing the acceptance or the rejection of each downward tertiary reserve offer with a quantity of p^{dn}_{kq} in MW and an offered price of c^{dn}_{kq} in CHF/MW in the weekly market [$x^{\mathrm{dn}}_{kq} \in \{0,1\}$]. Each downward tertiary offer can belong to a set of mutually exclusive N_q offers.
  - A continuous variable representing the contribution of upward secondary reserves in satisfying the probabilistic criteria [$\epsilon^{\mathrm{s}+} \in [0,1]$].
  - A continuous variable representing the contribution of downward secondary reserves in satisfying the probabilistic criteria [$\epsilon^{\mathrm{s}-} \in [0,1]$].
  - A continuous variable representing the contribution of upward overall reserves in satisfying the probabilistic criteria [$\epsilon^{\mathrm{o}+} \in [0,1]$].
  - A continuous variable representing the contribution of downward overall reserves in satisfying the probabilistic criteria [$\epsilon^{\mathrm{o}-} \in [0,1]$].
- The second-stage variables pertain to the daily market. They are wait-and-see decisions as they are made after the realization of offers in the daily market and involve:
  - Amount of upward tertiary reserves procured in each four-hour interval t and each scenario ω in the daily market [$y^{\mathrm{up}}_{t\omega}$, MW].

- Amount of downward tertiary reserves procured in each four-hour interval t and each scenario ω in the daily market [$y^{\text{dn}}_{t\omega}$, MW].
- Cost of the upward tertiary reserves procured in each four-hour interval t and each scenario ω in the daily market [$\gamma^{\text{up}}_{t\omega}$, CHF].
- Cost of the downward tertiary reserves procured in each four-hour interval t and each scenario ω in the daily market [$\gamma^{\text{dn}}_{t\omega}$, CHF].

Objective Function

The objective function consists of two terms pertaining to the reserve cost in the weekly market, and the expected reserve cost in the daily market:

- The reserve cost in the weekly market consists of secondary offers ($\sum_{i=1}^{N_{\text{SR}}}\sum_{r=1}^{N_r} c^{\text{s}}_{ir} p^{\text{s}}_{ir} x^{\text{s}}_{ir}$), upward tertiary offers ($\sum_{j=1}^{N_j}\sum_{m=1}^{N_m} c^{\text{up}}_{jm} p^{\text{up}}_{jm} x^{\text{up}}_{jm}$), and downward tertiary offers ($\sum_{k=1}^{N_k}\sum_{q=1}^{N_q} c^{\text{dn}}_{kq} p^{\text{dn}}_{kq} x^{\text{dn}}_{kq}$):

$$\sum_{i=1}^{N_{\text{SR}}}\sum_{r=1}^{N_r} c^{\text{s}}_{ir} p^{\text{s}}_{ir} x^{\text{s}}_{ir} + \sum_{j=1}^{N_j}\sum_{m=1}^{N_m} c^{\text{up}}_{jm} p^{\text{up}}_{jm} x^{\text{up}}_{jm} + \sum_{k=1}^{N_k}\sum_{q=1}^{N_q} c^{\text{dn}}_{kq} p^{\text{dn}}_{kq} x^{\text{dn}}_{kq} \tag{5.11}$$

  As an example, if secondary offer i is accepted, $x^{\text{s}}_{ir} = 1$ and in the objective function, the term $c^{\text{s}}_{ir} p^{\text{s}}_{ir}$ has a non-zero value.

- The expected reserve cost in the daily market includes the expected cost associated to upward tertiary reserves and downward tertiary reserves:

$$\sum_{\omega} \pi_\omega \Big(\sum_{t=1}^{N_t} \big(\gamma^{\text{up}}_{t\omega} + \gamma^{\text{dn}}_{t\omega} \big) \Big) \tag{5.12}$$

The summation of these cost components results in the total reserve cost. The objective of the two-stage clearing model is to minimize this cost, as expressed by (5.13):

$$\begin{aligned} \underset{\Xi^{\text{R}}}{\text{Minimize}} \quad & \sum_{i=1}^{N_{\text{SR}}}\sum_{r=1}^{N_r} c^{\text{s}}_{ir} p^{\text{s}}_{ir} x^{\text{s}}_{ir} + \sum_{j=1}^{N_j}\sum_{m=1}^{N_m} c^{\text{up}}_{jm} p^{\text{up}}_{jm} x^{\text{up}}_{jm} + \sum_{k=1}^{N_k}\sum_{q=1}^{N_q} c^{\text{dn}}_{kq} p^{\text{dn}}_{kq} x^{\text{dn}}_{kq} \\ & + \sum_{\omega} \pi_\omega \Big(\sum_{t=1}^{N_t} \big(\gamma^{\text{up}}_{t\omega} + \gamma^{\text{dn}}_{t\omega} \big) \Big) \end{aligned} \tag{5.13}$$

The minimization is over the set of variables $\Xi^{\text{R}} = \{x^{\text{s}}_{ir}, \forall i, \forall r; x^{\text{up}}_{jm}, \forall j, \forall m; x^{\text{dn}}_{kq}, \forall k, \forall q; \epsilon^{\text{s}+}; \epsilon^{\text{s}-}; \epsilon^{\text{o}+}; \epsilon^{\text{o}-}; y^{\text{up}}_{t\omega}, y^{\text{dn}}_{t\omega}, \gamma^{\text{up}}_{t\omega}, \gamma^{\text{dn}}_{t\omega}, \forall t, \forall \omega\}$, as described in Section 5.6.1.

Constraints

There are three groups of constraints: the first-stage constraints pertaining to the weekly market, the second-stage constraints related to the daily market, and the linking constraints coupling the first-stage decisions in the weekly market to the second-stage decisions in the daily market.

First-stage Constraints (Weekly Market):

One constraint is solely related to the first-stage market. This constraint models mutually exclusive offers in the weekly market, as described in Section 5.2.3.

Mutually Exclusive Offers:

If secondary reserve offer x^{s}_{ir} along with other N_r secondary offers are in a set of mutually exclusive offers, only one of them can be accepted. Since x^{s}_{ir} is a binary variable, constraint (5.14) enforces that at most only one offer among those in the set of mutually exclusive offers is accepted:

$$\sum_{r=1}^{N_r} x^{\mathrm{s}}_{ir} \leq 1, \forall i \tag{5.14}$$

If secondary reserve offer x^{s}_{ir} is not in a set of mutually exclusive offers (i.e., $N_r = 1$), constraint (5.14) becomes $x^{\mathrm{s}}_{i1} \leq 1$ that renders to $x^{\mathrm{s}}_{i} \leq 1$, which is consistent with x^{s}_{ir} being binary (i.e., $x^{\mathrm{s}}_{ir} \in \{0,1\}, \forall i, \forall r$).

In the same vein, mutually exclusive upward tertiary offers and downward tertiary offers are modeled through constraints (5.15) and (5.16), respectively:

$$\sum_{m=1}^{N_m} x^{\mathrm{up}}_{jm} \leq 1, \forall j \tag{5.15}$$

$$\sum_{q=1}^{N_q} x^{\mathrm{dn}}_{kq} \leq 1, \forall k \tag{5.16}$$

Second-Stage Constraints (Daily Market):

One constraint pertains solely to the daily market. This constraint models offers in this market.

Similar to the weekly market, the structure of the the daily offers include indivisible offers and mutually exclusive offers. An accurate modeling of such offers requires the use of binary variables in the second stage, where variables and constraints are defined per scenario. An increase in the number of scenarios results in an increase in the number of (binary) variables and constraints, and consequently, in the problem size. To ease the computational burden, we avoid to use the binary variables for modeling daily offers in the second stage.

For this, we approximate indivisible offers and mutually exclusive offers by a piece-wise linear offer curve.

Among a set of mutually exclusive offers, the one with the largest quantity offered is considered as the representative of this set. These offers along with other indivisible offers form a Merit Order List (MOL), where the offers are ranked based on ascending order of offer prices. A piece-wise linear offer curve is, then, fitted to the resultant MOL, as shown in Fig 5.7.

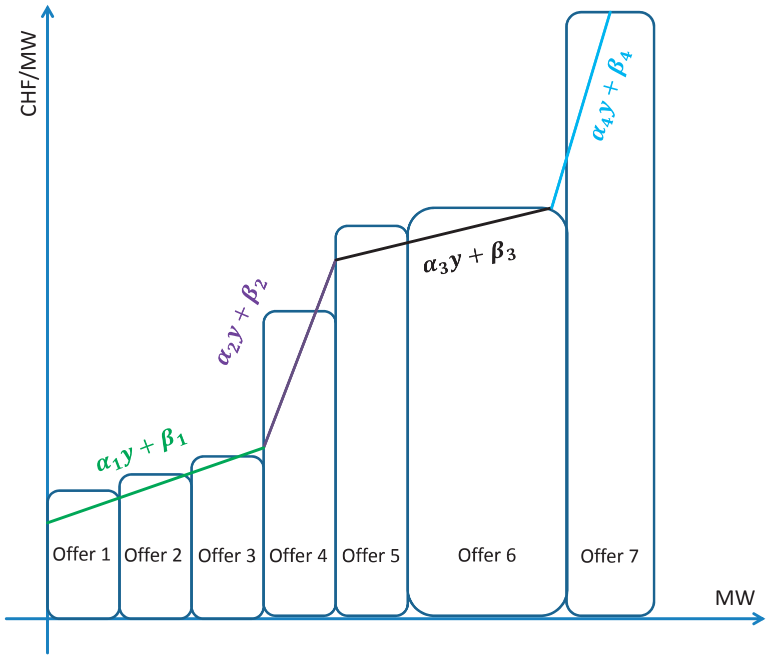

Figure 5.7 – The merit order list and its piece-wise linear curve

Considering upward tertiary offers, a linear curve consisting of l pieces at each four-hour interval t and each scenario ω is:

$$\gamma_{t\omega}^{\text{up}} = \begin{cases} \alpha_1^{\text{up}} y_{t\omega}^{\text{up}} + \beta_1^{\text{up}}, & y_{t\omega}^{\text{min,up}} \le y_{t\omega}^{\text{up}} \le y_{t\omega}^{2,\text{up}} \\ \alpha_2^{\text{up}} y_{t\omega}^{\text{up}} + \beta_3^{\text{up}}, & y_{t\omega}^{2,\text{up}} \le y_{t\omega}^{\text{up}} \le y_{t\omega}^{3,\text{up}} \\ \quad\vdots & \\ \alpha_L^{\text{up}} y_{t\omega}^{\text{up}} + \beta_L^{\text{up}}, & y_{t\omega}^{\text{L,up}} \le y_{t\omega}^{\text{up}} \le y_{t\omega}^{\text{max,up}} \end{cases} \tag{5.17}$$

which is equivalent to:

$$\underset{y_{t\omega}^{\text{up}}}{\text{Minimize}} \quad \gamma_{t\omega}^{\text{up}} \tag{5.18a}$$

$$\alpha_l^{\mathrm{up}} y_{t\omega}^{\mathrm{up}} + \beta_l^{\mathrm{up}} \leq \gamma_{t\omega}^{\mathrm{up}}, \forall l, \forall \omega, \forall t \tag{5.18b}$$

$$y_{t\omega}^{\mathrm{min,up}} \leq y_{t\omega}^{\mathrm{up}} \leq y_{t\omega}^{\mathrm{max,up}}, \forall \omega, \forall t \tag{5.18c}$$

In the same vein, we consider a piece-wise linear curve for downward tertiary offers:

$$\underset{y_{t\omega}^{\mathrm{dn}}}{\text{Minimize}} \quad \gamma_{t\omega}^{\mathrm{dn}} \tag{5.19a}$$

$$\alpha_l^{\mathrm{dn}} y_{t\omega}^{\mathrm{dn}} + \beta_l^{\mathrm{dn}} \leq \gamma_{t\omega}^{\mathrm{dn}}, \forall l, \forall \omega, \forall t \tag{5.19b}$$

$$y_{t\omega}^{\mathrm{min,dn}} \leq y_{t\omega}^{\mathrm{dn}} \leq y_{t\omega}^{\mathrm{max,dn}}, \forall \omega, \forall t \tag{5.19c}$$

Linking Constraints:

The weekly and daily markets are linked through the probabilistic and deterministic criteria.

Deterministic Criterion:

According to the deterministic criterion, the total amount of upward tertiary reserves must be at least 400 MW at each interval and each scenario:

$$400 \leq \Big(\sum_{j=1}^{N_j} \sum_{m=1}^{N_m} p_{jm}^{\mathrm{up}} x_{jm}^{\mathrm{up}}\Big) + y_{t\omega}^{\mathrm{T,up}}, \forall \omega, \forall t \tag{5.20}$$

Probabilistic Criterion:

Considering the probabilistic criterion formulated in (5.3), the amounts of upward secondary $R^{\mathrm{s,up}}$ and downward secondary $R^{\mathrm{s,dn}}$ are the same ($R^{\mathrm{s,up}} = R^{\mathrm{s,dn}} = R^{\mathrm{s}}$) due to symmetric secondary offers. Therefore, inequality (5.3) becomes:

$$\mathbb{P}(\Delta p^{\mathrm{s},+} > R^{\mathrm{s}}) + \mathbb{P}(\Delta p^{\mathrm{s},-} > R^{\mathrm{s}}) + \mathbb{P}(\Delta p^{\mathrm{o},+} > R^{o,\mathrm{up}}) + \mathbb{P}(\Delta p^{\mathrm{o},-} > R^{o,\mathrm{dn}}) \leq 0.2\% \tag{5.21}$$

The cumulative distribution functions of power imbalances are expressed as:

$$\mathbb{F}^{\mathrm{s}+}(R^{\mathrm{s}}) = \mathbb{P}(\Delta p^{\mathrm{s},+} > R^{\mathrm{s}}) \tag{5.22}$$

$$\mathbb{F}^{\mathrm{s}-}(R^{\mathrm{s}}) = \mathbb{P}(\Delta p^{\mathrm{s},-} > R^{\mathrm{s}}) \tag{5.23}$$

$$\mathbb{F}^{\mathrm{o}+}(R^{\mathrm{s}} + R^{\mathrm{T,up}}) = \mathbb{P}(\Delta p^{\mathrm{o},+} > (R^{\mathrm{s}} + R^{\mathrm{T,up}})) \tag{5.24}$$

$$\mathbb{F}^{\mathrm{o}-}(R^{\mathrm{s}} + R^{\mathrm{T,dn}}) = \mathbb{P}(\Delta p^{\mathrm{o},-} > (R^{\mathrm{s}} + R^{\mathrm{T,dn}})) \tag{5.25}$$

where $R^{\mathrm{s}} = \sum_{i=1}^{N_{\mathrm{SR}}} \sum_{r=1}^{N_r} p_{ir}^{\mathrm{s}} x_{ir}^{\mathrm{s}}$. Similarly, the amount of upward tertiary reserve is determined by the upward tertiary offers in the weekly market and the contribution of uncertain offers from the daily market. That is, $R^{\mathrm{T,up}} = \left(\sum_{j=1}^{N_j}\sum_{m=1}^{N_m} p_{jm}^{\mathrm{up}} x_{jm}^{\mathrm{up}}\right) + y_{t\omega}^{\mathrm{up}}, \forall\omega$. In the same vein, $R^{\mathrm{T,dn}} = \left(\sum_{k=1}^{N_k}\sum_{q=1}^{N_q} p_{kq}^{\mathrm{dn}} x_{kq}^{\mathrm{dn}}\right) + y_{t\omega}^{\mathrm{dn}}, \forall\omega$. Therefore, constraint (5.21) is recast to:

$$\mathbb{F}^{\mathrm{s+}}\Big(\sum_{i=1}^{N_{\mathrm{SR}}}\sum_{r=1}^{N_r} p_{ir}^{\mathrm{s}} x_{ir}^{\mathrm{s}}\Big) + \mathbb{F}^{\mathrm{s-}}\Big(\sum_{i=1}^{N_{\mathrm{SR}}}\sum_{r=1}^{N_r} p_{ir}^{\mathrm{s}} x_{ir}^{\mathrm{s}}\Big) + \mathbb{F}^{\mathrm{o+}}\Big(\sum_{i=1}^{N_{\mathrm{SR}}}\sum_{r=1}^{N_r} p_{ir}^{\mathrm{s}} x_{ir}^{\mathrm{s}} + \sum_{j=1}^{N_j}\sum_{m=1}^{N_m} p_{jm}^{\mathrm{up}} x_{jm}^{\mathrm{up}} + y_{t\omega}^{\mathrm{up}}\Big)$$
$$+ \mathbb{F}^{\mathrm{o-}}\Big(\sum_{i=1}^{N_{\mathrm{SR}}}\sum_{r=1}^{N_r} p_{ir}^{\mathrm{s}} x_{ir}^{\mathrm{s}} + \sum_{k=1}^{N_k}\sum_{q=1}^{N_q} p_{kq}^{\mathrm{dn}} x_{kq}^{\mathrm{dn}} + y_{t\omega}^{\mathrm{dn}}\Big) \leq 0.2\%, \forall\omega, \forall t \tag{5.26}$$

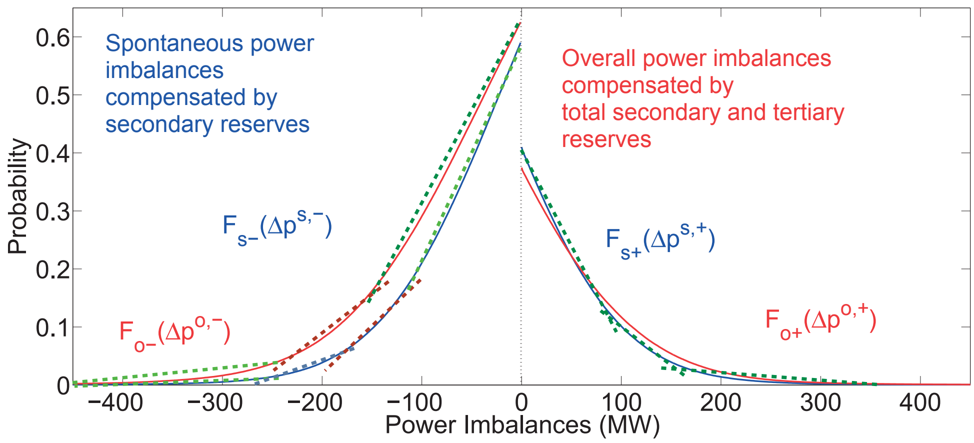

Figure 5.8 – Piece-wise linearization of cumulative distribution functions in dashed lines

As illustrated in Fig 5.8, the cumulative distribution functions are not linear. We use a piece-wise linearization to represent these functions. That is, any cumulative distribution function $\mathbb{F}(R)$ is represented by:

$$\mathbb{F}(R) = \begin{cases} a_1 R + b_1, & R_1 \leq R \leq R_2 \\ a_2 R + b_2, & R_2 \leq R \leq R_3 \\ \vdots & \\ a_N R + b_N, & R_N \leq R \leq R_{N+1} \end{cases} \tag{5.27}$$

which is recast as:

$$\underset{R_1 \leq R \leq R_{N+1}}{\text{Minimize}} \quad \epsilon \tag{5.28}$$

$$a_n R + b_n \leq \epsilon, \forall n$$

$$0 \leq \epsilon \leq 1$$

Thus, equation (5.26) is represented by equations (5.29) below:

$$\epsilon^{s+} + \epsilon^{s-} + \epsilon^{o+} + \epsilon^{o-} \leq 0.2\% \tag{5.29a}$$

$$a_n^{s+}\Big(\sum_{i=1}^{N_{SR}}\sum_{r=1}^{N_r} p_{ir}^{s} x_{ir}^{s}\Big) + b_n^{s+} \leq \epsilon^{s+}, \forall n \tag{5.29b}$$

$$a_n^{s-}\Big(\sum_{i=1}^{N_{SR}}\sum_{r=1}^{N_r} p_{ir}^{s} x_{ir}^{s}\Big) + b_n^{s-} \leq \epsilon^{s-}, \forall n \tag{5.29c}$$

$$a_n^{o+}\Big(\sum_{i=1}^{N_{SR}}\sum_{r=1}^{N_r} p_{ir}^{s} x_{ir}^{s} + \sum_{j=1}^{N_j}\sum_{m=1}^{N_m} p_{jm}^{up} x_{jm}^{up} + y_{t\omega}^{up}\Big) + b_n^{o+} \leq \epsilon^{o+}, \forall n, \forall t, \forall \omega \tag{5.29d}$$

$$a_n^{o-}\Big(\sum_{i=1}^{N_{SR}}\sum_{r=1}^{N_r} p_{ir}^{s} x_{ir}^{s} + \sum_{k=1}^{N_k}\sum_{q=1}^{N_q} p_{kq}^{dn} x_{kq}^{dn} + y_{t\omega}^{dn}\Big) + b_n^{o-} \leq \epsilon^{o-}, \forall n, \forall t, \forall \omega \tag{5.29e}$$

$$\epsilon^{s+}, \epsilon^{s-}, \epsilon^{o+}, \epsilon^{o-} \in [0,1] \tag{5.29f}$$

Complete Formulation of the Risk-Neutral Model

The complete formulation of the two-stage MILP reserve clearing model is:

$$\underset{\Xi^{R}}{\text{Minimize}}$$

$$\sum_{i=1}^{N_{SR}}\sum_{r=1}^{N_r} c_{ir}^{s} p_{ir}^{s} x_{ir}^{s} + \sum_{j=1}^{N_j}\sum_{m=1}^{N_m} c_{jm}^{up} p_{jm}^{up} x_{jm}^{up} + \sum_{k=1}^{N_k}\sum_{q=1}^{N_q} c_{kq}^{dn} p_{kq}^{dn} x_{kq}^{dn}$$

$$+ \sum_{\omega} \pi_\omega \Big(\sum_{t=1}^{N_t} \big(\gamma_{t\omega}^{up} + \gamma_{t\omega}^{dn}\big)\Big) \tag{5.30a}$$

subject to

$$\sum_{r=1}^{N_r} x_{ir}^{s} \leq 1, \forall i \tag{5.30b}$$

$$\sum_{m=1}^{N_m} x_{jm}^{up} \leq 1, \forall j \tag{5.30c}$$

$$\sum_{q=1}^{N_q} x_{kq}^{dn} \leq 1, \forall k \tag{5.30d}$$

$$400 \leq \big(\sum_{j=1}^{N_j}\sum_{m=1}^{N_m} p_{jm}^{up} x_{jm}^{up}\big) + y_{t\omega}^{up}, \forall \omega, \forall t \tag{5.30e}$$

$$\epsilon^{s+} + \epsilon^{s-} + \epsilon^{o+} + \epsilon^{o-} \leq 0.2\% \tag{5.30f}$$

$$a_n^{s+}\Big(\sum_{i=1}^{N_{SR}}\sum_{r=1}^{N_r} p_{ir}^{s} x_{ir}^{s}\Big) + b_n^{s+} \leq \epsilon^{s+}, \forall n \tag{5.30g}$$

$$a_n^{s-}\Big(\sum_{i=1}^{N_{SR}}\sum_{r=1}^{N_r} p_{ir}^{s} x_{ir}^{s}\Big) + b_n^{s-} \leq \epsilon^{s-}, \forall n \tag{5.30h}$$

$$a_n^{\mathrm{o+}}\Big(\sum_{i=1}^{N_{\mathrm{SR}}}\sum_{r=1}^{N_r} p_{ir}^{\mathrm{s}} x_{ir}^{\mathrm{s}} + \sum_{j=1}^{N_j}\sum_{m=1}^{N_m} p_{jm}^{\mathrm{up}} x_{jm}^{\mathrm{up}} + y_{t\omega}^{\mathrm{up}}\Big) + b_n^{\mathrm{o+}} \le \epsilon^{\mathrm{o+}}, \forall n, \forall t, \forall \omega \tag{5.30i}$$

$$a_n^{\mathrm{o-}}\Big(\sum_{i=1}^{N_{\mathrm{SR}}}\sum_{r=1}^{N_r} p_{ir}^{\mathrm{s}} x_{ir}^{\mathrm{s}} + \sum_{k=1}^{N_k}\sum_{q=1}^{N^{\mathrm{q}}} p_{kq}^{\mathrm{dn}} x_{kq}^{\mathrm{dn}} + y_{t\omega}^{\mathrm{dn}}\Big) + b_n^{\mathrm{o-}} \le \epsilon^{\mathrm{o-}}, \forall n, \forall t, \forall \omega \tag{5.30j}$$

$$\alpha_l^{\mathrm{up}} y_{t\omega}^{\mathrm{up}} + \beta_l^{\mathrm{up}} \le \gamma_{t\omega}^{\mathrm{up}}, \forall l, \forall \omega, \forall t \tag{5.30k}$$

$$\alpha_l^{\mathrm{dn}} y_{t\omega}^{\mathrm{dn}} + \beta_l^{\mathrm{dn}} \le \gamma_{t\omega}^{\mathrm{dn}}, \forall l, \forall \omega, \forall t \tag{5.30l}$$

$$0 \le y_{t\omega}^{\mathrm{up}} \le y_{t\omega}^{\mathrm{max,up}}, \forall \omega, \forall t \tag{5.30m}$$

$$0 \le y_{t\omega}^{\mathrm{dn}} \le y_{t\omega}^{\mathrm{max,dn}}, \forall \omega, \forall t \tag{5.30n}$$

$$x_{ir}^{\mathrm{s}} \in \{0,1\}, \forall i, \forall r \tag{5.30o}$$

$$x_{js}^{\mathrm{up}} \in \{0,1\}, \forall j, \forall s \tag{5.30p}$$

$$x_{kq}^{\mathrm{dn}} \in \{0,1\}, \forall k, \forall q \tag{5.30q}$$

$$\epsilon^{\mathrm{s+}}, \epsilon^{\mathrm{s-}}, \epsilon^{\mathrm{o+}}, \epsilon^{\mathrm{o-}} \in [0,1] \tag{5.30r}$$

5.6.2 Risk-Averse Model

In problem (5.30), the objective is to minimize the expected reserve cost. This may, however, lead to a situation where the TSO experiences high reserve costs if expensive offers occur in the daily market, although the corresponding scenario may have a low probability.

To avoid losses due to unfavorable scenarios, we incorporate the Conditional Value at Risk (CVaR) [57] as a risk control measure in problem (5.30).

The CVaR at the α_r confidence level is the expected value of the costs under the scenarios that lead to the $(1-\alpha_r)\times$ 100% worst outcomes. In other words, if the Value at Risk (VaR) γ is defined to be the largest threshold that is not exceeded by the cost with probability α_r, the CVaR is the expected value of this risk. Fig. 5.9 illustrates the Value at Risk (VaR) and the CVaR.

The mathematical description of the CVaR at the α_r confidence level is expressed by equation (5.31):

$$\mathrm{CVaR} = Min\{\gamma + \frac{1}{1-\alpha_r}\mathbb{E}[Max\{cost_\omega - \gamma, 0\}]\} \tag{5.31}$$

Since $cost_\omega$ is equal to $\sum_{i=1}^{N_{\mathrm{SR}}}\sum_{r=1}^{N_r} c_{ir}^{\mathrm{s}} p_{ir}^{\mathrm{s}} x_{ir}^{\mathrm{s}} + \sum_{j=1}^{N_j}\sum_{m=1}^{N_m} c_{jm}^{\mathrm{up}} p_{jm}^{\mathrm{up}} x_{jm}^{\mathrm{up}} + \sum_{k=1}^{N_k}\sum_{q=1}^{N_q} c_{kq}^{\mathrm{dn}} p_{kq}^{\mathrm{dn}} x_{kq}^{\mathrm{dn}} + \sum_{t=1}^{N_t}\big(\gamma_{t\omega}^{\mathrm{up}} + \gamma_{t\omega}^{\mathrm{dn}}\big), \forall \omega$, using continuous non-negative variable $\mathbf{s}_\omega$, equation (5.31) is recast as:

$$\underset{\Xi^{\mathrm{R}},\gamma,\mathbf{s}_\omega}{\text{Minimize}} \quad \gamma + (1-\alpha_r)^{-1}\sum_{\omega}\pi_\omega \mathbf{s}_\omega \tag{5.32a}$$

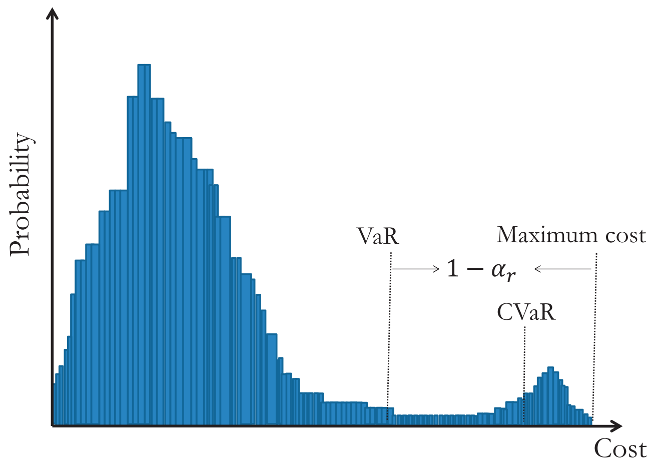

Figure 5.9 – Value at Risk (VaR) and Conditional Value at Risk (CVaR).

subject to

$$\sum_{i=1}^{N_{\mathrm{SR}}}\sum_{r=1}^{N_r} c_{ir}^{\mathrm{s}} p_{ir}^{\mathrm{s}} x_{ir}^{\mathrm{s}} + \sum_{j=1}^{N_j}\sum_{m=1}^{N_m} c_{jm}^{\mathrm{up}} p_{jm}^{\mathrm{up}} x_{jm}^{\mathrm{up}} + \sum_{k=1}^{N_k}\sum_{q=1}^{N_q} c_{kq}^{\mathrm{dn}} p_{kq}^{\mathrm{dn}} x_{kq}^{\mathrm{dn}} + \sum_{t=1}^{N_t}\left(\gamma_{t\omega}^{\mathrm{up}}+\gamma_{t\omega}^{\mathrm{dn}}\right) - \gamma \leq \mathbf{s}_\omega, \forall\omega \tag{5.32b}$$

$$0 \leq \mathbf{s}_\omega, \forall\omega \tag{5.32c}$$

Considering a trade-off between the expected reserve cost and the CVaR, the risk-averse formulation is:

$$\underset{\Xi^{\mathrm{CVaR}}}{\text{Minimize}}$$

$$(1-\beta_r)\Bigg[\sum_{i=1}^{N_{\mathrm{SR}}}\sum_{r=1}^{N_r} c_{ir}^{\mathrm{s}} p_{ir}^{\mathrm{s}} x_{ir}^{\mathrm{s}} + \sum_{j=1}^{N_j}\sum_{m=1}^{N_m} c_{jm}^{\mathrm{up}} p_{jm}^{\mathrm{up}} x_{jm}^{\mathrm{up}} + \sum_{k=1}^{N_k}\sum_{q=1}^{N_q} c_{kq}^{\mathrm{dn}} p_{kq}^{\mathrm{dn}} x_{kq}^{\mathrm{dn}}$$

$$+\sum_{\omega}\pi_\omega\left(\sum_{t=1}^{N_t}\left(\gamma_{t\omega}^{\mathrm{up}}+\gamma_{t\omega}^{\mathrm{dn}}\right)\right)\Bigg] + \beta_r\left(\gamma + (1-\alpha_r)^{-1}\sum_{\omega}\pi_\omega \mathbf{s}_\omega\right) \tag{5.33a}$$

subject to

$$\sum_{r=1}^{N_r} x_{ir}^{\mathrm{s}} \leq 1, \forall i \tag{5.33b}$$

$$\sum_{m=1}^{N_m} x_{jm}^{\mathrm{up}} \leq 1, \forall j \tag{5.33c}$$

$$\sum_{q=1}^{N_q} x_{kq}^{\mathrm{dn}} \leq 1, \forall k \tag{5.33d}$$

$$400 \leq \Big(\sum_{j=1}^{N_j}\sum_{m=1}^{N_m} p^{\text{up}}_{jm} x^{\text{up}}_{jm}\Big) + y^{\text{up}}_{t\omega}, \forall \omega, \forall t \tag{5.33e}$$

$$\epsilon^{\text{s}+} + \epsilon^{\text{s}-} + \epsilon^{\text{o}+} + \epsilon^{\text{o}-} \leq 0.2\% \tag{5.33f}$$

$$a^{\text{s}+}_n \Big(\sum_{i=1}^{N_{\text{SR}}}\sum_{r=1}^{N_r} p^{\text{s}}_{ir} x^{\text{s}}_{ir}\Big) + b^{\text{s}+}_n \leq \epsilon^{\text{s}+}, \forall n \tag{5.33g}$$

$$a^{\text{s}-}_n \Big(\sum_{i=1}^{N_{\text{SR}}}\sum_{r=1}^{N_r} p^{\text{s}}_{ir} x^{\text{s}}_{ir}\Big) + b^{\text{s}-}_n \leq \epsilon^{\text{s}-}, \forall n \tag{5.33h}$$

$$a^{\text{o}+}_n \Big(\sum_{i=1}^{N_{\text{SR}}}\sum_{r=1}^{N_r} p^{\text{s}}_{ir} x^{\text{s}}_{ir} + \sum_{j=1}^{N_j}\sum_{m=1}^{N_m} p^{\text{up}}_{jm} x^{\text{up}}_{jm} + y^{\text{up}}_{t\omega}\Big) + b^{\text{o}+}_n \leq \epsilon^{\text{o}+}, \forall n, \forall t, \forall \omega \tag{5.33i}$$

$$a^{\text{o}-}_n \Big(\sum_{i=1}^{N_{\text{SR}}}\sum_{r=1}^{N_r} p^{\text{s}}_{ir} x^{\text{s}}_{ir} + \sum_{k=1}^{N_k}\sum_{q=1}^{N^{\text{q}}} p^{\text{dn}}_{kq} x^{\text{dn}}_{kq} + y^{\text{dn}}_{t\omega}\Big) + b^{\text{o}-}_n \leq \epsilon^{\text{o}-}, \forall n, \forall t, \forall \omega \tag{5.33j}$$

$$\alpha^{\text{up}}_l y^{\text{up}}_{t\omega} + \beta^{\text{up}}_l \leq \gamma^{\text{up}}_{t\omega}, \forall l, \forall \omega, \forall t \tag{5.33k}$$

$$\alpha^{\text{dn}}_l y^{\text{dn}}_{t\omega} + \beta^{\text{dn}}_l \leq \gamma^{\text{dn}}_{t\omega}, \forall l, \forall \omega, \forall t \tag{5.33l}$$

$$\sum_{i=1}^{N_{\text{SR}}}\sum_{r=1}^{N_r} c^{\text{s}}_{ir} p^{\text{s}}_{ir} x^{\text{s}}_{ir} + \sum_{j=1}^{N_j}\sum_{m=1}^{N_m} c^{\text{up}}_{jm} p^{\text{up}}_{jm} x^{\text{up}}_{jm} + \sum_{k=1}^{N_k}\sum_{q=1}^{N_q} c^{\text{dn}}_{kq} p^{\text{dn}}_{kq} x^{\text{dn}}_{kq} + \sum_{t=1}^{N_t}\big(\gamma^{\text{up}}_{t\omega} + \gamma^{\text{dn}}_{t\omega}\big) - \gamma \leq \mathbf{s}_\omega, \forall \omega$$

$$0 \leq \mathbf{s}_\omega, \forall \omega \tag{5.33m}$$

$$0 \leq y^{\text{up}}_{t\omega} \leq y^{\text{max,up}}_{t\omega}, \forall \omega, \forall t \tag{5.33n}$$

$$0 \leq y^{\text{dn}}_{t\omega} \leq y^{\text{max,dn}}_{t\omega}, \forall \omega, \forall t \tag{5.33o}$$

$$x^{\text{s}}_{ir} \in \{0,1\}, \forall i, \forall r \tag{5.33p}$$

$$x^{\text{up}}_{js} \in \{0,1\}, \forall j, \forall s \tag{5.33q}$$

$$x^{\text{dn}}_{kq} \in \{0,1\}, \forall k, \forall q \tag{5.33r}$$

$$\epsilon^{\text{s}+}, \epsilon^{\text{s}-}, \epsilon^{\text{o}+}, \epsilon^{\text{o}-} \in [0,1] \tag{5.33s}$$

The trade-off between the expected reserve cost and the CVaR is materialized by the parameter $\beta_r \in (0,1)$. If $\beta_r = 0$, the risk measure is neglected and the problem becomes the risk-neutral problem (5.30). If $\beta_r = 1$, the CVaR is minimized for the scenarios, where the reserve cost is more than the risk γ, and hence, variable $\mathbf{s}_\omega$ takes a positive value.

The minimization is over the set of variables $\Xi^{\text{CVaR}} = \Xi^{\text{R}} \cup \{\gamma; \mathbf{s}_\omega \forall \omega\}$.

5.6.3 The Reference Model (Common Practice)

The reference model (common practice) separates the dimensioning process (technical component) and the clearing process (market component). The system operator determines that $\hat{R}^{\text{s}}$, $\hat{R}^{\text{T,w,up}}$, $\hat{R}^{\text{T,w,dn}}$ are the amounts of secondary reserves, upward tertiary reserves, and downward tertiary reserves, respectively, in the weekly market, while $\hat{R}^{\mathrm{T,d,up}}$ and $\hat{R}^{\mathrm{T,d,dn}}$ are the amounts of upward tertiary reserves and downward tertiary reserves, respectively, in the daily market. These amounts are next procured in the corresponding markets.

The mathematical description of the reference model includes the clearing models of the weekly and daily markets, which are represented by problems (5.34) and (5.35), respectively.

$$\underset{x^{\mathrm{s}}_{ir}, x^{\mathrm{up}}_{js}, x^{\mathrm{dn}}_{kq}}{\text{Minimize}} \quad \sum_{i=1}^{N_{\mathrm{SR}}} \sum_{r=1}^{N_r} c^{\mathrm{s}}_{ir} p^{\mathrm{s}}_{ir} x^{\mathrm{s}}_{ir} + \sum_{j=1}^{N_j} \sum_{m=1}^{N_m} c^{\mathrm{up}}_{jm} p^{\mathrm{up}}_{jm} x^{\mathrm{up}}_{jm} + \sum_{k=1}^{N_k} \sum_{q=1}^{N_q} c^{\mathrm{dn}}_{kq} p^{\mathrm{dn}}_{kq} x^{\mathrm{dn}}_{kq} \tag{5.34a}$$

$$\hat{R}^{\mathrm{s}} \leq \sum_{i=1}^{N_{\mathrm{SR}}} \sum_{r=1}^{N_r} p^{\mathrm{s}}_{ir} x^{\mathrm{s}}_{ir} \tag{5.34b}$$

$$\hat{R}^{\mathrm{T,w,up}} \leq \sum_{j=1}^{N_j} \sum_{m=1}^{N_m} p^{\mathrm{up}}_{jm} x^{\mathrm{up}}_{jm} \tag{5.34c}$$

$$\hat{R}^{\mathrm{T,w,dn}} \leq \sum_{k=1}^{N_k} \sum_{q=1}^{N_q} p^{\mathrm{dn}}_{kq} x^{\mathrm{dn}}_{kq} \tag{5.34d}$$

$$\sum_{r=1}^{N_r} x^{\mathrm{s}}_{ir} \leq 1, \forall i \tag{5.34e}$$

$$\sum_{m=1}^{N_m} x^{\mathrm{up}}_{jm} \leq 1, \forall j \tag{5.34f}$$

$$\sum_{q=1}^{N_q} x^{\mathrm{dn}}_{kq} \leq 1, \forall k \tag{5.34g}$$

$$x^{\mathrm{s}}_{ir} \in \{0,1\}, \forall i, \forall r \tag{5.34h}$$

$$x^{\mathrm{up}}_{js} \in \{0,1\}, \forall j, \forall s \tag{5.34i}$$

$$x^{\mathrm{dn}}_{kq} \in \{0,1\}, \forall k, \forall q \tag{5.34j}$$

In the weekly market, problem (5.34) minimizes the reserve cost (5.34a) over binary variables $\{x^{\mathrm{s}}_{ir}, \forall i, \forall r; x^{\mathrm{up}}_{js}, \forall j, \forall s; x^{\mathrm{dn}}_{kq}, \forall k, \forall q\}$, as described in Section 5.6.1.

Constraints (5.34b)-(5.34d) satisfy the amounts of secondary, upward tertiary, and downward tertiary reserves, respectively. Constraints (5.34e)-(5.34g) model mutually exclusive secondary reserve offers, upward tertiary reserve offers, and downward tertiary reserve offers, respectively. Finally, the indivisibility of offers related to secondary, upward tertiary, and downward tertiary reserves are expressed by constraints (5.34h)-(5.34j), respectively.

In the daily market, the decision variables are:

- Binary variables representing the acceptance or the rejection of each upward tertiary reserve offer in each four-hour interval t in the daily market $[y^{\mathrm{up}}_{j'm't}]$. Each upward tertiary reserve offer may be in a set of mutually exclusive $N_{m'}$ offers.

- Binary variables representing the acceptance or the rejection of each downward tertiary reserve offer in each four-hour interval t in the daily market $[y^{\text{dn}}_{k'q't}]$. Each downward tertiary reserve offer may be in a set of mutually exclusive $N_{q'}$ offers.

The MILP clearing model of the daily market is formulated in problem (5.35) below:

$$\underset{y^{\text{up}}_{j'm't}, y^{\text{dn}}_{k'q't}}{\text{Minimize}} \quad \sum_{t=1}^{N_t} \Big(\sum_{j'=1}^{N_{j'}} \sum_{m'=1}^{N_{m'}} c^{\text{up}}_{j'm't} p^{\text{up}}_{j'm't} y^{\text{up}}_{j'm't} + \sum_{k'=1}^{N_{k'}} \sum_{q'=1}^{N_{q'}} c^{\text{dn}}_{k'q't} p^{\text{dn}}_{k'q't} y^{\text{dn}}_{k'q't} \Big) \tag{5.35a}$$

$$\hat{R}^{\text{T,d,up}} \leq \sum_{j'=1}^{N_{j'}} \sum_{m'=1}^{N_{m'}} p^{\text{up}}_{j'm't} y^{\text{up}}_{j'm't} \tag{5.35b}$$

$$\hat{R}^{\text{T,d,dn}} \leq \sum_{k'=1}^{N_{k'}} \sum_{q'=1}^{N_{q'}} p^{\text{dn}}_{k'q't} y^{\text{dn}}_{k'q't} \tag{5.35c}$$

$$\sum_{j'=1}^{N_{j'}} \sum_{m'=1}^{N_{m'}} y^{\text{up}}_{j'm't} \leq 1, \forall j', \forall t \tag{5.35d}$$

$$\sum_{k'=1}^{N_{k'}} \sum_{q'=1}^{N_{q'}} y^{\text{dn}}_{k'q't} \leq 1, \forall k', \forall t \tag{5.35e}$$

$$y^{\text{up}}_{j'm't} \in \{0,1\}, \forall j', \forall m', \forall t, \tag{5.35f}$$

$$y^{\text{dn}}_{k'q't} \in \{0,1\}, \forall k', \forall q', \forall t \tag{5.35g}$$

Problem (5.35) minimizes the costs of the upward and downward tertiary reserves (5.35a) in the daily market over binary variables $\{y^{\text{up}}_{j'm't}, \forall j', \forall m', \forall t;\ y^{\text{dn}}_{k'q't}, \forall k', \forall q', \forall t\}$, as described above.

Constraints (5.35b) and (5.35c) satisfy the required amounts of upward and downward tertiary reserves, respectively. Constraints (5.35d) and (5.35e) model mutually exclusive upward tertiary offers and mutually exclusive downward tertiary offers, respectively. Indivisibility of upward and downward tertiary offers are modeled by constraints (5.35f) and (5.35g), respectively.

5.6.4 Metrics: Perfect Information Model & Actual Cost

To evaluate the performance of the proposed two-stage models (i.e., the risk-neutral model and the risk-averse model), we compute the actual reserve cost obtained from these models, and compare it to the reserve cost obtained from the deterministic reference model (common practice). We also compare the outcomes of the proposed models to an optimal solution obtained from a *perfect information* model. In the following, We first explain how to compute the actual cost, and next, we elaborate on the *perfect information* model.

The actual reserve cost is obtained as follows:

1. We solve the proposed two-stage model.
2. The variables pertaining to the weekly market are fixed at the optimal first-stage solution obtained (i.e., $x^{\text{s}}_{ir} = x^{*\text{s}}_{ir}$, $x^{\text{up}}_{jm} = x^{*\text{up}}_{jm}$ and $x^{\text{dn}}_{kq} = x^{*\text{dn}}_{kq}$).
3. The offers are updated in the daily market.
4. The resulting problem is then solved for the actual daily offers (and not the scenarios).
5. The optimal value of objective function is the actual reserve cost.

The mathematical description of obtaining the actual cost is expressed by problem (5.36):

$$\underset{y^{\text{up}}_{j'm't}, y^{\text{dn}}_{k'q't}, \epsilon^{\text{s}+}, \epsilon^{\text{s}-}, \epsilon^{\text{o}+}, \epsilon^{\text{o}-}}{\text{Minimize}}$$

$$\sum_{i=1}^{N_{\text{SR}}} \sum_{r=1}^{N_r} c^{\text{s}}_{ir} p^{\text{s}}_{ir} x^{*\text{s}}_{ir} + \sum_{j=1}^{N_j} \sum_{m=1}^{N_m} c^{\text{up}}_{jm} p^{\text{up}}_{jm} x^{*\text{up}}_{jm} + \sum_{k=1}^{N_k} \sum_{q=1}^{N_q} c^{\text{dn}}_{kq} p^{\text{dn}}_{kq} x^{*\text{dn}}_{kq}$$

$$+ \Big(\sum_{t=1}^{N_t} \big(\sum_{j'=1}^{N_{j'}} \sum_{m'=1}^{N_{m'}} c^{\text{up}}_{j'm't} p^{\text{up}}_{j'm't} y^{\text{up}}_{j'm't} + \sum_{k'=1}^{N_{k'}} \sum_{q'=1}^{N_{q'}} c^{\text{dn}}_{k'q't} p^{\text{dn}}_{k'q't} y^{\text{dn}}_{k'q't} \big) \Big) \tag{5.36a}$$

subject to

$$\sum_{j'=1}^{N_{j'}} \sum_{m'=1}^{N_{m'}} y^{\text{up}}_{j'm't} \leq 1, \forall j', \forall t \tag{5.36b}$$

$$\sum_{k'=1}^{N_{k'}} \sum_{q'=1}^{N_{q'}} y^{\text{dn}}_{k'q't} \leq 1, \forall k', \forall t \tag{5.36c}$$

$$400 \leq \big(\sum_{j=1}^{N_j} \sum_{m=1}^{N_m} p^{\text{up}}_{jm} x^{*\text{up}}_{jm} \big) + \big(\sum_{j'=1}^{N_{j'}} \sum_{m'=1}^{N_{m'}} p^{\text{up}}_{j'm't} y^{\text{up}}_{j'm't} \big), \forall \omega, \forall t \tag{5.36d}$$

$$\epsilon^{\text{s}+} + \epsilon^{\text{s}-} + \epsilon^{\text{o}+} + \epsilon^{\text{o}-} \leq 0.2\% \tag{5.36e}$$

$$a^{\text{s}+}_n \Big(\sum_{i=1}^{N_{\text{SR}}} \sum_{r=1}^{N_r} p^{\text{s}}_{ir} x^{*\text{s}}_{ir} \Big) + b^{\text{s}+}_n \leq \epsilon^{\text{s}+}, \forall n \tag{5.36f}$$

$$a^{\text{s}-}_n \Big(\sum_{i=1}^{N_{\text{SR}}} \sum_{r=1}^{N_r} p^{\text{s}}_{ir} x^{*\text{s}}_{ir} \Big) + b^{\text{s}-}_n \leq \epsilon^{\text{s}-}, \forall n \tag{5.36g}$$

$$a^{\text{o}+}_n \Big(\sum_{i=1}^{N_{\text{SR}}} \sum_{r=1}^{N_r} p^{\text{s}}_{ir} x^{*\text{s}}_{ir} + \sum_{j=1}^{N_j} \sum_{m=1}^{N_m} p^{\text{up}}_{jm} x^{*\text{up}}_{jm} + \big(\sum_{j'=1}^{N_{j'}} \sum_{m'=1}^{N_{m'}} p^{\text{up}}_{j'm't} y^{\text{up}}_{j'm't} \big) \Big) + b^{\text{o}+}_n \leq \epsilon^{\text{o}+}, \forall n, \forall t \tag{5.36h}$$

$$a_n^{\text{o}-}\Big(\sum_{i=1}^{N_{\text{SR}}}\sum_{r=1}^{N_r} p_{ir}^{\text{s}} x_{ir}^{*\text{s}} + \sum_{k=1}^{N_k}\sum_{q=1}^{N_q} p_{kq}^{\text{dn}} x_{kq}^{*\text{dn}} + \big(\sum_{k'=1}^{N_{k'}}\sum_{q'=1}^{N_{q'}} p_{k'q't}^{\text{dn}} y_{k'q't}^{\text{dn}}\big)\Big) + b_n^{\text{o}-} \le \epsilon^{\text{o}-}, \forall n, \forall t \quad (5.36\text{i})$$

$$y_{j'm't}^{\text{up}} \in \{0,1\}, \forall j', \forall m', \forall t \quad (5.36\text{j})$$

$$y_{k'q't}^{\text{dn}} \in \{0,1\}, \forall k', \forall q', \forall t \quad (5.36\text{k})$$

$$\epsilon^{\text{s}+}, \epsilon^{\text{s}-}, \epsilon^{\text{o}+}, \epsilon^{\text{o}-} \in [0,1] \quad (5.36\text{l})$$

Perfect Information Model

The *perfect information solution* identifies what optimal decisions would have been made if the daily offers were available in the weekly market. This solution is obtained by solving a deterministic model where the scenarios are replaced by actual daily offers. Note that scenarios constitute a discrete approximation, and thus, they may deviate from the actual offers. Therefore, this solution acts as a proxy to evaluate the accuracy of the scenarios.

We should note that this solution is different from the Expected Value of Perfect Information (EVPI). The EVPI is the expected optimal value of the two-stage model with relaxed non-anticipativity constraints [4]. Therefore, the EVPI still uses scenarios. However, in the *perfect information model*, there is one scenario with all actual offers, and not a number of representative scenarios.

The formulation of the perfect information model is as follows:

$$\underset{\Xi^{\text{PI}}}{\text{Minimize}}$$

$$\sum_{i=1}^{N_{\text{SR}}}\sum_{r=1}^{N_r} c_{ir}^{\text{s}} p_{ir}^{\text{s}} x_{ir}^{\text{s}} + \sum_{j=1}^{N_j}\sum_{m=1}^{N_m} c_{jm}^{\text{up}} p_{jm}^{\text{up}} x_{jm}^{\text{up}} + \sum_{k=1}^{N_k}\sum_{q=1}^{N_q} c_{kq}^{\text{dn}} p_{kq}^{\text{dn}} x_{kq}^{\text{dn}}$$

$$+ \Big(\sum_{t=1}^{N_t}\big(\sum_{j'=1}^{N_{j'}}\sum_{m'=1}^{N_{m'}} c_{j'm't}^{\text{up}} p_{j'm't}^{\text{up}} y_{j'm't}^{\text{up}} + \sum_{k'=1}^{N_{k'}}\sum_{q'=1}^{N_{q'}} c_{k'q't}^{\text{dn}} p_{k'q't}^{\text{dn}} y_{k'q't}^{\text{dn}}\big)\Big) \quad (5.37\text{a})$$

subject to

$$\sum_{r=1}^{N_r} x_{ir}^{\text{s}} \le 1, \forall i \quad (5.37\text{b})$$

$$\sum_{m=1}^{N_m} x_{jm}^{\text{up}} \le 1, \forall j \quad (5.37\text{c})$$

$$\sum_{q=1}^{N_q} x_{kq}^{\text{dn}} \le 1, \forall k \quad (5.37\text{d})$$

$$\sum_{j'=1}^{N_{j'}}\sum_{m'=1}^{N_{m'}} y_{j'm't}^{\text{up}} \le 1, \forall j', \forall t \quad (5.37\text{e})$$

$$\sum_{k'=1}^{N_{k'}} \sum_{q'=1}^{N_{q'}} y^{\text{dn}}_{k'q't} \le 1, \forall k', \forall t \tag{5.37f}$$

$$400 \le \Big(\sum_{j=1}^{N_j} \sum_{m=1}^{N_m} p^{\text{up}}_{jm} x^{\text{up}}_{jm}\Big) + \Big(\sum_{j'=1}^{N_{j'}} \sum_{m'=1}^{N_{m'}} p^{\text{up}}_{j'm't} y^{\text{up}}_{j'm't}\Big), \forall \omega, \forall t \tag{5.37g}$$

$$\epsilon^{\text{s}+} + \epsilon^{\text{s}-} + \epsilon^{\text{o}+} + \epsilon^{\text{o}-} \le 0.2\% \tag{5.37h}$$

$$a^{\text{s}+}_n \Big(\sum_{i=1}^{N_{\text{SR}}} \sum_{r=1}^{N_r} p^{\text{s}}_{ir} x^{\text{s}}_{ir}\Big) + b^{\text{s}+}_n \le \epsilon^{\text{s}+}, \forall n \tag{5.37i}$$

$$a^{\text{s}-}_n \Big(\sum_{i=1}^{N_{\text{SR}}} \sum_{r=1}^{N_r} p^{\text{s}}_{ir} x^{\text{s}}_{ir}\Big) + b^{\text{s}-}_n \le \epsilon^{\text{s}-}, \forall n \tag{5.37j}$$

$$a^{\text{o}+}_n \Big(\sum_{i=1}^{N_{\text{SR}}} \sum_{r=1}^{N_r} p^{\text{s}}_{ir} x^{\text{s}}_{ir} + \sum_{j=1}^{N_j} \sum_{m=1}^{N_m} p^{\text{up}}_{jm} x^{\text{up}}_{jm} + \Big(\sum_{j'=1}^{N_{j'}} \sum_{m'=1}^{N_{m'}} p^{\text{up}}_{j'm't} y^{\text{up}}_{j'm't}\Big)\Big) + b^{\text{o}+}_n \le \epsilon^{\text{o}+}, \forall n, \forall t \tag{5.37k}$$

$$a^{\text{o}-}_n \Big(\sum_{i=1}^{N_{\text{SR}}} \sum_{r=1}^{N_r} p^{\text{s}}_{ir} x^{\text{s}}_{ir} + \sum_{k=1}^{N_k} \sum_{q=1}^{N_q} p^{\text{dn}}_{kq} x^{\text{dn}}_{kq} + \Big(\sum_{k'=1}^{N_{k'}} \sum_{q'=1}^{N_{q'}} p^{\text{dn}}_{k'q't} y^{\text{dn}}_{k'q't}\Big)\Big) + b^{\text{o}-}_n \le \epsilon^{\text{o}-}, \forall n, \forall t \tag{5.37l}$$

$$x^{\text{s}}_{ir} \in \{0,1\}, \forall i, \forall r \tag{5.37m}$$

$$x^{\text{up}}_{js} \in \{0,1\}, \forall j, \forall s \tag{5.37n}$$

$$x^{\text{dn}}_{kq} \in \{0,1\}, \forall k, \forall q \tag{5.37o}$$

$$y^{\text{up}}_{j'm't} \in \{0,1\}, \forall j', \forall m', \forall t \tag{5.37p}$$

$$y^{\text{dn}}_{k'q't} \in \{0,1\}, \forall k', \forall q', \forall t \tag{5.37q}$$

$$\epsilon^{\text{s}+}, \epsilon^{\text{s}-}, \epsilon^{\text{o}+}, \epsilon^{\text{o}-} \in [0,1] \tag{5.37r}$$

Problem (5.37) minimizes the reserve cost (5.37a) over the set of variables $\Xi^{\text{PI}} = \{x^{\text{s}}_{ir}, \forall i, \forall r; x^{\text{up}}_{jm}, \forall j, \forall m; x^{\text{dn}}_{kq}, \forall k, \forall q; y^{\text{up}}_{j'm't}, \forall j', \forall m', \forall t; y^{\text{dn}}_{k'q't}, \forall k', \forall q', \forall t\}$ considering constraints (5.37b)-(5.37f) modeling mutually exclusive offers, constraint (5.37g) representing the deterministic criterion, constraints (5.37h)-(5.37l) modeling the probability criterion, and constraints (5.37m)-(5.37q) enforcing indivisibility of offers.

5.7 Case Studies

For the case studies presented in this chapter, we analyze the outcomes from the proposed risk-neutral model, problem (5.30), and from the proposed risk-averse model, problem (5.33), in the Swiss reserve market.

5.7.1 Outcomes of the Risk-Neutral Model

The proposed risk-neutral two-stage model has been used to clear the Swiss reserve market since February 2014.

In this section, we provide the outcomes obtained from the actual implementation of the risk-neutral model (5.30) and compare them to the results of the reference model (i.e., problems (5.34) and (5.35)), as well as the solution of the perfect information model (i.e., problem (5.37)).

Given the limited data due to the short history of the Swiss reserve market, we use the experience and judgment of the operators to select scenarios. The experience pertaining to the offering behavior of market participants indicate that offers of daily markets do not usually change much over two consecutive weeks. As previously mentioned, the best available offers that represent the offers in the daily markets in week *w* are those in week *w-2*. Therefore, we take offers from week *w-2* and assume three equi-probable scenarios representing price offers higher than, lower than, and equal to the price offers in week *w-2*.

We provide the clearing outcomes for week 27, 2016 (the second week of July) and week 46, 2016 (the third week of November), as two examples of the season with high precipitation, and thus, low price offers, and of the season with low precipitation and high price offers.

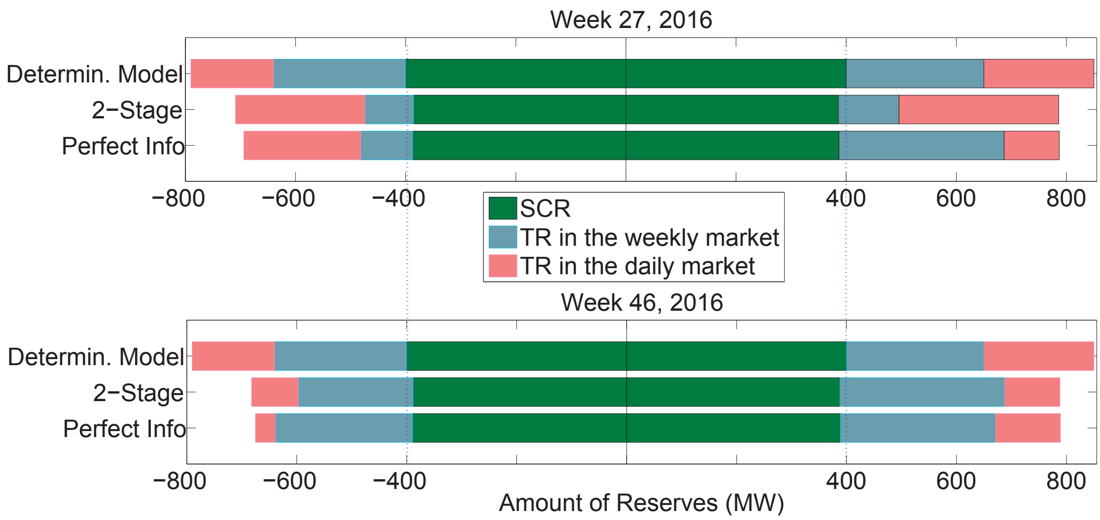

Figure 5.10 – The amounts of reserves obtained from the perfect information model, the risk-neutral two-stage model, and the deterministic reference model (SCR and TR denote secondary and tertiary reserves, respectively.)

Fig 5.10 shows the amounts of reserves obtained from the perfect information model, the risk-neutral two-stage model, and the deterministic reference model in weeks 27 and 46, 2016. The details about the levels of reserves are provided in Tables 5.1. We should note that the SCR and TR denote secondary reserve and tertiary reserves, respectively.

Comparing the outcomes from the proposed two-stage model and those from the reference model, the following observations are in order.

In week 27, the amount of secondary reserve decreases from 400 MW in the reference model to 386 MW in the two-stage approach. The total amount of upward tertiary reserve (i.e., the total amount from the weekly and daily markets) decreases from 450 MW in the reference model to 400 MW using the proposed two-stage approach. Also, the total amount of downward tertiary reserve decreases from 390 MW in the reference model to 323 MW using the two-stage approach. Therefore, the total amount of reserves (i.e., the total amount of secondary, upward tertiary and downward tertiary) decreases from 1240 MW in the reference model to 1110 MW in the two-stage model.

A similar observation is valid in week 46. That is, the levels of reserves decrease under the two-stage model as compared to those from the reference model.

We also benchmark the outcomes of the risk-neutral two-stage model against those of the perfect information model to evaluate the performance of the two-stage model.

In week 27, the amounts of secondary reserves are almost the same (differing only by 1 MW). The total amount of upward tertiary reserve are also the same, as it is enforced by constraint (5.20) to be at least 400 MW. Eventually, the total amount of downward tertiary reserve obtained from the perfect information model is 16 MW smaller than that of the corresponding amount from the two-stage model (307 MW vs. 323 MW). This is translated into the following. If actual daily offers were available, the cheapest would be to buy 387 MW of secondary reserve and 307 MW of downward tertiary reserve. In the absence of actual offers in the daily market and the use of scenarios in the two-stage model, these amounts are 386 MW of secondary reserve (1 MW smaller than 387 MW) and 323 MW of downward tertiary reserve (16 MW greater than 307 MW).

Similar observations are valid in week 46. The total amount of reserves from the two-stage model are only 7 MW greater than that of the perfect information model. The outcomes of the prefect information model are also used to benchmark how accurate is the allocation of tertiary reserve amounts to the weekly and daily markets.

Focusing on week 27 and downward tertiary reserves, the trend of buying a smaller share of the total amount in the weekly market and a larger share in the daily market is similar in the two-stage model and the perfect information model. The corresponding amounts are, however, slightly different; the perfect information model procures 95 MW in the weekly market and 212 MW in the daily market, while the two-stage model procures 88 MW and 235 MW in the weekly and daily markets, respectively. This shows that the scenarios modeling downward offers in the daily market are good representatives of actual offers and the two-stage model has a good performance. We should also note that in the reference model a higher share of tertiary reserves is allocated to the weekly market based on the judgment that the weekly market would have a higher liquidity and cheaper offers than the daily market. However, this example shows that such a judgment is not always correct.

Regarding upward tertiary reserves in week 27, the two-stage model allocates a higher share of the total amount to the daily market. However, this is the opposite if the prefect information model is used. Noting that in both models, 100 MW is procured in the daily market, we conclude that upward tertiary scenarios are good representatives of the actual offers up to 100 MW; however, they are cheaper than actual offers for quantities larger than 100 MW. This implies that a better modeling of scenarios representing upward tertiary reserves is desired.

Focusing on week 46, the trend of buying a higher share of tertiary reserves (both upward and downward) in the weekly market is similar under both the two-stage model and perfect information model; the amounts are, however, slightly different. That is, in the weekly market the two-stage model procures 8 MW in addition to 282 MW of upward tertiary reserve resulting from the perfect information model, and a 41 MW smaller than 250 MW of downward tertiary reserve obtained from the perfect information model.

Details regarding reserve costs are provided in Table 5.2. We should note that Table 5.2 provides the expected reserve cost (equation (5.13)) as well as the actual reserve cost (equation (5.36a)) obtained from the two-stage model.

In week 27, the expected reserve cost from the two-stage model is CHF1.34M, and after actualization of daily offers, the actual reserve cost is CHF1.40M. Therefore, a cost saving of 4.6% is achieved considering the cost of the reference model (CHF1.47M).

Considering the expected reserve cost of CHF1.34M and the perfect information cost of CHF1.37M, we conclude that the reserve cost is underestimated by the scenarios in the two-stage model. This results from the scenarios representing upward tertiary reserve offers that are cheaper than the corresponding actual offers, as mentioned above. Note that the actual cost from the two-stage model is only 2% higher than the cost obtained from the prefect information model. This implies that there is still a potential of cost saving by better choosing scenarios that represent daily offers.

In week 46, the expected reserve cost from the two-stage model is CHF5.72M, and after actualization of daily offers, the actual reserve cost is CHF6.00M. A cost saving of 13.7% is

Table 5.1 – Reserves [MW]

	SCR	Up TR		Down TR		Total R.
week 27		weekly	daily	weekly	daily	
Perfect Info.	387	300	100	95	212	1094
Two-stage Model	386	110	290	88	235	1109
Reference Model	400	250	200	240	150	1240
	SCR	Up TR		Down TR		Total R.
week 46		weekly	daily	weekly	daily	
Perfect Info.	389	282	118	250	36	1075
Two-stage Model	388	300	100	209	85	1082
Reference Model	400	250	200	240	150	1240

Table 5.2 – Costs of Reserves [CHF]

	Weekly cost			Total	Total cost	
week 27	SCR	Up TR	Down TR	weekly cost	Exp.	Act.
Perfect Info.	1198437	91583	15643	1305663	–	1372716
Two-stage Model	1195459	30227	14341	1240027	1340186	1404820
Reference Model	1240595	73833	50302	1364730	–	1473258
week 46						
Perfect Info	4850598	271091	292132	5413821	–	5668418
Two-stage Model	4835450	307975	222866	5366291	5716644	6002171
Reference Model	5018841	222417	272752	5514010	–	6956193

obtained by considering this actual cost and the cost of the reference model (CHF6.96M).

The actual cost of the two-stage model is 5.56% higher than the cost from the perfect information model. That is, there is a potential of cost saving of about 5% by improving the scenarios.

These outcomes show that the proposed two-stage model results in a smaller reserve cost than that of the deterministic reference model as a result of procuring a smaller amount of reserves, as well as of procuring a considerable share of tertiary reserves in the market stage with cheaper offers.

We should note that the reserve amounts from the reference model, determined by Swissgrid in 2008, result in a deficit probability of 0.18% that is smaller than 0.2%. In other words, the reference model results in reserve over-procurement. The two-stage model, however, determines an adequate level of the reserves while avoiding over-procurement, and consequently, attains a smaller reserve cost.

5.7.2 Discussion on the Number of Scenarios, Optimal Expected Reserve Cost and Computation Time

In this section, we elaborate on the number of scenarios and its impact on the solution accuracy and the computation time.

An increase in the number of scenarios may improve representation of the daily offers, and therefore, the expected reserve cost. However, on the other hand, it may increase the required computation time. We investigate the impact of the number of scenarios on the computation time and the expected reserve cost in the following.

For the simulations, we use CPLEX 12.5.0 under MATLAB on a computer with two Intel(R) Core(TM) processors clocking at 2.7 GHz and 8 GB of RAM.

Table 5.3 provides the problem size in terms of the number of variables and constraints, the computation time and the expected cost for different numbers of scenarios. With the increase in the number of scenarios, the problem size and the computation time increase; however, the expected cost remains unaltered.

Table 5.3 – Number of scenarios, computation time and expected reserve cost

week 46			
Number of scenarios	3	10	20
No. of binary variables	452	452	452
No. of continuous variables	762	2533	5063
No. of total variables	1214	2985	5515
No. of constraints	9017	29891	59711
Computation time (s)	28	257	445
Expected cost (CHFM)	5.67	5.67	5.67
week 27			
Number of scenarios	3	10	20
No. of binary variables	357	357	357
No. of continuous variables	762	2533	5063
No. of total variables	1119	2890	5420
No. of constraints	9009	29883	59703
Computation time (s)	15	88	258
Expected cost (CHFM)	1.32	1.32	1.32

These analyses imply that an increase in the number of scenarios does not necessarily improve the representation of the daily offers. Hence, the same expected costs are obtained using different numbers of scenarios.

5.7.3 Simulation Results for the Risk-Averse Model

In this section, we present outcomes from the risk-averse model (5.33) and compare them to those from the risk-neutral two-stage model. These outcomes are also benchmarked against the outputs from the perfect information model.

The CVaR is computed at the 0.9 confidence level; that is, the expected reserve cost pertaining to the 10% worse scenarios is minimized.

We assume 20 equi-probable scenarios, where scenarios representing upward tertiary offers in weeks 27 and 46 are within a range from 80% to 250% of the price offers in the daily market in weeks 25 and 44, and those representing downward tertiary offers cover a range from 75% to 115% of the price offers in the daily market in weeks 25 and 44.

We select this number of scenarios so that it covers sufficiently probable scenarios while avoiding high computational burden.

The results for week 27 are provided below.

The quantities of reserves including their allocations in the weekly and daily markets, as well as the expected cost and the CVaR are provided in Table 5.4 for the risk-neutral case ($\beta_r = 0$) and the risk-averse case ($\beta_r = 1$).

Using the risk-neutral model, the expected reserve cost is CHF1.34M and the CVaR is CHF1.39M. That is, with a probability of 90%, the final reserve cost is less than or equal to CHF1.39M.

The amounts of upward and downward tertiary reserves in the weekly market are 110 MW, and 88 MW, respectively. That is, the risk-neutral model allocates a larger share of tertiary reserves in the daily market.

Using the risk-averse model with $\beta_r = 1$, the amount of upward tertiary reserve is 300 MW in the weekly market. That is, a higher share of upward tertiary reserves is procured in the weekly market to reduce the risk of being exposed to expensive offers in the daily market.

The expected cost of the risk-averse model is CHF1.36M, which is higher than CHF1.34M obtained from the risk-neutral model. This higher expected cost is obtained at the benefit of a smaller risk, i.e., the CVaR is CHF1.37M. In other words, with a probability of 90%, the final reserve cost is less than or equal to CHF1.37M if the CVaR is minimized.

The efficient frontier is shown in Fig. 5.11. It is relevant to observe that moving from the risk-neutral case with $\beta = 0$ to the risk-averse case with $\beta = 0.5$, there is a comparatively sharp decrease in the risk (i.e, in the CVaR), but a slightly different expected cost, while moving from

Table 5.4 – Reserves, expected cost and CVaR (week 27, 2016)

week 27	SCR [MW]	Up TR [MW]		Down TR [MW]		Total R. [MW]	Exp. cost [CHF]	CVaR [CHF]
		weekly	daily	weekly	daily			
$\beta_r = 0$	386	110	290	88	235	1109	1341931	1394645
$\beta_r = 1$	386	300	100	88	235	1109	1368091	1371527

$\beta = 0.5$ to $\beta = 1$ the risk does not noticeably alter. This suggests that the risk-averse model with $\beta = 0.5$ avoids that the TSO is exposed to expensive reserve offers in the daily market, while still minimizing the expected cost.

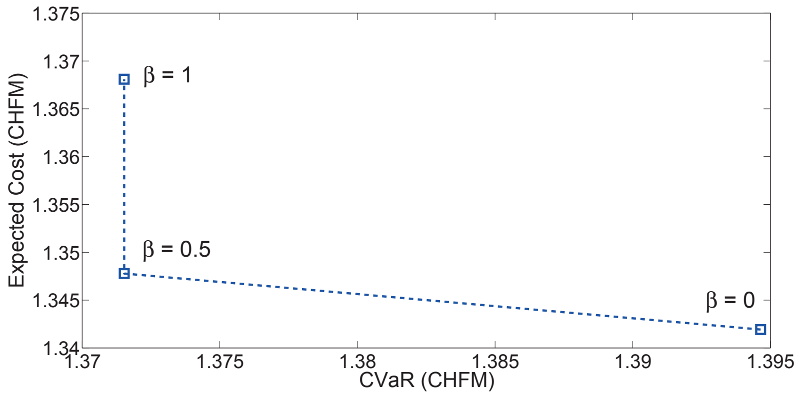

Figure 5.11 – Efficient Frontier in term of the expected reserve cost and CVaR (week 27, 2016)

Considering the risk-averse model with $\beta_r = 0.5$, the per-scenario reserve cost and the optimal value of $\mathbf{s}_\omega$ are provided in Table 5.5. The CVaR is CHF1.37M and results from scenarios 19 and 20, where high reserve costs occur.

The actual costs obtained from the risk-neutral and risk-averse models with $\beta_r = 0.5$ and $\beta_r = 1$, and from the perfect information model are provided in Table 5.6.

The actual costs from the risk-averse models with $\beta_r = 0.5$ and $\beta_r = 1$ are close to the cost of the perfect information model. The reason is that the risk-averse model procures a higher portion of upward tertiary reserves (300 MW from the total 400 MW) in the weekly market in order to minimize the risk of being exposed to the expensive offers in the daily market. Eventually, since the actual offers are expensive, the actual costs of the risk-averse cases are smaller than that of the risk-neutral model.

Table 5.7 provides the reserves, the expected cost, and the CVaR obtained from the risk-neutral case ($\beta_r = 0$) and the risk-averse one ($\beta_r = 1$) for week 46.

Table 5.5 – Cost and $\mathbf{s}_\omega$ per Scenario for $\beta_r = 0.5$ (week 27, 2016)

Scenario	Cost (CHF)	$\mathbf{s}_\omega$ (CHF)	Scenario	Cost (CHF)	$\mathbf{s}_\omega$ (CHF)
1	1322700.71	0.00	11	1349106.58	0.00
2	1325344.77	0.00	12	1351745.06	0.00
3	1327987.09	0.00	13	1354383.54	0.00
4	1330627.89	0.00	14	1357021.92	0.00
5	1333268.17	0.00	15	1359659.54	0.00
6	1335908.38	0.00	16	1362297.16	0.00
7	1338548.58	0.00	17	1364934.78	0.00
8	1341188.79	0.00	18	1367572.41	0.00
9	1343828.65	0.00	19	1370209.85	2637.44
10	1346468.10	0.00	20	1372846.66	5274.25

Table 5.6 – Actual costs (week 27, 2016)

Approach	Actual cost (M CHF)
Perfect info	1372716
Risk-neutral, $\beta_r = 0$	1404820
Risk-averse, $\beta_r = 0.5$	1372962
Risk-averse, $\beta_r = 1$	1372939

The expected cost and the CVaR of the risk-neutral model are CHF5.85M ad CHF6.15M, respectively, and of the risk-averse model are CHF6.09M and CHF6.13M, respectively. That is, the risk-averse model decreases the CVaR at the expense of increasing the expected cost.

Table 5.7 – Reserves, expected cost and CVaR (week 46, 2016)

week 46	SCR [MW]	Up TR [MW]		Down TR [MW]		Total R. [MW]	Exp. cost [CHF]	CVaR [CHF]
		weekly	daily	weekly	daily			
$\beta_r = 0$	388	300	100	204	86	1078	5845596	6149647
$\beta_r = 1$	388	300	100	214	80	1082	6089771	6131757

The efficient frontier for week 46 is shown in Fig. 5.12. Moving from $\beta = 0$ to $\beta = 0.5$, there is a comparatively sharp decrease in the CVaR and a slight increase in the expected cost, while moving from $\beta = 0.5$ to $\beta = 1$, the CVaR gently decreases but the expected cost sharply increases. The difference of the CVaR between the extreme points (i.e., the case with $\beta = 0$ and the case with $\beta = 1$) is of order of 0.3% (CHF18k).

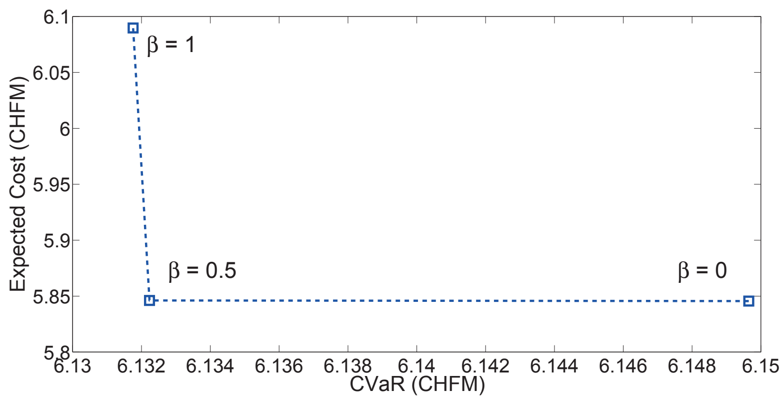

Figure 5.12 – Efficient Frontier in term of the expected reserve cost and the CVaR (week 46, 2016)

Considering the actual costs, provided in Table 5.8, the risk-averse model with $\beta_r = 1$ results in a cost with the smallest deviation from the cost of perfect information model, while the actual cost of the risk-neutral model is the highest. The reason is that the risk-averse model with $\beta_r = 1$ procures 214 MW downward tertiary reserves in the weekly market in order to minimize the risk of being exposed to the expensive offers in the daily market. Eventually, since the actual offers are expensive, the actual costs of the risk-averse cases are smaller than that of the risk-neutral model.

Table 5.8 – Actual costs (week 46, 2016)

Approach	Actual cost (M CHF)
Perfect info	5668418
Risk-neutral, $\beta_r = 0$	6050277
Risk-averse, $\beta_r = 0.5$	6002171
Risk-averse, $\beta_r = 1$	5956934

5.7.4 Case Study Conclusions

We propose a risk-neutral stochastic two-stage clearing model to replace the deterministic reference model in the Swiss reserve market.

The proposed two-stage model results in cost savings ranging from 4% to 14% over different weeks. This is due to procuring a smaller quantity of reserves under the proposed model than that of the reference model, as well as procuring a considerable share of tertiary reserves in the market with cheaper offers.

The proposed model is benchmarked against a perfect information solution, which is the optimal solution obtained from a deterministic model with actual offers. This comparison confirms that the two-stage model generally has a good performance in term of procuring the right amounts of reserves in the market with cheaper offers. However, the scenarios modeling offers in the daily market can be still improved. Such improvements have potential cost savings in the range of 2% to 5%.

From a computational point of view, the proposed two-stage model is tractable and requires a reasonable solution time.

We also propose a risk-averse two-stage model, where the risk measure is the CVaR, to minimize the risk pertaining to expensive reserve offers in the daily market. If expensive offers ocurr in the daily market, the use of the proposed risk-averse model may result in a smaller actual cost than that of the risk-neutral model. Therefore, if Swissgrid wishes to implement a risk-averse model, the proposed risk-averse model results in appropriate outcomes.

5.8 Summary and Conclusion of the Chapter

To cope with the drawbacks associated with the common practice of reserve provision in Switzerland, we propose a risk-neutral two-stage stochastic clearing model, and also, a risk-averse one.

The decision-making problem consists of determining which amount of reserves to procure in the weekly market and which one in the daily market. In the proposed two-stage model, the first stage represents the weekly market and the second stage the daily market. The source of uncertainty is the unknown offers in the daily market, which are represented by scenarios. Additionally, to minimize the risk pertaining to expensive reserve offers in the daily market, a risk-averse instance of this two-stage clearing model is proposed.

We compare the performance of the risk-neutral two-stage model with the common deterministic approach, which sacrifices optimality in favor of simplicity.

The proposed risk-neutral two-stage model results in a smaller reserve cost than that of the deterministic approach as a result of procuring smaller reserve quantities, as well as procuring these quantities in the market with cheaper offers.

We also compare the outcomes of the proposed models with the results of a perfect information model, where the optimal solution is obtained from a deterministic model with actual weekly and daily offers. This comparison shows that the two-stage model has a good performance in term of procuring the right amounts of reserves in the market with cheaper offers. However, that scenarios modeling offers in the daily market can still be improved.

The risk-neutral two-stage model has been clearing the Swiss reserve market since February 2014. Also, this study suggests that if Swissgrid wishes to implement a risk-averse model, the proposed risk-averse model results in appropriate outcomes.

6 Closure

In this concluding chapter, we provide a summary, the main conclusions and contributions of the work developed in this dissertation. We also provide suggestions for future research work.

6.1 Summary and Conclusions

In this thesis, we analyze some of the challenges associated with the operation of electricity market under uncertainty. To tackle such challenges, mathematical models for decision making are proposed, illustrated and analyzed. Below, we summarize the main characteristics of these models and provide concluding remarks.

6.1.1 Multi-Stage Stochastic Clearing Model

Power systems across the world are moving to integrate a significant amount of renewable power production and as a result to consider a number of intra-day markets. This calls for a revise in market-clearing approaches.

To make informed day-ahead decisions in the presence of uncertain renewable power production, we propose a multi-stage stochastic clearing model, where the first stage represents the day-ahead market, n additional stages model n intra-day markets, and a final stage stands for real-time operation. As an instance of multi-stage stochastic models, we present a three-stage one, where uncertainty stems from wind power production. The stochastic clearing process includes the first stage representing the day-ahead market, the second stage modeling an intra-day market, and the third stage standing for real-time operation. Therefore, the day-ahead schedules are decided with a detailed prognosis of the future, which includes the intra-day market and real-time operation.

The proposed model is illustrated and analyzed through an example and larger case studies, and benchmarked against a two-stage stochastic model. The simulation outcomes show that the proposed three-stage model has a better performance than the two-stage one as a result of more informed decisions at the day-ahead market. That is, the three-stage model results in lower day-ahead cost, expected cost, total expected profit, and consumer payment than those from the two-stage model.

Additionally, the day-ahead peak prices obtained from the three-stage model are lower than those derived from a two-stage model. This results from the use of more precise information on evolving wind power forecast across market stages in the three-stage model, and therefore, more efficient positioning of the units in term of day-ahead power production schedules, as well as intra-day power adjustments and deployed reserves. This is concluded by applying the three-stage model to different load profiles, and by considering different values of adjustment bounds and flexibility of units to provide reserves. Our simulation results also indicate that the outcomes from a three-stage model and a two-stage one get closer as restrictions get tighter. Small bounds are translated into reduced energy trading in the intra-day market, and hence, the results of the three-stage model get closer to those from two-stage one.

Therefore, we conclude that if a stochastic clearing model is adopted in systems with a large amount of renewable production, it should be a multi-stage stochastic model, and not a two-stage one. The advantage of a multi-stage clearing model stems from how renewable power output forecasts evolve from the day-ahead market to real-time operation. The information on how uncertain renewable production develops across the market floors, as well as, allowing flexibility for the contribution of renewable generation in both the day-ahead and intra-day markets improve the market outcomes and the integration of renewable generation.

6.1.2 Pricing Scheme Pertaining to A Stochastic Non-Convex Market-Clearing Model

Apart from the scheduling component of the market operation discussed in Chapter 2, other key component is pricing. While the use of non-convex clearing models might be inevitable due to the technical operating conditions of a power system, non-convex clearing models fail to result in linear marginal prices. On the other hand, uncertainty adds another layer of complexity.

We approach this problem by formulating a stochastic non-convex clearing model. We define three variants of cost-recovery conditions for producers in the presence of uncertainty including cost-recovery condition in the day-ahead market, cost-recovery condition in expectation, and cost-recovery condition per scenario. We next develop models that enforce these cost-recovery conditions. These models minimize the duality gap of the stochastic non-convex model and the dual problem of a relaxed version of the non-convex model subject to primal constraints, dual constraints, cost-recovery constraints, and integrity constraints. The cost-recovery conditions make this model non-linear, as it includes bi-linear terms. For computational tractability, the bi-linear terms are linearized using auxiliary integer variables and additional constraints. Therefore, the non-linear optimization model with cost-recovery constraints is recast as a MILP model with a higher problem size.

This model is benchmarked against the standard marginal pricing model through a simple example as well as large case studies. Day-ahead prices obtained from the proposed approaches are higher than conventional marginal prices in some periods. This, consequently, causes higher producer profits, and therefore, higher consumer payments. However, the new prices eliminate the need of uplifts and allow the market to fully rely on these " modified" marginal prices. Our conclusions are not affected by network congestion, as well as by considering other sources of non-convexity such as minimum up/down time constraints of units.

From a social welfare point of view, the social welfare obtained from the proposed models with cost-recovery features deviates the least possible amount from the optimal social welfare. The approach with day-ahead cost-recovery constraints results in the same expected cost as the original primal two-stage problem for the different load profiles considered. The other proposed approaches attain optimal expected costs close to the one of the original problem. The duality gaps are also small.

From the computational point of view, the models proposed have bi-linear terms, which need to be linearized using integer variables. In this process, a smaller linearization step leads to slightly more precise results at the expense of higher computation burden, but still the same conclusions are derived. Generally, the models proposed are tractable and solvable in a reasonable time using an MILP state-of-the-art solver.

Therefore, the proposed pricing schemes result in linear marginal prices without the need for uplift at the expense of deviating slightly from the optimal value of social welfare.

6.1.3 Economic Impact of Flexible Demands

While the main stream research emphasizes advantages arisen from demand flexibility, we take a closer look at the economic impacts of flexible demands and investigate economic consequences of demand flexibility in details.

We consider a power system with significant renewable production, comparatively expensive fast-ramping units, and flexible demands (ability of demands to move load from peak periods to off-peak periods). In this market environment, we explore the impacts of demand flexibility on operation costs, prices, consumer payments, and producer profits. We compare the cases of flexible and inflexible demands through a simple example and large case studies.

Demand flexibility is beneficial to the system, as it shifts its consumption from day hours to night hours, when cheap renewable production is available. In other words, demand flexibility adapts its consumption pattern to the production pattern of renewable production. This leads to a considerable cost reduction as compared to the cost obtained from the case with inflexible demands. Due to the notable shift in consumption in the case with demand flexibility, prices from the flexible demand case are higher over the off-peak periods and lower over the peak-periods with respect to the prices from the case with inflexible demands. Network congestion and ramping limits of the conventional units do not generally change these observations. Higher off-peak prices may result in higher consumer payments in the flexible demand case than those in the case with inflexible demands.

On one hand, demand flexibility is beneficial for the system as a whole since it decreases the expected operation cost, but on the other hand, demand flexibility can result in price increases that in turn increase demand expenses. Therefore, demands might be better off being inflexible in systems with a generation mix dominated by comparatively cheap renewable units and comparatively expensive fast-ramping units.

6.1.4 Stochastic Clearing model for the Reserve Market

In the context of self-dispatch markets with separated energy and reserve trading, we present a reserve scheduling problem motivated by the reserve market in Switzerland.

The Swiss reserve market consists of a weekly market and a daily market. The decision-making problem consists of determining which amount of reserves to procure in the weekly market and which one in the daily market.

We propose a risk-neutral two-stage stochastic clearing model to replace the common deterministic clearing approach in the Swiss reserve market. In the proposed two-stage model, the first stage represents the weekly market and the second stage the daily market. The source of uncertainty is the unknown offers in the daily market, which are represented by scenarios. We also introduce a risk-averse instance of this two-stage clearing model, where the risk measure is the CVaR. In other words, we aim to minimize the risk pertaining to expensive reserve offers in the daily market.

The proposed models are analyzed using real cases from the Swiss reserve market. We compare the performance of the risk-neutral two-stage model with the common deterministic approach, which sacrifices optimality in favor of simplicity. The proposed model results in a notable cost saving as compared to the deterministic approach. This is the result of procuring a smaller quantity of reserves under the proposed model than that of the deterministic approach, as well as procuring a considerable share of tertiary reserves in the market with cheaper reserve offers.

The proposed model is also benchmarked against a perfect information solution, which is obtained from a deterministic model with actual weekly and daily offers. This comparison shows that the two-stage model has a good performance in term of procuring the right amounts of reserves in the market with cheaper offers. However, the scenarios modeling offers in the daily market can still be improved.

The risk-neutral two-stage model has been clearing the Swiss reserve market since February 2014.

Also, this study suggests that if Swissgrid wishes to implement a risk-averse model, the proposed risk-averse model results in appropriate outcomes.

6.2 Contributions

The contributions of the work carried out in this dissertation are enumerated below:

1. To develop a multi-stage stochastic market-clearing model which takes into account the day-ahead market, a number of intra-day markets and the real-time operation. The propose model provides informed day-ahead decisions in renewable-dominated systems.
2. To carry out a comprehensive analysis of the performance of a three-stage model and its comparison with respect to a two-stage one.
3. To develop pricing methodologies for a stochastic non-convex market that result in linear marginal prices guaranteeing cost-recovery for producers.
4. To mathematically formulate the cost-recovery conditions of the producers: cost recovery in the day-ahead market, cost recovery in expectation, and cost recovery per scenario.
5. To carry out a comprehensive analysis to evaluate the performance of the proposed pricing methodologies.
6. To investigate the economic impacts of flexible demands in a power system with comparatively expensive fast-ramping units and comparatively cheap renewable units.

7. To develop and implement a risk-neutral two-stage stochastic market-clearing model for the Swiss reserve market.

8. To develop a risk-averse two-stage stochastic market-clearing model for the Swiss reserve market.

9. To mathematically describe all technical and market constraints of the Swiss reserve market.

10. To characterize the scenarios modeling uncertain offers in the Swiss daily reserve market.

6.3 Future Research Work

Finally, future research suggestions are provided below:

1. To consider quick-start units in intra-day markets and real-time operation in the market-clearing model. This requires the use of integer variables in all stages (and not only in the first stage) of the proposed multi-stage model.

2. To make the proposed clearing model more realistic by including security criteria such as the n-1 one and an AC representation of the transmission network.

3. To consider in the clearing model topological control. The core idea is to co-optimize topological changes such as line switching along with energy and reserves.

4. To apply appropriate decomposition algorithms for computational tractability.

5. To apply the proposed pricing methodologies to this model and evaluate their performance in term of optimality of solutions and tractability of the problem.

6. To apply appropriate decomposition techniques to efficiently solve the proposed pricing models.

7. To propose novel pricing schemes to encourage demand flexibility in a market with high renewable production.

8. To consider scenarios that explicitly represent indivisible daily offers (and not an approximated piece-wise linear curve) in the reserve clearing model.

Appendices

A Some Notions on Multi-Stage Stochastic Programming

This appendix provides the mathematical description of two topics relevant to multi-stage stochastic programming: the general formulation of a multi-stage stochastic programming problem and an instance of the VSS computed for this multi-stage stochastic problem.

A.1 Mathematical Description of Multi-Stage Stochastic Programming

Considering a decision-making process with s points in time to make a decision, the decision-making sequence is as follows: First, the decisions x^1 are made. Second, the stochastic process ζ^1 is realized as $\zeta^1_{\omega^1}$. Third, the decisions x^2 which depend on x^1 and the realization of ζ^1 are generated (denoted by $x^2(x^1,\omega^1)$). Next, the stochastic process ζ^2 is realized as $\zeta^2_{\omega^2}$, and consequently, the decisions $x^3(x^1,\omega^1,x^2,\omega^2)$ are taken. It continues till stage s, where decisions $x^{\mathrm{s}}(x^1,\omega^1,\cdots,x^{\mathrm{s}-1},\omega^{\mathrm{s}-1})$ are made after realization of the stochastic process $\zeta^{\mathrm{s}-1}_{\omega^{\mathrm{s}-1}}$. Note that at each stage the decisions are made independent of future realizations of the stochastic processes. In other words, the decisions are unique for all possible realizations of the stochastic processes in future. Thus, the non-anticipativity of the decisions is considered in the decision making sequence.

The formulation of the described multi-stage decision-making problem is:

$$
\begin{aligned}
&\underset{x^1}{\text{Maximize}} \quad f^1(x^1) + \mathbb{E}_{\omega^1}\Big(\underset{x^2(\omega^1)}{\text{Maximize}} \quad f^2(x^1,\omega^1,x^2(\omega^1)) \\
&+ \mathbb{E}_{\omega^2|\omega^1}\big[\underset{x^3(\omega^1,\omega^2)}{\text{Maximize}} \quad f^3(x^1,\omega^1,x^2(\omega^1),\omega^2,x^3(\omega^2)) \\
&+ \cdots + \mathbb{E}_{\omega^{\mathrm{s}}|\omega^1,\cdots,\omega^{\mathrm{s}-1}}\big[\underset{x^{\mathrm{s}}(\omega^1,\cdots,\omega^{\mathrm{s}-1})}{\text{Maximize}} \quad f^{\mathrm{s}}(x^1,\omega^1,\cdots,\omega^{\mathrm{s}-1},x^s(\omega^{\mathrm{s}-1}))\big]\cdots\big]\Big)
\end{aligned}
\tag{1}
$$

$$\text{subject to} \begin{cases} g^1(x^1) \leq 0 \\ g^2(x^1, \omega^1, x^2(\omega^1)) \leq 0, & \forall \omega^1 \in \Omega^1 \\ \vdots \\ g^{\mathrm{s}}(x^1, \omega^1, \cdots, \omega^{\mathrm{s}-1}, x^{\mathrm{s}}(\omega^{\mathrm{s}-1})) \leq 0, & \forall \omega^1 \in \Omega^1, \cdots, \forall \omega^{\mathrm{s}-1} \in \Omega^{\mathrm{s}-1} \\ x^1, x^2(\omega^1), \cdots, x^s(\omega^{\mathrm{s}-1}) \in \mathbb{R}^n \end{cases}$$

According to [4], if all the random variables are finitely distributed and the objective and constraints are linear functions, the equivalent of problem (1) is:

$$\underset{x^1, x^2(\omega^1), \cdots, x^s(\omega^{\mathrm{s}-1})}{\text{Maximize}} \quad c^{1\top} x^1 + \sum_{\omega^1 \in \Omega^1} \pi(\omega^1) \Big(c^{2\top}(\omega^1) x^2(\omega^1) + \sum_{\omega^2 \in \Omega^2} \pi(\omega^2) \big[c^{3\top}(\omega^2) x^3(\omega^2) + \cdots \tag{2}$$

$$+ \sum_{\omega^{\mathrm{s}-1} \in \Omega^{\mathrm{s}-1}} \pi(\omega^{\mathrm{s}-1}) c^{\mathrm{s}\top}(\omega^{\mathrm{s}-1}) x^s(\omega^{\mathrm{s}-1}) \cdots \big] \Big)$$

$$\text{subject to} \begin{cases} A^{11} x^1 \leq 0 \\ A^{21}(\omega^1) x^1 + A^{22}(\omega^1) x^2(\omega^1) \leq 0, & \forall \omega^1 \in \Omega^1 \\ \vdots \\ A^{\mathrm{s}1}(\omega^1, \cdots, \omega^{\mathrm{s}-1}) x^1 + \cdots + A^{\mathrm{ss}}(\omega^1, \cdots, \omega^{\mathrm{s}-1}) x^s(\omega^{\mathrm{s}-1}) \leq 0 \\ \qquad \forall \omega^1 \in \Omega^1 \cdots, \forall \omega^{\mathrm{s}-1} \in \Omega^{\mathrm{s}-1} \\ x^1, x^2(\omega^1), \cdots, x^s(\omega^{\mathrm{s}-1}) \in \mathbb{R}^n \end{cases}$$

A.2 Value of the Stochastic Solution for Multi-Stage Stochastic Programming

In a multi-stage problem with s stages, the $\mathrm{VSS_s}$ is defined for stage s as follows. First, the uncertain parameters are replaced by their expected value, and a deterministic problem without recourse is solved. We call this problem MV model (standing for Mean-Value):

$$\underset{x^1, \cdots, x^{\mathrm{s}}}{\text{Maximize}} \quad c^{1\top} x^1 + \overline{c}^{2\top} x^2 + \cdots + \overline{c}^{\mathrm{s}\top} x^{\mathrm{s}} \tag{3}$$

$$\text{subject to} \begin{cases} A^{11} x^1 \leq 0, \\ \overline{A}^{21} x^1 + \overline{A}^{22} x^2 \leq 0 \\ \vdots \\ \overline{A}^{\mathrm{s}1} x^1 + \cdots + \overline{A}^{\mathrm{ss}} x^{\mathrm{s}} \leq 0, \\ x^1, \cdots, x^{\mathrm{s}} \in \mathbb{R}^n \end{cases}$$

where $\overline{c}^{\circ}$ and $\overline{A}^{\circ}$ are the expected value of parameters c° and A°, resoectively (i.e., $\overline{c}^{\circ} = \mathbb{E}[c(\omega^{\circ})]$ and $\overline{A}^{\circ} = \mathbb{E}[A(\omega^{\circ})]$).

Considering that $\{\overline{x}^{*,1}, \cdots, \overline{x}^{*,\mathrm{s}}\}$ are optimizers of MV problem (3), the next step to compute the VSS is to fix the decisions of stages 1 to s − 1 to $\overline{x}^{*,1}$ to $\overline{x}^{*,\mathrm{s}-1}$, and solve the resulting problem for each scenario:

$$\underset{x^{s}(\omega^{\mathrm{s}-1})}{\text{Maximize}} \quad c^{1\top}\overline{x}^{*,1} + \sum_{\omega^{1}\in\Omega^{1}} \pi(\omega^{1}) c^{2\top}(\omega^{1})\overline{x}^{*,2} + \cdots + \sum_{\omega^{\mathrm{s}-1}\in\Omega^{\mathrm{s}-1}} \pi(\omega^{\mathrm{s}-1}) c^{\mathrm{s}\top}(\omega^{\mathrm{s}-1}) x^{s}(\omega^{\mathrm{s}-1}) \tag{4}$$

$$\text{subject to} \begin{cases} A^{11}\overline{x}^{*,1} \leq 0 \\ A^{21}(\omega^{1})\overline{x}^{*,1} + A^{22}(\omega^{1})\overline{x}^{*,2} \leq 0, \qquad \forall \omega^{1} \in \Omega^{1} \\ \vdots \\ A^{\mathrm{s}1}(\omega^{1}, \cdots, \omega^{\mathrm{s}-1})\overline{x}^{*,1} + \cdots + A^{\mathrm{ss}}(\omega^{1}, \cdots, \omega^{\mathrm{s}-1}) x^{s}(\omega^{\mathrm{s}-1}) \leq 0, \\ \qquad\qquad \forall \omega^{1} \in \Omega^{1}, \cdots, \forall \omega^{\mathrm{s}-1} \in \Omega^{\mathrm{s}-1} \\ x^{s}(\omega^{\mathrm{s}-1}) \in \mathbb{R}^{n} \end{cases}$$

Denoting the optimal value of problem (4) by $z^{\mathrm{D,s}}$ and the optimal value of multi-stage problem (2) by z^{*}, $\mathrm{VSS_s}$ is:

$$\mathrm{VSS_s} = \mathrm{z^{D,s}} - \mathrm{z}^{*}, \quad \forall \mathrm{n} > 1 \tag{5}$$

and as a percentage of the optimal value of stochastic problem:

$$\mathrm{VSS_{s\%}} = \frac{\mathrm{z^{D,s}} - \mathrm{z}^{*}}{\mathrm{z}^{*}}, \quad \forall \mathrm{n} > 1 \tag{6}$$

B IEEE 24-Node System Data

This appendix provides the technical characteristics of the IEEE 24-node system considered in the case studies of Chapters 2, 3 and 4.

The considered 24-node network is based on the single-area IEEE Reliability Test System (RTS) [72] and is illustrated in Figure 1. Line resistances are null and thus, active power losses are disregarded. The values of reactance and capacity of transmission lines are listed in Table 1. We should note that line reactances are given in per unit on a 100-MVA base.

For the sake of clarity, the particular characteristics of the generating units are provided in each case study of the corresponding chapters.

Table 1 – 24-node system: reactance and capacity of transmission lines

From node	To node	Reactance (p.u.)	Capacity (MW)
1	2	0.014	200
1	3	0.211	220
1	5	0.085	510
2	4	0.127	220
2	6	0.192	220
3	9	0.119	220
3	24	0.084	510
4	9	0.104	220
5	10	0.088	220
6	10	0.061	200
7	8	0.061	220
8	9	0.165	220
8	10	0.165	220
9	11	0.084	510
9	12	0.084	510
10	11	0.084	510
10	12	0.084	510
11	13	0.048	600
11	14	0.042	600
12	13	0.048	600
12	23	0.097	600
13	23	0.087	600
14	16	0.059	600
15	16	0.071	600
15	21	0.049	600
15	21	0.049	600
15	24	0.052	600
16	17	0.026	600
16	19	0.023	600
17	18	0.014	600
17	22	0.105	600
18	21	0.026	600
18	21	0.026	600
19	20	0.040	600
19	20	0.040	600
20	23	0.022	600
20	23	0.022	600
21	22	0.068	600

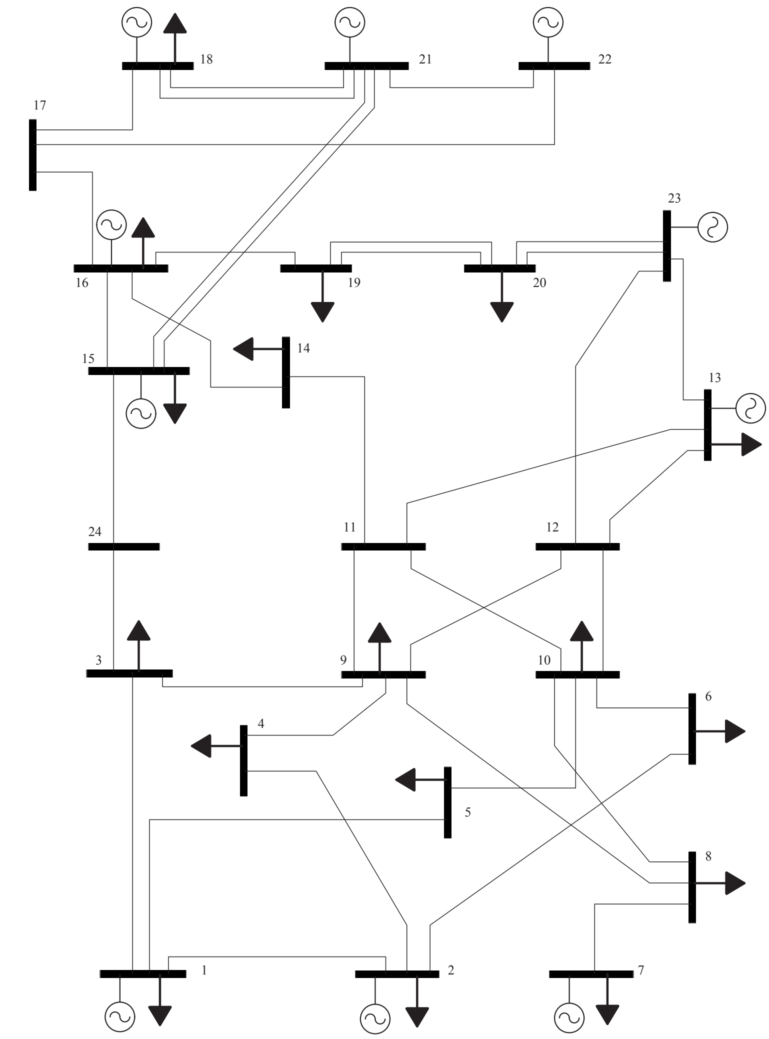

Figure 1 – Schematic of 24-node system

C Minimum Up- and Down-Time Constraints

In the following, we provide the mathematical description of minimum up- and down-time constraints.

For the sake of simplicity, we use a single-binary variable formulation [10], but recognize that a three-binary variable formulation is more efficient [49]. The minimum up/down time constraints are as follow:

$$\sum_{t=1}^{\mathrm{H_i^U}}(1-u_{it})=0,\forall i \tag{7a}$$

$$\mathrm{UT}_i(u_{it}-u_{i,t-1})\leq\sum_{k=t}^{t+\mathrm{UT}_i-1}u_{ik},\forall i,\forall t=\mathrm{H}_i^U+1,\cdots,N_T-\mathrm{UT}_i+1 \tag{7b}$$

$$\sum_{k=t}^{N_T}\big(u_{ik}-(u_{it}-u_{i,t-1})\big)\geq 0,\forall i,\forall t=N_T-\mathrm{UT}_i+2,\cdots,N_T \tag{7c}$$

$$\sum_{t=1}^{\mathrm{H_i^D}}u_{it}=0,\forall i \tag{7d}$$

$$\mathrm{DT}_i(u_{i,t-1}-u_{it})\leq\sum_{k=t}^{t+\mathrm{DT}_i-1}(1-u_{ik}),\forall i,\forall t=\mathrm{H}_i^D+1,\cdots,N_T-\mathrm{DT}_i+1 \tag{7e}$$

$$\sum_{k=t}^{N_T}\big(1-u_{ik}-(u_{i,t-1}-u_{it})\big)\geq 0,\forall i,\forall t=N_T-\mathrm{DT}_i+2,\cdots,N_T \tag{7f}$$

where constants UT_i and DT_i denote minimum up-time and minimum down-time of unit i, respectively. Parameter H_i^U is the number of initial periods that unit i must be online, and H_i^D is the number of initial periods that unit i must be off-line.

Constraints (7a) and (7d) are related to initial conditions for the units as defined by H_i^U and H_i^D, respectively. Constraints (7b) and (7e) enforce that in subsequent periods (of “sizes” UT_i and DT_i) minimum up-time and minimum down-time constraints are, respectively, satisfied. Constraints (7c) pertain to the last periods of the study horizon and enforce that started-up unit i remains online until the end of time span if required by its minimum up-time constraint. Similarly, constraints (7f) enforce that already-off-line unit i remains off-line until the end of time span if required by its minimum down-time constraints.

Bibliography

[1] M. H. Albadi and E. F. El-Saadany. Demand response in electricity markets: An overview. In *Power Engineering Society General Meeting, 2007. IEEE*, pages 1–5, June 2007.

[2] Alliance for Sustainable Energy (Alliance), National Renewable Energy Laboratory (NREL). Solar advisor model version 2012.5.11.

[3] R. Baldick, U. Helman, B. F. Hobbs, and R. P. O'Neill. Design of efficient generation markets. *Proceedings of the IEEE*, 93(11):1998–2012, Nov 2005.

[4] J. R. Birge and F. Louveaux. *Introduction to stochastic programming*. Springer, New York, 1997.

[5] P. N. Biskas, D. I. Chatzigiannis, and A. G. Bakirtzis. European electricity market integration with mixed market designs; part I: Formulation. *IEEE Transactions on Power Systems*, 29(1):458–465, Jan 2014.

[6] M. Bjørndal and K. Jörnsten. Equilibrium prices supported by dual price functions in markets with non-convexities. *European Journal of Operational Research*, 190(3):768–789, Nov. 2008.

[7] S. Borenstein, M. Jaske, and A. Rosenfeld. Dynamic pricing, advanced metering, and demand response in electricity markets. *Center for the Study of Energy Markets. UC Berkeley: Center for the Study of Energy Markets*, 2002.

[8] F. Bouffard and F. D. Galiana. Stochastic security for operations planning with significant wind power generation. *IEEE Transactions on Power Systems*, 23(2):306–316, May 2008.

[9] F. Bouffard, F. D. Galiana, and A. J. Conejo. Market-clearing with stochastic security-Part I: formulation. *Power Systems, IEEE Transactions on*, 20(4):1818 – 1826, nov. 2005.

[10] M. Carrion and J. M. Arroyo. A computationally efficient mixed-integer linear formulation for the thermal unit commitment problem. *IEEE Transactions on Power Systems*, 21(3):1371–1378, Aug 2006.

[11] S. Ceria. Solving hard mixed-integer programs for electricity generation. In B. F. Hobbs, M. Rothkopf, R. P. O'Neil, and H. P. Chao, editors, *The Next Generation of Electric Power Unit Commitment Models*, pages 153–166. Springer US, 2001.

[12] H.-P. Chao, S. S. Oren, A. Papalexopoulos, D. J. Sobajic, and R. Wilson. Interface between engineering and market operations in restructured electricity systems. *Proceedings of the IEEE*, 93(11):1984–1997, Nov 2005.

[13] European Comission. Guideline Electricity Balancing. March 2017. https://www.entsoe.eu/major-projects/network-code-development/electricity-balancing/Pages/default.aspx.

[14] A. J. Conejo, M. Carrion, and J. M. Morales. *Decision Making Under Uncertainty in Electricity Markets*. Springer, 2010.

[15] A. J. Conejo, J. M. Morales, and L. Baringo. Real-time demand response model. *IEEE Transactions on Smart Grid*, 1(3):236–242, Dec 2010.

[16] Danish Wind Industry Association. Wind Turbine Power Calculator. http://www.windpower.org.

[17] G. B. Dantzig. Linear programming under uncertainty. *Management Science*, 1(3):197–206, 1955.

[18] R. Doherty and M. O'Malley. A new approach to quantify reserve demand in systems with significant installed wind capacity. *IEEE Transactions on Power Systems*, 20(2):587–595, May 2005.

[19] J. Dupačová, G. Consigli, and S. W. Wallace. Scenarios for multistage stochastic programs. *Annals of Operations Research*, 100(1):25–53, 2000.

[20] J. Dupačová, N. Gröwe-Kuska, and W. Römisch. Scenario reduction in stochastic programming. *Mathematical Programming*, 95(3):493–511, 2003.

[21] EPEX. EPEX Intraday Market. https://www.epexspot.com/en/market-data/intradaycontinuous.

[22] L. F. Escudero, A. Garín, M. Merino, and G. Pérez. The value of the stochastic solution in multistage problems. *TOP*, 15(1):48–64, 2007.

[23] F. D. Galiana, F. Bouffard, J. M. Arroyo, and J. F. Restrepo. Scheduling and pricing of coupled energy and primary, secondary, and tertiary reserves. *Proceedings of the IEEE*, 93(11):1970–1983, Nov 2005.

[24] P. R. Gribik, W. W. Hogan, and S. L. Pope. Market-clearing prices and energy uplift. *Unpublished, downloadable at: http://www.hks.harvard.edu/fs/whogan/*, 2007.

[25] H. Heitsch and W. Römisch. Scenario reduction algorithms in stochastic programming. *Computational Optimization and Applications*, 24(2):187–206, 2003.

[26] I. Herrero, P. Rodilla, and C. Batlle. Enhancing intraday price signals in us iso markets for a better integration of variable energy resources. *Working Paper IIT-15-168A*, 2016.

[27] B.F. Hobbs, M. Rothkopf, and R.P. O'Neil. *The Next Generation of Electric Power Unit Commitment Models*. International Series on Operations Research and Management Science, 2001.

[28] W. Hogan. Demand response pricing in organized wholesale markets. *IRC Comments, Demand Response Notice of Proposed Rule-making, FERC Docket RM10-17-000*, May 2010.

[29] W. Hogan and B. J. Ring. On minimum-uplift pricing for electricity markets. *Unpublished, downloadable at:http://www.hks.harvard.edu/fs/whogan/*, 2003.

[30] K. Hoyland and W. S. Wallace. Generating scenario trees for multi-stage decision problems. *Management Science*, 47(2):295–307, 2 2001.

[31] International Energy Agency (IEA). Technology Roadmap: Wind Energy - 2013 edition. http://www.iea.org/publications/freepublications/publication/technology-roadmap-wind-energy—2013-edition.html.

[32] A. M. Jafari, H. Zareipour, A. Schellenberg, and N. Amjady. The value of intra-day markets in power systems with high wind power penetration. *IEEE Transactions on Power Systems*, 29(3):1121–1132, May 2014.

[33] D. S. Kirschen, G. Strbac, P. Cumperayot, and D. de Paiva Mendes. Factoring the elasticity of demand in electricity prices. *IEEE Transactions on Power Systems*, 15(2):612–617, May 2000.

[34] P. Sh. Kundur, N. J. Balu, and M. G. Lauby. *Power System Stability and Control*. McGraw-Hill, Inc., 1994.

[35] I. Lamprinos, N. D. Hatziargyriou, I. Kokos, and A. D. Dimeas. Making demand response a reality in europe: Policy, regulations, and deployment status. *IEEE Communications Magazine*, 54(12):108–113, December 2016.

[36] D. G Luenberger and Y. Ye. *Linear and nonlinear programming*, volume 228. Springer, 2015.

[37] H. M. Markowitz. *Portfolio selection: Efficient Diversification of Investments, 2nd Edition*. Wiley, 1991.

[38] J. M. Morales, A. J. Conejo, K. Liu, and J. Zhong. Pricing electricity in pools with wind producers. *Power Systems, IEEE Transactions on*, 27(3):1366–1376, Aug 2012.

[39] J. M. Morales, A. J. Conejo, H. Madseon, P. Pinson, and M. Zugno. *Integrating Renewables in Electricity Markets*. Springer, New York, 2014.

[40] J. M. Morales, A. J. Conejo, and J. Perez-Ruiz. Economic valuation of reserves in power systems with high penetration of wind power. *Power Systems, IEEE Transactions on*, 24(2):900–910, May 2009.

[41] J. M. Morales, S. Pineda, A. J. Conejo, and M. Carrion. Scenario reduction for futures market trading in electricity markets. *IEEE Transactions on Power Systems*, 24(2):878–888, May 2009.

[42] J.M. Morales, R. Minguez, and A.J. Conejo. A methodology to generate statistically dependent wind speed scenarios. *Applied Energy*, 87(3):843–855, 2010.

[43] Nord Pool. Nord Pool Intraday Market. http://www.nordpoolspot.com/How-does-it-work/Intraday-market/.

[44] U.S. Department of Energy. Benefits of demand response in electricity markets and recommendations for achieving them. In *A report to the United States congress pursuant to Section 1252 of the energy policy act OF 2005*, February 2006.

[45] OMIE. OMIE Intraday Market. http://www.omie.es/en/home/markets-and-products/electricity-market/our-electricity-markets/intraday-market.

[46] R. P. O'Neill, P. M. Sotkiewicz, B. F. Hobbs, M. H. Rothkopf, and W. R. Stewart Jr. Efficient market-clearing prices in markets with non-convexities. *European Journal of Operational Research*, 164(1):269 – 285, 2005.

[47] OpHB-Team. Policy 1 – Load-Frequency Control and Performance. In *UCTE Operation Handbook*, March 2009. www.entsoe.eu.

[48] M. A. Ortega-Vazquez and D. S. Kirschen. Estimating the spinning reserve requirements in systems with significant wind power generation penetration. *IEEE Transactions on Power Systems*, 24(1):114–124, Feb 2009.

[49] J. Ostrowski, M. F. Anjos, and A. Vannelli. Tight mixed integer linear programming formulations for the unit commitment problem. *IEEE Transactions on Power Systems*, 27(1):39–46, Feb 2012.

[50] A. L. Ott. Experience with pjm market operation, system design, and implementation. *Power Systems, IEEE Transactions on*, 18(2):528–534, May 2003.

[51] D. Papadaskalopoulos and G. Strbac. Decentralized participation of flexible demand in electricity markets; part I: Market mechanism. *IEEE Transactions on Power Systems*, 28(4):3658–3666, Nov 2013.

[52] A. Papavasiliou, S. S. Oren, and R. P. O'Neill. Reserve requirements for wind power integration: A scenario-based stochastic programming framework. *Power Systems, IEEE Transactions on*, 26(4):2197–2206, Nov 2011.

[53] I. J. Perez-Arriaga and C. Meseguer. Wholesale marginal prices in competitive generation markets. *IEEE Transactions on Power Systems*, 12(2):710–717, May 1997.

[54] G. Pritchard, G. Zakeri, and A. Philpott. A single-settlement, energy-only electric power market for unpredictable and intermittent participants. *Operations Research*, 58(4-part-2):1210–1219, 2010.

[55] G. C. Pug and W. Römisch. *Modeling, measuring and managing risk*. World Scientific, 2007.

[56] Y. G. Rebours, D. S. Kirschen, M. Trotignon, and S. Rossignol. A Survey of Frequency and Voltage Control Ancillary Services; Part I: Technical Features. *IEEE Transactions on Power Systems*, 22:350–357, 2007.

[57] R. Tyrrell Rockafellar and S. Uryasev. Optimization of conditional value-at-risk. *Journal of Risk*, 2:21–41, 2000.

[58] M. Roozbehani, M. A. Dahleh, and S. K. Mitter. Volatility of power grids under real-time pricing. *IEEE Transactions on Power Systems*, 27(4):1926–1940, Nov 2012.

[59] C. Ruiz, A. J. Conejo, and S. A. Gabriel. Pricing non-convexities in an electricity pool. *Power Systems, IEEE Transactions on*, 27(3):1334–1342, Aug 2012.

[60] A. Shabbir. Convexity and decomposition of mean-risk stochastic programs. *Mathematical Programming*, 106(3):433–446, 2006.

[61] S. Stoft. *Power System Economics: Designing Markets for Electricity*. IEEE Press, WILEY-INTERSCIENCE, 2002.

[62] G. Strbac. Demand side management: Benefits and challenges. *Energy Policy*, 36(12):4419 – 4426, 2008. Foresight Sustainable Energy Management and the Built Environment Project.

[63] C. L. Su and D. Kirschen. Quantifying the effect of demand response on electricity markets. *IEEE Transactions on Power Systems*, 24(3):1199–1207, Aug 2009.

[64] Swissgrid Ltd. Principles of ancillary services products. www.swissgrid.ch, May 2011.

[65] J. N. Tsitsiklis and Y. Xu. Pricing of fluctuations in electricity markets. *European Journal of Operational Research*, 246(1):199 – 208, 2015.

[66] A. Tuohy, P. Meibom, E. Denny, and M. O'Malley. Unit commitment for systems with significant wind penetration. *IEEE Transactions on Power Systems*, 24(2):592–601, May 2009.

[67] S. W. Wallace and S. Fleten. Stochastic programming models in energy. In *Handbooks in Operations Research and Management Science*. Elsevier Science, 2003.

[68] C. Wang, P. B. Luh, P. Gribik, L. Zhang, and T. Peng. A study of commitment cost in approximate extended locational marginal prices. In *Power and Energy Society General Meeting, 2012 IEEE*, pages 1–7, July 2012.

[69] G. Wang, U. V. Shanbhag, T. Zheng, E. Litvinov, and S. P. Meyn. An extreme-point global optimization technique for convex hull pricing. *in Proc. IEEE Power Energy Society General Meeting*, pages 1 – 8, 2011.

[70] J. Wang, M. Shahidehpour, and Z. Li. Security-constrained unit commitment with volatile wind power generation. *IEEE Transactions on Power Systems*, 23(3):1319–1327, Aug 2008.

[71] R. Wilson. Architecture of power markets. *Econometrica*, 70(4):1299–1340, 2002.

[72] P. Wong et al. The IEEE reliability test system-1996. *Power Systems, IEEE Transactions on*, 14(3):1010–1020, Aug 1999.

[73] S. Wong and J. D. Fuller. Pricing energy and reserves using stochastic optimization in an alternative electricity market. *IEEE Transactions on Power Systems*, 22(2):631–638, May 2007.

[74] H. Wu, M. Shahidehpour, and A. Al-Abdulwahab. Hourly demand response in day-ahead scheduling for managing the variability of renewable energy. *IET Generation, Transmission Distribution*, 7(3):226–234, March 2013.

[75] H. Wu, M. Shahidehpour, A. Alabdulwahab, and A. Abusorrah. Thermal generation flexibility with ramping costs and hourly demand response in stochastic security-constrained scheduling of variable energy sources. *IEEE Transactions on Power Systems*, 30(6):2955–2964, Nov 2015.

Farzaneh Abbaspourtorbati

Iran, 31 May 1984
Add: Funkwisenstrasse 100,
8050 Zurich, Switzerland

Email: Farzaneh.Abbaspourtorbati@epfl.ch

Education

- Ph.D. in Electrical Engineering, EPFL, Lausanne, Switzerland.
  Thesis title: *Electricity Market Operations under Uncertainty*
  2013 – 2017
- Visiting Scholar, Department of Integrated Systems Engineering, The Ohio State University, Columbus, Ohio, USA.
  Feb – April 2015
- M.Sc. in Energy Science and Technology, ETH Zurich, Zurich, Switzerland.
  2009 – 2011
- B.Sc. in Electrical Engineering, Sharif University of Technology, Tehran, Iran.
  2002 – 2007

Professional Experiences

- TSO Market Specialist, TSO Market Development, Swissgrid, Switzerland.
  Dec 2012 – now
- Application Engineer, Grid Application, Swissgrid, Switzerland.
  Nov 2011 – Nov 2012
- Internship, Ancillary Service Development, Swissgrid, Switzerland.
  Sep 2010 – Nov 2011

Invited Talk

- "Pricing Electricity in a Stochastic Market Model with Non-Convexities", IEEE PES General Meeting, Chicago, US, July 2017.
- "Stochastic Programming in Practice: Swiss Reserve Marketp", IEEE PES General Meeting, Chicago, US, July 2017.
- "Pricing Electricity in a Stochastic Market Model with Non-Convexities", PowerTech, Manchester, UK, June 2017.
- "Is Being Flexible Advantageous for Demands?", INFORMS Annual meeting, Nashville, USA, Nov 2016.
- "Stochastic Programming in Practice: Swiss Reserve Market", ENTSO-E Ancillary Service Workshop, Brussels, Belgium, Oct, 2016.
- "Stochastic Programming in Practice: Swiss Reserve Market", Swiss Association for Energy Economics (SAEE), Zurich, Switzerland, Nov 2015.
- "Pricing Electricity in a Stochastic Market Model with Non-Convexities", INFORMS Annual meeting, Philadelphia, USA, Nov 2015.
- "Stochastic Programming in Practice: Swiss Reserve Market", 5th Annual European Electricity Ancillary Services and Balancing Forum, Frankfurt, Germany, Sep 2014.

Student Supervision

- Master Thesis, EPFL, 2015, Student: Anneta Matenli,
  Title: *"Assessment of Centralized and Decentralized Dispatch Methodologies in Day-Ahead Contingency Analysis"*
- Master Thesis, ETH Zurich, 2015, Student: Georgios Chatzis,
  Title: *"A Framework for Joint Dimesnioning and Scheduling of Frequency Control Reserves and Energy Dispatch under OSTRAL Islanding Operation"*
- Master Thesis, ETH Zurich, 2015, Student: Haoyuan Qu,
  Title: *"Three-Stage Stochastic Market-Clearing Model for the Swiss Reserve Market "*
- Master Thesis, ETH Zurich, 2013, Student: Athanasios Troupakis,
  Title: *"Integrated Market for Manually Activated Ancillary Services Energy Products in Switzerland "*

List of Publications

Journal Papers

[J4] **F. Abbaspourtorbati**, A. J. Conejo, J. Wang, R. Cherkaoui, *Is Being Flexible Advantageous for Demands?*, IEEE Transactions on Power Systems, vol. 32, no. 3, pp. 2337-2345, May 2017.

[J3] **F. Abbaspourtorbati**, A. J. Conejo, J. Wang, R. Cherkaoui, *Three- or Two-stage Stochastic Market-Clearing Algorithm?*, IEEE Transactions on Power Systems, in press, 2016.

[J2] **F. Abbaspourtorbati**, A. J. Conejo, J. Wang, R. Cherkaoui, *Pricing Electricity in a Stochastic Market Model with Non-Convexities*, IEEE Transactions on Power Systems, vol. 32, no. 2, pp. 1248-1259, March 2017.

[J1] **F. Abbaspourtorbati**, and M. Zima, *The Swiss Reserve Market: Stochastic Programming in Practice*, IEEE Transactions on Power Systems, vol. 31, no. 2, pp. 1188-1194, March 2016.

Conference Papers

[C9] **F. Abbaspourtorbati**, R. Cherkaoui, and M. Zima, *Scarcity Mitigation in the Swiss Reserve Market*, Power System Computation Conference (PSCC), Genoa, Italy, 2016.

[C8] G. Chatzis, I. Avramiotis-Falireas, L. Roald,**F. Abbaspourtorbati**, G. Andersson, M. Zima, *Joint Scheduling Of Frequency Control Reserves And Energy Dispatch For Islanded Power Systems*, Power System Computation Conference (PSCC), Genoa, Italy, 2016.

[C7] A. Matenli, **F. Abbaspourtorbati**, F. Mende, L. Luongo, and R. Cherkaoui, *Centralized and Decentralized Electricity Market Settings: Assessment of Operational and Economic Aspects*, European Energy Market (EEM), Porto, Portugal, 2016.

[C6] I. Avramiotis-Falireas, H. Qu, **F. Abbaspourtorbati**, M. Zima, *The Importance of Accurate Transmission System Model for Cross-Border Exchange of Balancing Energy*, European Energy Market (EEM), Porto, Portugal, 2016.

[C5] **F. Abbaspourtorbati**, R. Cherkaoui, and M. Zima, *Balancing Market under Uncertainty*

with a Rolling Horizon for European Market Structure, PowerTech Conference, Eindhoven, Netherland, 2015.

[C4] A. Troupakis, M. Vrakopoulou, **F. Abbaspourtorbati**, G. Andersson, and M. Zima, *Market clearing framework for an integrated market for manually activated control reserves and redispatch in Switzerland*, European Energy Market (EEM), Krakow, Poland, 2014.

[C3] **F. Abbaspourtorbati**, M. Zima, *Procurement of frequency control reserves in self-scheduling markets using stochastic programming approach: Swiss case*, European Energy Market (EEM), Stockholm, Sweden, 2013.

[C2] I. Avramiotis, A. Troupakis, **F. Abbaspourtorbati**, and M.Zima, *An MPC Strategy for Automatic Generation Control with Consideration of Deterministic Power Imbalances*, IREP Symposium, Crete, Greece, 2013.

[C1] **F. Abbaspourtorbati**, M. Scherer, A. Ulbig, and G. Andersson, *Towards an optimal activation pattern of tertiary control reserves in the power system of Switzerland*, American Control Conference (ACC), Montreal, Canada, 2012.